THE DARLING GRANITE BATHOLITH

by

A.E.SCHOCH, M.Sc.

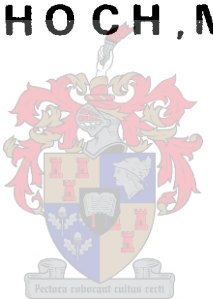

Thesis presented for the degree of Doctor of Science at the University of Stellenbosch.

Promotor: prof. W.J. Verwoerd

September 1972

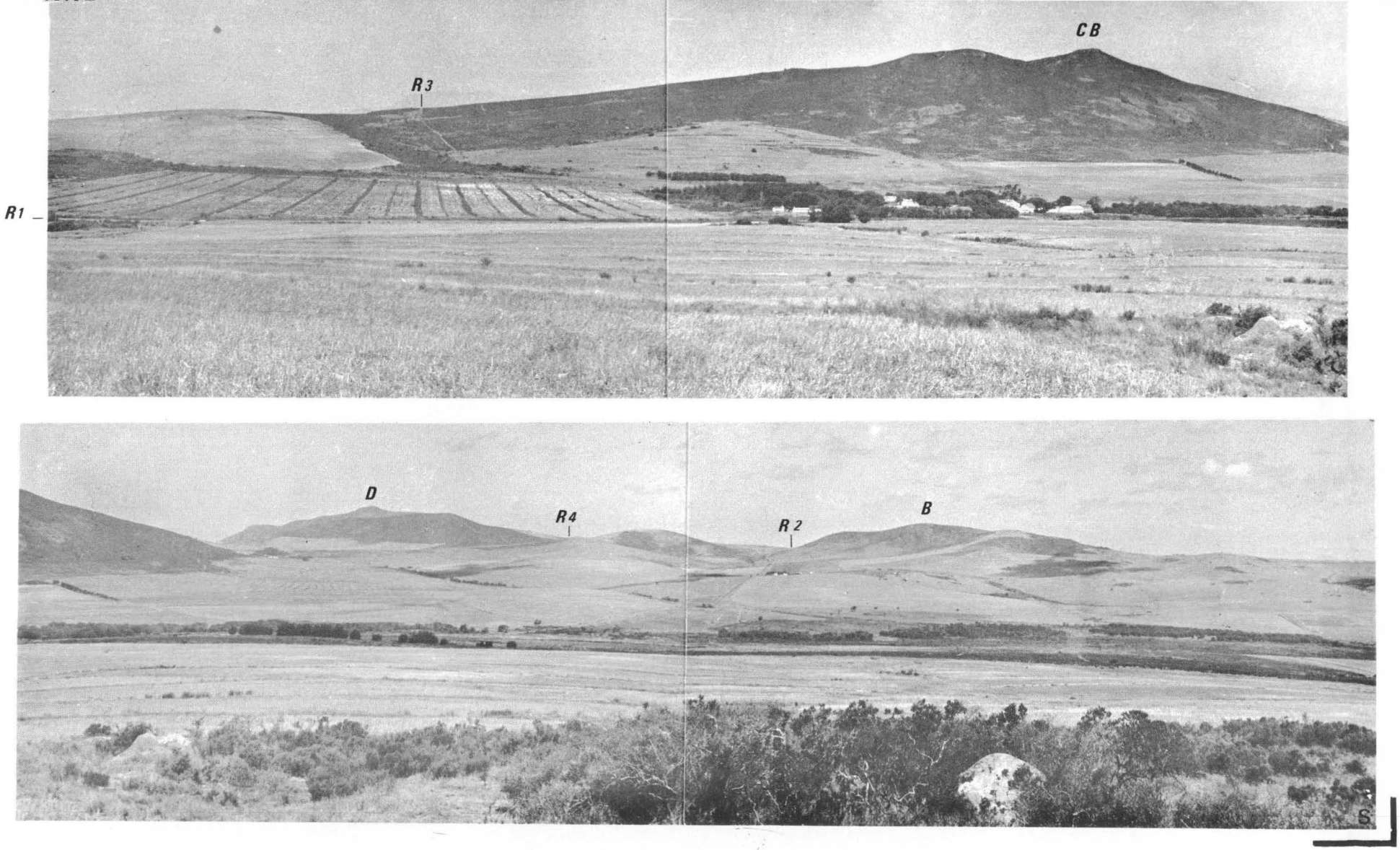

Panoramic view of some prominent topographic features in the Darling batholith, spanning approximately 150°. Round outcrop in right foreground is part of a dyke of young granite, while the other rock represents hybrid granodiorite. (R1 - Main road to Darling. R2 - Main road to Cape Town. R3 - Farm road between Contreberg and Vrededal. R4 - Road between Mamre and Mamre road station skirting foot of Dassenberg. CB - Contreberg. Farm below mountain is Contreberg farm. D - Dassenberg. Farm barely visible below and left of mountain is Waterkloof. B - Bobbejaanberg. Farm barely visible next to road and left of mountain is Commercial Dale).

ABSTRACT

The Darling batholith is characterised by large scale hybridisation, but mainly consists of the coarsely porphyritic Darling granite. This granite changes gradationally into a biotite-rich variety which occupies a roughly elliptical area with a major, northwesterly trending axis of 30 km. The biotite granite envelops a large irregular body of hybrid granodiorite. Small intrusions of younger granite occur within the batholith namely the Klipberg and Contreberg granites and possibly the biotite-rich Dassenberg granite. Dassen Island is underlain by fine-grained granite which could be related to either the younger or coarsely porphyritic granites. A prominent northwesterly trending mylonite zone can be traced through Darling to Swartberg, and ultimately to Trekoskraal in the Saldanha batholith, but is not continuous since it occasionally changes into gneissic granite and is also interrupted by the younger intrusives.

Quantitative mapping included measurement of matrix grain size, average maximum phenocryst length, xenolith distribution density, quartz nodule distribution density and average size, lineation, dark mineral index and gneissosity. On Dassen Island the distribution of tourmaline nodules was determined. The results are displayed as small scale contour maps which show strong correlation between the various parameters. The average values of matrix grain size, average phenocryst length and xenolith distribution density are respectively 2-5mm, 20-60mm and 0-1,5 per m^2 for the Darling granite, and 1-2 mm, 5-20 mm and 1-9 per m^2 for the hybrid granodiorite. It was found that the matrix grain size decreases with increase in hybridisation. The spotty distribution pattern of tourmaline nodules on Dassen Island indicates addition of boron by assimilation of metamorphites and a late stage liquid immiscibility process.

The granites have normal mineralogy and the K-feldspar of the phenocrysts is maximum microcline (Δ = 0,9 - 1,0).

The/

The hybrid granodiorite contains much pinitised cordierite and locally garnet. The deeply pleochroic biotite is probably of the $2M_1$ polytype and has a higher Fe:Mg ratio in the hybrid granodiorite than in the granite (2,8 - 3,0 vs. 2,2 - 2,3). The intimately associated chlorite seems to be of the Ia polytype. The cordierite is of the normal and low temperature type with average intensity index of 2,7 , distortion index of 0,3 and $2V_\alpha$ of 63°. The xenoliths are predominantly quartzitic metagraywackes, but lime-rich types holding sphene and diopside were occasionally encountered.

Thirteen new chemical analyses and thirty-one previously published analyses are used to calculate average composite analyses of the various rock types. The results of calculations employing Barth standard cell values indicate that the hybrid granodiorite could have originated by reaction between granite magma and Malmesbury quartzitic metagraywacke and pelite with a little limestone. A "granite differentiation index" based on weight percentages of (TiO_2 + MgO + FeO + Fe_2O_3) and (SiO_2 + Na_2O + K_2O) shows a linear relationship between the granites in probable order of age. The magmatic differentiation trend is separated from the hybridisation trend on a 6alk - 2(al - alk) - (100 - 2al) diagram.

Mesonorms and their cordierite variants are used to effect comparison with the experimental granitic system of von Platen (1965). The Darling and Contreberg granites plot near the relevant cotectic surfaces. A pilot experimental study of melting behaviour indicates that the Contreberg granite is closer to a minimum melt composition than the Darling granite. Comparison of alkali values with a $\mu_{Na_2O} - \mu_{K_2O}$ Schreinemakers diagram of Korzhinskii (1959), shows that the alkali ratio of the older analyses may be incorrect, and indicates that the dark minerals have a greater effect on plagioclase composition than the amount of K-feldspar. The classification of granites by means of Harpum diagrams is shown to have little relevance to the reconstruction of the ancient thermodynamical variants.

The/

The Darling granite is correlated with the Hoedjies Point granite of the Saldanha batholith and on geochronological evidence probably corresponds in age (500 - 600 m.y.) with the Cape Peninsula granite. The younger granites of Darling are tentatively correlated with the Cape Columbine granite of the Saldanha batholith. The northeastern boundary of the Darling batholith is a major fault, the Colenso fault, which is considered to extend as far as Northwest Bay, Saldanha. It is proposed that the Darling batholith occupies a down-faulted block within a graben and that the hybrid granodiorite represents a remnant synform of the roof rocks intruded by the granite. The younger granites constitute only four percent by volume of the batholith and may represent anatectic melts from a nearby subjacent source.

CONTENTS

THE DARLING GRANITE BATHOLITH

I INTRODUCTION

The Cape granites have attracted attention since an early date, at first because of the exceptional contact relations and related phenomena in the Cape Peninsula (Playfair and Hall, 1815; Charles Darwin, 1844; Walker and Mathias, 1946; Shand, 1949), but later on a regional basis (Corstorphine, 1897; Rogers, 1897; Haughton 1933). The regional interpretation received its major increment with the unparalleled synthesis of D.L. Scholtz (1946), which evoked the seldom-used adjective of "masterly" from S.J. Shand (1948). Excellent summaries of the literature are numerous, notably by Kolbe (1966), Otto (1957) and McIver (1957).

For a long time the term "Cape granite" was understood by most geologists to signify an intrusive high-level granite of post-Malmesbury age, occurring as isolated but consanguineous plutons from Namaqualand through the Western Cape to as far as Steytlerville (Scholtz, fig. 1 and map, 1946; van Biljon, 1939, and for the extremities of the area Söhnge and de Villiers, 1948; Middlemost, 1967, and de Villiers, 1941, 1944). While working in the Saldanha area (1958), the author observed the likelihood of multiple intrusion on a grand scale encompassing a significant slice of the Precambrian geological column. Since that time this impression has been reinforced by numerous new observations, making reinterpretation of all the previously published data necessary.

Because the field relations are complex, study of the Cape granites should commence in well-exposed areas such as the coastal outcrops, before extending the observations to districts where the inference-to-fact ratio becomes less favourable. Such investigations have reached an advanced

stage/

stage for the Saldanha batholith (Otto, 1957; McIver, 1957; Schoch, 1962; Packham, in progress). At the suggestion of Prof. D.L. Scholtz a comprehensive study of the neighbouring less well-exposed Darling batholith in the interior was initiated. The previous work proved to be invaluable for the understanding of this body.

The Darling granites have received little attention in the literature. The earliest reports (Rogers, 1896; Corstorphine, 1897), merely point out that the "Saldanha - Klein Dassenberg granite" or "Kapoc Berg - St.Helena Bay mass" which is gneissic in part, represents the largest pluton of Cape granite. The sporadic occurrence of gneissic textures as well as the presence of xenoliths identified as "various kinds of granulite", and which sometimes contain sphene, were recorded in a few sentences (Rogers and du Toit, 1909; Haughton, 1933). It was recognised that the attitudes of the inclusions do not always conform with the foliation of the granite. The portions of the published maps relevant to the Darling area recorded only the barest outlines of the contact between the granite and the Malmesbury Formation (Geological Commission of the Cape of Good Hope Sheet IV, 1906; Geological Survey of the Union of South Africa Sheet 247, 1933). Scholtz (1946) mentioned the occasional presence of garnet in Darling granites and briefly described the mineralogy of some xenoliths, including calcareous types. He included two analyses of granite and two of hybrid rocks. On the accompanying generalised structural map some data for foliation, lineation and joint orientations were shown and reference was made to "sheared quartz porphyry" and "cordierite and garnet bearing granitites and hybrid rocks". Photomicrographs which illustrate cataclastic features were also included (plate XIV fig. 1, and plate XV). Kolbe (1966) gave three new analyses of Darling granites in his study of the regional geochemistry of the Cape granites. Unfortunately the rock types selected were

not/

not typical of the average granite of the Darling pluton (Schoch, 1966), and the results are therefore more useful for the present investigation than for the intended purpose.

The field work was done during university vacations since 1963 and completed in 1969. In order to gain an insight into the local geological relations, that portion of the mass nearest to the Saldanha batholith and bounded by the roads to Ysterfontein and Burgerspan was mapped on aerial photographs with an average scale of 1 : 18 600. The rest of the mapping was then conducted on 1 : 50 000 and the final map presented on the same scale (see folder). The portion of this map to the west of longitude 18°30'E and to the north of latitude 30°30'S was incorporated in Geological Survey Sheet ~~255~~, 3318A-3218C, Saldanha (in preparation).

There are four major intrusives in the Saldanha batholith and at least two in the Darling mass. These two granite provinces are probably connected, as they are separated to the east of Langebaan by a strip, only a few kilometres wide, of thin recent limestones covered by dune sand. The broad synthesis is summarised in Table 1 in which the granites are symbolised in vertical order of age.

Table 1/

TABLE 1

SALDANHA BATHOLITH	DARLING BATHOLITH	Belts of Mylonitisation
a CCG 1	KB,CB 3	Mild NE, sometimes NW
VG ? ?		Shear streaks NE, NW
SQP 2		Mild to strong, NW belts
b HPG	DAR c	NW belts of severe mylonitisation

CCG = Cape Columbine Granite
VG = Vredenburg Granite
SQP = Saldanha Quartz Porphyry
HPG = Hoedjies Point Granite
KB = Klipberg Granite
CB = Contreberg Granite
DAR = Darling Granite
1 = Intrusive contact, South-west of Cape Columbine.
2 = Intrusive contact, Hoedjies Point Peninsula.
3 = Intrusive contacts on farms Wolwefontein, Contreberg.
a = Intrusive into Malmesbury Hornfels, Slippers Bay.
b = Intrusive into Malmesbury Hornfels, Trekoskraal, near Vredenburg.
c = Intrusive but sheared contact with Malmesbury Hornfels, on farm Klawervlei.

 = Intrusive contact

II DESCRIPTIVE FIELD PETROLOGY

Various granites occur in the region centred around Darling, and are bordered by metamorphites of the Malmesbury Formation to the south, west and north-east. The mutual relations of the Darling granites are highly complex, and exposed contacts are rare.

The most significant single result of the present study was the recognition of large bodies of young granite, previously unknown. For convenience the different geological features will be discussed with the aid of suitable small scale maps in order to limit the description of geographical distributions to essentials. Grid markings on these figures refer to the intersections of east longitudes 18°30' and 18°15' with south latitudes 33°15' and 33°30'.

1. The Darling granite

The distribution of the regional granite of the Darling batholith is displayed in fig. 1. Recent limestones, covered by dune sand, separate these occurrences from the easternmost exposures of the Hoedjies Point granite east of Langebaan, and probably rest on a continuous basement of granite.

The Darling granite is usually encountered as scattered outcrops which exhibit distinctive dome-like features due to exfoliation. The northernmost exposures at Swartberg and Betjieskop represent topographical high points projecting through the recent limestone beds.

The distribution of the granite can be roughly described as peripheral to an elliptical area with major and minor axes of 30 and 8 km respectively.

It can easily be distinguished from the other intrusives owing to its light colour and the presence of large potash

feldspar/

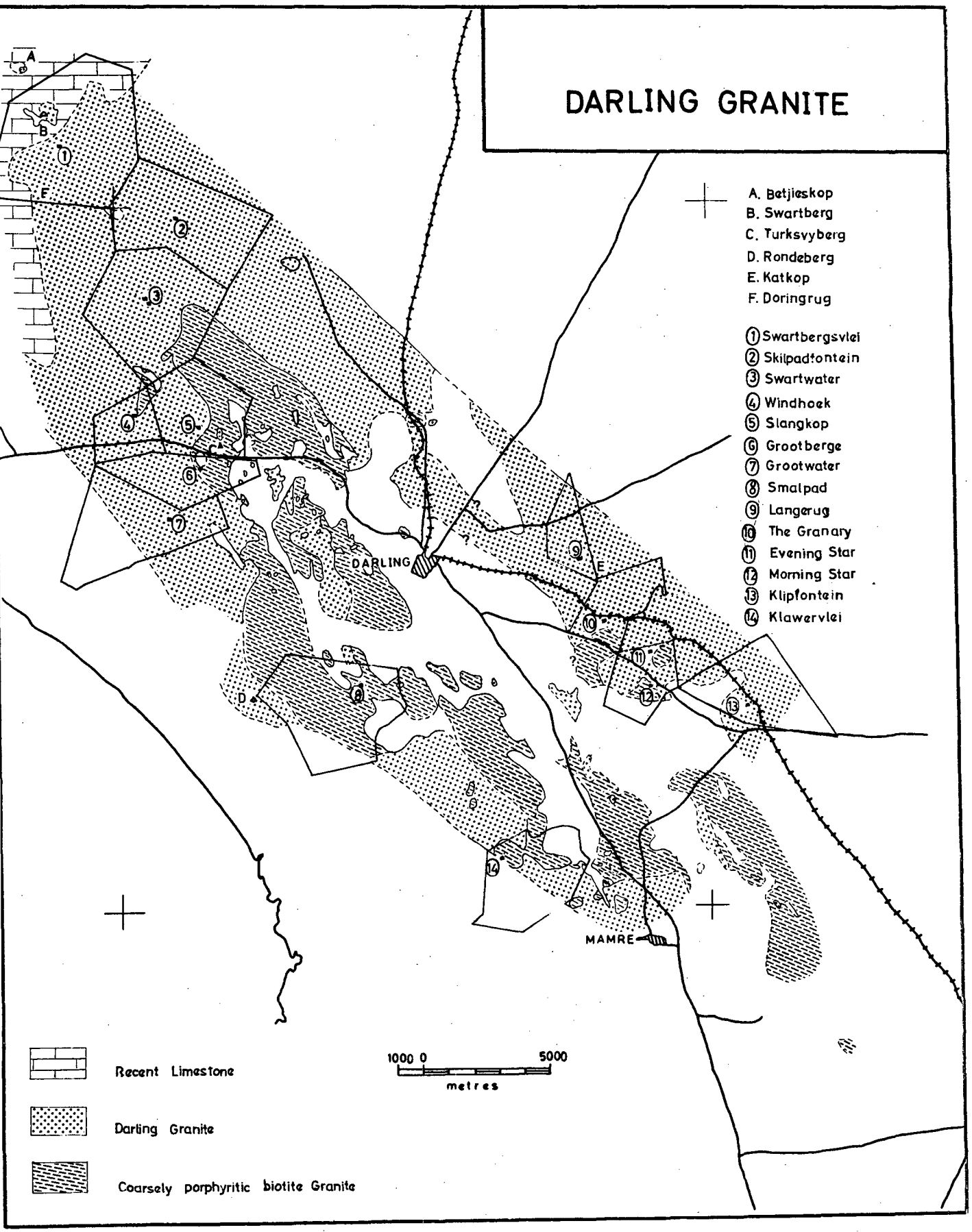

Fig.1

feldspar phenocrysts of rectangular outline (plate XVI). Biotite is common, while cordierite is occasionally present. This coarsely porphyritic granite is correlated with the Hoedjies Point granite of the Saldanha region because of the similarity in distribution, texture, nature of phenocrysts, deformation features, types of xenoliths, reaction products, and chemistry (p.79).

2. The porphyritic biotite granite

The Darling granite commonly grades into a biotite-rich variety (plate XIII, below), which has been mapped separately. This change is not gradual but reasonably abrupt on a regional scale. In general the biotite granite occupies a roughly elliptical area, centrally and concentrically disposed with respect to the biotite-poor Darling granite (fig. 1). It is however much better developed on the southwestern side of the town of Darling. The porphyritic biotite granite in turn, envelops the hybrid granodiorite discussed below. On Dassen Island (fig. 9), an occurrence of similar porphyritic biotite granite was noted in the northeastern corner, as well as an isolated body near the extremity of the northwestern peninsula (plates XV and XVII, above).

In the unusually well exposed coastal outcrop areas of the Saldanha batholith various steps in the progressive assimilative reaction between granite magma and Malmesbury metamorphites have been preserved at a host of localities, exhibiting a concomitant reduction of grain size and percentage of feldspar phenocrysts in the granitic products, apart from an increase in dark mineral content. If these observations are applied to the Darling mass, it seems likely that the porphyritic biotite granite would grade into less porphyritic varieties impossible to distinguish from the younger biotite granite described on p. 14. It is therefore possible that the rock type under discussion enjoys a wider distribution than is indicated on the map.

Fig. 2/

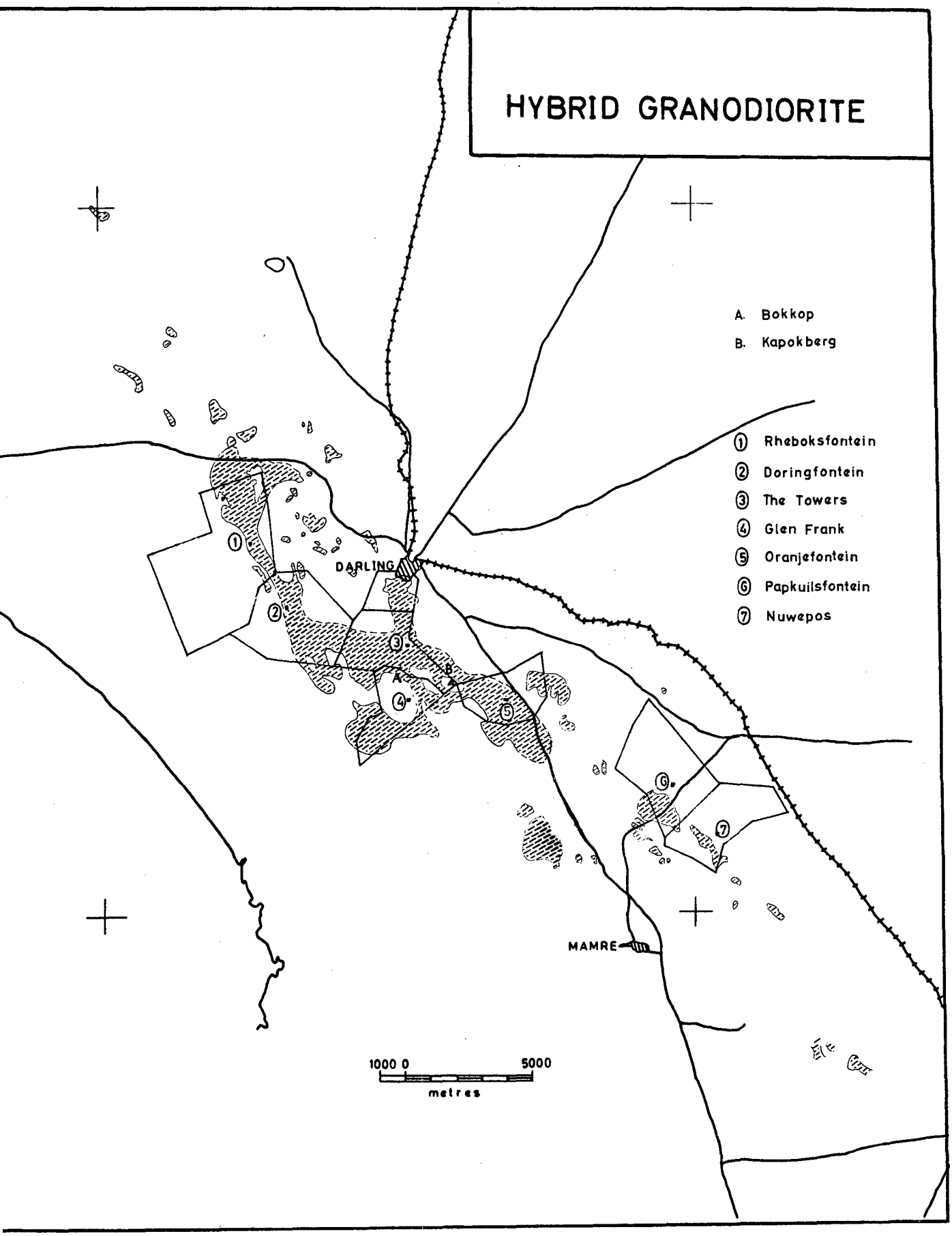

Fig. 2

3. The hybrid granodiorite

The hybrid granodiorite occupies the central position with respect to the concentric and approximately ellipse-shaped distribution of granites already discussed. It is a fine, even-grained and nonporphyritic dark-coloured rock (plates X, XI and XII), which can be mapped easily. In plan (fig. 2), as well as in section the distribution is irregular in outline but trends northwesterly over the farms Oranje-fontein, The Towers, Glen Frank, Doringfontein and Rheboks-fontein, including numerous isolated patches. As prominent parts of the mass occupy high ground as in the vicinity of Kapokberg, some form of topographical control over the distribution might be expected, which would enable deductions on the three-dimensional shape of the body to be made. No obvious control was found, even though it was diligently sought.

The main reason for the dark colour is the presence of much biotite. In some regions garnet is locally abundant as on the northern part of The Towers, and on the flank of Kapokberg on Groote Post. Cordierite is usually abundant but much altered.

4. The young granites

Younger granites within the Darling mass were first recognised during the present study (Schoch, 1966).

(a) Part of a large pluton of equigranular granite builds the prominent landmark Klipberg to the north-west of Darling, and occurs on the farms Klipberg, Alexanderfontein, Wolwefontein and Kraalbosdam (fig. 3). It is well-jointed, with prominent horizontal joints, appearing like an outlier of Table Mountain sandstone when viewed from a distance. On Wolwefontein undeformed apophyses were observed which project into a gneissic facies of the porphyritic biotite granite, the grain size of the dykes decreasing with width and therefore grading from granite through granite porphyry to quartz porphyry. The

intrusion/

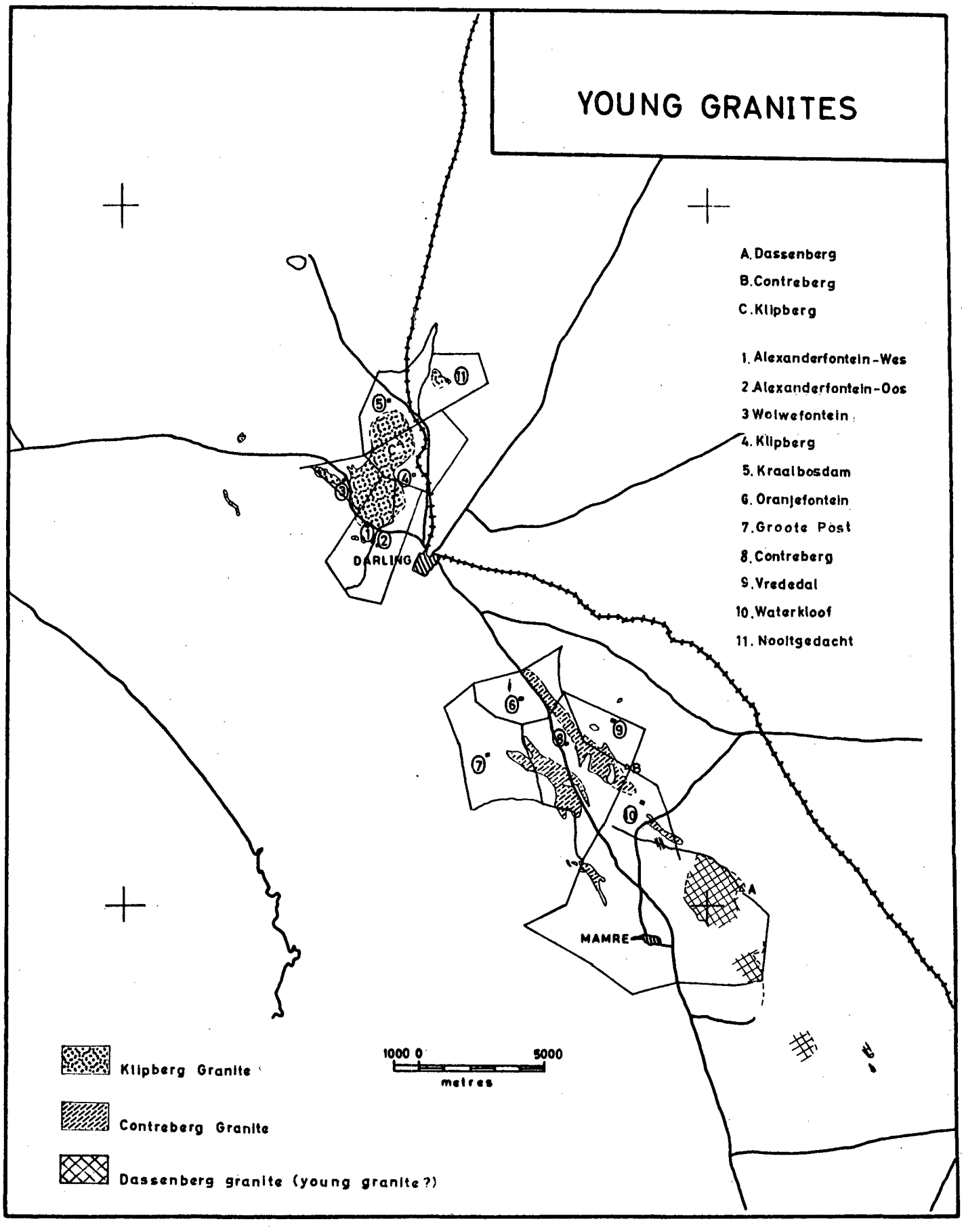

Fig. 3

intrusion must have taken place subsequent to the locally pronounced cataclastic deformation of the older granite.

Similar equigranular granite was also exposed on Nooitgedacht during the construction of a dam and subsoiling in a vineyard. The paucity of outcrops precludes the mapping of boundaries, but this body does not appear to be connected to the main one.

A small dyke of comparable material was noted on Rheboksfontein.

(b) Two major bodies of a porphyritic finegrained granite occur on the farms Contreberg and Groote Post. Once again a prominent landmark (Contreberg hill) is associated with part of the young granite. The intrusions strike northwesterly and seem to be essentially dyke-shaped. The larger body stretches from Oranjefontein over Contreberg and Vrededal to Waterkloof (frontispiece). Small dykes were also located on Waterkloof on the northwestern slope of Dassenberg and on Bobbejaanberg in the Mamre area.

This granite does not resemble the young granite discussed above (a), and for convenience they will be referred to as the Contreberg and Klipberg granites respectively. The Contreberg granite holds a large percentage of euhedral to subhedral and small phenocrysts, which are highly directed. At Contreberg hill pronounced swirl structures are sometimes seen with wavelengths of a few cm.

(c) To the south of Dassenberg in the Mamre area, and at Kanonkop, bodies of medium-grained porphyritic granite occur which exhibit characteristics of both younger and older granites. This once again illustrates the hazards of attempting correlation on grounds of texture. The author therefore places this occurrence in a division of its own for the time being.

(d)/

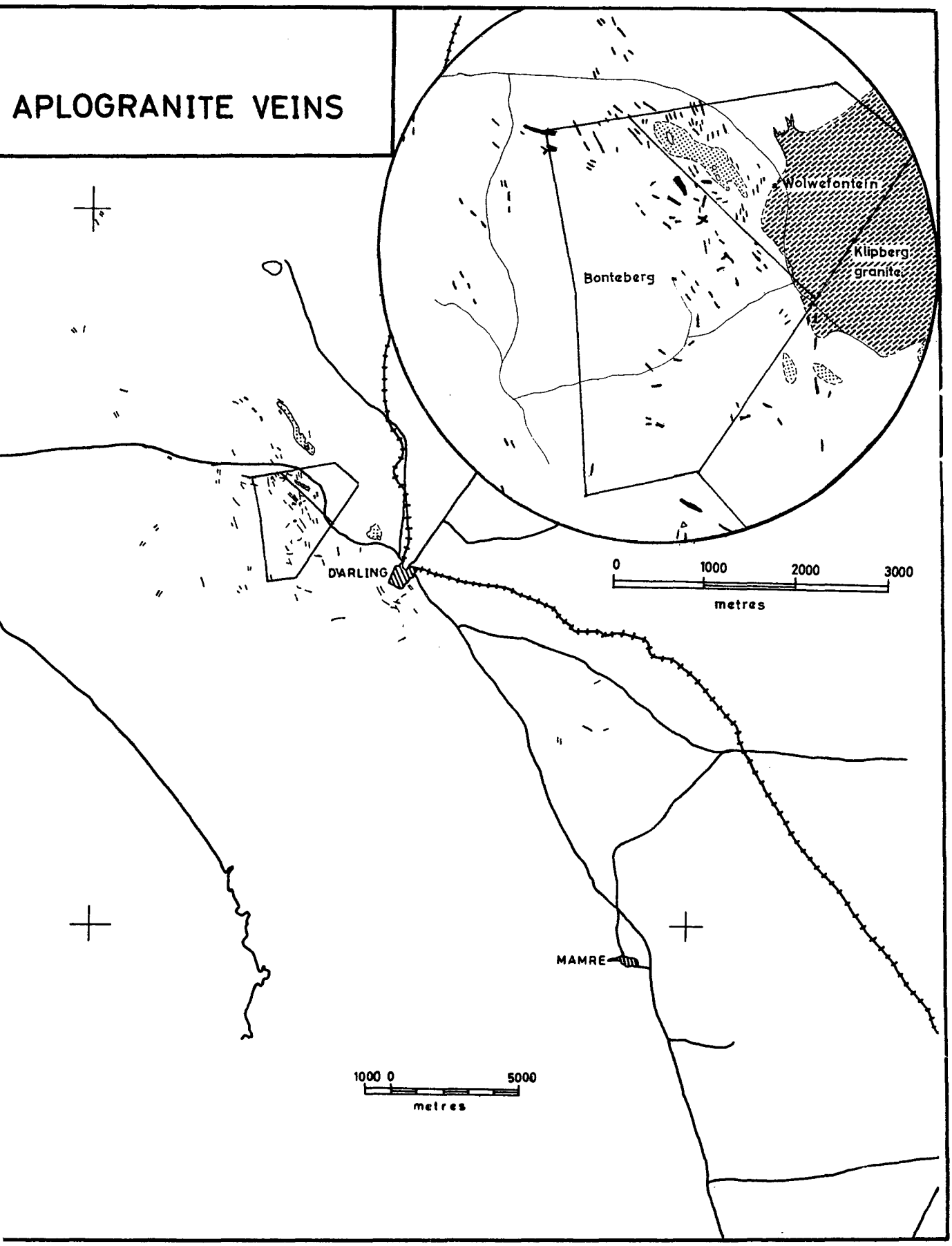

Fig. 4

(d) Small veins and dykes of aplogranite are often encountered, but show the best development in the hill called Bonteberg on the farm of the same name (fig. 4). The origin of the veins and the reason for their relative concentration on Bonteberg are obscure. There are also numerous true aplite dykes and veins in the Klipberg granite, which are not included here. Many of the aplogranite veins hold tiny needles of tourmaline.

5. The non-porphyritic biotite granite

The name for this rock type was deliberately chosen to indicate the contrast with the porphyritic biotite granite. It is not really devoid of phenocrysts, but large ones are few by comparison (plate XI, middle). While the Darling granite grades into porphyritic biotite granite, the young granites grade into the rock type under discussion, though not on so grand a scale. In such instances the non-porphyritic biotite granite is obviously a young feature. However, since progressive contamination of the older granite goes hand-in-hand with reduction of grain size as well as percentage of phenocrysts, there is no infallible field criterion by means of which to distinguish young contaminated granite from non-porphyritic older biotite-rich materials, with the exclusion of the hybrid granodiorite. It is therefore realised that various products may have been grouped together in this mapping unit. The regional distribution (fig. 5) nevertheless shows marked correlation with that of the young granites (fig. 3).

6. Mylonite

(a) A belt of magnificent mylonites with a northwesterly strike appears intermittently from Darling to Swartberg (fig.6). The rocks were crushed to microscopic grain size, retaining elongated augen of feldspar and quartz (Schoch, 1962, p. 740). The belt traverses the town, adjacent to which it is well exposed in various quarries.

This/

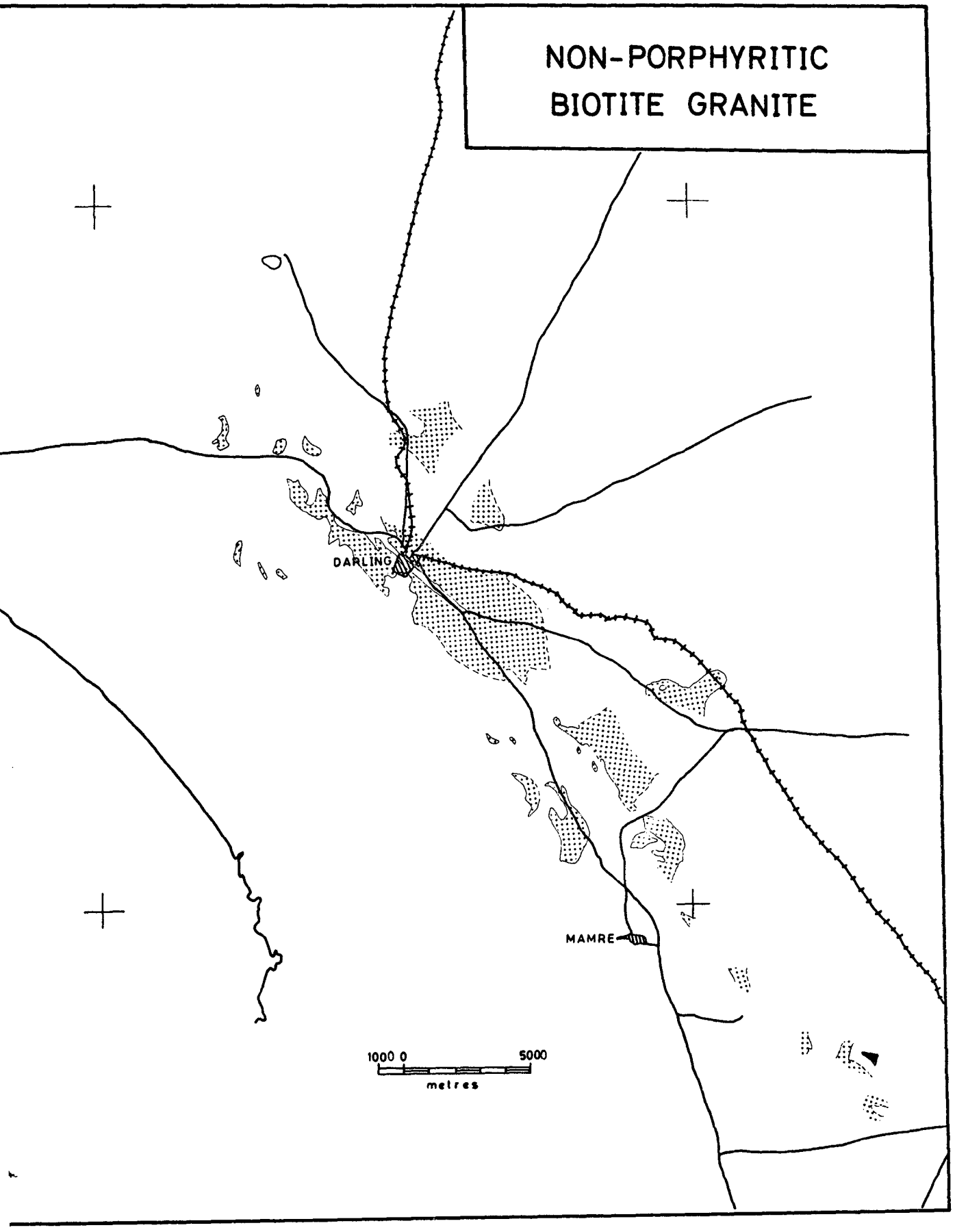

Fig.5

This particular continuous band ends to the south-east on the farm Oude Post, probably against a transverse fault, and to the north-west against the Klipberg granite. The young granite clearly postdates the main episode of mylonitisation, but does exhibit feeble deformation on strike, indicating slight later movements along the same direction. The most intense crushing phenomena, interpreted by Scholtz (1946) as pseudotachylite veins, are now admirably exposed in a new quarry on Oude Post.

Beyond the interruption caused by the Klipberg mass, thin lens-shaped mylonite bodies occur along strike on the farms Wolwefontein, Wildschutsvlei and Droëvlei. Surprisingly, the occurrences are now arranged en echelon. A coarse secondary fracturing in the cm range is visible on many weathered surfaces, reinforcing the evidence for a resumption of movements along the same zone after mylonitisation.

Towards the north-west the next exposure is a conspicuous zone of identical material on the southwestern flank of Swartberg on the farm Swartbergsvlei. The most northerly outcrop of Darling batholith plutonites on the farm Langfontein northwest of Swartberg, is a hill called Betjieskop which projects through the limestone cover, and is composed of mylonite as well.

All the evidence indicates that this prominent mylonite belt is the same as the one which appears on strike on the west coast in the Saldanha batholith at Northwest Bay (Schoch, 1962, p. 740).

(b) Small occurrences of mylonite with the same strike appear near the Colenso fault on Colenso, on Kraalbosdam and on Klipfontein. It was also encountered on the fault itself at Hartebeesvlei.

(c) Halfway between the Colenso fault and the main mylonite zone, a subsidiary belt is indicated by a few outcrops of

mylonite/

mylonite bands on Rooihoogtevlei and Langerug. The same zone is probably represented by occurrences on Nuwepos and against the flanks of Dassenberg on the farms Hill Side and Burgerspost, though with a slightly different strike. The change in orientation correlates with a similar rotation of the Colenso fault (fig. 6).

The sporadic disappearance of the mylonites does not seem remarkable if it is realised that the same movements could have caused gneissic textures wherever the forces acted over greater widths. If this is true the mylonites could have developed only in areas of more constricted movement. This possibility is clearly indicated when the distribution of mylonites (fig. 6) is compared with the gneissosity map (fig. 19, chapter III). Ordinary shear streaks, so well exhibited in the Saldanha region (Schoch, 1962), are quite common at many localities, for instance in Darling granite at Swartberg. The study at Trekoskraal in the Saldanha pluton indicated that the streaks and mylonite zones were caused by the same forces.

7. Faults

(a) A major fault forms the northeastern boundary of the batholith (fig. 6). This dislocation will be referred to as the Colenso fault. Outcrops are scanty in the northeastern parts of the batholith, but the narrow fault zone is easily located owing to the massive though intermittent development of chalcedonic fault breccia (plate XX) with a pronounced northwesterly trend. A spectacular occurrence of the breccia can be seen on Colenso on the southeastern side of the main road to Hopefield. The small white hill is immediately conspicuous in the locally flat terrain. Equally conspicuous outcrops are present on strike on Môrelig and Klipfontein. On the same trend line small outcrops were also observed on the northern corner of Kraalbosdam (formerly a portion of Nooitgedacht, plate XX), and on Brakrivier. Mylonite was located on the fault trend at Hartebeesvlei. The fault line

is/

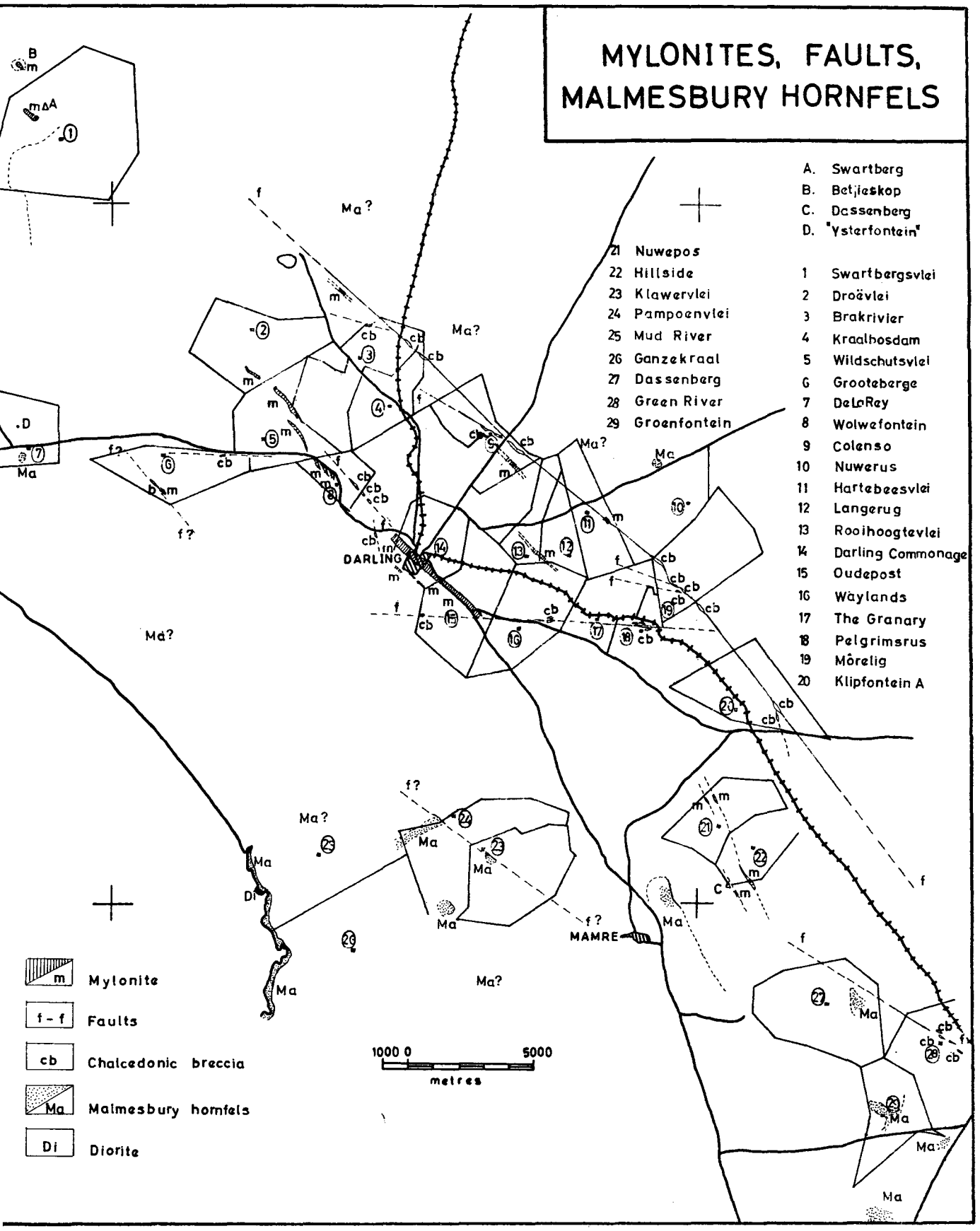

Fig. 6

is very straight, a fact which is locally very useful for the siting of drill holes for water, but a slight rotation to a new trend occurs in the southeastern part, the hinge being situated on Môrelig.

Lines of small outcrops of chalcedonic breccia indicate subsidiary faults at several localities. Examples of this are to be seen at the hinge on Môrelig, as well as on Colenso, Brakrivier and possibly on Klipfontein. The fact that the Colenso fault forms the boundary between granite and Malmesbury Formation rocks, can be explained by either a vertical or horizontal movement on the fault. No evidence of a vertical component was observed but the available evidence is too meagre to exclude such a possibility.

In the south-east, on Green River, large exposures of chalcedonic breccia have a similar orientation as the secondary faults described above. This fault may change to a similar strike as that of the Colenso fault before reaching Dassenberg (C in fig. 6).

(b) A westerly trending transverse fault is indicated by a lineament of chalcedonic breccia suboutcrops in a vineyard on Waylands, with another possible outcrop on strike to the west on the boundary between Oude Post and The Towers, and a magnificent breccia occurrence to the east on Pelgrimsrus. Paucity of outcrops precludes the tracing of this feature farther to the west, within the long valley in which Doringfontein is situated, but this may well be a physiographic expression of the line of weakness. The sense of movement of this interesting fault is not immediately apparent, and its determination would require detailed structural research which falls outside the scope of the present study. For convenience this feature will be called the Pelgrimsrus fault. On Waylands a high yield borehole is situated on it.

(c) An occurrence of schistose chalcedony on Alexanderfontein

and/

and Wolwefontein, striking parallel to the Colenso fault, may indicate a small dislocation traversing the Klipberg granite. Minor indications of the same character are present on the northern boundary of Grootberge, and are orientated east-west, while a small possible fault with associated mylonite exhibiting the Colenso fault trend was observed on the southern portion of the same farm.

(d) The granite-hornfels contact on Klawervlei discussed below represents a northwesterly trending fault plane as well, but the outcrops are too few to supply definite evidence.

It is instructive to compare the orientation of the mylonites, dolerite dykes and linear grouping of large xenoliths with the fault pattern (figs. 6 and 8). It has already been pointed out that the major episode of mylonitisation antedates the younger granite, but that the last movements on the faults are apparently later than this. It is quite possible that movements along the same vectors were active at various times during the geological history of the area. The latest large-scale movements may well post-date the Cape System, and it is predicted that the Colenso fault will eventually prove to connect with the Jonkershoek fault, the Franschhoek fault or one of their subsidiaries.

8. Dolerite:

Dolerite dykes in the Darling area are scarce and also difficult to locate, considering that they are commonly between 30cm and 1m wide (plate XXI, below right). Four dykes were observed (fig. 8), namely (a) on Platteklip, (b) Wolwefontein and Alexanderfontein, and (c and d) on Oranjefontein. All of them strike northwesterly.

9. The Malmesbury Formation

The country to the northeast of the Colenso fault is

flat/

flat and very deeply weathered. It is believed to consist of metamorphites of the Malmesbury Formation, as can occasionally be surmised in areas of weathered outcrop rather than soil.

To the west the boundary of the batholith must lie somewhere between De La Rey and the western corner of Grootberge, as hornfels is exposed on the firstmentioned farm. The buried contact may strike a few degrees west of true north, for many springs favour this orientation, sometimes providing veritable oases in the dune country. The original "ysterfontein" from which the name of the holiday resort was derived, is a group of chalybeate springs with a large development of ferricrete on De La Rey (D in fig. 6).

The only exposed granite-hornfels contact in the batholith can be seen below the dam on Klawervlei. Significantly, it exhibits the northwesterly trend encountered so frequently in the district. Although the exposure is only a few metres long, it is clear that movement has taken place along the contact zone. To the south-east the springs which feed the Mud River are situated on strike. To the north-west on Pampoenvlei the actual contact is not exposed, but a mere few metres of cover separate outcrops of hornfels and granite. On Pampoenvlei the Mud River changes its direction from parallel to the contact to nearly perpendicular to it, and has exposed a section across the folded Malmesbury rocks.

The structure of the Malmesbury Formation is admirably displayed on the coastal strip starting from the mouth of the Mud River, over the farm Ganzekraal (plate XXI, above), and onwards towards a point north of Melkbosch-strand. The intense thermal metamorphism of these folded quartzitic metagraywackes and spotted shales is in excess of the grade expected for the normal hornfelsic aureole around a Cape granite, for the rocks are several km distant from the contact. This observation, coupled with the presence of numerous anastomosing quartz veinlets, may indicate proximity of another

granitic/

granitic body, either subjacent or in the sea.

Outcrops of the Malmesbury Formation north-east of Mamre may represent a protuberance projecting into the batholith from its eastern margin along which some exposures of Malmesbury rocks appear on the farm Dassenberg and Groenfontein, while the Klipheuwel Formation occurs farther to the east. Outside the mapped area intermittent exposures of small granite bodies are known in the valley of the Mosselbank river to the south-east in the direction of elongation of the Darling batholith.

10. The Mud River diorite

A small diorite body was discovered in 1967 on the farm Mud River by the author and Mr. H.S. Pienaar during a students' excursion. This is the first known occurrence of diorite in hornfels on the west coast. The exposed portion of the body measures approximately 125 by 50 metres. The diorite displays considerable heterogeneity, such as schlieric structures and various types of xenoliths. An inclusion of metamorphosed limestone was observed at one locality. Parts of the diorite are rich in pyrite.

11. Xenoliths

Xenoliths are common, especially in the biotite-rich rock types. By far the largest number are very quartz-rich, including spotted types, and all exhibit typical metamorphic textures. Spotted pelitic kinds are somewhat less frequent, and occasionally impure limestone inclusions are also encountered (plate XIV). The xenoliths are invariably ellipsoidal (plate X), and the size and shape of many are reminiscent of watermelons. Quantitative data will be presented in chapter III.

The structure of individual inclusions is often complex, contrasting with the enveloping homogeneous granite. Two typical xenoliths of quartzitic metagraywacke are depicted in

fig. 7/

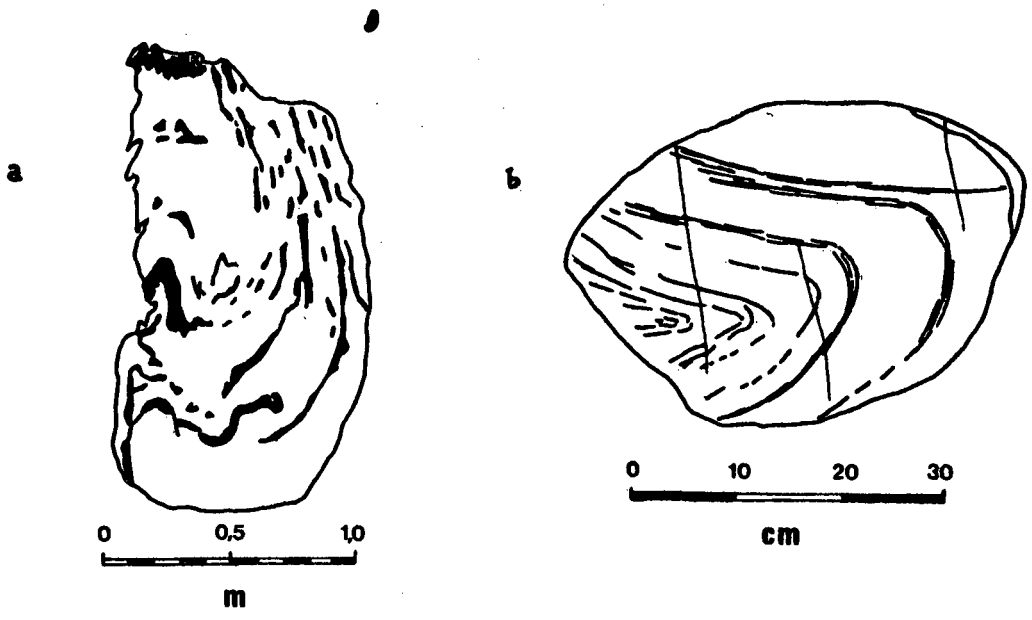

FIG. 7. DETAILED STRUCTURE OF XENOLITHS

a. Xenolith exposed on vertical east-west orientated surface. The xenolith is enveloped by even-grained biotite granite. The structure is visible because of quartz veinlets (shown in black) which sometimes merge with an enveloping quartz-rich reaction rim. (South of the farm dwellings on Vredehoek, near the boundary with Contreberg).

b. Xenolith exposed on horizontal rock surface. The xenolith is enveloped by hybrid granodiorite. The structure is eminently visible owing to etching by weathering. The three vertical lines represent joints in the xenolith. (Halfway between the farm dwellings on Oranjefontein and the boundary with Waylands, in a northwesterly direction).

fig. 7, and it is obvious that the original Malmesbury rocks were severely deformed. The present outlines of the inclusions must be due to reaction since they are ellipsoidal and often enveloped by a thin quartz-rich rim (not shown). As can therefore be expected inclusions with borders suggestive of the original shapes of the blocks were not observed at Darling, but a few examples with straight edges and blocklike shapes were encountered in granite on Dassen Island (plate XV).

High xenolith distribution densities are commonly associated with the appearance of large augen-shaped segregations of milky quartz (plate XXI, below left), in the enveloping granite and granodiorite. The quartz blebs range from 1 to 15 cm in major diameter, (fig.15), and are in rare instances visibly zoned, exhibiting cores of rosy quartz.

At several localities unusually large inclusions, mappable on 1 : 50 000 scale, have been encountered (fig. 8). The largest one is nearly 3 km in length and occurs on Rheboksfontein and Grootwater. The others are much smaller. Examples can be seen at the boundary between Oranjefontein and Oude Post halfway between the main road and the Kapokberg beacon, on Oranjefontein approximately 1km north-west of the main road and near the boundary with Waylands (plate XIV) and also at the beacon on Bobbejaanberg. Swarms of large xenoliths occur on top of the mountain northwest of the farm dwellings at Groote Post, north of Bokkop on The Towers and at Turksvyberg on Slangkop. A northwesterly orientated streak of scattered inclusions can be observed just to the south of the main road from the boundary between Alexanderfontein and Bonteberg, up to Wolwefontein.

In some cases large xenoliths are enveloped by a coarse-grained to pegmatitic reaction product. Examples are present at the Bonteberg-Wolwefontein and Turksvyberg occurrences mentioned above. At the lastmentioned locality the xenoliths include limestones, and diopside is present in the enveloping material.

As/

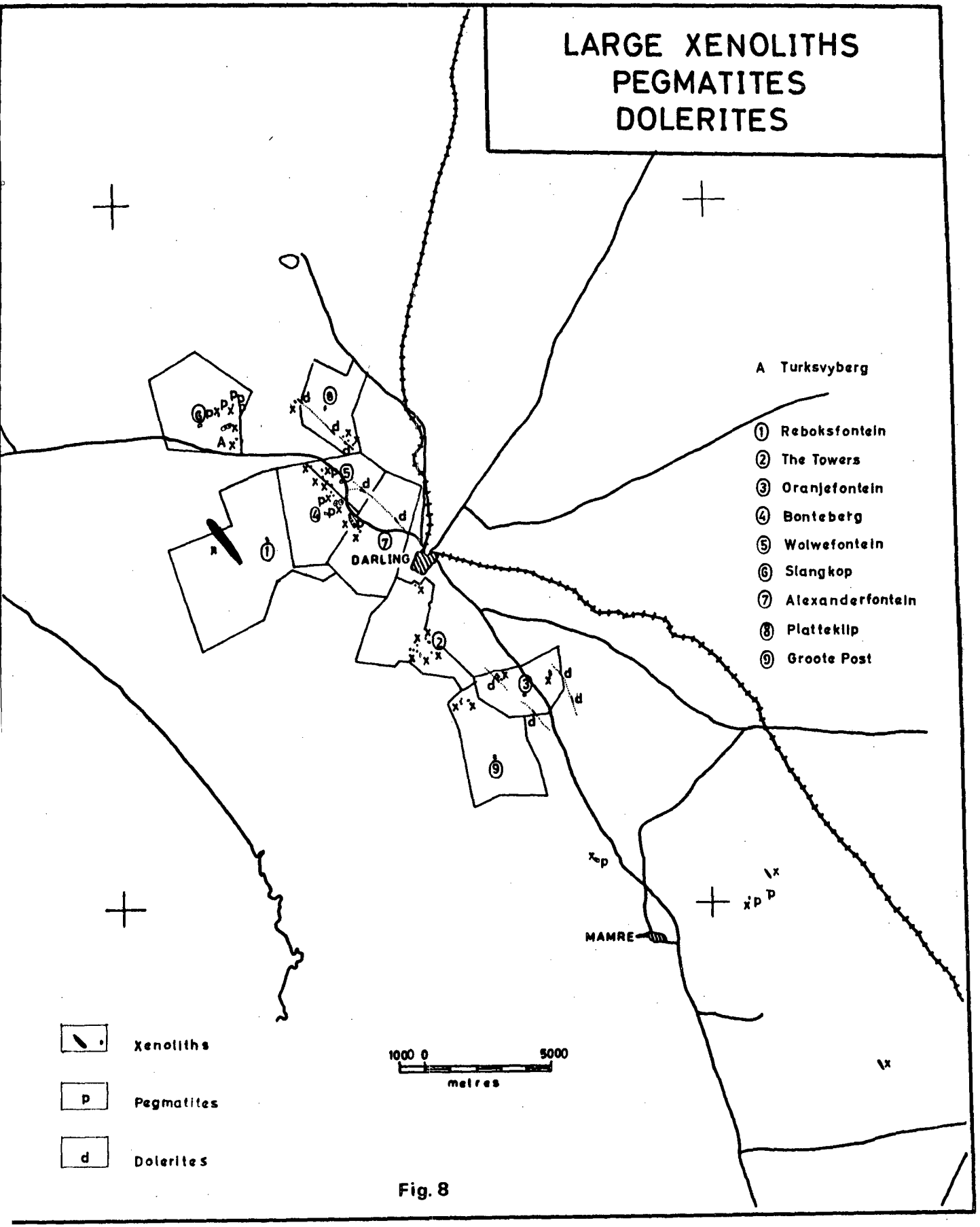

Fig. 8

As a rule the long axes of xenoliths are orientated northwesterly and nearly horizontally. However, contrasting orientations of neighbouring inclusions of differing compositions in a particular xenolith swarm (plate X) often indicate that the enveloping material must at some stage have been mobile. That it was hot as well, is shown by the wide variety of plastic deformation features in the xenoliths. The borders are clearly due to reaction and the smooth but sometimes fluted surfaces of the watermelon-shaped inclusions can often be observed where they have been dislodged by weathering.

12. Dassen Island

Dassen Island consists mainly of a fine- and even-grained granite grading into granite porphyry, and holding dispersed tourmaline nodules. It was first described by McLachlan (1949) and remapped by the author in 1963 (fig. 9). The relationship of the main granite with a coarsely porphyritic granite is ambiguous, since a tapering dykelike body of the coarse granite seems to have intruded into the fine-grained granite at the northwestern peninsula, while the reverse appears to have taken place in the southwestern area near the lighthouse. Since the lastmentioned exposure is a good one and because a gradation to smaller grain sizes is evident in the fine-grained granite as the sharp contact with porphyritic granite at the northwestern occurrence is approached, the fine-grained granite may be justifiably regarded as the younger intrusive.
It should however, be kept in mind that similar nodular tourmaline rocks known elsewhere in the Cape granites seem to be intimately associated with the coarsely porphyritic varieties as a marginal phase. The observations and arguments of D.L. Scholtz (1946, p. lxi, plate XI and plate XII) concerning nodular tourmaline Cape granites as products of late liquid immiscibility are still valid, also for the granite under consideration.

Hornfels/

DASSEN ISLAND

Geology and matrix grain size

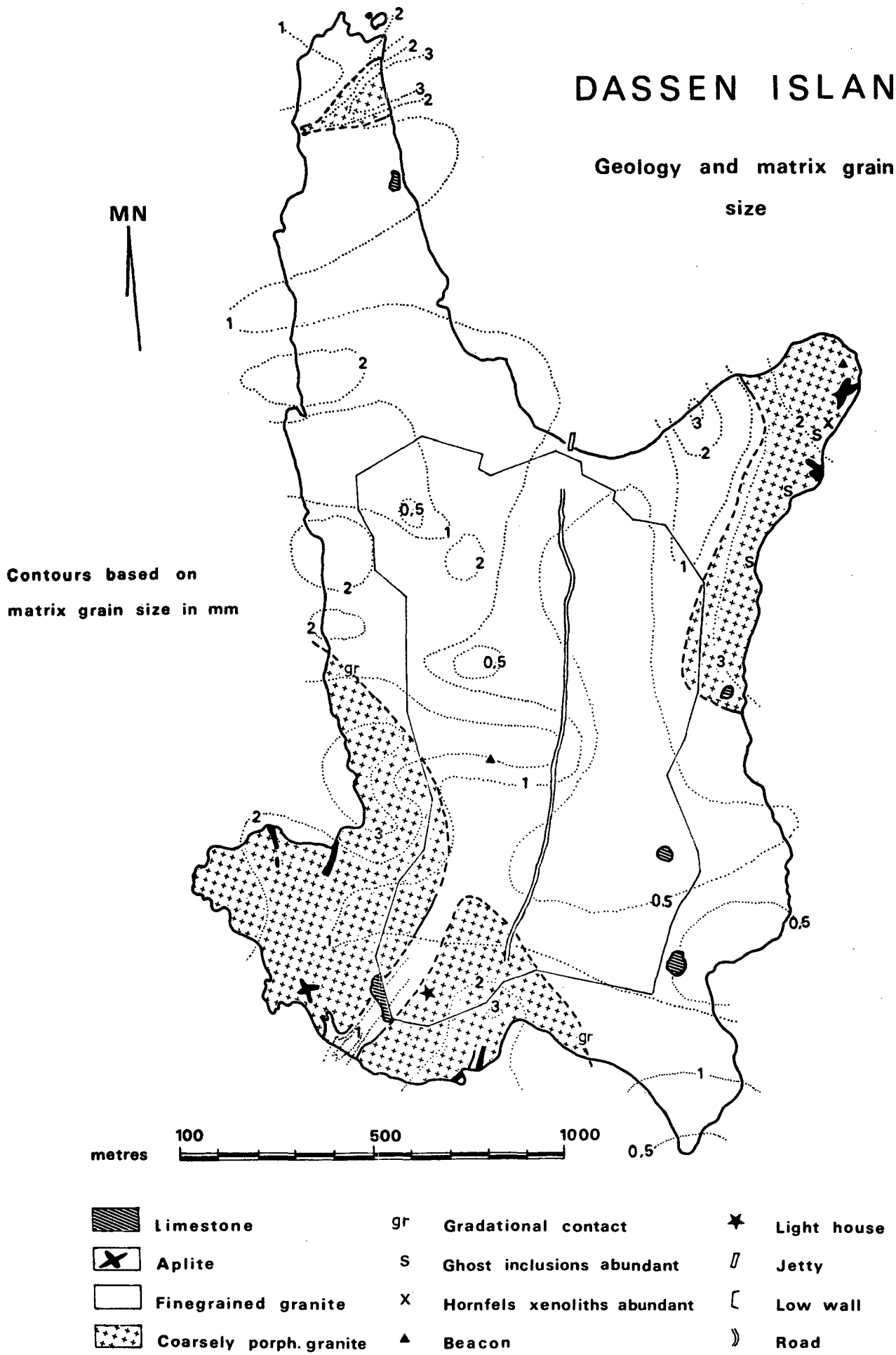

Fig. 9

Hornfels inclusions are often seen in the coarsely porphyritic granite, and are sometimes of angular dimensions suggestive of fracturing along joint planes. Such xenoliths are pitch black quartzitic metagraywackes (plate XV) with no corrosion features on the contact with the granite, and therefore very conspicuous against the light coloured background. Partly digested inclusions were also encountered as well as ghost inclusions, particularly in the northeastern part of the island.

The porphyritic granite in the south-west is singular, since it exhibits gradational contacts with the fine-grained granite, and is itself characterised by tourmaline nodules. These features are in contrast with the characteristics of the porphyritic granite of the northwestern peninsula (plate XVII, above) and the northeastern area.

III QUANTITATIVE FIELD PETROLOGY

The main task of the author was to record the basic field relations because so little was known of the Darling batholith. It was nevertheless attempted to produce more than a merely descriptive study. It was therefore decided at the outset to expand a semiquantitative method of field investigation initiated at the University of Stellenbosch by prof. D.L. Scholtz into quantitative procedures. The previous methods included measurements of texture (Scholtz, 1946, p. xlvii; Otto, 1957, fig. 5; McIver, 1957, p. 551; Schoch, 1962) and classification of mylonitisation features (Schoch, 1962, pp. 693 - 695). In the meantime the use of quantitative analysis in the study of batholiths has gained wide acceptance in the literature owing to the excellent work of authors such as Whitten (eg.1961, 1964) and Peikert (1965), although there seems to have been a tendency to overemphasize "sampling problems" and computer application.

As many observations of matrix grain size, phenocryst size, xenolith distribution density and other selected factors were made as was practicable over the entire area studied, and it was hoped that these would aid in arriving at acceptable solutions to some petrogenetic problems. Seen in retrospect this was a fortunate decision in view of the paucity of contacts, the gradual nature of transitions and the sparse distribution of outcrops in some areas, but it was sometimes regretted in the field during the recording of tedious measurements.

The number of outcrops per unit area of study ranges from one extreme to the other over the district. The dots in fig. 10 represent localities where measurements were made and provides a rough indication of the outcrop distribution density. Naturally all the parameters were not measured at all stations. Roughly 10 000 observations have been recorded of which approximately 2 000 pertained to texture. The accumulated data are

obviously/

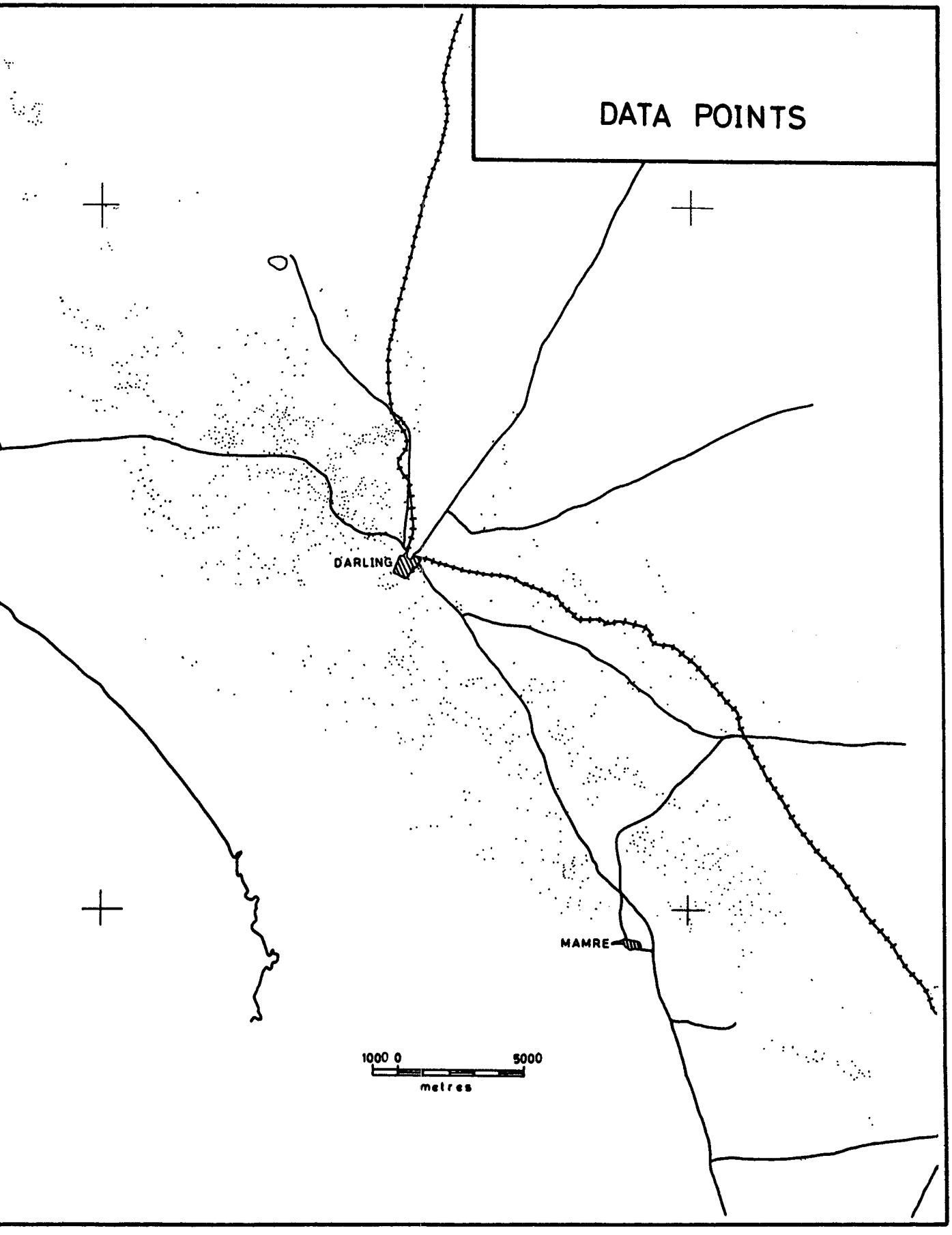

Fig .10

obviously ample for the purpose of this study, but it seems advisable that the matter should be pursued further with the aid of a computer and three-dimensional trend surface analysis.

The syntheses presented in this chapter can be divided into two categories, namely those based on objective measurements and those based on observations which entailed judgement and are therefore to some degree subjective. The results are given in the form of text figures which summarise the quantitative data obtained, thus eliminating the use of lengthy tables or descriptions. Owing to the geological complexity of the area it was never apparent during field work what the final maps would look like. All the figures were originally constructed as contour maps on 1 : 50 000 (1 : 18 600 in part) and subsequently reduced by a ratio of roughly 1 in 4 (1 in 10 in part), which considerably adds to the confidence with which they may be used. Diagrams based on the "objective" criteria namely matrix grain size, average maximum phenocryst length, xenolith distribution density, quartz nodule distribution, and lineation will be presented first, but the data for Dassen Island will be discussed at the end of the chapter.

1. Matrix grain size

The initial expectation that measurement of this parameter would aid discovery of chill phases proved to be naïve, as is clearly indicated by fig. 11. Chill phases are of course known in the Cape granites (Scholtz, 1946; Otto, 1957; Schoch, 1966), at Paardeberg, Paarl mountain, Cape St. Martin, Trekoskraal and elsewhere in the Western Province. However, reduction of grain size is not only caused by steep thermal gradients during crystallisation but also by a mechanism seldom considered in the literature, namely reaction between the granite and inclusions of its metamorphosed wall-rock, for which the Darling area supplies the best developed regional display imaginable. This is also clearly shown on a small scale at certain exposures in the Saldanha area, for instance at the hybrid grano-

diorites/

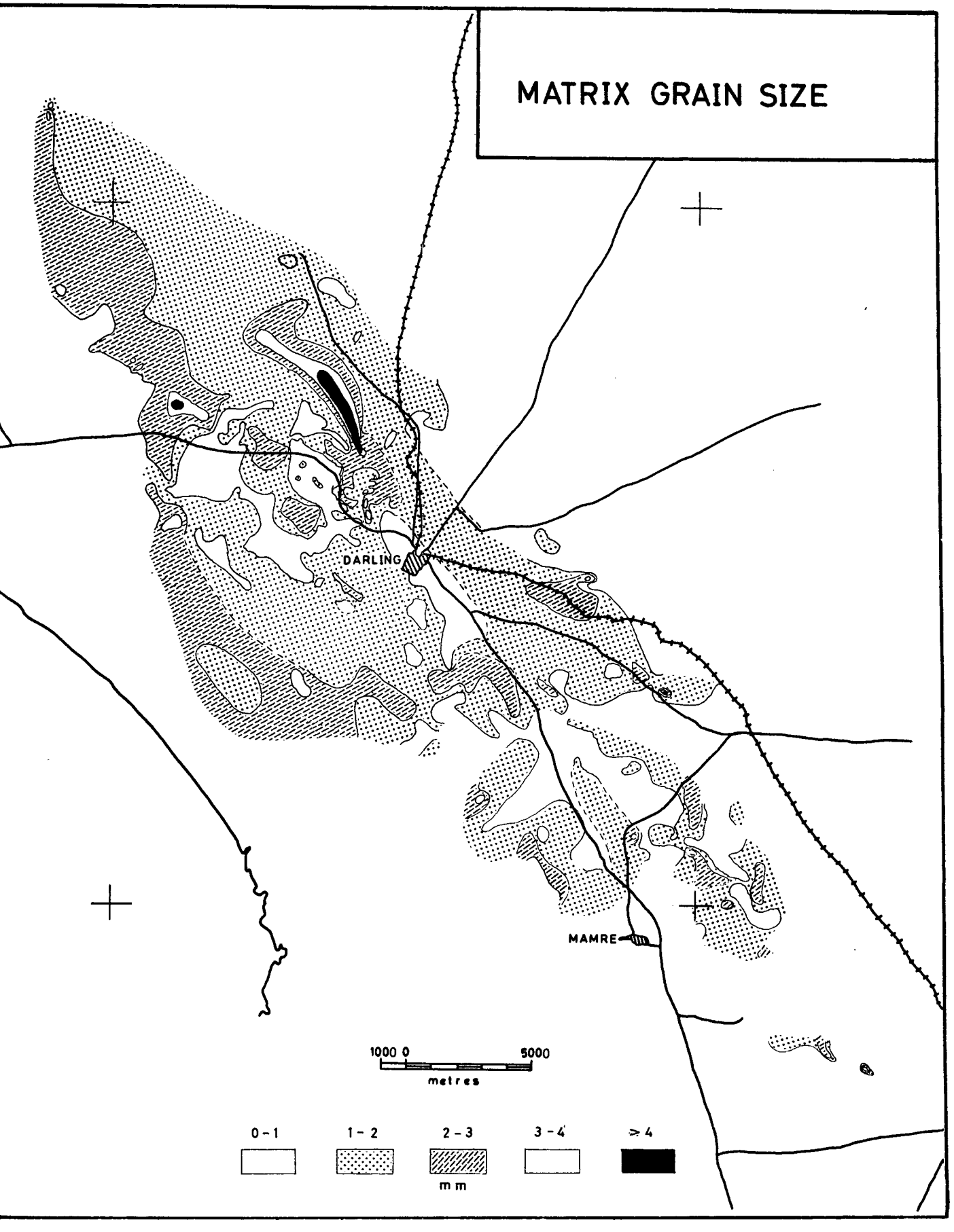

Fig. 11

diorites of Groot Paternoster on the farm Duikereiland and in the Slippers Bay hills (Scholtz, 1946).

The grain size characteristics of the various rock types of the Darling batholith can be summarised as follows:

Darling granite - Coarse average matrix grain size which varies gradationally from 2 mm to 5 mm, reaching as much as 9 mm in isolated cases.
Porphyritic biotite granite - 1 mm to 3 mm.
Hybrid granodiorite - Commonly slightly less than 1 mm, to 2 mm.
Non-porphyritic biotite granite - Varies from 0,5 mm to 1,5 mm.
Klipberg granite - 1 mm to 2 mm.
Contreberg granite - 0,3 mm to 0,6 mm.

As shown in chapter II the first three rock types form a hybridisation sequence. The fact that they show a progressive reduction of matrix grain size with increasing hybridisation provides the best explanation of the highly involved distribution map (compare fig. 11 with figs. 1, 2, 5, 13, and 18). The young granites are finegrained and obviously responsible for corresponding minima (compare fig. 11 with fig. 3), but the general northwesterly "grain" and spotty nature of most anomalies correspond with the hybrid rock types.

2. Average maximum phenocryst lengths

While the matrix grain size may reflect emplacement conditions, phenocryst sizes are not necessarily affected by the same environmental controls, as is well shown for instance by the occurrence of quartz porphyries with small phenocrysts (Saldanha) compared with other exposures holding very large ones (Franschhoek). Phenocryst size is much more difficult to interpret than matrix grain size, since single crystal growth is controlled by complex environmental factors (Grigoriev, 1961; Chalmers, 1964). Phenocryst kernels may represent crystallisation under very different physicochemical conditions than the rest of the observed rock and may even

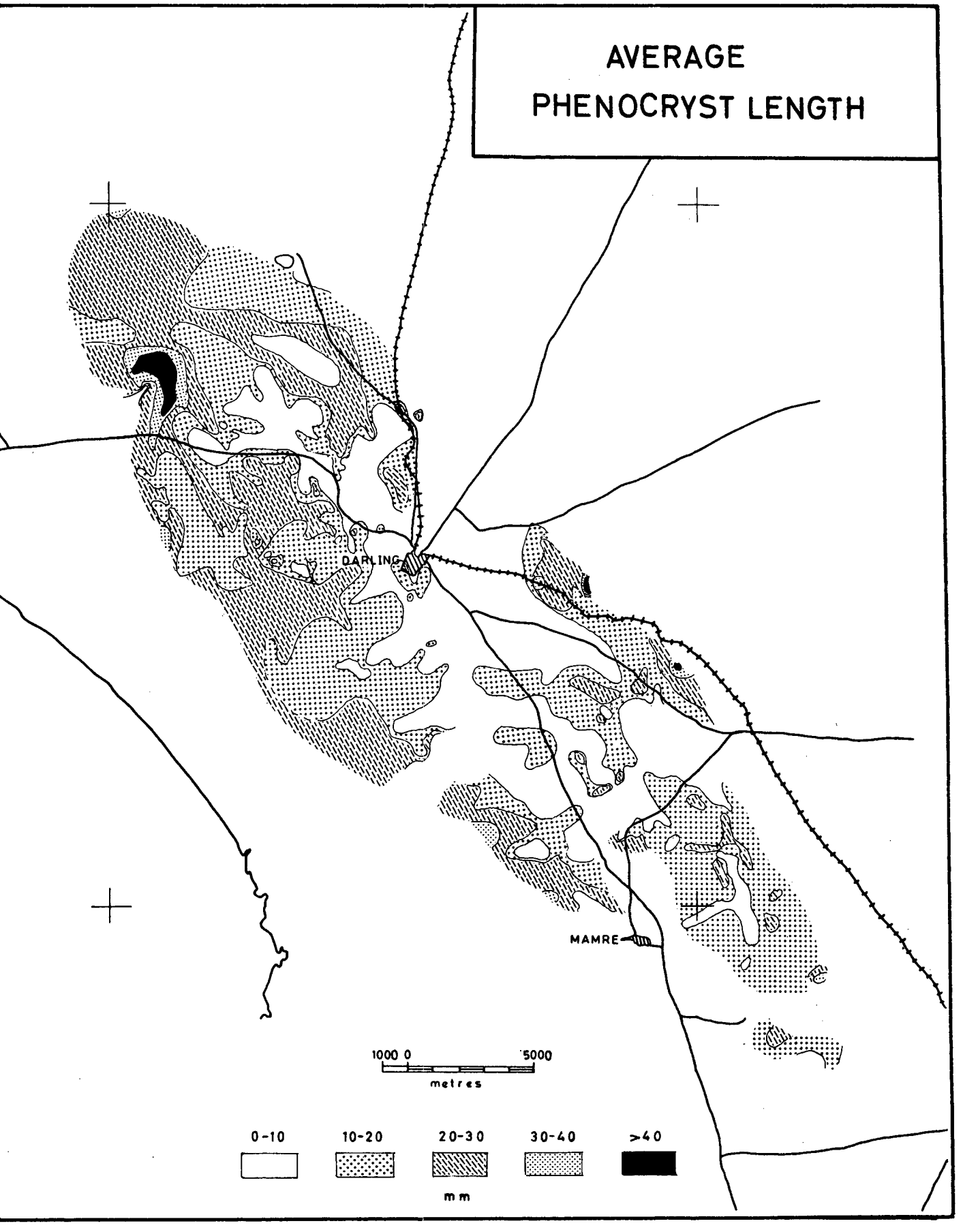

Fig. 12

be xenocrystal from parent material deep down in the crust. At some localities in the Darling batholith two or more generations of phenocrysts were observed, which creates further difficulties, but these cases were too few to be significant on the reconnaissance scale adopted here.

The average maximum lengths of abundant potash feldspar phenocrysts were measured. The relevant map (fig. 12), shows a surprising correlation with the hybridisation phenomena as well as the matrix grain size. For the various rock types the characteristics are:

Darling granite - Gradational variation from 20 mm to 60 mm.
Porphyritic biotite granite - 16 mm to 30 mm.
Hybrid granodiorite - 5 mm to 10 mm, rarely as much as 20 mm.
Non- porphyritic biotite granite - 5 mm to 15 mm.
Klipberg granite - None.
Contreberg granite - 2 mm to 8 mm.

3. Xenolith distribution density

Xenoliths are frequently seen in all the rock types except in most of the young granite exposures. The number of xenoliths larger than 5 cm in diameter in a unit surface area was counted at each observation point. In certain areas large xenoliths are more numerous than in other regions, but no systematic measurements were made of average sizes. The density of distribution correlates quite well with increasing dark mineral content (compare fig. 13 with figs. 1, 2, 5 and 18). The following variations were found:

Darling granite - 0 - 1,5 xenoliths per m^2.
Porphyritic biotite granite - 1 to 2 xenoliths per m^2.
Hybrid granodiorite - Between 1 and 3 per m^2, but up to 9 in local areas, and occasionally as high as 45.
Non- porphyritic biotite granite - Between 1 and 3 per m^2 but in local areas as high as 10.

4./

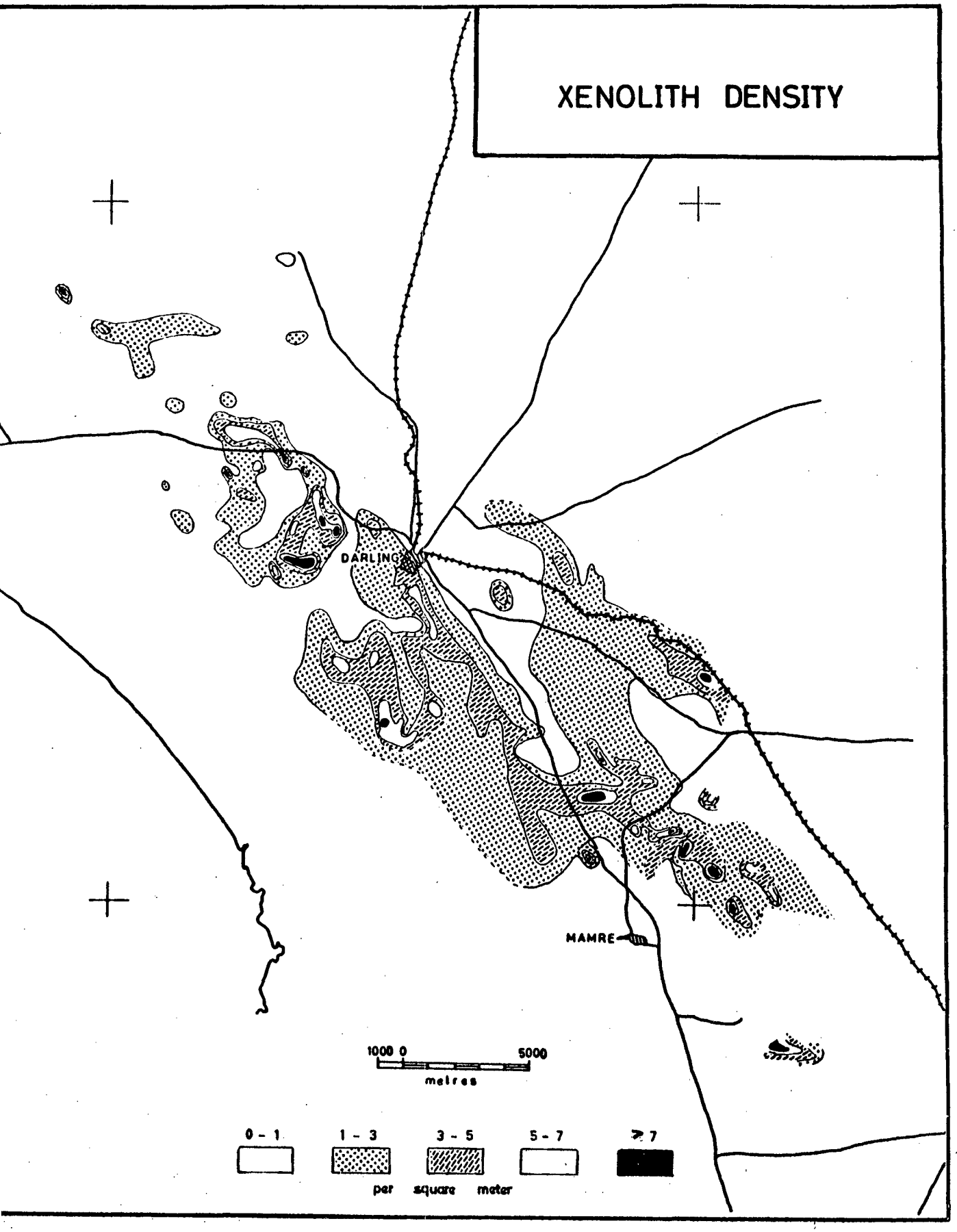

Fig. 13

4. Quartz nodules

Quartz segregations are present as small ellipsoidal augen in the granite and hybrid granite. The distribution density is shown in fig. 14. This diagram is somewhat less reliable than the others shown in this chapter because only about 300 measurements were available. The spacing between the nodules is closest in the hybrid and biotite-rich granites including parts of the Contreberg granite, averaging 1 per square metre with as many as 30 per square metre in isolated patches. The spotty pattern which emerges from the synthesis is similar to the one obtained for xenolith distribution density (fig. 13). Because the number of nodules per unit surface must be a reflection of the factors which effected nucleation of the migrating silica, the patch-like distribution probably indicates slight local differences of environmental conditions during the forming of the segregations. It is interesting to note that Carmichael (1969) recorded silica as the most mobile component during medium-grade metamorphism in pelites of the Grenville Formation, Canada. A siliceous melt phase must have been present at Darling but it is significant that the silica segregated as nodules as in metamorphic rocks rather than as veins, and that the inter-nodule distance is relatively small. This observation suggests that nodule size should be taken into account as well.

The average nodule size (fig. 15) is 5 - 10 cm but may be more than 20 cm in small areas. It is clear from a comparison of figs. 14 and 15 that a sparse distribution does not necessarily go hand-in-hand with large nodules. From this fact it can be deduced that the values of the thermodynamic variants favouring nucleation of quartz did not always coincide with those responsible for the mobility of silica.

The stress field active during consolidation of the hybrid granites would have influenced the orientation of the long axes of the nodules. This aspect was not explored fully, but fig.16

shows/

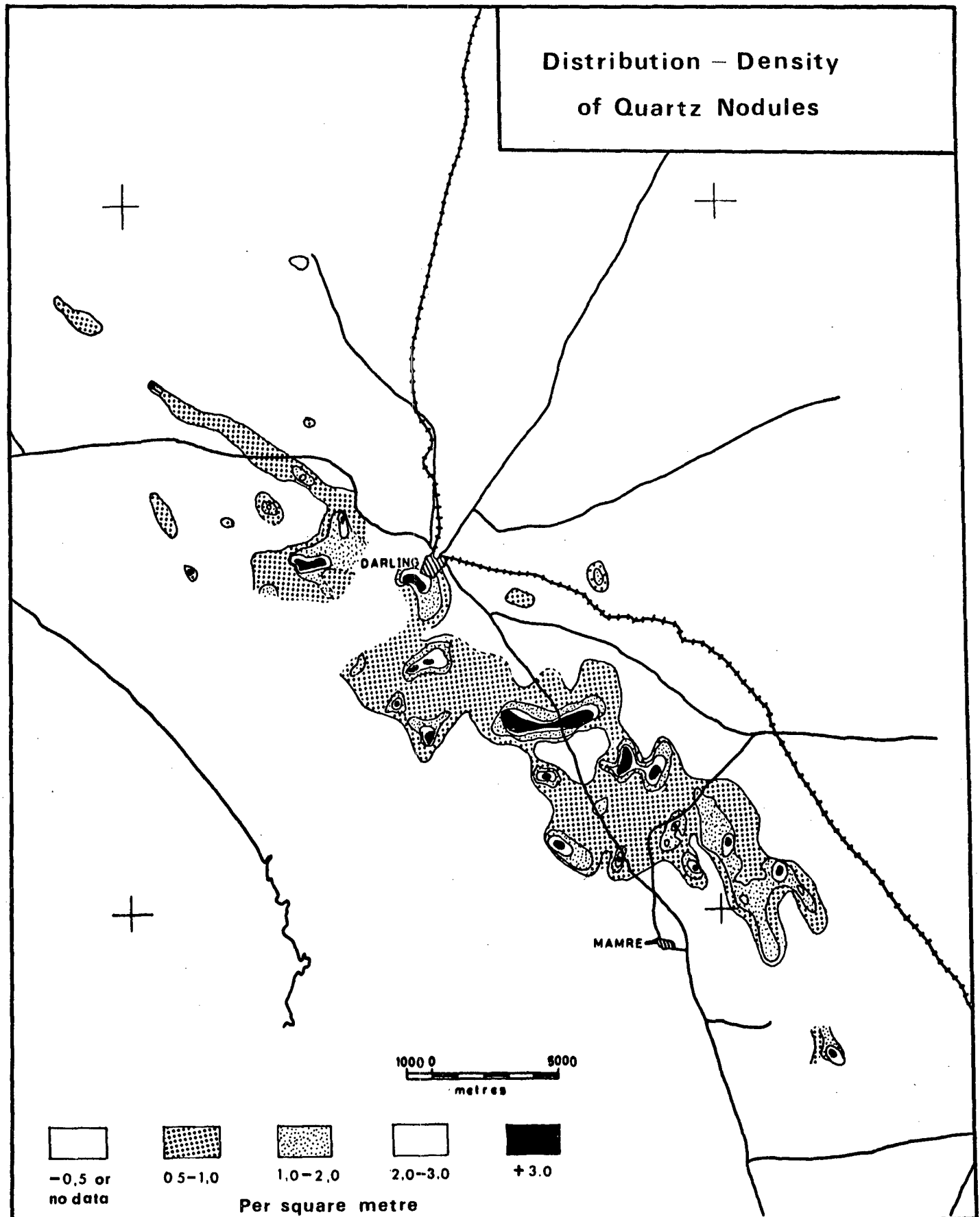

Fig. 14

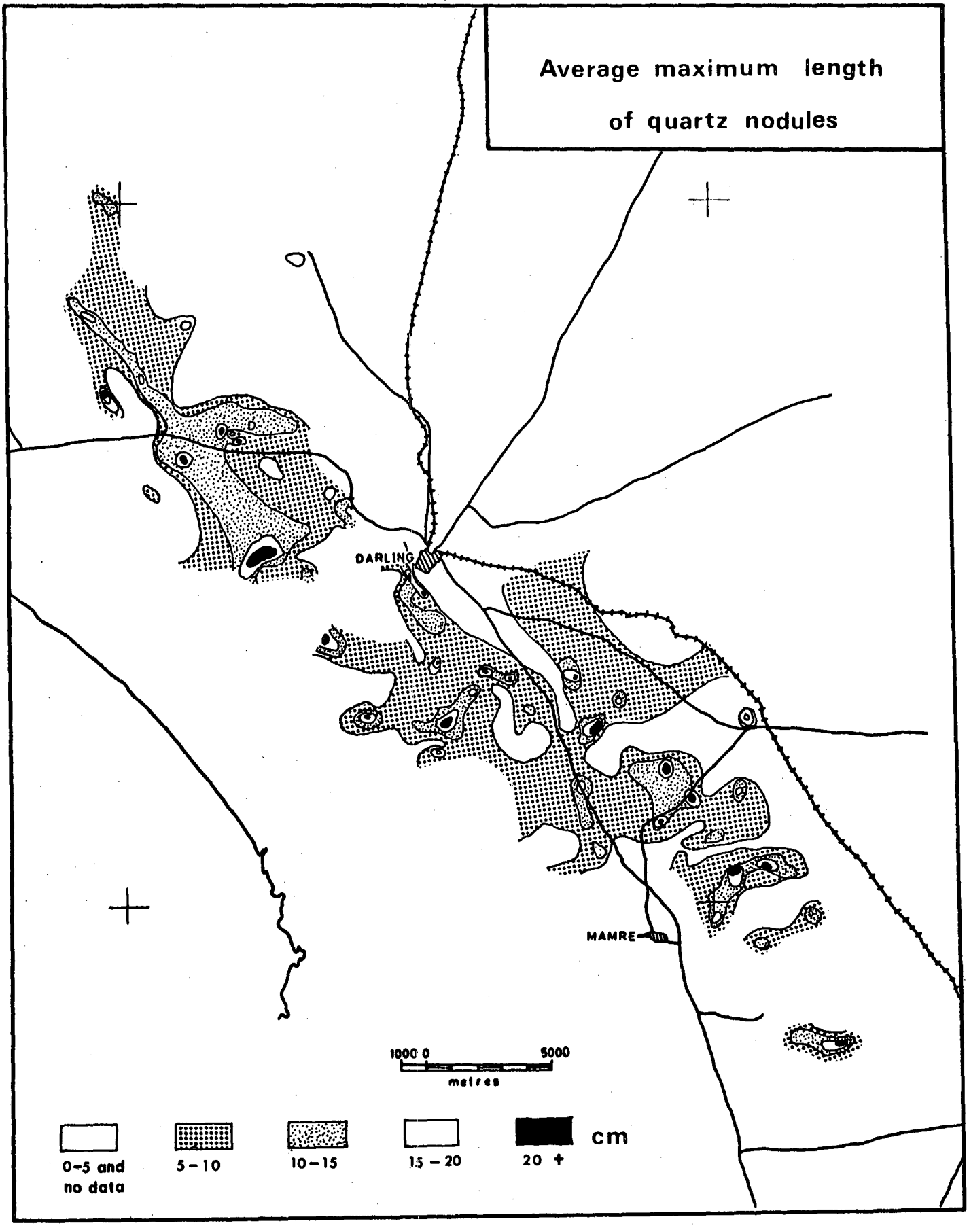

Fig.15

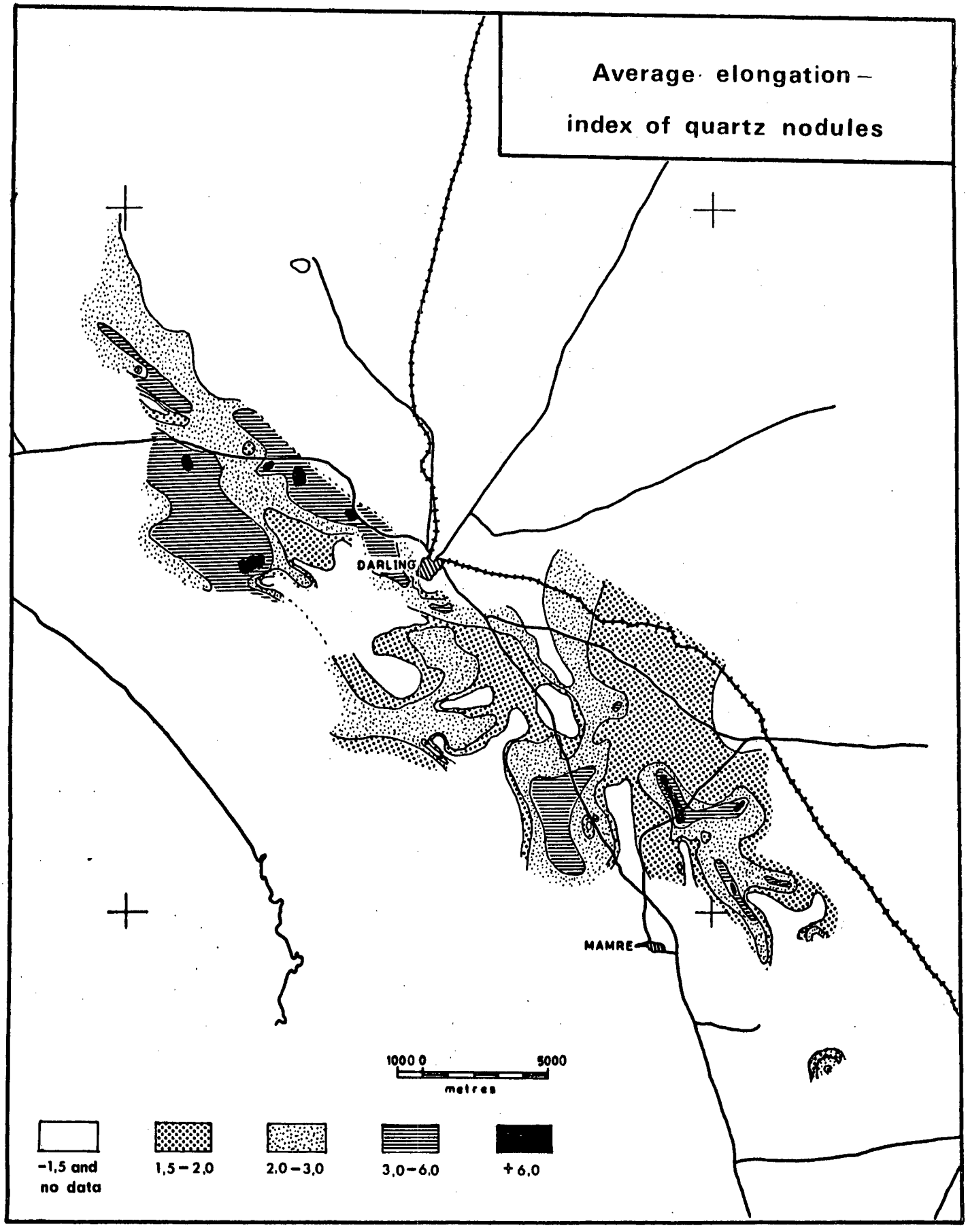

Fig. 16

shows that nodule elongation agrees very well with the north-westerly "grain" of the district, evident in most of the figures given in chapter II. Comparison of fig. 16 and fig. 19 reveals a positive correlation.

Most of the nodules are unzoned or not visibly zoned milky quartz, but many instances of isolated segregations with rims of milky quartz enclosing cores of clear or sometimes rosy quartz were recorded. Unfortunately too few observations of this aspect were made to allow determination of any possible regional variation but it would seem that zoned types are more likely to be found in porphyritic biotite granite and hybrid granodiorite than elsewhere. A future study of this phenomenon may aid in interpreting the transport and nucleation processes which took place, eg. with reference to the presence of titanium and/or manganese in rose quartz (Frondel, 1962).

5. Structure

This study was not intended as a structural investigation, but lineations were measured wherever expedient. The most conspicuous linear structure is the parallel orientation of feldspar phenocrysts. The measurement of feldspar lineation is difficult at the best of times because the crystals tend to be tabular rather than columnar. To eliminate bias on the part of the observer it is necessary to do the observations on a statistical basis, entailing stereographic construction of the linear element from readings taken on at least seven rock faces of differing orientation at each locality (Lowe, 1946; Turner and Weiss, 1963, p. 82). This method was adopted but bias was not considered to be ruled out for any specific feldspar lineation unless corroborative evidence was obtained from the measurement of the orientation of the long axes of ellipsoidal xenoliths as well as quartz segregations at the same locality. Experience showed that the quartz nodules were very reliable for this purpose.

The/

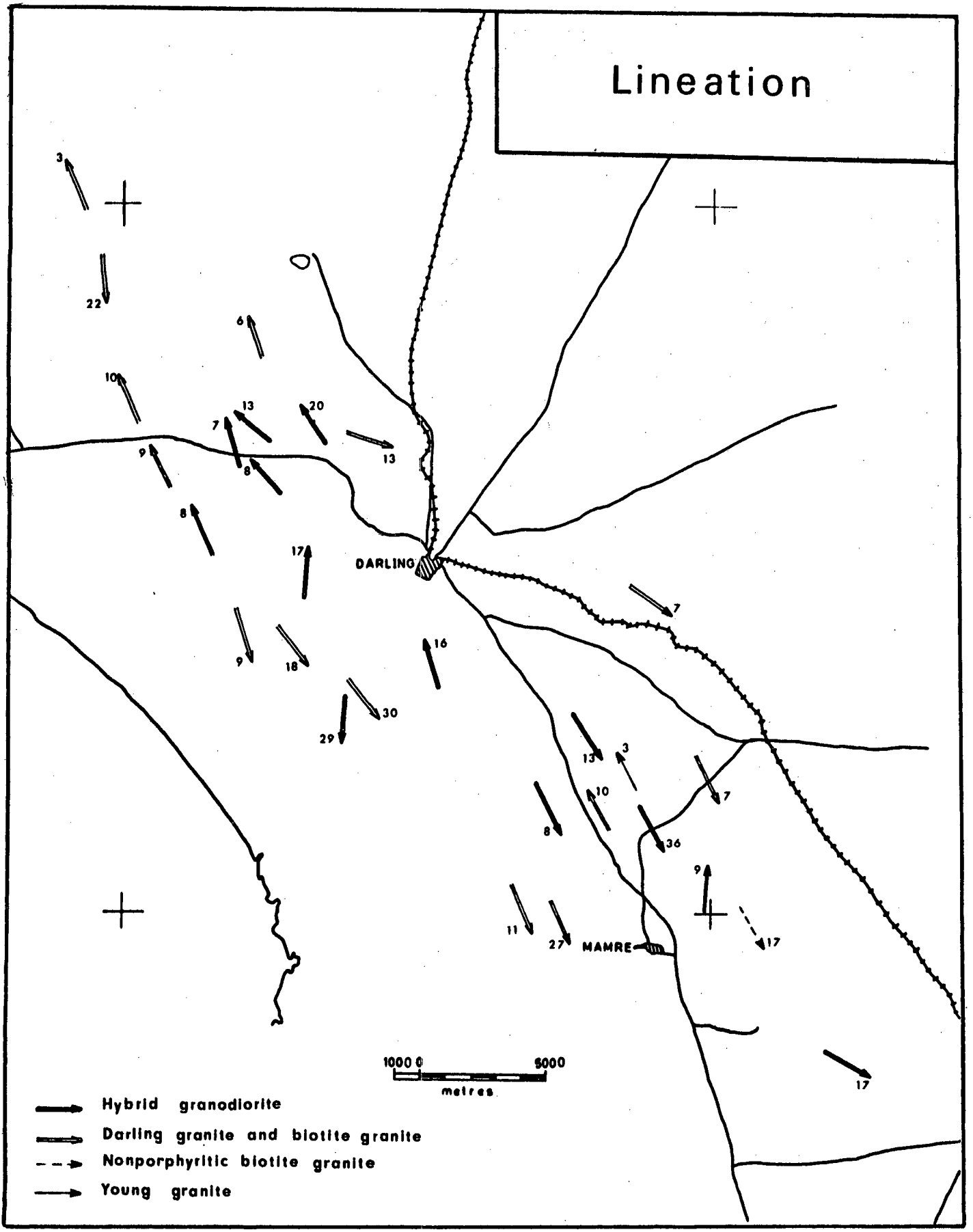

Fig. 17

The average lineations revealed by the stereograms are shown in fig. 17. It is clear that the batholith as a whole tends towards a flow line dome or arch (Cloos, 1936). This corroborates the findings of Scholtz (plate XX, 1946) which were based on only a few measurements.

6. Dark mineral index

This is one of the subjective criteria, as it was considered impractical to measure colour index quantitatively in the field. In order to minimise the personal factor it was found convenient to judge the dark mineral content on an arbitrary scale of ten divisions, which was applied wherever other readings had to be taken. Such a procedure is better than merely noting down the general appearance of the rock by comparison with observations made at other localities, and therefore subject to the vagaries of memory. Since the distribution of rock types appeared to be completely random during much of the field work and mapping deliberately did not proceed systematically from one farm to the next, the author could not possibly have anticipated the final distribution pattern.

Biotite is the principal dark mineral with negligible pyroxene, hornblende and magnetite. This parameter may therefore be regarded as approximately a biotite index. The biotite content increases together with an increase in degree of hybridisation in the Darling as well as the Saldanha batholiths, and should therefore be parallel to the trends previously discussed. The results are presented in fig. 18.

7. Gneissosity

Although not a particularly imposing feature of the Darling mass, gneissose textures may be well-developed locally, as on Burgerspost. At an early stage some relationship between mylonite development and gneissosity of the granites became apparent. Like the previous parameter this factor was arbitrarily

judged/

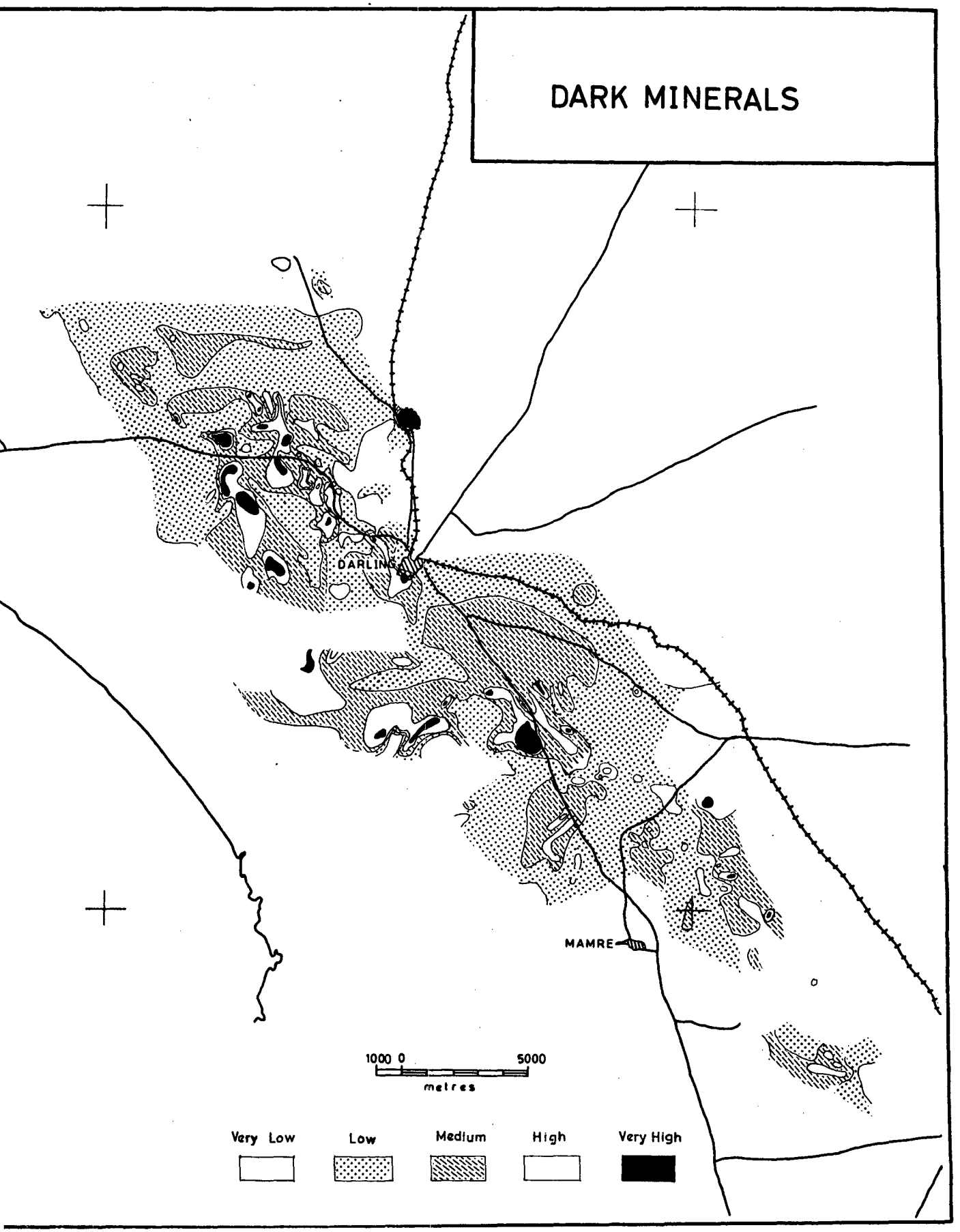

Fig. 18

judged on a scale of ten. It is of course possible to approach objective evaluation by counting the number of schistosity plane traces per unit length perpendicular to the strike, but this was considered to be too time-consuming.

The synthesis (fig. 19) is surprising to say the least. Although the mylonite bands are interrupted and even arranged en echelon in some regions, comparison of figs. 19 and 6 shows that there is always a continuation on strike in the form of a gneissose band. The pronounced northwesterly trend, parallel to the large Colenso fault, is particularly striking. Some suggestion of transverse faulting is also present.

8. Amount of feldspar phenocrysts

The percentage of phenocrysts was estimated visually at numerous localities. The resulting contour map (fig. 20), shows the same northwesterly trend encountered in the previously discussed diagrams. The high percentage of small phenocrysts in the Contreberg granite contrasts markedly with the absence of insets in the Klipberg granite.

9. Dassen Island

The grain size variation of the Dassen Island granites is shown in fig. 9. The grain size of the fine-grained nodular tourmaline granite varies serially between 0,5 and 2,0 mm , but reaches values as high as 3,5 mm in local areas. The average matrix grain size of the coarsely porphyritic granite is greater than that of the fine-grained granite.

The size of the tourmaline nodules varies serially from 5 to 20 mm in the eastern and northwestern parts of the island, but becomes as much as 30 mm in the southeastern corner (fig.21). In the western areas however, the nodules are larger, usually varying between 20 and 50 mm, with a maximum of 90 mm at one locality near the central beacon north of the light-house. The figures quoted are for the nodules themselves, the leuco-

cratic/

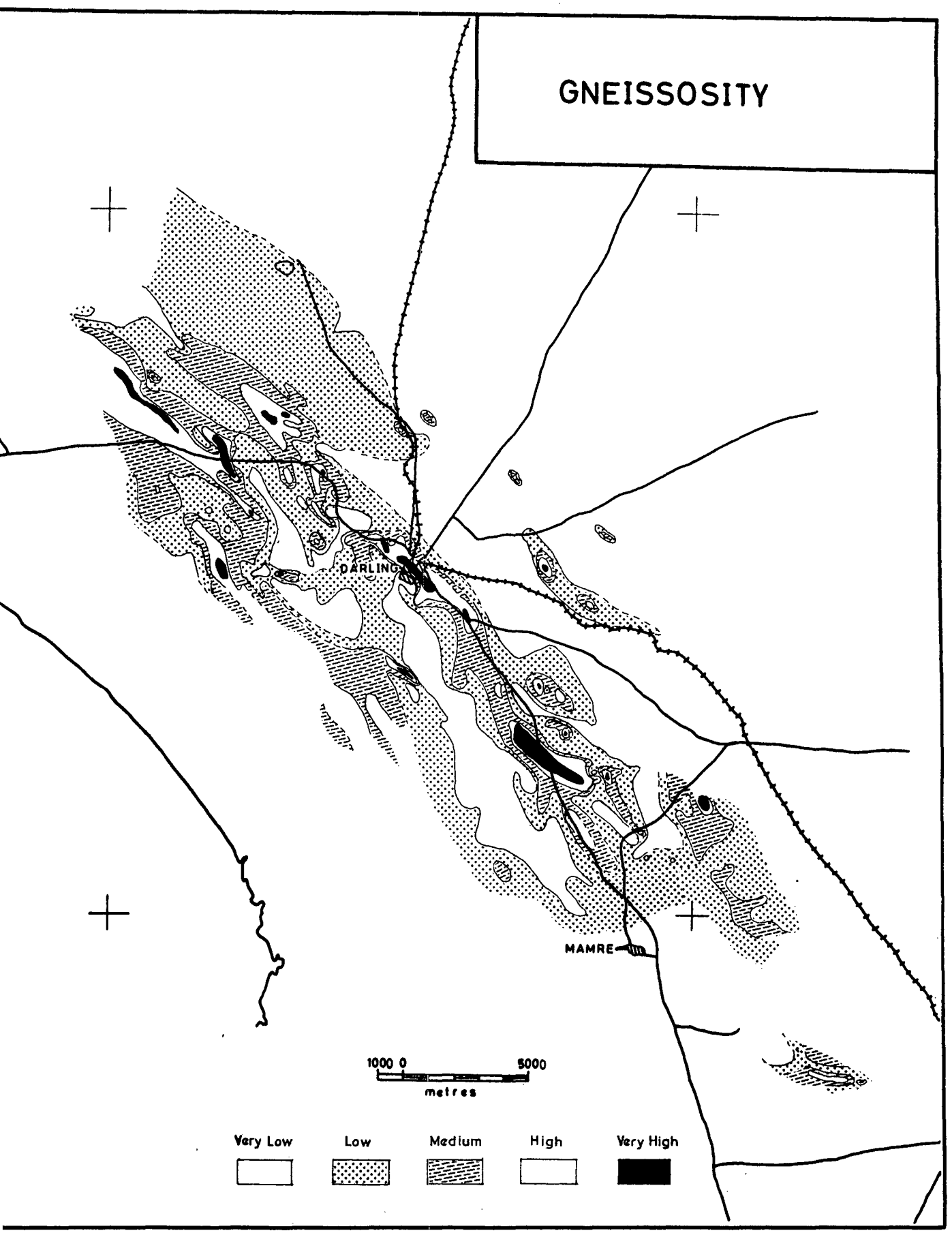

Fig.19

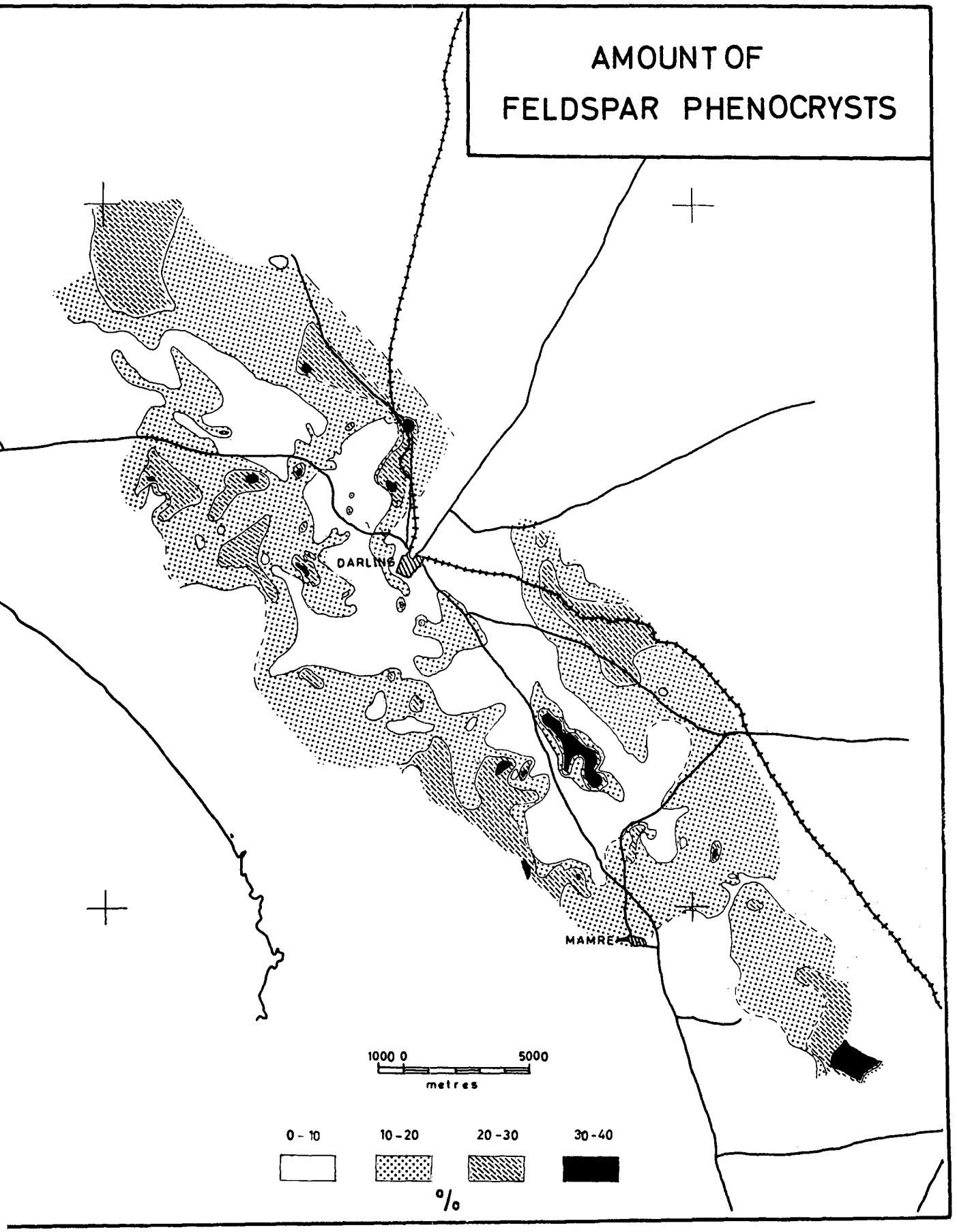

Fig. 20

cratic borders being excluded. Usually however, the light-coloured rims are not conspicuous. In a few rare instances sparsely distributed nodules of large size are present in granite with a dense population of smaller ones, the firstmentioned invariably showing well-developed leucocratic rims.

The average distance between nodules varies nearly but not quite sympathetically with their size (fig. 21). For the east and north-west the distance was measured at between 10 and 30 mm, with a maximum of 60 mm in the southeastern corner, but it increases gradually up to more than 100 mm in the west, where as much as 200 mm was recorded in a local area not exactly coinciding with the occurrence of the largest nodules.

The deviation from a sympathetic relationship between nodule sizes and inter-nodule distances is revealed when a ratio map is constructed (fig. 22a). The nodules in the coarsely porphyritic granite of the south-west are much more widely spaced (spacing 6 - 7 times size) than in the corresponding fine-grained granite (spacing 1 - 1,5 times size, gradually increasing to a ratio of 2 in some areas). Distances of diffusion towards nucleation centres depend on small local variations of temperature, pressure, oxygen fugacity and other environmental factors. This could explain the variation in inter-nodule distances and their independence of nodule size.

It is possible to construct another map from the data in figure 21 showing nodule content as a percentage, the values of which will be proportional to the actual tourmaline content of the granite. The individual nodules hold up to nearly fifty percent schorl, which replaces earlier formed minerals. From figure 22c it is evident that the granites under consideration have exceedingly high volume percentages of tourmaline. The coarsely porphyritic granite of the south-west holds less tourmaline than the fine-grained granite, since the average nodule content is 20% for the former and 40% for the latter. A very interesting observation is the presence of areas with relatively

high/

DASSEN ISLAND

Tourmaline nodules

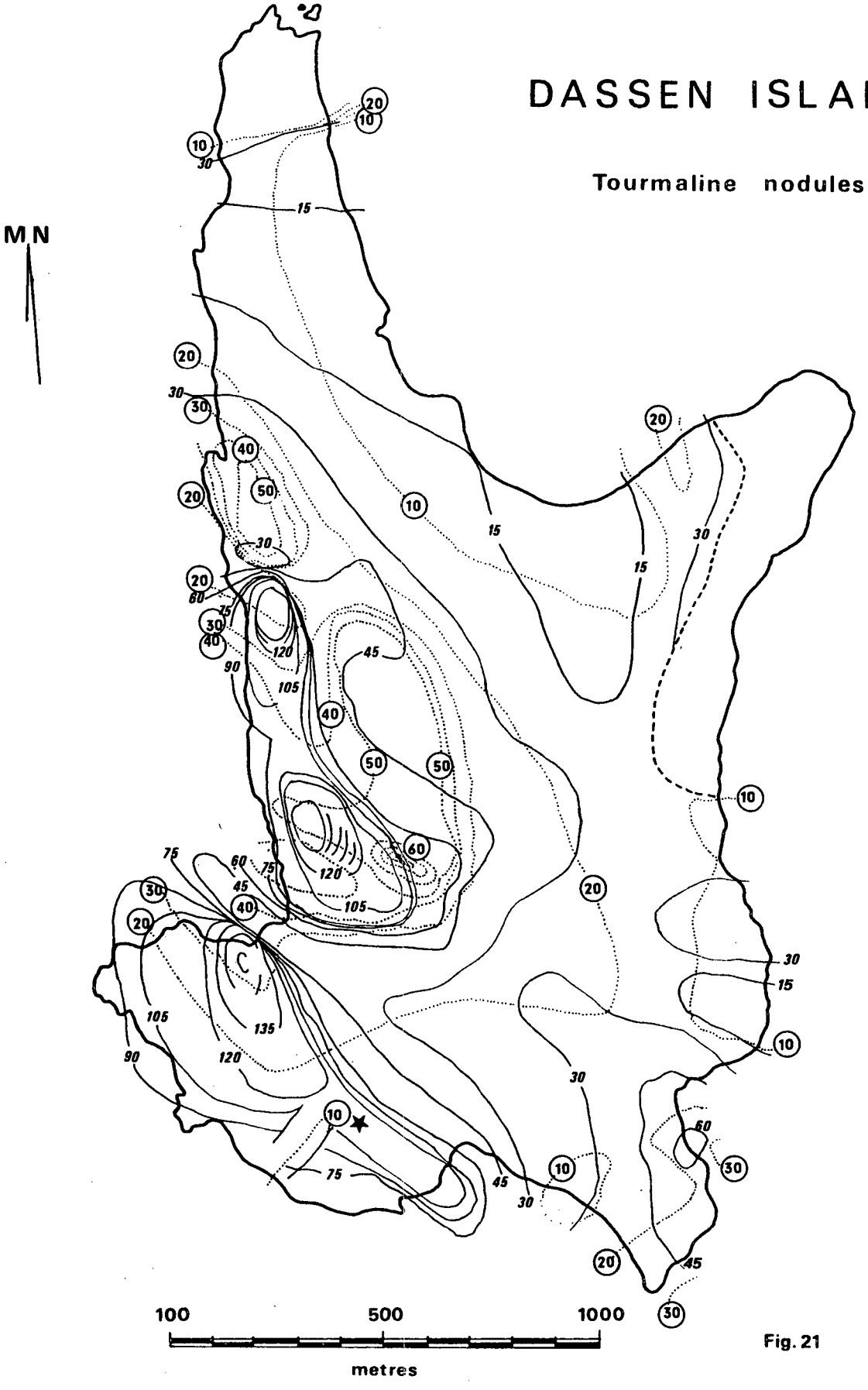

Fig. 21

No tourmaline nodules

Diameter of tourmaline nodules, mm (excluding leucocratic borders)

Distance between tourmaline nodules mm

high tourmaline content within the fine-grained granite. Two small lows are present on the west coast and one on the east coast, while as many as three highs may be present adjacent to the lows in the west.

The matrix grain size, which is usually a function of cooling rate during genesis, is not sympathetic with tourmaline content (fig. 22). The fine-grained granite is richer in tourmaline than the coarse granite, while the tourmaline content and relative nodule sizes with respect to grain size shows a spotty distribution. Taking all these facts into consideration it is concluded that we are dealing with the products of

(i) a late segregation process and/or
(ii) local additions of boron.

It is therefore possible that some of the boron was obtained from metasediments by means of assimilative reactions, a process which would have aided the formation of local enrichments of boron-rich liquids in the terminal stages of consolidation. The thermodynamics of supercritical boron-alkali-bearing liquids would seem to be a fruitful subject which still awaits laboratory investigation.

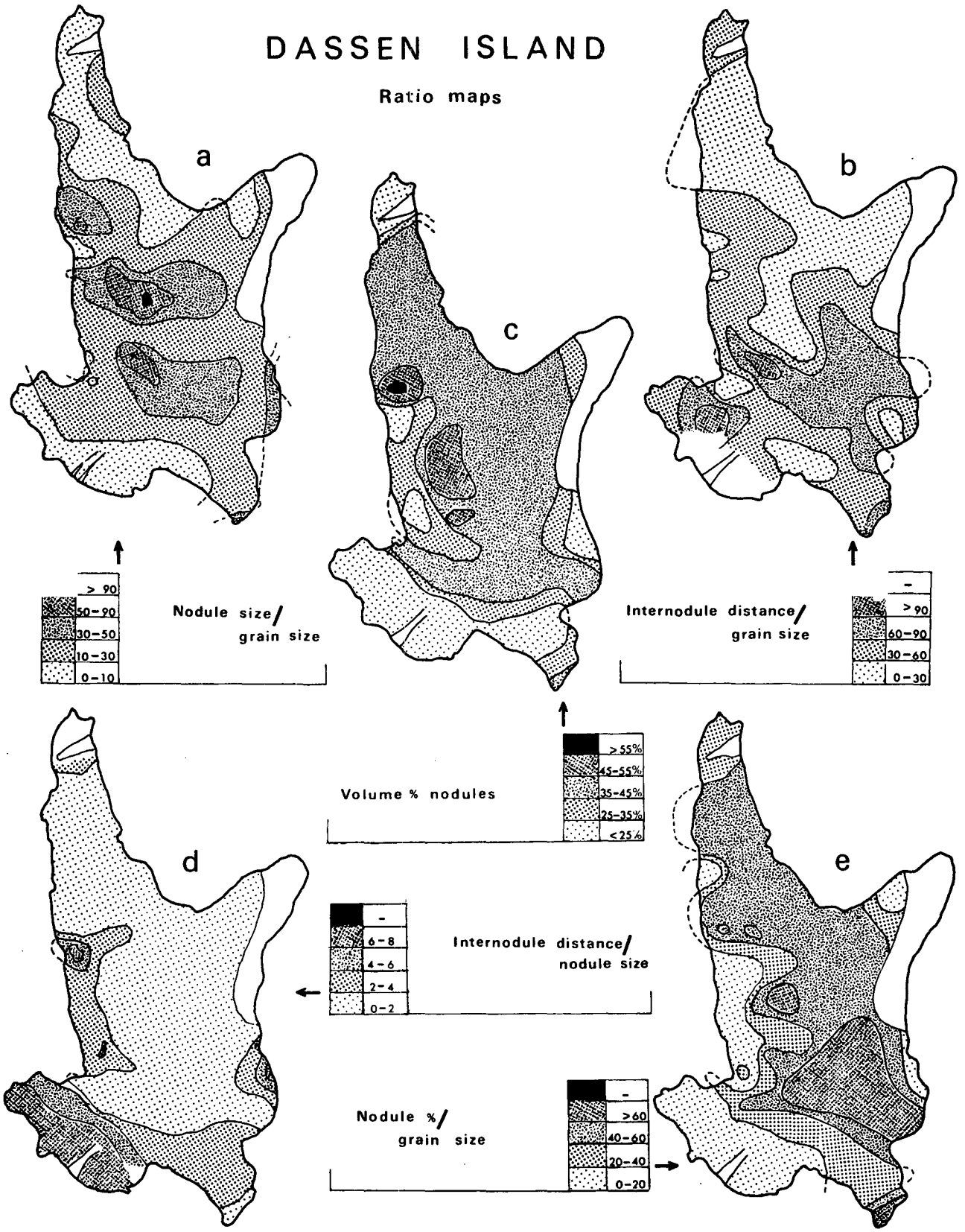

Fig. 22

IV PETROGRAPHY

This thesis deals mainly with the regional aspects of a complex batholith. Therefore only those petrographical aspects were investigated which could be useful in the broad context. The average properties of the various mapping units are discussed below with special emphasis on the hybridisation phenomena.

1. Darling granite and porphyritic biotite granite

The Darling granite is characterised by large microcline microperthite and microperthite phenocrysts, the perthitic segregations being of the types known as rods and strings (plate IV,3). Inclusions of andesine, (An_{32}), and sometimes biotite or its chloritised product, are frequently present in these crystals. The plagioclase is markedly zonal, resorption and repair structures occasionally being evident, but with the normal continuous type predominant (plate IV, 1,2). The cores are andesine (An_{33}, but sometimes as basic as An_{40}) with the broad mantles grading towards oligoclase (An_{20}) and followed by narrow oligoclase albite rims. Saussuritisation of the more anorthite-rich cores and mantles varies from slight to extreme. The quartz of the granite exhibits the familiar strain extinction and mosaic structures with sutured contacts between adjacent grains. The biotite crystals are large and intensely pleochroic in redbrown, holding numerous inclusions of zircon with attendant pleochroic haloes. Cordierite is sometimes present, but is usually severely pinitised (plate II), grading towards large muscovite flakes on the borders of crystals. Apart from cordierite, the most important accessory minerals are apatite and clinozoisite ($2V_{\alpha} = 85°$).

In certain areas of Darling granite fairly narrow bands of northwesterly orientation are characterised by gneissic texture, as for instance near the northeastern border of the batholith, particularly on Hill Side and Burgerspost, and in the south-

western/

western portion of the mass, as on Grootberge and Grootwater. The conclusion based on fieldwork that these gneissic bands form part of the deformational suite including the mylonite zones (chapter III) is corroborated by the microscopic study, since unmistakable signs of considerable cataclasis are always present. Although tartan twinning is not conspicuous in the alkali feldspars of the undeformed samples, it is particularly striking in the cataclastically affected microcline microperthites. The strained mosaics of quartz have a much smaller average grain size than in undeformed granite, and have bands of more intense cataclasis marked by mosaics with a shredded appearance. The biotites show kink banding as well as a tendency to develop "neurocytal" structures, (i.e. resembling the shape of multipolar nerve-cells with their attendant dendrites), and are in addition much chloritised. The plagioclases are much saussuritised and sometimes exhibit deformed twin lamellae. The chloritisation of biotite and saussuritisation of plagioclase can not be interpreted as indicative of cataclasis only since the same effects were also observed in undeformed granite, although less often. This is of course to be expected since the same effects can result from deuteric alteration as from low-grade adaptations typical of the greenschist facies caused by dynamic metamorphism. However, the rarity of these features in normal granites does indicate relatively dry conditions with deviations of only local importance, and it is interesting to note that several petrologists of standing (eg. Brown and Fyfe, 1970) are today of the opinion that "granitic liquids are not generally water saturated", in contrast with the classical viewpoints (eg. Tuttle and Bowen, 1958).

2. Hybrid Granodiorite

The average hybrid granodiorite consists of the following minerals, if the numerous xenoliths and quartz segregations are not taken into account:

Plagioclase (Andesine). Zoned from An_{51} to An_{23}, but through only 6-7 end member percentage units per individual crystal.

Cordierite/

Cordierite. Always pinitised on the edges and frequently completely replaced (plates I and III).
Biotite. Pleochroic in deep red-brown.
Quartz.

Accessory minerals include muscovite, apatite, garnet, zircon and occasionally brownish green tourmaline. Garnet is sometimes locally a major constituent, as in the outcrops to the south of the town of Darling on the farm The Towers, and on the northern flank of Kapokberg. Since the hybrid granodiorite grades towards porphyritic biotite granite, varieties were also encountered which hold large crystals of microperthite and microcline microperthite, and of which the matrix is more coarse-grained than usual. The pinite is very fine-grained and passes gradationally into large muscovite flakes (plate I). Occasionally two distinct types of pinite, zonally distributed around the cordierite cores, can be distinguished under the microscope (plateII). The plagioclase is saussuritised to a varying degree but is commonly relatively unaltered.

Modal analyses indicate that the mineralogical composition of the hybrid granodiorite varies between the following limits in volume percent:

Quartz	28 - 36		
Biotite	24 - 35		
Plagioclase	17 - 23		
Cordierite	2 - 6	7 - 9	8 - 15
Pinite	2 - 6		
Muscovite	1 - 7		
Potash feldspar	0 - 3		
Garnet	0 - 4		
Apatite	0,2		

These rocks may therefore be described as biotite-cordierite granites (or -adamellites or -granodiorites, cf. chapter VI).

3./

3. Xenoliths

Xenoliths of various kinds are relatively concentrated in the hybrid granodiorite with respect to the other Darling rock types.

(i) Quartzitic metagraywacke

This is the predominant type of xenolith. Although the texture is not notable in handspecimen, it is markedly foliated in thin section owing primarily to the highly directed nature of the biotite flakes. The mineral composition is quartz, biotite, and plagioclase (andesine) with accessory pyroxene (usually augite but occasionally diopside), apatite, muscovite, garnet, chlorite and magnetite. The grain size varies from 0,05 to 0,24 mm, but is nearly constant in individual specimens (plates VI and VII).

(ii) Amphibole-bearing xenoliths

In handspecimens these rocks are very similar in appearance to the quartzitic metagraywacke. The constituents are hornblende, biotite, quartz, andesine-labradorite and magnetite with accessory epidote and apatite.

(iii) Lime-rich xenoliths

The minerals are diopside, microperthite, sphene, plagioclase (zoned andesine), calcite and sometimes quartz with accessory chlorite, serpentinous alteration products of diopside, and saussurite (plate VIII). A typical mode (in volume percentage) is as follows:

Microperthite	Diopside	Plagioclase	Calcite	Sphene	Chlorite	Apatite	Others
38,0	37,7	9,5	9,2	2,0	1,0	0,7	2,0

A sample which was chemically analysed (table 4, analysis 13) can not be regarded as typical; it has the following mode:

Quartz	"Chlorite"	Plagioclase	Diopside	Sphene	Calcite
43	21	18	14	1	1

(iv)/

(iv) Spotted lime-rich xenoliths

These rare rock types consist of poikiloblasts of diopside with sphene, set in a matrix of plagioclase, quartz and calcite.

The association of calcite and quartz with only a thin intervening diopside rim in many lime-rich xenoliths (plate VIII), indicates a disequilibrium condition which may be due only to the timely congealing of the surrounding magma. However, many xenoliths are enveloped by a pegmatoid product, notably on the farms Alexanderfontein and Bonteheuwel, indicating that the release of CO_2 stimulated abnormal crystallisation in the enveloping granite. These pegmatoid rims are granitic, but hold diopside and sphene in addition to microperthite, quartz and plagioclase.

4. Young granites

The young granites are characterised by typical granitic mineralogy. Microperthite and microcline microperthite are present mostly as small phenocrysts except in the Klipberg granite, and where they have the same grain size as the rest of the constituents. Quartz and oligoclase-andesine are abundant. The plagioclase is commonly much saussuritised, and the biotite which is occasionally abundant as in the Contreberg granite, is chloritised to a large extent. Augite with hornblende rims illustrating a Bowen reaction was observed in significant amounts only in some of the dykes near Mamre. The accessory minerals of the young granites are apatite, green to bluish green tourmaline, zircon, magnetite and rarely, sphene and epidote.

The Klipberg granite is even-grained and the texture can best be described as aplogranitic, if it is realised that this intrusive is traversed by numerous aplite veins as well. In the Contreberg granite textures were often encountered which are indicative of crushing (perhaps protoclastic in part), and myrmekitic intergrowths are common.

The Dassen Island granite is remarkable for the preponderance

of/

of tourmaline nodules, but in the aplogranite veins on Bonteberg tiny tourmaline needles are also ubiquitous.

5. Non-porphyritic biotite granite

This division was instituted as a mapping unit because it proved impossible in the field to distinguish between biotite-rich varieties of the younger granite, and biotite-rich even-grained material which holds less xenoliths than the hybrid granodiorite, and weathers more readily. As can therefore be expected the non-porphyritic biotite granite exhibits a mixed mineralogy, on the one hand often approaching that of the younger granites, but on the other hand resembling the hybrid granodiorite. The minerals recorded are quartz, cordierite with pinite rims (occasionally completely pinitised), biotite (plate V), microperthite and microcline microperthite, with accessory apatite. It is interesting to note that evidence of cataclasis was often observed under the microscope.

6. Mylonite:

The various mylonite bands of the Darling area are all orientated northwesterly, and are mostly mylonites sensu stricto, ultramylonites and streaky granular mylonites (Schoch, 1962, fig. 9), but they also encompass a wide variety of crushed rocks. The microfragmental matrix often has an average grain size of one micron and smaller (plate IX). The ratio of matrix to augen varies widely, but the familiar neurocytal structures are always evident, being particularly noticeable owing to a pervading dust of pleochroic fragments and related alteration products. In most instances very little recrystallisation has taken place, with the exception of some of the bands near the Colenso fault which display considerable reconstitution (the β - γ grades, op. cit., p. 625). It is known that mylonitisation can cause a rise of more than 100° C in the prevailing temperature (P.H. Reitan, 1968), and the present study disclosed that the dynamic metamorphism generated lowgrade adaptations which belong in the greenschist facies. The biotite has been

extensively/

extensively chloritised and most of the plagioclase augen much saussuritised, while clinozoisite crystals have often grown in the microfragmental matrix. Younger veinlets holding undeformed alkali feldspar, green biotite and clinozoisite occasionally traverse the crushed materials.

Most of the mylonites were clearly derived from Darling granite and the related porphyritic biotite granite if the mineralogy of the crushed rocks are considered, particularly the preponderance of large microcline microperthite augen. The mylonite on the Colenso fault at Hartebeesvlei must, however, originally have been a fine-grained granite and could represent deformed young granite. In some examples of intense cataclasis near the town of Darling previous authors have interpreted the products as the mylonitised equivalents of coarsely porphyritic quartz porphyry (Scholtz, 1946, plate XV, figs. 2 and 4; Schoch, 1962, p. 740). The only new evidence offered here includes the distribution of the mylonite (map, folder) and a new chemical analysis (table 4, no. 3). Another new analysis, viz. of the mylonite at Trekoskraal in the Saldanha batholith (Schoch, 1962) is included for comparison. (This mylonite developed from the coarsely porphyritic Hoedjies Point granite, and the sample analysed and reported in 1962 was too small to be representative of a coarsely porphyritic granite, an error of judgment which has now been rectified. The sample from Darling was traversed by numerous quartz veins , a few mm in width, which were removed by handpicking after the primary crushing during preparation of a representative powder for analysis). The author thinks the possibility that this rock was originally a quartz porphyry must at present be regarded as remote, since this particular band occupies a central position in the batholith and because no other dykes of quartz porphyry were encountered in the area studied, except some of the apophyses from the Klipberg granite.

The mylonites provide strong petrographic evidence for a periodic recurrence of deformation. The first mylonitic

fragmentation/

fragmentation produced grains with an average diameter of 0,003 mm, enveloping porphyroclasts of 0,08 to 0,32 mm. A superimposed macrofragmental crushing visible on weathered surfaces at Wildschutsvlei and Droëvlei, is clearly later since it traverses all structures of the mylonite, and yields fragments which range in diameter from 0,05 to 2,12 mm as determined under the microscope, but with pieces as large as a few cm being discernible megascopically. This can only be interpreted as a later recurrence of the forces which caused cataclasis in the Darling batholith, possibly more than twice, and corroborates observations made on the better exposed mylonites in the Saldanha batholith (op. cit.).

V PETROGRAPHIC MINERALOGY

1. Microcline

The microcline of the microperthite in both the Darling and the younger granites is maximum microcline exhibiting obliquities near 1,0 when calculated according to $\Delta = 12{,}5\ (d_{131} - d_{1\bar{3}1})$ after Goldsmith and Laves (1954). A typical example from a sample of Contreberg granite and determined by high resolution X-ray diffractometry, yielded a value of $\Delta = 0{,}9750$.

2. Biotite and chlorite

The average refractive index of the biotites is $\beta = 1{,}642$ but as is well known, the optical properties give no indication of the chemical composition. The pleochroism is α, γ = red-brown to deep red-brown, β = brownish yellow to pale yellow.

It was considered important from the petrogenetic viewpoint to determine the composition of the biotite and therefore an attempt was made to prepare clean biotite concentrates for X-ray investigation. It is very difficult to separate biotite from chlorite. The best result that could be obtained on a powder of Contreberg granite by a combination of the Frantz isodynamic separator and an electrostatic drum separator, was a product with 6 volume percent chlorite, and 94 percent biotite. The grain size varied between 85 and 100 mesh A.S.T.M. and the chlorite content before separation was 18 percent. In order to obtain a still cleaner biotite concentrate, handpicking was essential, and this time-consuming task was undertaken for one sample. In most cases however, study by X-ray diffraction on the mixtures yielded satisfactory results.

As can be seen from table 2 the biotites of the Contreberg granite, hybrid granodiorites and the Darling granite closely resemble the synthetic $2M_1$ phlogopite of Yoder and Smith (1956). Selected diffractometer traces are shown in figure 23.

According/

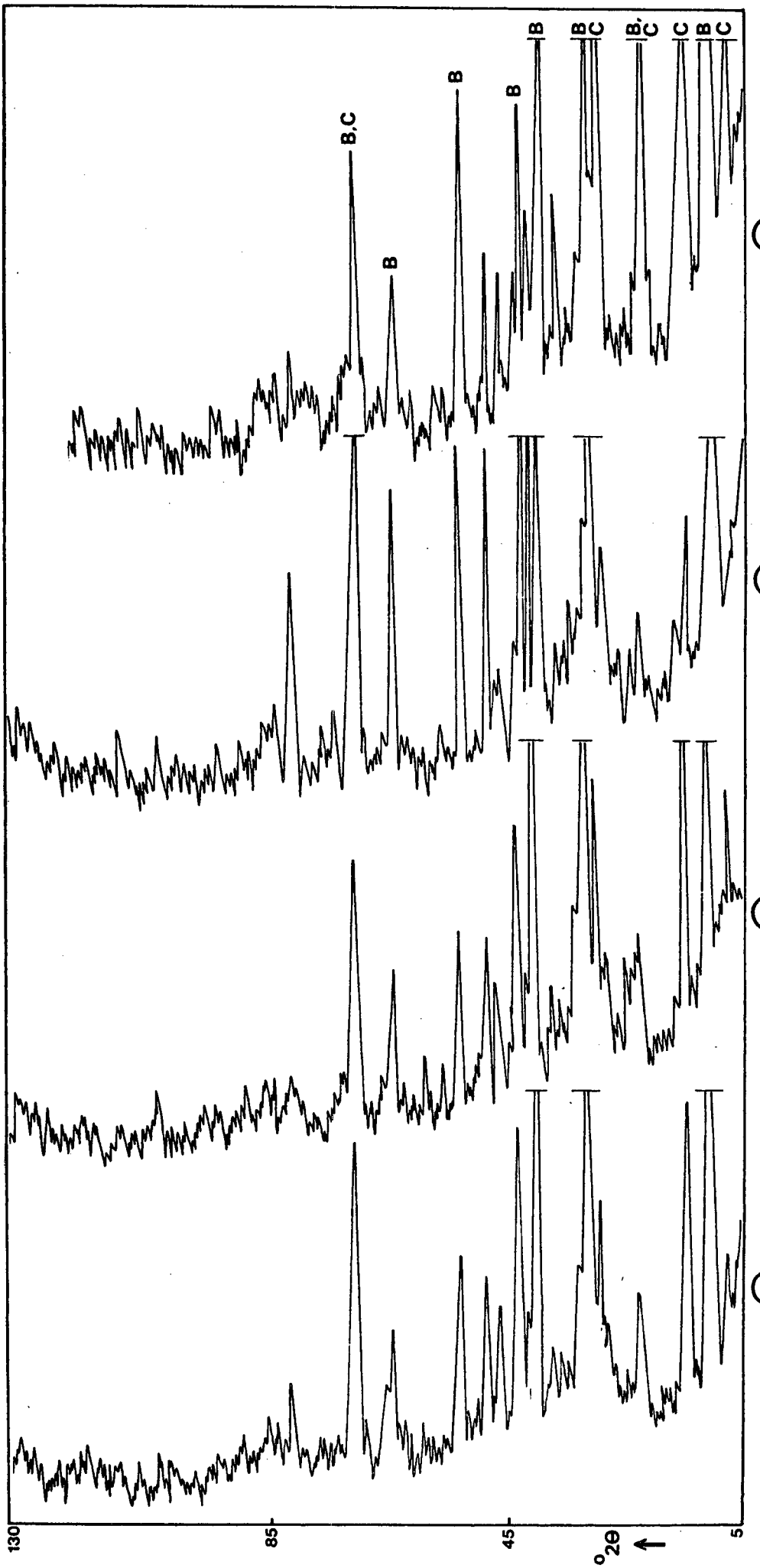

Fig. 23

According to many authors it is not possible to distinguish 1M and 3T micas by powder methods, but the 2M types can often be recognised, and the Darling micas resemble the available data for 2M phlogopite much more closely than the 3T and 1M patterns. There are exceptions in the case of some (00ℓ) back angle reflections which are closer to 1M positions when the observed d-values are compared with those calculated by the author from the published lattice parameters for Smith and Yoder's phlogopites, and for biotite and lepidomelane (A.S.T.M. Powder diffraction file, 1970), but the ambiguity is most likely due to inaccuracy of the parameters assumed. The calculations are easy if it is realised that the general formulae for monoclinic and trigonal lattices, which are respectively

$$d_{hk\ell} = \frac{1}{\sqrt{\dfrac{\dfrac{h^2}{a^2} + \dfrac{\ell^2}{c^2} + \dfrac{2h\ell}{ac}\cos\beta}{\sin^2\beta} + \dfrac{k^2}{b^2}}} \quad \text{and} \quad d^2_{hk\ell} = \frac{1}{\dfrac{4(h^2 + hk + k^2)}{3a^2} + \dfrac{\ell^2}{c^2}}$$

(Azároff and Buerger, 1958, p. 83, 89; Azároff, 1968; Nuffield, 1966), reduce to $d = \frac{c \sin\beta}{\ell}$ and $d = \frac{c}{\ell}$ for the special case of (00ℓ) reflections.

Fig. 23

DIFFRACTOMETER TRACES OF SELECTED BIOTITE-CONCENTRATES

(Co K_α radiation, Fe-filtered)

(1) Biotite + 11% chlorite, sample no. 7, table 4, Contreberg granite.

(2) Same as (1), biotite hand-picked.

(3) Biotite + chlorite, sample 12, table 4, hybrid granodiorite.

(4) Biotite + chlorite, sample 1, table 4, Darling granite.

C = Chlorite peak B = Biotite peak

From left to right the indices of the marked peaks are:
C(001), B(002), C(002), B(110,020) + C(003), C(004), B(006), B(116), B(133), B(137), B(153), B(330,060) + C(060).

Table 2/

TABLE 2

d-Values of biotite from the Darling batholith (Co K_α radiation, Fe-filtered).

$2M_1$ Phlogopite, Yoder and Eugster, 1954 Yoder and Smith, 1952	7 Biotite Contreberg Granite	12 Biotite Hybrid Granodiorite	1 Biotite Darling Granite
10,13 (100+) 5,056 (25) 4,612 (20)	10,11 (100+) 4,61 (15)	10,16 (100+) 4,61 (15)	10,11 (100+) 4,75 (55)(+ chlorite?)
3,814 (20) 3,540 (35) 3,362 (100)	3,54 (15?)(+ chlorite) 3,35 (100)	3,54 (15) 3,36 (100)	3,37 (100+)
3,283 (40) 3,040 (40) 2,818 (20)			2,83 (15)
2,651 (20) 2,624 (100) 2,522 (30)	2,63 (60) 2,51 (15?)(+ chlorite)	2,63 (70) 2,51 (40)	2,63 (25) 2,52 (20)
2,439 (40) 2,180 (45) 2,039 (20)	2,44 (30)	2,44 (30) 2,18 (20)	2,45 (30)
2,017 (65) 2,000 (20) 1,677 (45)	2,01 (20) 1,67 (15)	2,02 (40) 1,68 (20)	2,00 (30) 1,68 (15)
1,538 (50)	1,54 (25)	1,54 (30) 1,44 (25) 1,36 (20)	1,54 (20)
		1,26 (15)	

It is concluded that most of the Darling biotites are of the $2M_1$ polytype. The nomenclature of mica polytypes is in a state of flux at present and vector stacking symbols (the modified Ross-Takeda-Wones symbols) are superior to the Yoder-Smith symbols (Takeda, 1971), but this is not important for the data here presented, in view of the rarity of micas with very large unit cells. The author is also convinced that most of the common polytypes, including 1M and 3T, can be distinguished by careful X-ray diffractometer work since they do not only belong to different space groups, but to different diffraction groups as well. It will be necessary, however, to obtain a high degree of preferred orientation of the flakes in order to record the full series of basal reflections in each case.

The similarity between Darling biotite and synthetic phlogopite does not necessarily imply that these biotites are high in magnesium, since they are very deeply coloured. Gower (1957), showed that the ratio of intensities of the (004) and (005) peaks for 1M biotite is proportional to the Fe:Mg ratio of the octahedral lattice site population. For 2M mica the corresponding peak indices would be (008) and (00.10). This measurement could not be attempted quantitatively in view of the fact that Gower did not take polytypism sufficiently into account, that the biotite concentrates studied contained significant amounts of chlorite which lowered the lesser peaks owing to the dilution effect, and thirdly, that Gower's curve was constructed from data obtained by FeK_α radiation while the author employed CoK_α radiation. Nevertheless it can be stated qualitatively that the Fe:Mg ratio in biotite is significantly lower in the hybrid granodiorite than in both the Darling and Contreberg granites. It is interesting to note that this would in a certain sense be contrary to the conclusions of Engel and Engel (1960), who showed that the Fe content of biotite decreases with increasing metamorphic grade. However, in their area of study coexisting garnet had a major influence on the Fe:Mg distribution, while in the Darling area cordierite is much more important.

Analyses/

Analyses of biotite from hybrid granodiorite from The Towers, Wildschutsvlei and Kapokberg yielded Fe:Mg values of 2,24 , 2,18 and 2,30. The corresponding value for a separate from Darling Granite, Morning Star, was 2,89 which correlates well with a value of 3,04 for Hoedjies Point Granite from Hoedjies Point, Saldanha. (Four of these values were obtained from unpublished analyses made for the author by the National Institute for Metallurgy in 1972 and the figure for Kapokberg is from Kolbe, 1966, table 12, no. 174).

The division between the phlogopite and biotite fields on the annite-siderophyllite-phlogopite-eastonite square is customarily taken at Mg:Fe = 2:1 (e.g. Deer, Howie and Zussman, 1962, vol. 3, p. 57), so that the Darling biotites are definitely not magnesian.

In all thin sections examined alteration of biotite to chlorite was observed usually around the edges but occasionally extensively. The chlorite in the concentrates employed for X-ray study is therefore genetically linked to the biotite, and can provide additional information about the composition of the biotite. No chlorite concentrates were made and the chlorite content of the powders studied ranges from 2 to 15 volume percent, so that only the most intense peaks would be revealed by X-ray diffraction. The data obtained was nevertheless sufficient to indicate that the chlorites are identical in the different rock types, and that they belong to either the Ia or Ib polytypes of Bailey and Brown (1962) because of the distinctive primary peak at d = 7,10 (table 3). The Ia polytype is favoured because the distinctive though fairly weak peak at d = 2,395 was recorded in some samples. It is believed that this chlorite may belong to the diabantite-penninite series on grounds of similar diffraction patterns, but only chemical analysis could prove this since the diffractometry of the chlorites reflects structure more than chemistry.

TABLE 3./

TABLE 3

d-Values of Chlorite Fraction in Biotite Concentrates

(Co K_α-radiation, Fe-filtered)

Ia CHLORITE, (Bailey and Brown, 1962)	7 Chlorite, Contreberg Granite	12 Chlorite, Hybrid Granodiorite	1 Chlorite, Darling Granite
14,2 (60)	14,24 (80)(b)		14,30 (80)
7,10 (100)	7,11 (100+)	7,09	7,09 (100)
4,73 (40)	4,73		4,75
3,55 (80)	3,55 (50)		3,56 (100)
2,66 (40)			
2,395 (60)			2,39 (10)
1,549 (60)			

3. Cordierite/

3. Cordierite

The hybrid granodiorite is particularly rich in cordierite which often exhibits the familiar yellow pleochroic haloes around radioactive inclusions of zircon. It has been established that cordierite deviates to an increasing extent from hexagonal symmetry with lower temperatures of formation or tempering. In order to measure this effect quantitatively Miyashiro (1957) instituted the distortion index, which is calculated by the relation:

$$\Delta = 2\theta_{131} - \frac{2\theta_{511} + 2\theta_{421}}{2}$$

Some authors favour a different orientation in which the lines (131), (511) and (421) are indexed as (311), (241) and (151) respectively. (A.S.T.M. Powder diffraction file, 1970).
In an important paper Schreyer and Schairer (1961) presented much new data on the structural state of synthetic cordierite. Apart from the normal or Δ-type, there is also an "anomalous" or i-type which maintains a constant distortion index over the whole thermal range. However, the i-cordierites vary in terms of the intensity index, for which the intensities of the relevant peaks are now taken into account, namely:

$$i = \frac{I\ (511\ +\ 421)}{I\ (131)}$$

The cordierite of the hybrid granodiorite is of the normal type, since the average intensity index is 2,7 which is far outside the range of 0 - 1,31 reported by Schreyer and Schairer for i-type cordierite. This fact, in conjunction with the relative positions of the peaks, corresponds with the properties of the normal cordierite series (fig. 24a). The average distortion index is 0,248, and the Darling cordierites are therefore low cordierites (fig. 24b). The splitting of peaks into doublets and triplets characteristic of high cordierite,

is/

STRUCTURAL DATA OF CORDIERITE

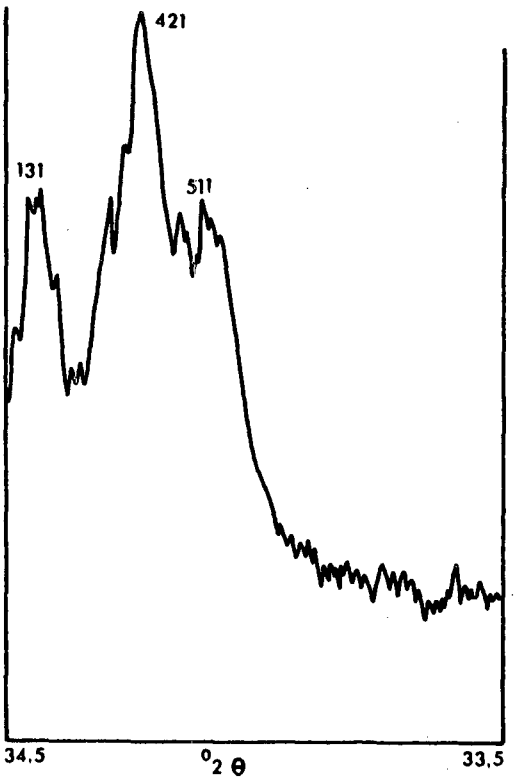

(a) Diffractometer trace (Co Kα -radiation) of Cordierite from Hybrid Granodiorite (Darling)

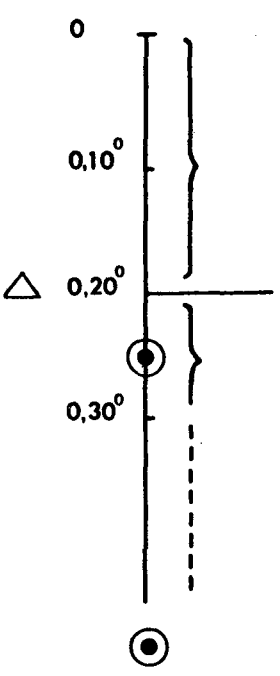

(b) Structural relations of Cordierite according to Schreyer and Schairer (1961)

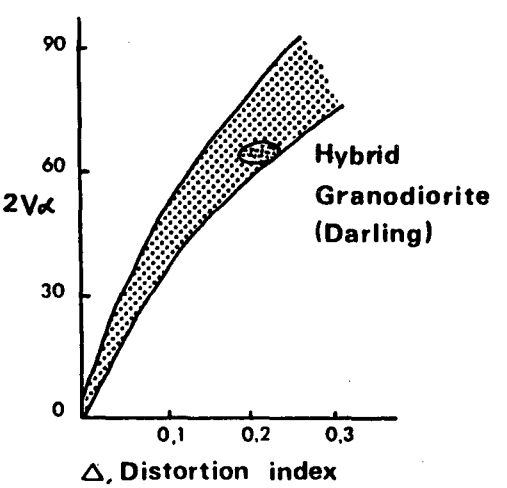

(c) Relation between optical properties and △ according to Miyashiro (1957)

Fig 24

is apparent at numerous points in the X-ray diffraction spectrum and should be further investigated experimentally.

The average refractive indices of the cordierite in the hybrid granodiorite is $\alpha = 1{,}540$, $\beta = 1{,}546$, $\gamma = 1{,}554$. Consequently we are dealing with a magnesian cordierite, which leads to speculation on the actual distribution ratio of Fe and Mg between biotite and coexisting cordierite, another topic for future detailed research. The average $2V_{\alpha}$ as determined by universal stage, is 63°, which agrees well with the correlation between optical properties and distortion index discovered by Miyashiro (fig. 24c).

VI PETROGRAPHIC GEOCHEMISTRY

The preparation of representative material for chemical analysis is an arduous task in the case of coarsely porphyritic granites, and should always be done by the investigator himself. For this reason, only a few well-chosen samples were submitted and the results (table 4) can now be integrated with the previously known data (table 5).

When the alkali ratio is taken into account, as was suggested by Harpum (1963), it is revealed that we are dealing with rocks ranging from granodiorite to granite (fig. 25). This classification is so easy to use that it has already gained wide acceptance, but it must be remembered that there is an absolute dependence on (i) truly representative sampling, and (ii) accurate determinations of Na and K. Unfortunately these two conditions are not always met by the data available in literature.

The younger granites in the Saldanha and Darling areas plot well within the granite field sensu stricto with some gradation towards adamellite. Most pertinent for the present study is the fact that, on the average, the contaminated rocks of the Darling batholith are adamellites with the new analyses clustering in the granite field, and the older data of Scholtz (22, 23 in table 5), overlapping with granodiorite. A suspicion is therefore created that the alkali ratios of the older gravimetric analyses are not comparable with those of the newer XRF determinations. Since it is not yet beyond doubt that the modern work is more accurate, the historical designation of these rocks as "hybrid granodiorite" will be retained for the time being. The uncertainty will only be removed by many more dependable analyses.

The problem central to the geology of the Darling area, is the relationship between the hybrid rocks and the regional granite (DAR, table 6). Field evidence for reaction between granite magma and Malmesbury metamorphites is irrefutable and

$K_2O - Na_2O$ diagram

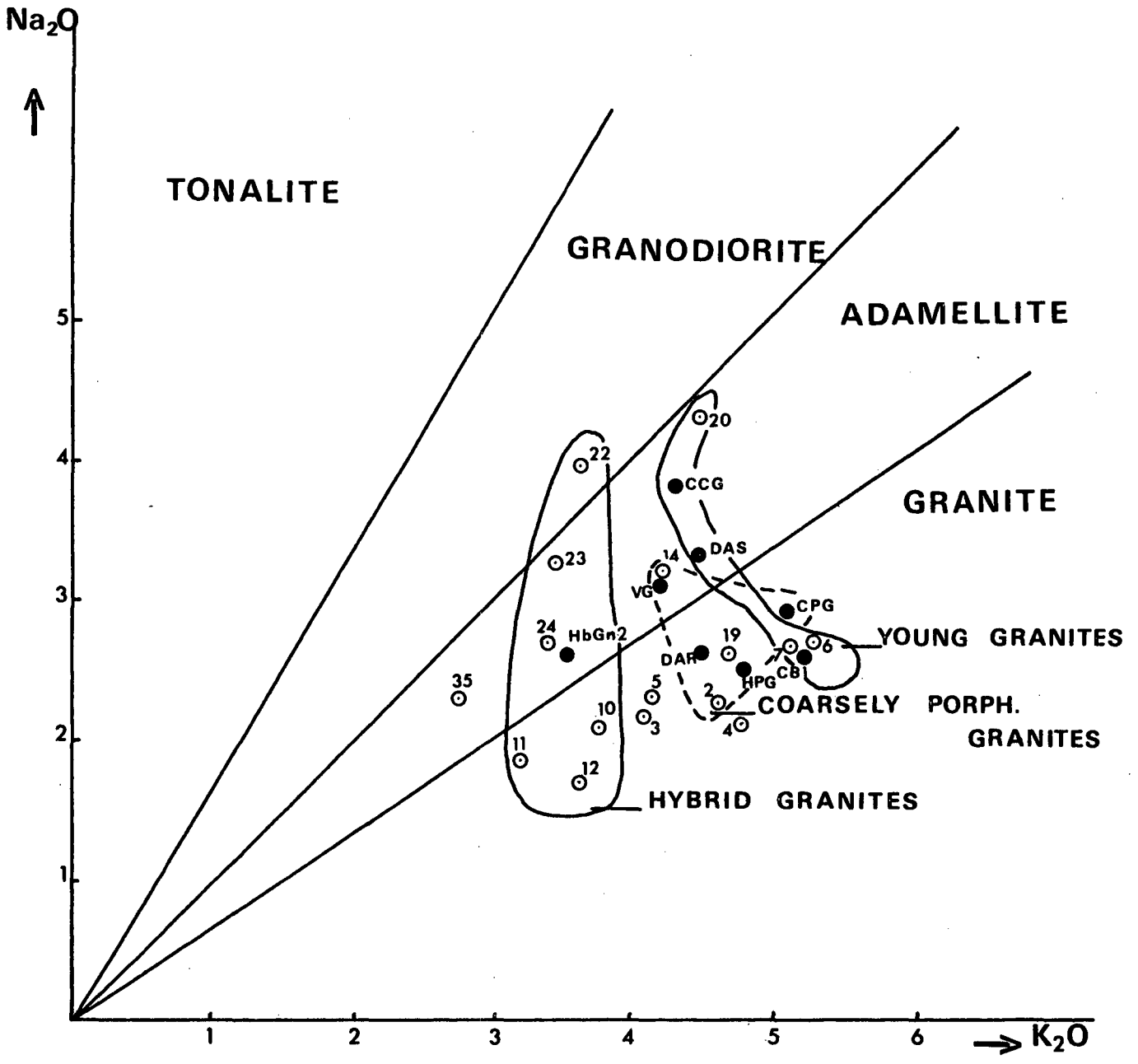

Fig. 25

TABLE 4

New Analyses

No.	SiO_2	Al_2O_3	Fe_2O_3	FeO	MgO	CaO	Na_2O	K_2O	TiO_2	P_2O_5	MnO	H_2O+	H_2O-	CO_2	B_2O_3	S	Sum
1	69,58	14,29	0,11	3,32	1,43	1,73	2,25	4,84	0,57	0,22	0,07	1,18	0,01	0,15		0,016	99,77
2	70,91	13,88	0,19	3,19	1,11	1,61	2,28	4,63	0,56	0,22	0,06	1,09	0,02	0,08		0,004	99,38
3	65,73	14,47	0,38	4,17	2,49	3,85	2,21	4,09	0,83	0,21	0,09	1,16	0,02	0,09		0,006	99,80
4	71,58	14,27	0,67	2,11	0,79	1,62	2,22	4,81	0,43	0,21	0,09	0,97	0,02	0,04		0,007	99,84
5	66,57	14,61	0,55	4,61	2,30	2,17	2,34	4,16	0,92	0,27	0,09	1,19	0,03	0,04		0,005	99,86
6	71,70	14,70	0,37	1,94	0,81	1,24	2,63	5,34	0,35	0,09	0,05	0,82	0,02	0,11	0,05	0,002	100,22
7	71,86	14,44	0,12	2,08	0,77	1,37	2,61	5,22	0,34	0,09	0,06	0,88	0,02	0,07	0,16	0,002	100,09
8	74,10	14,14	0,52	0,69	0,24	0,51	2,85	4,73	0,11	0,56	0,04	0,94	0,09	0,14	0,25	0,008	99,92
9	74,78	14,22	0,10	0,79	0,07	0,52	3,20	4,65	0,04	0,58	0,06	0,71	0,05	0,22	0,19	0,003	100,18
10	68,38	14,61	0,26	4,50	2,16	1,56	2,14	3,79	0,75	0,19	0,09	1,29	0,05	0,12		0,014	99,90
11	63,77	15,40	0,85	6,11	3,38	1,59	1,89	3,21	1,04	0,22	0,12	1,97	0,02	0,20		0,005	99,78
12	64,41	15,66	1,03	5,39	3,29	2,09	1,76	3,62	1,00	0,08	0,15	1,07	0,02	0,12		0,007	99,70
13	67,32	12,07	0,26	3,90	2,45	9,50	0,34	0,39	0,93	0,26	0,38	1,27	0,02	0,93		0,11	100,13

1 Coarsely porphyritic granite, Morning Star, Darling.
2 Porphyritic granite, Rondeberg, Darling.
3 Mylonite, Oude Post, Darling.
4 Mylonite, Trekoskraal, Vredenburg.
5 Biotite granite, Mamre.
6 Porphyritic fine-grained granite, northern part of farm, Contreberg, Darling.
7 Porphyritic fine-grained granite, eastern part of farm, Contreberg, Darling.
8 Nodular tourmaline granite, north of lighthouse, Dassen Island.
9 Nodular tourmaline granite, near cross in centre of island, Dassen Island.
10 Hybrid granite, Wildschutsvlei, Darling.
11 Hybrid granite, Doringfontein, Darling.
12 Hybrid granite, The Towers, Darling.
13 Feldspar-quartz-diopside-calcite-sphene xenolith, Glen Frank, Darling.

Analyses by the National Institute for Metallurgy, Johannesburg (1971)

Methods:

(a) SiO_2, Al_2O_3, total Fe, MgO, CaO, Na_2O, K_2O, TiO_2, P_2O_5, S, MnO by X-ray fluorescence.
(b) H_2O+, H_2O-, CO_2 by gravimetric procedures.
(c) FeO, B_2O_3 by volumetric procedures.

TABLE 5

Other Analyses

No.	SiO_2	Al_2O_3	Fe_2O_3	FeO	MgO	CaO	Na_2O	K_2O	TiO_2	P_2O_5	MnO	H_2O+	H_2O-	CO_2	B_2O_3	Cl	F	S	Sum
14	67,96	13,99	0,21	4,25	1,52	2,93	3,26	4,24	0,55	0,23		0,84	0,07	0,11					100,16
15	68,03	14,20	0,61	3,70	0,80	2,15	3,50	5,20	0,50	0,27		1,02	0,13	0,02					100,13
16	67,76	15,5		4,22	1,39	1,54	2,02	5,43	0,57										
17	74,67	13,9		2,78	0,68	1,54	3,18	4,99	0,32										
18	70,74	14,36	0,73	2,16	1,35	2,55	2,49	3,81	0,56	0,33	0,10	1,02	0,08						100,28
19	72,54	14,52	0,21	1,86	0,67	1,90	2,68	4,73	0,26			0,63	0,12						100,02
20	75,95	13,8		0,32	0,02	0,07	4,30	4,53	0,05										
21	73,44	14,58	0,71	0,85	0,24	0,52	4,11	3,88	0,08	0,48	0,06	0,97	0,23						100,15
22	62,26	15,90	0,99	6,17	3,09	1,65	3,99	3,60	0,70	0,25		1,40	0,22	0,04					100,26
23	63,33	16,40	1,09	5,69	2,90	1,87	3,30	3,42	0,40	0,26		1,31	0,22	0,07					100,26
24	67,13	15,8		4,97	2,25	2,14	2,70	3,42	0,66										
25	71,34	13,92	0,23	3,09	1,06	2,52	2,54	3,98		0,11		0,64	0,06						99,90
26	71,40	13,41	0,62	2,67	0,45	2,58	3,62	4,41		0,19	0,04	0,41	0,09	0,06					100,07
27	76,22	12,39	0,80	0,72	0,43	1,01	3,67	4,67	0,13	tr.	tr.	0,26	0,11						100,41
28	75,71	11,65	0,48	0,72	0,39	1,55	3,95	4,80	0,20	0,03	0,01	0,27	0,07			0,43	0,07		100,33
29	75,78	12,46	0,49	1,29	0,38	0,85	4,50	3,40	0,32	0,01	0,03	0,34	0,24			0,13	0,10		100,32
30	76,16	11,67	0,64	0,86	0,20	0,38	5,60	2,70	0,25		0,03	0,66	0,12			0,50	0,05		99,82
31	77,08	12,1		1,17	0,06	0,85	3,92	5,04	0,06										

TABLE 5 (Continued)

No.	SiO_2	Al_2O_3	Fe_2O_3	FeO	MgO	CaO	Na_2O	K_2O	TiO_2	P_2O_5	MnO	H_2O+	H_2O-	CO_2	B_2O_3	Cl	F	S	Sum
32	69,17	14,59	0,79	2,88	1,64	2,80	3,27	3,64	0,66	0,10	0,09	0,72	0,14						100,49
33	70,26	14,50	0,64	2,01	1,20	2,80	3,47	3,53	0,50	0,09	0,05	0,76	0,11						99,92
34	71,75	15,20	0,32	1,58	0,89	2,52	3,40	3,71	0,31	0,07	0,05	0,56	0,08						100,44
35	61,26	16,98	2,18	5,34	2,64	1,82	2,30	2,80	0,89	tr.	0,20	2,78	0,21	0,50					99,90
35A	60,31	18,20	1,94	5,47	2,44	1,35	2,37	3,32	0,67	0,20	0,10	3,52	0,11						100,00
36	74,98	11,05	0,27	4,64	1,33	2,08	2,19	2,06	1,05	0,17	0,04	0,41	0,09	tr.		0,01		0,06	99,94
37	75,29	10,63	0,86	3,02	1,55	1,17	2,62	2,22	0,68	0,17	0,06	LOI =	0,37	0,10		0,01		0,08	
38	61,07	15,55	1,69	6,18	3,62	0,86	1,43	4,14	0,82	0,15	0,09	LOI =	1,96	0,10		0,01		0,11	
39	60,19	17,68	1,33	5,96	3,36	0,47	1,90	4,59	0,79	0,17	0,06	LOI =	2,38	0,10		0,01		0,03	
40	59,34	17,59	2,59	5,03	3,77	0,64	1,16	4,81	0,80	0,12	0,07	LOI =	2,64	0,10					
41	71,06	11,34	0,50	4,15	2,49	1,83	2,79	2,54	0,60	0,21	0,09	1,92	0,07						99,59
42	56,31	15,87	3,24	4,27	4,35	6,00	3,00	3,95	0,79	0,43	0,16	1,23	0,08						

	Insolubles	$(Fe,Al)_2O_3$	$CaCO_3$	$MgCO_3$	Moisture	P_2O_5
43	4,0	2,0	85,0	5,1	2,0	tr.
44	6,5	3,0	62,5	27,62		
45	2,5	3,5	91,0		2,0	tr.

LOI = Loss on ignition

14 Coarsely porphyritic granodiorite, Mamre Station (DLS, 1A,15)
15 Coarsely porphyritic granite, Hoedjies Bay Peninsula (DLS, 1A,10)
16 Coarsely porphyritic granite, coastline 40 m east of Hoedjies Bay contact (PK, 6, 127)
17 Strongly sheared porphyritic granite, old quarries, main road, 750 m S.E. of Darling (PK, 6, 123)
18 Triturated coarsely porphyritic granite, Trekoskraal, Vredenburg (AES, 4, 1)
19 Granite, Darling (DLS, 1A, 16)
20 Microgranite, Klipberg, Darling, 500 m west of beacon 247 (PK, 6, 151)
21 Tourmaline granite, Huis-baai, Dassen Island (GRM, I, a)
22 Highly contaminated granodiorite, Doornfontein, Darling (DLS, 1A, 42)
23 Highly contaminated granodiorite, Klavervlei, Darling (DLS, 1A, 43)
24 Melanocratic granite, Kapokberg, Darling, 500 m S.E. of beacon 11 (PK, 6, 174)
25 Coarsely porphyritic granite, Klein Paternoster (DLS, 1A, 11)
26 Porphyritic granite, Vredenburg (DLS, 1A, 12)
27 Medium even-grained granite, south of Cape Castle (DLS, 1A, 13)
28 Coarse even-grained granite 1 000 ft west of Slippers Bay contact (JRM, IIa, 2)
29 Coarse even-grained granite 1 200 ft north of Slippers Bay contact (JRM, IIa, 3)
30 Even-grained granite, 7 ft north of Slippers Bay contact (JRM, IIa, 7)
31 Microgranite, coastline 1,5 m from Slippers Bay contact (PK, 6, 153)
32 Partially incorporated xenolith, Klein Paternoster (DLS, 1A, 44)
33 Hybrid microgranite, Great Paternoster (DLS, 1A, 45)
34 Hybrid granitised xenolith, Slippers Bay Hills (DLS, 1A, 46)
35 Fresh Malmesbury shale, borehole, Philadelphia (DLS,1A, 47)
35A Average of four typical Malmesbury shales (CTP, 1, a)
36 Medium grey shale, Ciollis' quarry near road Cape Town - Malmesbury (RVD, 6A, Ma3)

37 Argillaceous Malmesbury sediment, quarry, Bellville, road Cape Town - Paarl (RVD, 6A, Ma5)

38 Dark grey indurated argillaceous shale, Table View quarry, Milnerton (RVD, 6A, Ma7)

39 Arenaceous Malmesbury sediment, Ciollis' quarry, near road Cape Town - Malmesbury (RVD, 6A, Ma4)

40 Psammitic hornfels, quarry on De Waal Drive, Cape Town (FW and MM, II, 8)

41 Average analysis of three Malmesbury - Wellington greywacke analyses (PJZ, IV, 15)

42 Average analysis of four Ysterfontein diorite analyses (SM, Ic, D)

43 Limestone, De Hoek, Piketberg (WW, p37, no 878)

44 Dolomite, Voëlvlei, Gouda (WW, p42, no 890)

45 Limestone, Botmans' Drift, Hermon (WW,p42, no 890; ALH, p128, no 635)

(Author, Table, Analysis number)

PK = P. Kolbe (1966)
AES = A.E. Schoch (1962)
JRM = J.R. McIver (1957)
DLS = D.L. Scholtz (1946)
RVD = R.V. Danchin (1970, vol. II)
FW and MM = F. Walker and M. Mathias (1946)
PJZ = P.J. van Zijl (1950)
SM = S. Maske (1957)
WW = W. Wybergh (1918)
CTP = C.T. Potgieter (1950)
ALH = A.L. Hall (1938)
GRM = G.R. McLachlan (1949)

TABLE 6

New Composite Analyses

No.	SiO_2	Al_2O_3	Fe_2O_3	FeO	MgO	CaO	Na_2O	K_2O	TiO_2	P_2O_5	MnO	H_2O+	H_2O-	CO_2	B_2O_3	S	Cl	F	C	Sum
DAR	69,49	14,05	0,17	3,59	1,35	2,09	2,60	4,57	0,56	0,22	0,06	1,04	0,03	0,11		0,010				99,94
HPG	69,50	14,58	0,66	2,92	1,08	1,96	2,56	4,81	0,51	0,27	0,09	1,02	0,08	0,03		0,007				100,08
CPG	69,48	15,15	0,33	2,68	0,92	1,53	2,92	5,17	0,44	0,12	0,12	0,76	0,10	0,01	0,10					99,89
OG	69,49	14,59	0,39	3,06	1,12	1,86	2,69	4,85	0,50	0,20	0,09	0,94	0,07	0,05	0,10	0,008				100,01
VG	71,37	13,66	0,42	2,88	0,75	2,55	3,08	4,19	0,41	0,14	0,04	0,52	0,08	0,06						100,15
CB1	71,78	14,57	0,24	2,01	0,79	1,30	2,62	5,28	0,34	0,09	0,05	0,85	0,02	0,09	0,10	0,002				100,13
CB2	72,03	14,55	0,23	1,96	0,75	1,50	2,64	4,96	0,32	0,09	0,05	0,81	0,05	0,09	0,10	0,002				100,13
CCG	76,13	12,29	0,59	0,79	0,32	1,05	3,81	4,36	0,15	0,01	0,02	0,32	0,07			0,08	0,24	0,07		100,15
DAS	74,11	14,31	0,44	0,78	0,18	0,52	3,31	4,50	0,08	0,54	0,05	0,12	0,87	0,18	0,22	0,01				100,22
HbGn1	65,69	15,32	0,71	5,31	2,76	1,84	2,11	3,50	0,86	0,16	0,12	1,44	0,03	0,15		0,009				100,01
	± 1,10	± 0,27	±0,23	±0,46	±0,33	±0,02	±0,21	±0,01	±0,00	±0,00	±0,00	±0,27	±0,00	±0,00		±0,00				
HbGn2	64,62	15,57	0,84	5,55	2,83	1,81	2,62	3,50	0,76	0,16	0,08	1,40	0,11	0,11		0,009				100,01
	± 0,96	± 0,24	±0,15	±0,30	±0,21	±0,01	±0,36	±0,01	±0,00	±0,00	±0,00	±0,15	±0,00	±0,00		±0,00				
SH	60,82	17,05	1,96	5,66	3,37	0,96	1,71	4,10	0,82	0,12	0,10	2,80	0,21	0,20		0,07	0,01		0,03	100,00
QG	74,88	11,38	0,56	3,81	1,88	1,67	2,39	2,13	0,86	0,08	0,05	0,20	0,04	0,05		0,03				100,00

DAR = Darling Granite (Analyses 1 + 2 + 14)

HPG = Hoedjies Point Granite (Analyses 15 + 16)

CPG = Cape Peninsula Granite (Scholtz, 1946, analyses 28a + 28b + 29 + 30 + 31 and Kolbe, 1966, analyses 104 + 105 + 106 + 117 + 118)

OG = Old Granite (DAR + HPG + CPG)

VG = Vredenburg Granite (Analyses 25 + 26)

CB = Contreberg Granite (CB1, analyses 6 + 7; CB2, analyses 6 + 7 + 19)

CCG = Cape Columbine Granite (Analyses 27 + 28 + 29 and Kolbe, 1966, analysis 152)

DAS = Dassen Island Granite (Analyses 8 + 9 and McLachlan, 1949, analysis a)

HbGn = Hybrid Granodiorite (HbGn1, Analyses 10 + 11 + 12 + 24; HbGn2, analyses 10 + 11 + 12 + 22 + 23 + 24. Standard deviation of the mean, ($\sigma/\sqrt{n}$) given)

SH = Malmesbury Shale (Analyses 35 + 36 + 37 + 38)

QG = Malmesbury Quartzitic Graywacke (Analyses 39 + 40 and partial analysis supplied by J.D.T. Otto, 1971, personal communication)

in line with the documented data for the Saldanha batholith. The field facts include the distribution of xenoliths (chapter III) and the nature of the xenoliths.

A model is now proposed to account for the composition and nature of the hybrid granodiorite, and ultimately for its spatial position in the batholith, as well as its relatively large volume. In essence, this model depends on the following reaction:

GRANITE (Magma) + METAMORPHITES → HYBRID GRANODIORITE COMPLEX

The writer is fully aware of the justified criticism levelled against the indiscriminate use of linear mixing exercises. Liniar mixing of components can be applied if closed conditions can be assumed. The designation of any system as open, semi-closed or closed, is dependent on the definition of the system boundaries employed, and therefore subjective. Any open system becomes closed when the limits are sufficiently enlarged. On the relatively large (batholithic) scale adopted here, which is the correct scale on which to discuss the hybrid granodiorite, the system under contemplation can be regarded as closed or very nearly so. In the author's opinion the only possible exception pertains to part of the volatile components CO_2 and H_2O.

Adhering to the convention that an argument should proceed from the known to the unknown, the chemistry of the hybrid granodiorite will be discussed before that of the Darling granite and the Malmesbury metamorphites for which the available data are meagre.

Sampling of the hybrid granodiorite did not present great problems since the material is fairly homogeneous, but naturally no attempt was made to include the xenolith content of this rock type, or the sparsely distributed quartz segregations. Quantitative field measurements reveal that the hybrid granodiorite holds the following volumetric percentages of these components:

Quartz segregations	0,3
Xenoliths (quartzitic, pelitic and lime-rich, with the first-mentioned predominant)	1,0

The/

The chemical data for the average hybrid granodiorite (HbGn, table 6), should therefore be altered slightly in order to conform to the average material observed in the field. The composite analysis HbGn2 was therefore adapted to include 0,3% quartz and 1,0% Malmesbury quartzitic graywacke, QG. The result is shown in table 7 (HbGn2C = Hybrid granodiorite complex).

The process of reaction between magma and metamorphites should have been isovolumetric or very nearly isovolumetric. Consequently comparison of chemical data is best done when recalculated to a constant volume basis. For this purpose the Barth standard cell, referred to 160 oxygen ions, is admirably suitable, and relevant Barth cells are given in table 7. After having gained considerable experience with calculation and interpretation of standard cells, the author would like to emphasize that this approach is useful only when data of very high precision are available. If there is any doubt at all concerning the "difficult" components such as CO_2 and H_2O+ and those expressed by the $Fe^{+++}:Fe^{++}$ and $K^+:Na^+$ ratios, the utilisation of Niggli values would be superior, since they are specifically designed to circumvent the doubtful portions of analyses. (The alkali ratio is consolidated in the al-k value, and the ferrous: ferric ratio is recalculated to ferrous iron to form part of the fm value, while the summation is independent of the volatile components). In the case under consideration, however, the fact that the Niggli values are based on al + alk + c + fm = 100 presents insuperable difficulties if quartzitic materials are to be compared with more average rock types.

Having obtained an average standard cell for the right hand side of the proposed reaction, we can now consider the components on the left. The composite analysis calculated for the Darling granite (DAR, table 6, table 7), includes types of varying biotite content, but confidence in the use of these figures is enhanced by the close correspondence of the cell with that of the composite analysis of the comparable Hoedjies

Point/

TABLE 7

Barth Standard Cells

No.	Si^{++++}	Al^{+++}	Fe^{+++}	Fe^{++}	Mn^{++}	Mg^{++}	Ca^{++}	Na^{+}	K^{+}	Ti^{++++}	P^{+++++}	C^{++++}	C	B^{+++}	Sum	OH^{-}	$S^{=}$	$O^{=}$
1	62,04	14,99	0,11	2,46	0,05	1,93	1,61	1,82	2,68	0,37	0,11	0,18			88,35	7,16		152,84
10	60,00	15,07	0,31	3,32	0,05	2,84	1,48	3,58	4,22	0,47	0,10	0,10			91,54	7,80		152,20
11	56,54	16,08	0,53	4,53	0,05	4,47	1,54	3,30	3,62	0,69	0,11	0,26			91,72	11,50		148,50
12	57,54	16,53	0,65	4,03	0,05	4,40	1,99	3,00	4,08	0,70	0,11	0,10			93,18	6,54		153,46
13	58,62	12,45	0,31	2,82	0,26	3,19	8,84	0,52	0,42	0,57	0,31	1,10			89,41	7,52	0,16	152,32
14	56,38	14,63	0,11	3,15		1,98	2,78	5,66	4,80	0,37	0,11	0,10			94,12	5,34		151,02
22	55,86	16,80	0,65	4,63		4,15	1,56	7,00	4,10	0,48	0,11	0,05			95,39	9,70		150,30
23	56,38	17,23	0,75	4,23		3,85	1,77	5,68	3,86	0,26	0,11	0,05			94,27	8,98		151,02
22+23	56,12	17,01	0,70	4,43		4,00	1,66	6,34	3,98	0,37	0,16	0,05			94,82	9,34		150,66
32	60,59	15,04	0,10	2,10	0,00	2,16	2,63	5,58	4,00	0,47	0,10				92,77	5,04		154,95
33	61,35	14,89	0,08	1,47	0,37	1,57	2,62	5,88	3,88	0,31	0,10				92,52	5,02		154,97
34	62,27	15,54	0,04	1,15	0,00	1,15	2,35	5,74	4,06	0,21	0,02				92,53	3,66		156,33
42	52,14	17,37	2,23	3,34	0,11	6,01	5,95	5,34	4,56	0,55	0,33	0,00			97,93	8,02		151,98
SH	53,43	17,69	1,28	4,15	0,05	4,42	0,91	2,88	5,12	0,53	0,11	0,26	0,11		90,94	17,58	0,11	142,31
QG	64,92	11,61	0,41	2,75	0,00	2,44	1,55	4,04	2,28	0,57	0,10	0,05			90,72	1,34	0,05	158,61
SH:QG 80:20	55,73	16,47	1,11	3,87	0,04	4,02	1,04	3,11	4,55	0,54	0,11	0,22	0,09		90,90	14,27	0,10	145,57
HbGn2	57,37	16,31	0,53	4,11	0,05	3,74	1,71	4,48	3,94	0,53	0,11	0,10			92,99	8,96	0,16	150,88
	±0,85	± 0,21	±0,11	±0,21	±0,00	±0,27	±0,00	±0,64	±0,00	±0,00	±0,00	±0,00				±0,74		
HbGn2C	57,77	16,32	0,53	4,11	0,05	3,73	1,71	4,48	3,94	0,53	0,11	0,10			93,38	8,92		151,08
DAR	61,51	14,55	0,11	2,66	0,05	1,81	1,97	4,46	5,20	0,10	0,04	0,10			92,52	6,26	0,00	153,74
HPG	61,09	15,10	0,08	2,11	0,05	1,43	1,85	4,34	5,38	0,31	0,10	0,05			91,89	6,44		153,55
VG	62,52	14,10	0,06	2,11	0,32	0,94	2,37	5,16	4,74	0,26	0,10	0,05			92,73	3,48		156,53
CB1	62,29	14,89	0,11	1,46	0,00	1,04	1,20	4,38	5,84	0,21	0,21	0,10		0,31	92,04	5,00		154,99
	62,47	14,94	0,11	1,46	0,00	1,04	1,20	4,38	5,86	0,21	0,21	0,10			91,98	5,02		154,98
CCG	65,89	12,57	0,08	0,57	0,00	0,36	0,99	6,34	4,88	0,05	0,00	0,00			91,73	2,20		147,79

Point granite in the Saldanha batholith (HPG, tables 6 and 7).

What was the composition of Malmesbury metamorphites which could have been assimilated? No direct evidence is available, since the northeastern contact of the batholith is faulted and the southwestern one probably as well, apart from being covered by recent unconsolidated deposits, while the northwestern extremity is overlain by Langebaan limestone and sand and the southeastern end is obscured by deep weathering. However, the Malmesbury rocks can be observed at De la Rey in the west, and on the coast at Mud River and Ganzekraal to the south, apart from existing knowledge concerning the rock types occurring on the line of strike of the major axis of the batholith to the south-east. In the first two instances we find alternating thermally metamorphosed quartzitic graywacke and spotted shale. Unmetamorphosed Malmesbury rocks are present in some areas near the abovementioned strike line, but metamorphic domes which are extensively quarried also exist, as for instance to the west of Durbanville.

Unfortunately very few reliable analyses are available and these are summarised in table 5. Taking all facts into consideration the first approximation to Malmesbury composition is a mixture of 80% quartzitic graywacke and 20% pelites (shale, spotted shale).

The obvious method by which comparison of the actual composition of a rock with the calculated composition by linear mixing of reactants can be done, is by effecting coincidence of the amount of a major constituent. For this purpose silica or silicon is the most convenient component. Alumina or aluminium may also be used for this purpose, but it constitutes a much smaller percentage of the rock, and in addition many reported alumina values in silicate analyses are not sufficiently precise. Carmichael (1969) advocated the use of Al^{+++} as the most inert component with reference to local systems, indicating that its limit of migration is only 0,3 mm in the meta-

pelites/

pelites of the Whetstone Lake area, Ontario, Canada. Under higher grade conditions such as undoubtedly obtained during hybridisation in the Darling batholith this limit was probably considerably exceeded.

Isovolumetric (constant oxygen) mixing of 35,3% DAR with 64,7% of the 80:20 Malmesbury material yields a very good fit with the composition of the hybrid granodiorite (table 8). The sum of differences (excluding oxygen), is only +0,77 ions per cell and -1,30 valencies per cell. In the view of the imponderables present from the outset, such as the real regional Malmesbury composition, the model is considered to be acceptable.

If the constituents are compared individually, no serious obstacles are encountered either. Thus it was apparent on the Harpum-diagram that the alkali ratios of older analyses may not be in line with the more recent figures, and it is therefore interesting to note that the anomalies for K^+ and Na^+ of -0,89 and +0,84 ions respectively, are nearly balanced. A similar argument may be applied to the Fe^{++} and Fe^{+++} differences. The relatively large anomaly for OH^- of +2,52 ions may well be a reflection of loss of water from the batholith through the roof, so that the assumption of closed system conditions may not be applicable to this component. All the relatively large specific anomalies can therefore easily be accommodated in the model except for deficiencies of Mg^{++} (-0,49) and Ca^{++} (-0,34). However, the utilisation of the 80:20 mixture for the Malmesbury component represents the broadest of possibilities, and the actual material certainly included some biotite schists or phyllites, adding more Mg, and also a little lime-rich material, taking care of the Ca. Xenoliths of both rock types have been observed everywhere in the hybrid granodiorite.

The presence of limestone xenoliths should be taken into account if the above calculations are to be improved, but unfortunately only partial analyses of ancient vintage are available

for/

TABLE 8

Comparison of Calculated and Determined Cells

	Si^{++++}	Al^{+++}	Fe^{+++}	Fe^{++}	Mg^{++}	Ca^{++}	Na^{+}	K^{+}	Ti^{++++}	P^{+++++}	Mn^{++}	C^{++++}			OH^{-}	$S^{=}$	$(O^{=})$		
35,3% DAR 64,7% 80:20	57,77	15,79	0,76	3,44	3,24	1,37	3,59	4,78	0,38	0,09	0,04	0,24			11,44	0,06	(148,45)		
HbGnC	57,77	16,32	0,53	4,11	3,73	1,71	4,48	3,94	0,53	0,11	0,05	0,10	Cations	Valencies	8,92	0,00	(151,08)	Ions	Valencies
+			0,23					0,84				0,12	1,19	2,01	2,52	0,06		3,77	4,59
-		0,43		0,67	0,49	0,34	0,89		0,15	0,02	0,01		3,00	5,89			(2,63)	3,00	5,89
												△	-1,81	-3,88			△	+0,77	-1,30

	Si^{++++}	Al^{+++}	Fe^{+++}	Fe^{++}	Mg^{++}	Ca^{++}	Na^{+}	K^{+}	Ti^{++++}	P^{+++++}	Mn^{++}	C^{++++}			OH^{-}	$S^{=}$	$(O^{=})$		
30,0% DAR 59,5% 80:20 10,5% 13	57,77	15,47	0,73	3,54	3,27	2,14	3,24	4,31	0,41	0,11	0,07	0,33			11,16	0,08	(148,73)		
HbGnC	57,77	16,32	0,53	4,11	3,73	1,71	4,48	3,94	0,53	0,11	0,05	0,10	Cations	Valencies	8,92	0,00	(151,08)	Ions	Valencies
+			0,20			0,43		0,37			0,02	0,23	1,25	2,79	2,24	0,08		3,65	5,19
-		0,85		0,57	0,46		1,24		0,12				3,24	6,33			(2,35)	3,24	6,33
												△	-1,99	-3,54			△	+0,41	-1,14

for Malmesbury limestones and dolomites (table 5), and even then for occurrences distant from the area of investigation. One of the new analyses (table 4,13) represents a xenolith, and although it must have been extensively altered by metasomatic processes, it can be utilised to provide a rough measure of the original Ca and Mg content. Only a small percentage of the Malmesbury mixture could have been lime-rich or lime-magnesia-rich in any case. The resulting calculation yields an even better fit than before (table 8).

All the features of the proposed model have now been discussed, but it would still be interesting to calculate the chemical composition of the "missing" portion on the assumption that the observed anomalies are actual and not apparent as was argued above. One can attribute the anomaly to the left hand portion of the assimilation equation in particular to the 80:20 Malmesbury mixture, or to the hybrid granodiorite on the right hand side. The results (table 9) show that the rock type with which the 80:20 mixture must be replaced in order to remove the anomaly approximates a diorite as the percentage of replacement is increased. (The low Ca^{++} value can be ignored, since it was already shown that lime-rich Malmesbury materials were present which were not taken into account here). The boxes in the table indicate cases where the specific anomalies were too large to be accommodated, and which were then taken as 0,00. Diorites of local importance are of course known in the Darling region, viz. at Ysterfontein (Maske, 1957), and at Mud River (chapter II). The possible implications of this calculation are encumbered by too many uncertainties at present, so that further discussion would be premature. However, it is clear that the chemistry of the diorite is very near to a 80:20 Malmesbury mixture with a little limestone!

When the anomaly is solely attributed to the hybrid granodiorite, low replacement-percentages are impossible. The figures obtained in this case yield a more granitic material which

leads/

TABLE 9

Calculated Standard Cell Composition

of Anomalous Factor

Percentage of 80:20 mixture	Si^{++++}	Al^{+++}	Fe^{+++}	Fe^{++}	Mg^{++}	Ca^{++}	Na^{+}	K^{+}	Ti^{++++}	P^{+++++}	Mn^{++}	C^{++++}	Sum	OH^{-}	$S^{=}$	$O^{=}$
5	39,24	20,93	□	17,44	13,51	8,07	21,58	□	3,71	0,44	0,22	□		□		160,00
10	47,93	19,92	□	12,22	9,96	5,44	14,47	□	2,93	0,40	0,13	□		□		160,00
20	53,73	19,08	□	8,72	7,53	3,50	9,61	□	1,64	0,22	0,07	□		□		160,00
30	55,60	18,65	0,00	7,30	6,53	2,77	7,66	0,21	1,28	0,21	0,10	□		1,28	0,00	158,73
50	55,40	17,70	0,40	5,90	5,50	2,06	5,65	1,94	0,98	0,15	0,06	0,00		6,42	0,00	153,58
100	55,73	17,74	0,76	4,90	4,78	1,56	4,40	3,25	0,77	0,14	0,06	0,12		10,37	0,00	149,63
Diorite (Analysis 42)	52,14	17,37	2,23	3,34	6,01	5,95	5,34	4,56	0,55	0,33	0,11	0,00		8,02		151,98
Percentage of HbGn2C																
20	60,22	14,75	1,77	0,78	1,36	0,00	0,05	8,50	□	0,00	0,00	0,73	88,16	5,85	0,31	143,83
30	57,83	14,92	1,27	1,87	2,10	0,57	1,50	6,74	0,03	0,03	0,00	0,50	87,35	17,35	0,20	142,45
40	57,82	15,26	1,10	2,43	2,50	0,85	2,25	6,05	0,15	0,05	0,03	0,40	88,89	15,24	0,15	144,61

leads to speculation on the close association in the field between relatively small bodies of younger granite and hybrid rocks in both the Saldanha and Darling batholiths.

This is as far as can be progressed at present. The anomalous factor, if really anomalous at all, is most likely attributable to both sides of the equation.

During the assimilative reactions a considerable amount of water must have been introduced by the Malmesbury component, as well as by the process of transvaporisation (Szádeczky-Kardoss, 1960). This is illustrated by the calculated OH^- contents of the standard cells (table 7), and it would be interesting to obtain data on the isotopic ratios of both oxygen and hydrogen (Turi and Taylor, 1971). The possibility that some H^+ ions may be present in micas is slight (Wedepohl et al., 1969, p. 1 - 5), but would cause the calculated OH^- values to be too high. At high temperatures the release of combined water is accompanied by an increase in the degree of dissociation, and hence in a rise of the fugacity of oxygen.

The considerable advances made in petrogenesis in recent years owing to recognition of the primary rôle of oxygen fugacity levels in natural reactions has been well documented (eg. Eugster and Wones, 1962; Ernst, 1968). The most important effect of a rise in fO_2 is the oxidation of iron, and most deductions on the original level of oxygen pressure are in fact based on recognition of buffer-pairs of iron-bearing minerals. Unfortunately the determination of ferrous iron is not always reliable. Great caution was exercised to prevent oxidation during preparation of the material for the new analyses reported here, such as final grinding under acetone. The $Fe^{+++}:Fe^{++}$ ratios are shown in fig. 26. The resulting trends are enhanced when standard cell values rather than gravimetric figures are used (fig. 27). The former presentation is preferred since comparisons are nearly isovolumetric.

The/

FIG. 26 Fe_2O_3 - FeO IN WEIGHT %

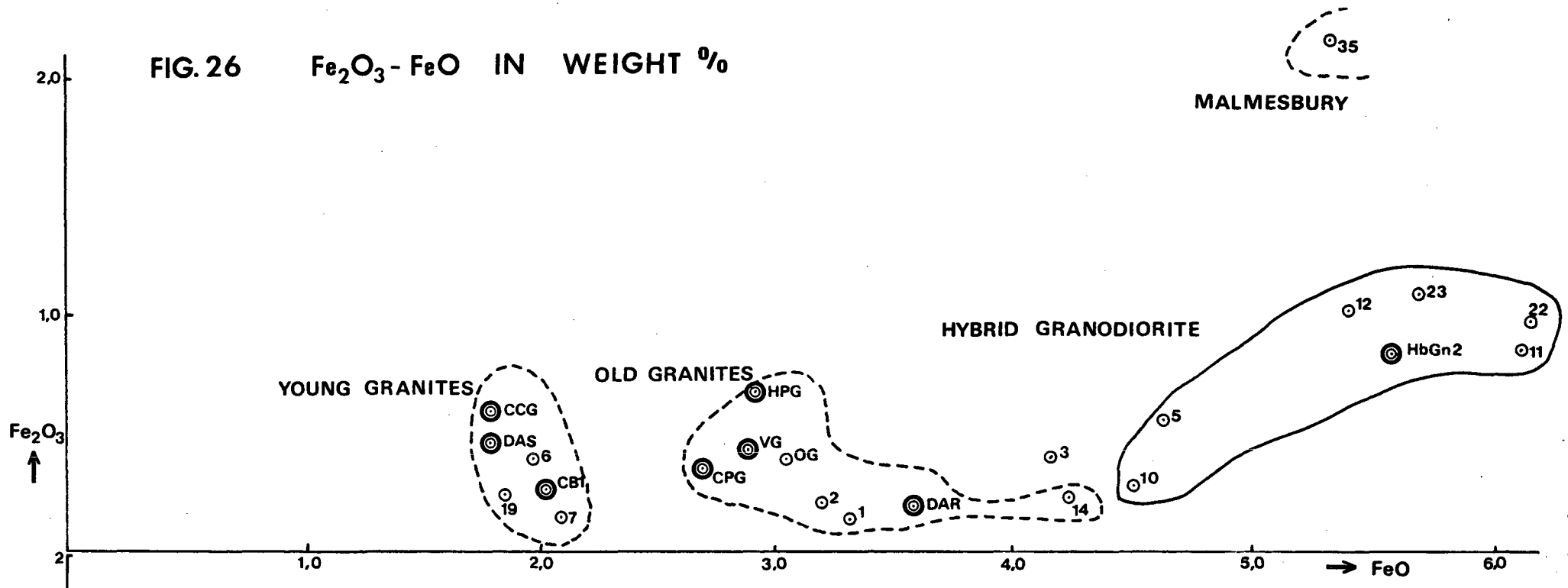

FIG. 27 Fe^{+++} - Fe^{++} IN STANDARD CELL VALUES

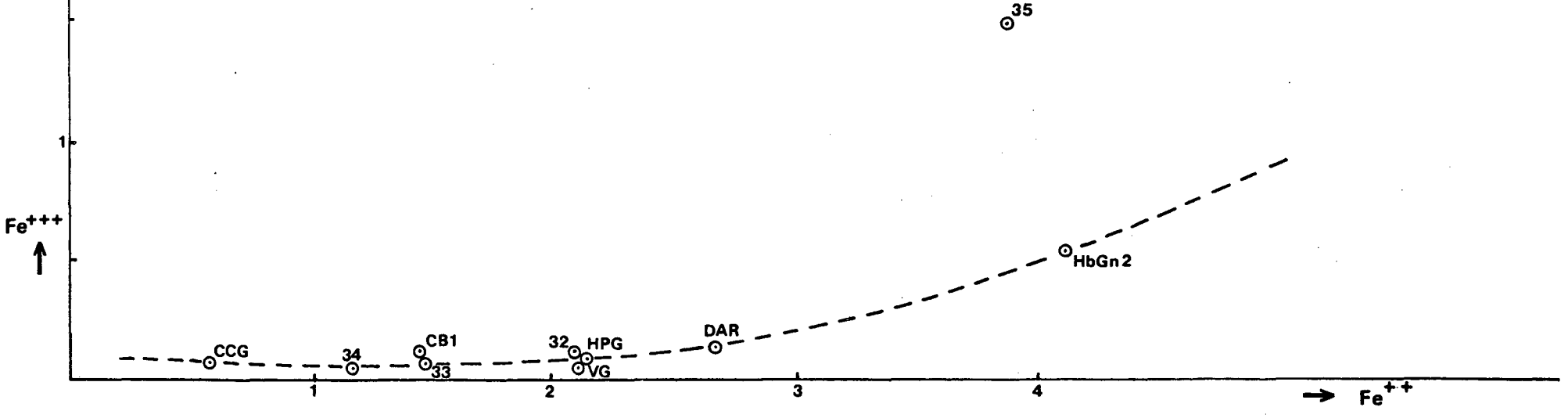

The conversion of ferrous to ferric iron is surprisingly slight, although discernible in the hybrid rocks, compared with the parent materials. The younger and older granites returned similar ratios but the former has less total iron. It is evident that the fO_2 must have been high, specifically during the hybridisation reactions, but not high enough to exceed the Fe_2O_3 - Fe_3O_4 buffer conditions. That the various granites experienced rather similar conditions may have been expected, but more pronounced oxidation might have been predicted for the hybrid rocks of sedimentary derivation. The author believes it possible that release of CO_2 from the lime-rich Malmesbury component was sufficient to modify the P_{H_2O} and may have tempered the rise in partial pressure of oxygen. The consequences of addition of CO_2 on the oxygen fugacity of a hydrous system are at present very difficult to calculate since the reactions between CO_2 and H_2 have to be taken into account as well, and the answer will be different for differing H_2O/CO_2 mixtures (Krauskopf, 1967, chapter 16), but the mineralogy of dolomite-limestone intruded by granites in the Marble Delta of Natal indicates that the effect may in fact be a lowering of oxygen fugacity (J.D.T. Otto, personal communication, 1970).

The postulated influence of P_{CO_2} would have been particularly marked if the system was effectively closed, although modern isotopic studies on some batholiths indicate considerable movement of volatiles inwards from the sides and upwards, for which the magmatic "heat engine" supplied the energy (Turi and Taylor, 1971a and 1971b). However, we are here dealing with the central part of the batholith and with continuous internal additions. The fact that many limestone xenoliths are enveloped by pegmatoid zones (eg. on Alexanderfontein and The Towers), coupled with the calcium content of the hybrid granodiorite, indicates arrestation of the reaction after initial rapid assimilation. A gradual build-up of the CO_2:O_2 ratio during the reactions, may also have something to do with the lesser amount of assimila-

tion/

tion of quartzitic xenoliths compared to other types, and the production of ellipsoidal quartz segregations rather than normal late stage veins. The psammite-pelite ratio of xenoliths is certainly much higher than allowed for in the 80:20 Malmesbury mixture previously discussed. The absence of comparable large scale features in the Saldanha batholith except for the area nearest to the Darling batholith may reflect more "open" conditions with respect to the volatiles. The Saldanha quartz porphyry must have reached a level very near the ancient surface.

It is interesting to note that the assimilative model presented above for the hybrid granodiorites of Darling is corroborated when the classical and well-exposed localities of the Saldanha batholith are subjected to the same tests (table 10), provided that the latest correlations are taken into account (Schoch, 1971; Visser and Schoch, in press). Excellent fits are obtained for the hybrid materials of both Klein Paternoster and Great Paternoster (Duikereiland), while the greater percentage of Vredenburg granite used for the latter (82,8%) than for the former (71,6%) is in agreement with the field evidence and of the correct magnitude. With respect to the Fe^{+++}:Fe^{++} and K^{+}:Na^{+} ratios the same features as at Darling are evident but the Mg^{++} balances and the Ca^{++} anomaly is negligible in the one case.

A poor correlation is obtained for the hybrid granite of the Slippers Bay Hills. This material is today known to occur in Cape Columbine granite (Geological Survey, sheet 3318A-3218C, in press) and the results are even worse if other granites are used in the calculations, as one would have been forced to do three years ago. The two Paternoster localities are situated not far from the extended strike line of the major axis of the Darling pluton as well as the enveloped hybrid granodiorite. This is not true of Slippers Bay, and it may well be that the 80:20 Malmesbury mixture employed is unrealistic in this case. If Malmesbury shale alone is in fact used (SH, table 7), the

correlation/

TABLE 10

Saldanha Hybrid Granites Compared with Appropriate Mixtures

	Si^{++++}	Al^{+++}	Fe^{+++}	Fe^{++}	Mg^{++}	Ca^{++}	Na^{+}	K^{+}	Ti^{++++}	P^{+++++}	Mn^{++}	C^{++++}		OH^{-}	$S^{=}$	$O^{=}$	
71,6% VG 28,4% 80:20	60,59	14,77	0,36	2,61	1,81	2,64	4,58	4,69	0,34	0,10	0,24	0,12		6,54	0,02	153,12	
Analysis 32	60,59	15,04	0,10	2,10	2,16	2,63	5,58	4,00	0,47	0,10	0,00		Cations	5,04		154,95	Ions
+			0,26	0,51		0,01		0,69			0,24		1,83	1,50	(0,02)		3,53
-		0,27			0,35		1,00		0,13			0,12	1,75			1,53	1,75
												△	+0,08			△	+1,60
82,8% VG 17,2% 80:20	61,35	14,51	0,24	2,41	1,47	2,14	4,81	4,71	0,31	0,10	0,27	0,09		5,34	0,02	154,74	
Analysis 33	61,35	14,89	0,08	1,47	1,57	2,62	5,88	3,88	0,31	0,10	0,37		Cations	5,02		154,97	Ions
+			0,16	0,94				0,83				0,09	2,02	0,32	(0,02)		2,36
-		0,38			0,10	0,48	1,07				0,10		2,13			0,33	2,13
												△	-0,11			△	+0,23
64,4% CCG 35,6% 80:20	62,27	13,96	0,45	1,74	1,66	1,01	5,19	4,76	0,22	0,04	0,01	0,11		6,50	0,03	153,44	
Analysis 34	62,27	15,54	0,04	1,15	1,15	2,35	5,74	4,06	0,21	0,02	0,00		Cations	3,66		156,33	Ions
+			0,42	0,59	0,51			0,77	0,01	0,02	0,01	0,11	2,37	2,84	(0,03)		5,21
-		1,58				1,34	0,55						3,47			2,89	3,47
												△	-1,10			△	+1,74

	Valencies	
	Valencies	
	4,97	
	3,03	
	+1,94	
	Valencies	
	3,91	
	3,57	
	+0,34	
	Valencies	
	7,63	
	7,97	
	-0,34	

correlation improves to values of: Δ cations = -1,01; Δ ions = +2,03; Δ cation valencies = -3,32 and Δ ion valencies = +0,25. This is still unsatisfactory, but it is also known that parts of the nearby Malmesbury outcrops are unusual, amphibolite having been discovered there recently (T. Erlank, personal communication, 1971).

The impressive variation curve of D.L. Scholtz (1946, fig.3) for the regional aspects of the hybridisation phenomena utilised one composite analysis of two hybrid granodiorites. This "granitisation variation curve" contrasted markedly with his "magmatic" diagram (plate XIX), both constructed from the relevant Niggli values. When the Darling hybridisation data are compared on the basis of Niggli values, the new curves are highly irregular and show almost no correlation with those of Scholtz. However, attention must be drawn to the fact that the latest evidence from the Saldanha region (Visser and Schoch, in press; Schoch, 1971, 1966), indicates that two of the plotted hybrids are in Vredenburg granite and one in a correlative of the Cape Columbine granite. At Darling we are dealing with hybrid Darling granite which is correlated with the Hoedjies Point granite of Saldanha. Since the abovementioned granites are of various ages according to preliminary geochronologic ages (chapter IX), although geochemically related, the respective contamination features are only qualitatively comparable. In addition, the author is convinced that comparison on an isovolumetric basis is superior.

The new data were consequently plotted in terms of standard cell values and compared with the recalculated version of the previous data. In order to conform to the previous presentation, parameters similar to Niggli values were employed, namely the number of ions per standard cell for Si^{++++}, Al^{+++}, (Fe^{+++} + Fe^{++} + Mn^{++} + Mg^{++}) = "fm", Ca^{++} and (Na^{+} + K^{+}) = "alk". The results indicate that the poor correlation obtained with Niggli value plots was more apparent than real. This is explained if

it/

it is realised that Niggli values are not suitable for comparison of extreme rock types rich in other components than al, alk, c or fm, with intermediate varieties. Since we have deduced that Malmesbury quartzitic graywacke must have been important during hybridisation reactions at Darling, and probably less so in Saldanha, the isovolumetric curves are bound to be better.

The new curves (fig. 28), show strong similarities with those of Scholtz and corroborate his conclusions. The "alk" values of the new plot are consistently lower than for the older analyses. The higher points on the new curve are due to samples 22 and 23, two analyses of Darling hybrid granodiorite reported by Scholtz. The disparity between the K:Na ratios of older and modern analyses discussed before may therefore apply to total alkalis as well.

A plot of the values discussed above against the standard cell cation content (fig. 29), is not very instructive in view of the rather constant values returned for the components utilised. The high level of "geological oxidation" of these rocks (Barth, 1948) is in line with the previous conclusions concerning the Fe^{+++}: Fe^{++} ratio. The lower values for OH^- ions per standard cell returned for the Saldanha hybrids compared with the Darling rocks may be a function of the greater loss of water from the former, considering the relatively small volume of materials involved at the two Saldanha sample localities and of lower biotite contents in the Saldanha hybrids. The nearly linear relationship of OH^- with "fm" (fig. 30) reflects the association of OH^- with biotite content, but the spread of the values for the Darling hybrid rocks indicates the utilisation of "fm" by anhydrous minerals as well.

Seen from the regional viewpoint several other interesting geochemical features come to light. From the composite analyses it is apparent that a marked trend exists from the older granites to the younger intrusives, displaying a <u>decrease</u> in TiO_2, MgO and FeO, and an <u>increase</u> in SiO_2, Na_2O, CaO and to a

lesser/

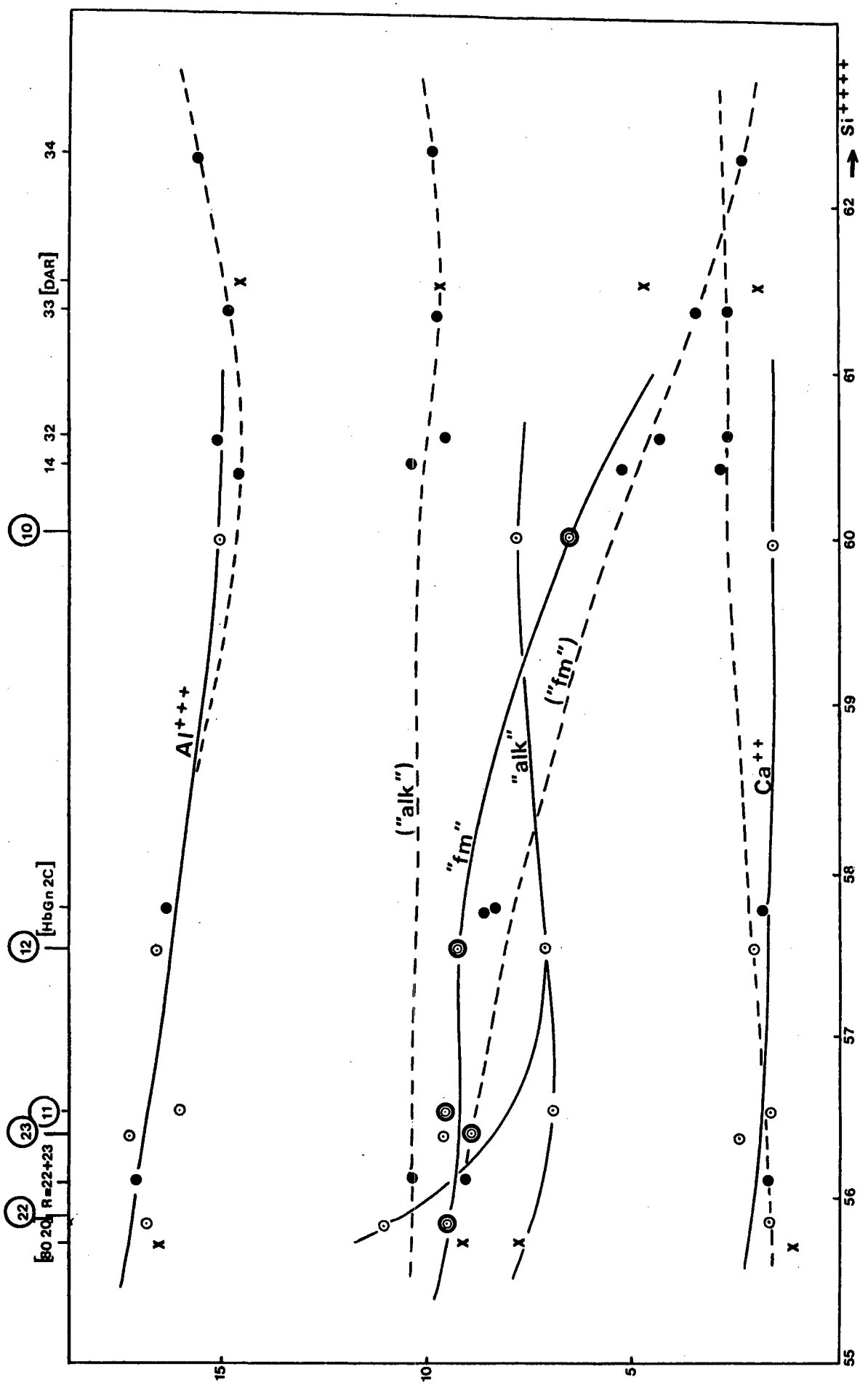

FIG. 28. VARIATION DIAGRAM UTILISING STANDARD CELL VALUES PLOTTED AGAINST [Si] ++++
(Curves for the Darling hybrid rocks shown in bold, compared with regional hybridisation curves based on data from Scholtz, 1946, shown in dashed lines. The data for the 80:20 Malmesbury mixture, DAR and HbGnC2 have been added for comparison, but were not used during construction of the curves).

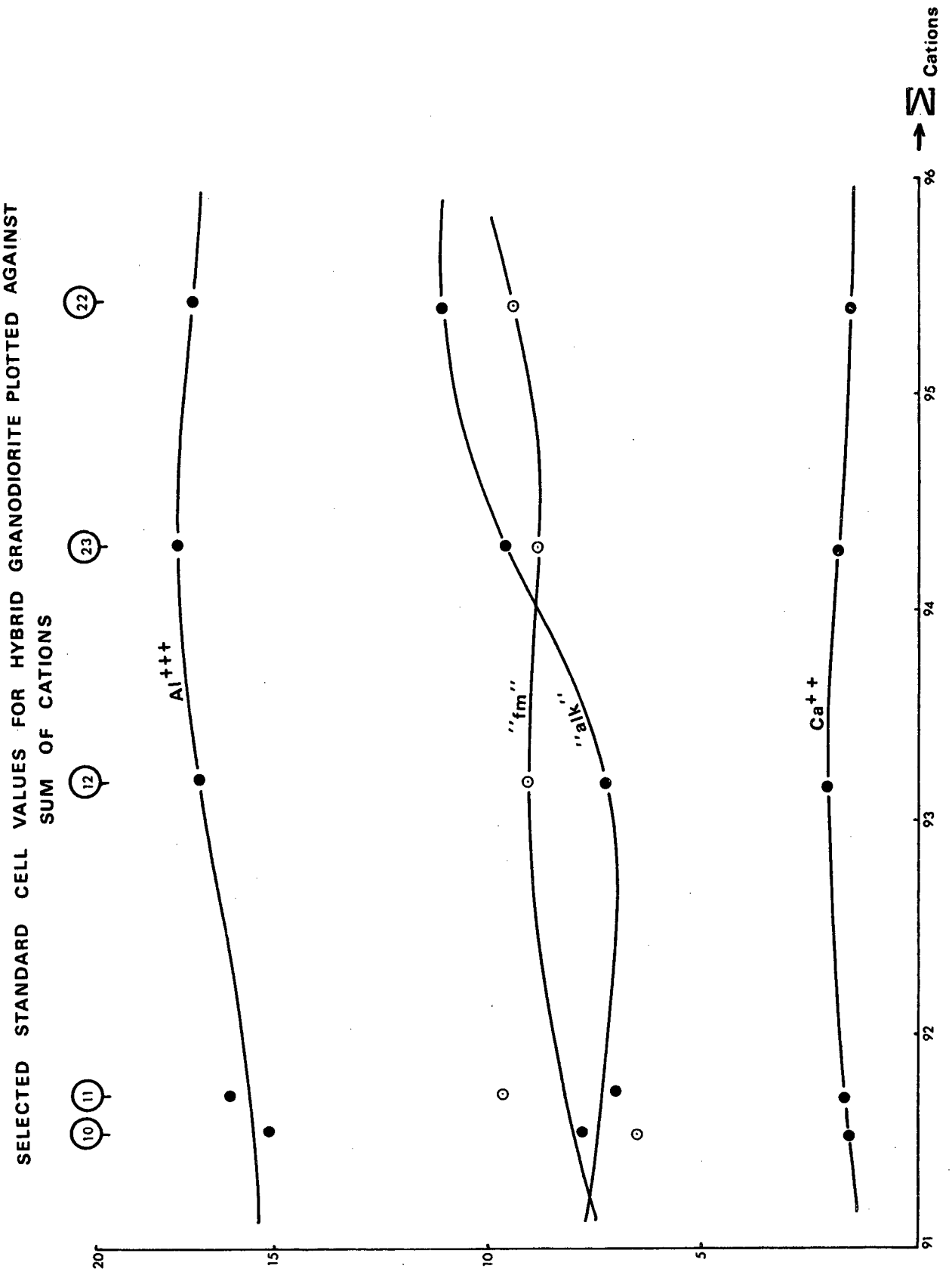

Fig. 29

STANDARD CELL VALUES

FOR OH^- PLOTTED AGAINST

$(Fe^{+++} + Fe^{++} + Mn^{++} + Mg^{++})$

⊙ Darling hybrid rocks

● Recalculated from data given by D.L. Scholtz (1946), for regional investigation of hybridisation

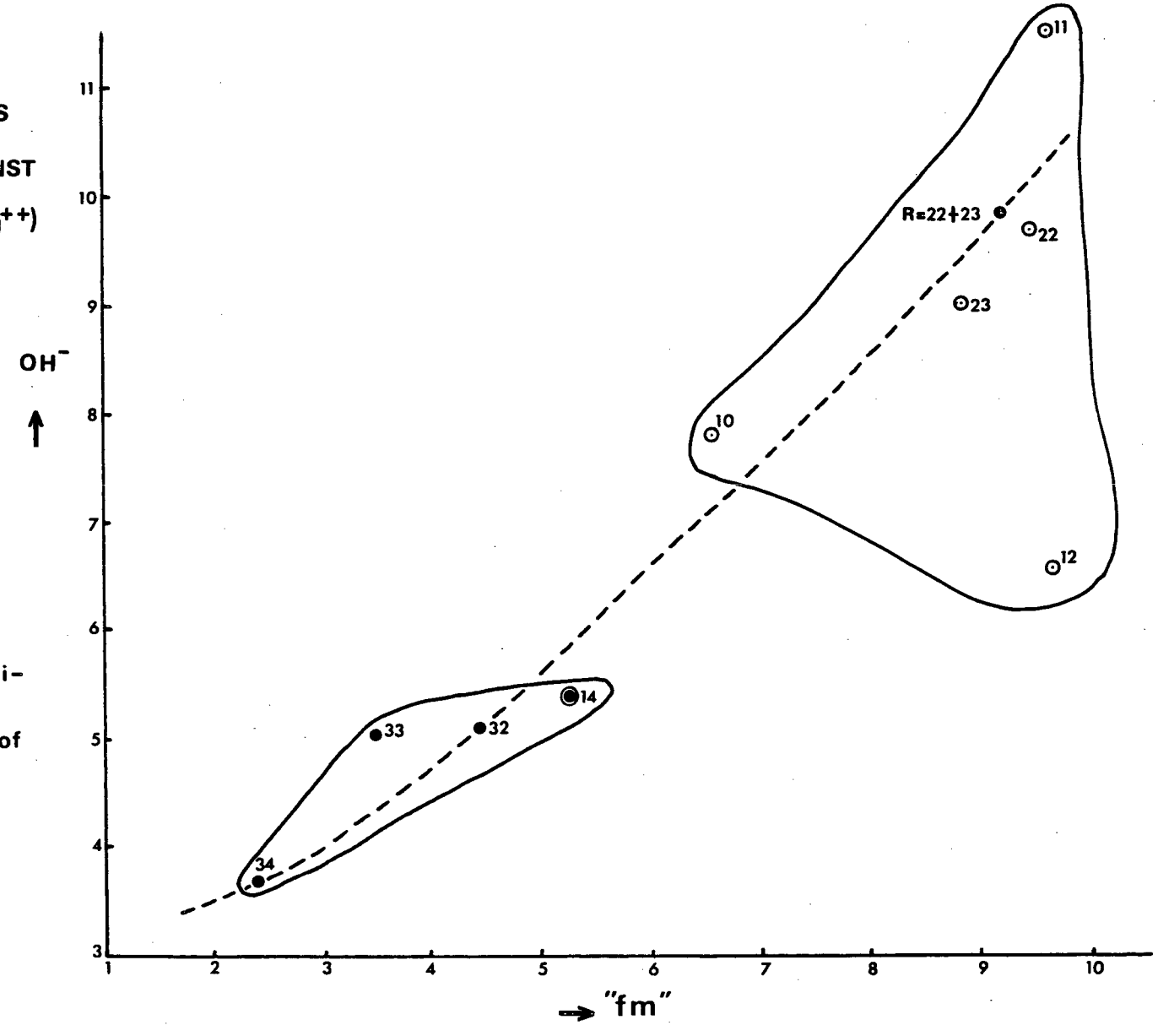

Fig. 30

lesser extent K_2O and P_2O_5. Kolbe (1966) came to similar conclusions on the basis of an impressive array of mineral analyses, trace element determinations and general geochemical information such as K/Rb, Fe/Mg, Ti/Mg and Ti/Fe-trends, but he related his findings to textural variation of the granites only. Such trends will in the main be topologically similar to variation based on age, since the younger intrusives in the Cape are often more fine-grained than older ones, but this is by no means to be taken for granted. Analyses of chill phases and filter-press products will for instance be grouped with much younger intrusives than they should be.

A convenient "differentiation index" can be constructed to summarise the situation, based on the increasing and decreasing components mentioned above. It was decided to employ (FeO + Fe_2O_3 + MgO + TiO_2) and (Na_2O + K_2O + SiO_2) in weight percentages. The resulting trend is shown in figs. 31 and 32, exhibiting a continuous gradation from the older granites on the left to the younger granites on the right. The hybrid phases have higher index values than the corresponding normal granites, while the opposite effect is observed with chill phases.

In fig. 33 the younger and older granites are separated on the degree of silication (Si°) versus degree of acidity (Az°) plot of Burri (1959, p. 76). This merely illustrates that the younger granites are more quartz-rich as well as more siliceous but there is an unexpected gap between the two groups.

The customary method for calculating the silica saturation from Niggli values, is based on the relationship si' (bound silica value) = 100 + 4alk, in the case of ordinary igneous rocks. This is derived from the simplification that most rocks consist of alkali feldspar (alk : al : si = 1 : 1 : 6), anorthite (c : al : si = 1 : 1 : 2) and dark minerals such as diopside, as well as quartz. The bound silica is therefore given by alkali feldspar = 6alk, anorthite = 2(al - alk) and, "diopside" = c - (al - alk) + fm , which adds up to 100 + 4alk (since al + alk + c + fm = 100). A comparison of "normative" feldspar -

dark/

"GRANITE DIFFERENTIATION INDEX" VALUES

PLOTTED FOR REGIONAL GRANITES

(CSM = Cape St. Martin quartz porphyry dykes composite analysis, after data in Otto, 1957)

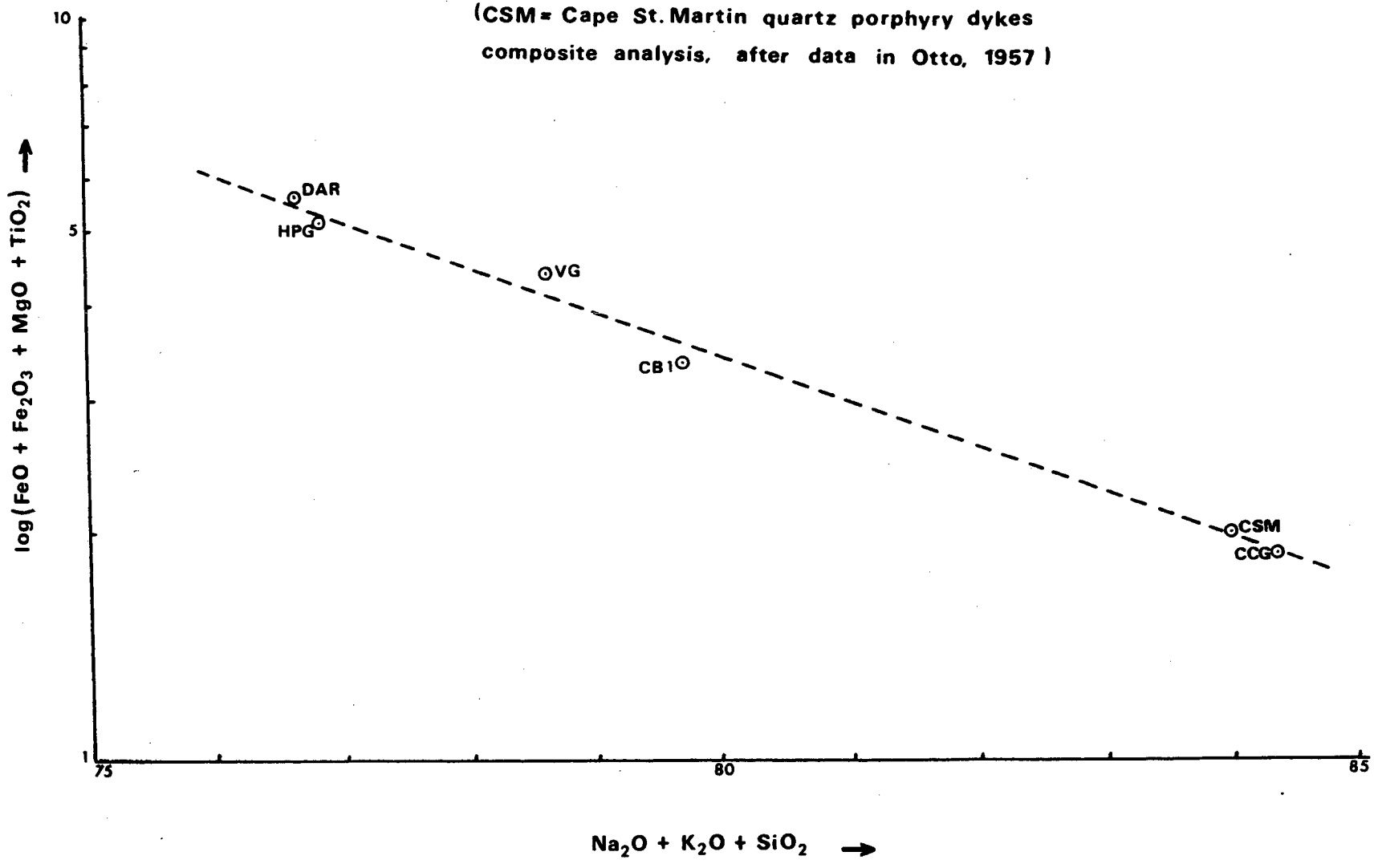

Fig. 31

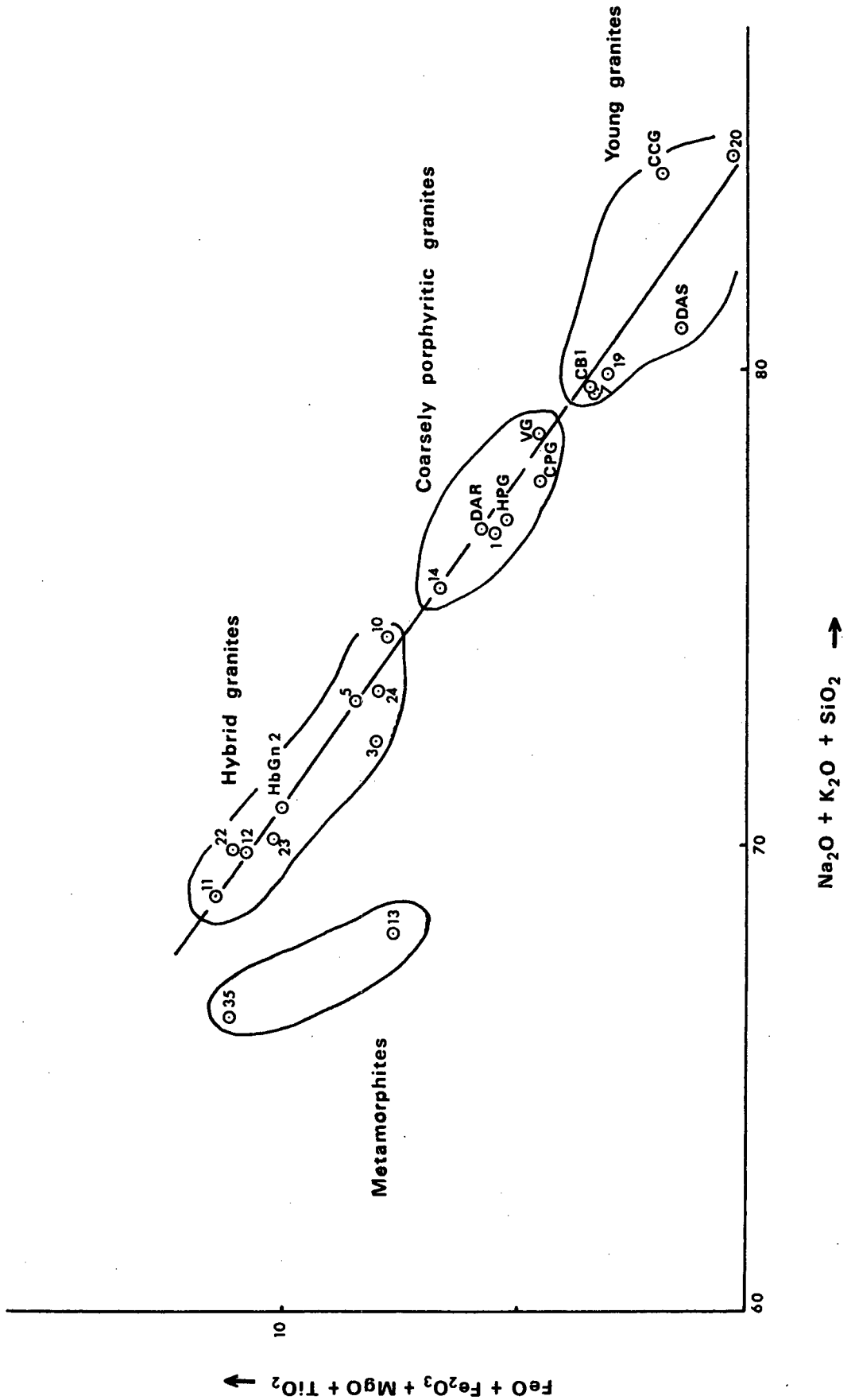

Fig.32

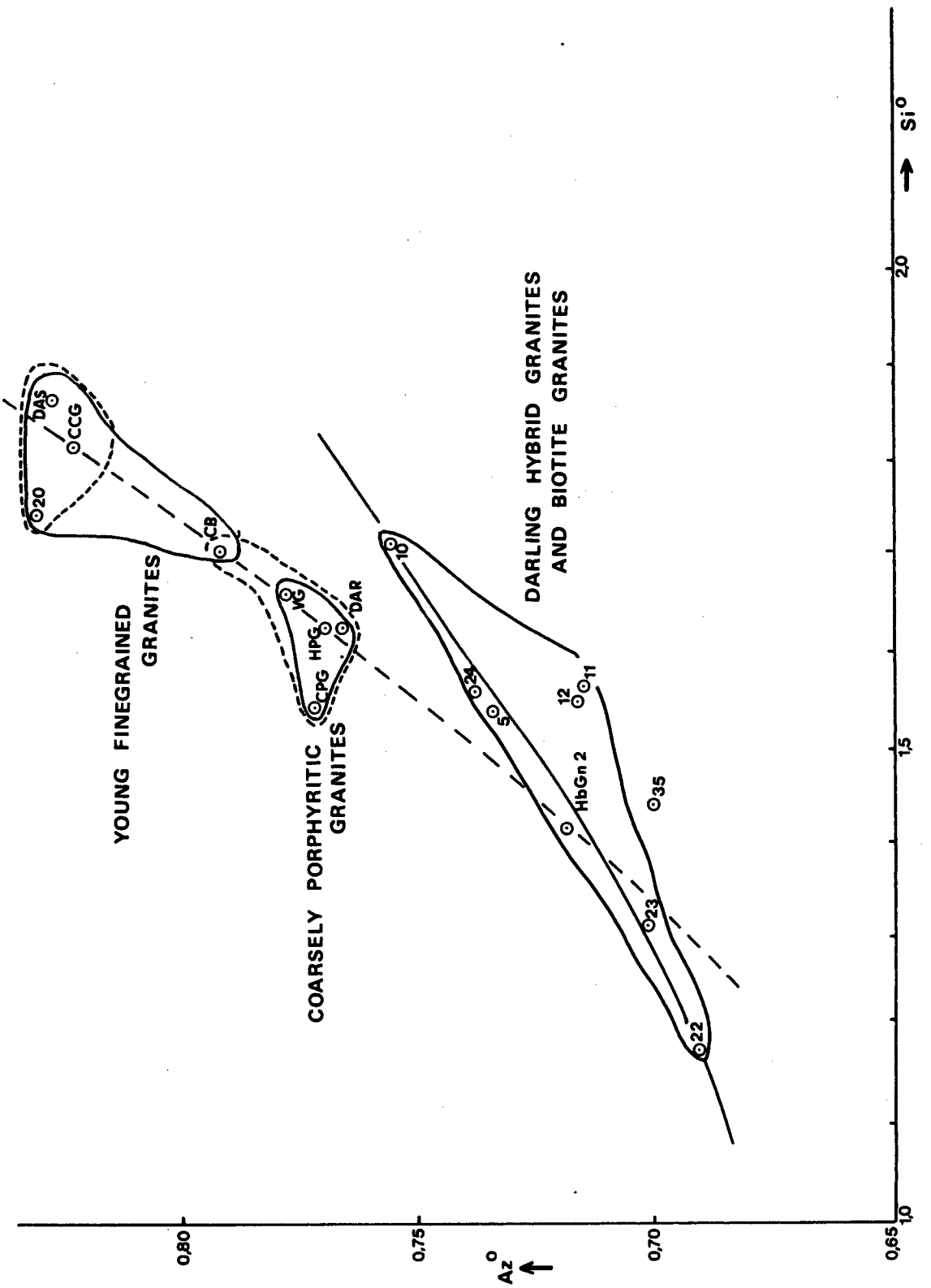

Fig. 33

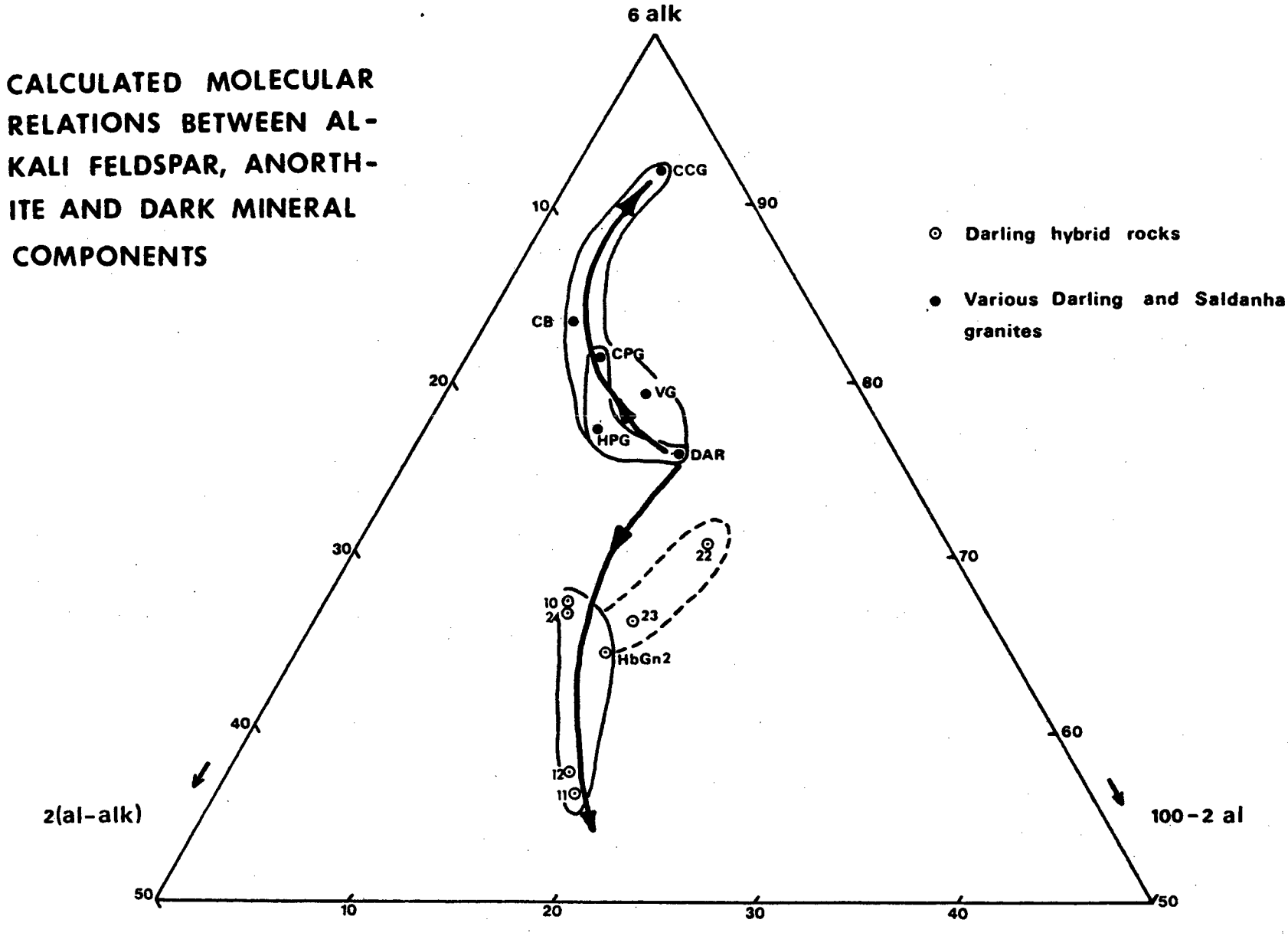

Fig. 34

dark mineral relations, which is of great interest for the understanding of the Darling phenomena, can therefore be obtained by displaying the Niggli values on a triangle with corners 6alk, 2(al - alk) and c - (al + alk) + fm = 100 - 2al.

The resulting plot is shown in fig. 34. The differentiation trend of older to younger granites is once again markedly different from the contamination trend for the Darling hybrid rocks. In the former the alkali feldspar decreases with decrease in age of the granite, the dark minerals are at first constant but then decreases from the older towards the younger granites, with an antipathetic relationship for the anorthite content. Starting from Darling granite, it can be seen that the contamination or granitisation trend is characterised by a decrease in alkali feldspar and an increase in dark minerals and anorthite end member, which merely illustrates the obvious fact that the hybrid rocks became more basic as hybridisation increased. Since alkali feldspars are responsible for most of the large phenocrysts in the granites, the hybrid rocks can be expected to be more finegrained than the parent granite, as is the case (chapter II).

Finally, the regional as well as the local chemical data, are summarised on a standard Niggli diagram (fig. 35).

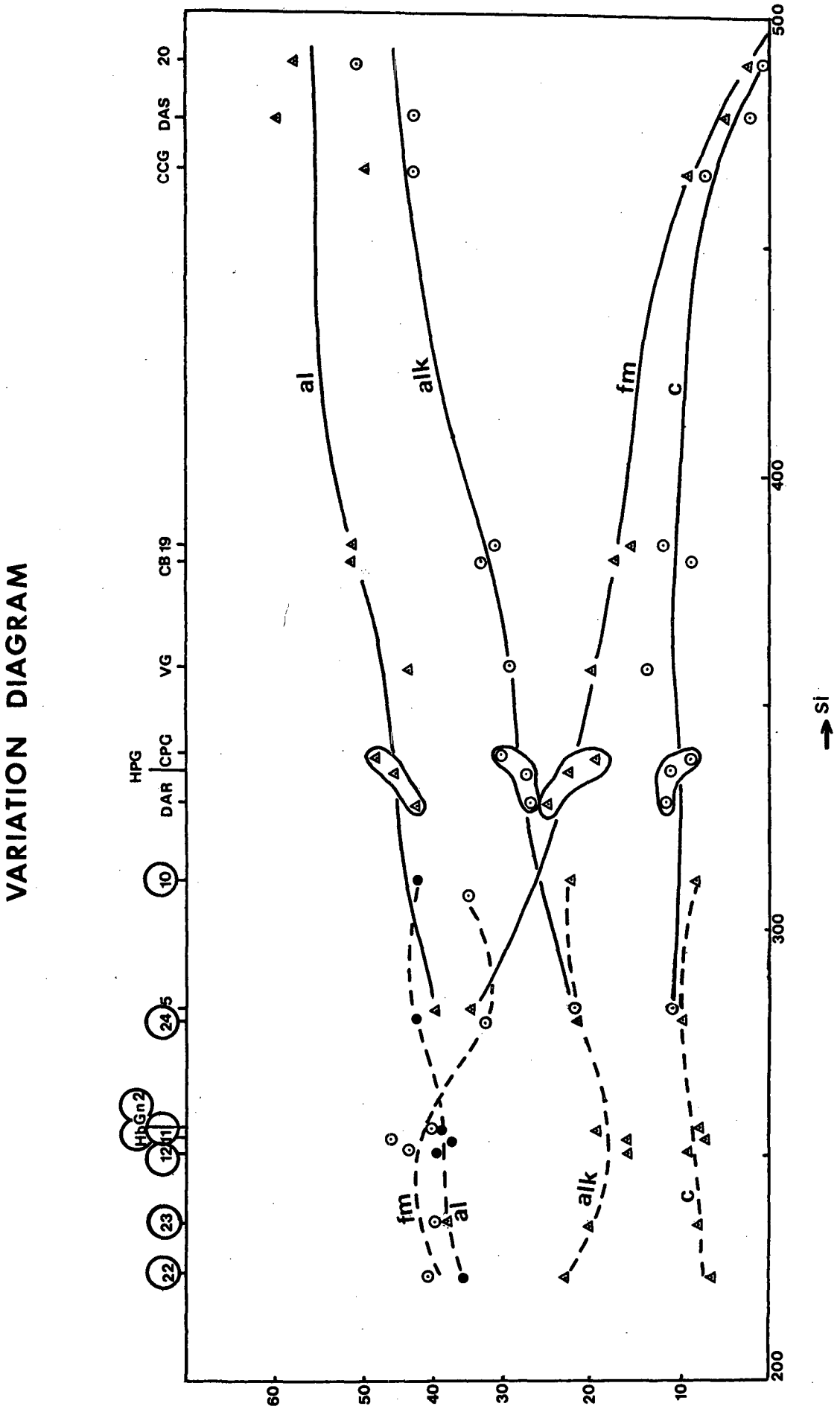

Fig. 35

VII EXPERIMENTAL PETROLOGY

1. Comparison with the experimental granitic system

Because the understanding of the granitic system Quartz - Orthoclase - Plagioclase - Water has reached an advanced stage (von Platen, 1965; Tuttle and Bowen, 1958) it was decided to attempt correlation of the granites under discussion as well as some Saldanha granites with the available experimental results. Since modes have not been determined accurately for the coarsely porphyritic varieties whilst representative chemical analyses are available, appropiate norms will be utilised for this purpose. The most representative data available are the composite analyses (table 6), from which the nearest approach to modes, namely mesonorms and variant mesonorms were calculated.

Several authors correctly advocated mesonorms as the most suitable representations of granites following P. Niggli (Barth, 1959; Kolbe, 1966). These authors were also right in insisting that the normative values should be retained in a molecular form, because of the ease with which variants can be calculated at any stage when needed, as illustrated below by the tourmaline variants for the Contreberg and Dassen Island granites (table 11). The argument to the contrary, in favour of weight percentages, in order merely to preserve the status quo, is not convincing (Chayes and Métais, 1964). The calculated Barth-Niggli mesonorms are therefore listed as molecular percentages (table 11), but all values utilised for plotting on the triangular diagrams were recast as weight percentages. The normative tourmaline and cordierite have the same Mg : Fe ratios as the biotite. Cordierite was formed according to the equation:

$$4C + 5Q + 16/3\ Bi = 11\ Cord + 10/3\ Or$$

The standard mesonorms contain biotite but no cordierite, These standard norms and the cordierite variants constitute two

"end members"/

TABLE 11

Mesonorms of Selected Composite Analyses

	Q	Or	Ab	An	C	Ap	Cc	Mt	Tit	Bi	Di	Ho	Tourmaline	Cord	Py	Ms	Zo	Sum
HPG	31,68	23,04	23,44	6,58	3,20	0,57		0,69	1,03	9,78								100,01
	27,68	25,71	23,44	6,58		0,57		0,69	1,03	5,51				8,80				100,01
DAR	35,20	19,89	20,57	7,43	2,40	0,29	0,23	0,17	1,20	12,63								100,01
	32,20	21,89	20,57	7,43		0,29	0,23	0,17	1,20	9,43				6,60				100,01
CPG	26,98	25,97	26,42	8,38	1,36	0,14		0,34	0,85	8,47			1,08					99,99
	25,28	27,13	26,42	8,38		0,14		0,34	0,85	6,65			1,08	3,74				100,01
OG	30,47	23,03	24,45	6,15	2,73	0,42	0,12	0,42	1,02	10,11			1,08					100,00
	27,06	25,30	24,45	6,15		0,42	0,12	0,42	1,02	6,47			1,08	7,51				100,00
VG	30,71	20,22	28,33	10,20	0,34	0,28	0,11	0,51	0,85	8,45								100,00
	30,29	20,50	28,33	10,20		0,28	0,11	0,51	0,85	8,00				0,93				100,00
CB1	32,71	27,14	23,57	3,98	3,24	0,28	0,23	0,23	0,91	6,64			1,08					100,01
	28,66	29,84	23,57	3,98		0,28	0,23	0,23	0,91	2,32			1,08	8,91				100,01
CB2	33,36	25,90	23,80	4,90	3,15	0,26	0,34	0,25	0,69	6,24			1,08					99,97
	29,42	28,52	23,80	4,90		0,26	0,34	0,25	0,69	2,04			1,08	8,66				99,96
CCG	32,49	26,46	34,35	3,10	0,0			0,68	0,34		0,34	2,08			0,17			100,01
HbGn1	36,00	8,02	19,55	4,60	7,26	0,30	0,34	0,78	1,89	21,25								99,99
	26,93	14,07	19,55	4,60		0,30	0,34	0,78	1,89	11,57				19,96				99,99
	30,84	3,72	19,55			0,30	0,34	0,78	1,89	15,25				12,37		11,27	3,68	99,99
HbGn2	31,80	7,52	24,35	5,00	6,38	0,26	0,22	0,85	1,71	21,89								99,98
	23,83	12,84	24,35	5,00		0,26	0,22	0,85	1,71	13,38				17,54				99,98
	28,08	1,59	24,35			0,26	0,22	0,85	1,71	17,38				9,29		12,25	4,00	99,98
HbGn2C	32,30	7,50	24,00	4,85	6,52	0,30	0,22	0,85	1,71	21,76								100,01
	24,15	12,93	24,00	4,85		0,30	0,22	0,85	1,71	13,07				17,93				100,01
	28,27	2,02	24,00			0,30	0,22	0,85	1,71	16,95				9,93		11,88	3,88	100,01
																Graphite		
SH:QG	35,13	11,68	17,10	0,65	9,42	0,30	0,48	1,83	1,77	21,31					0,22	0,10		99,99
80:20	23,36	19,53	17,10	0,65		0,30	0,48	1,83	1,77	8,75				25,90	0,22	0,10		99,99

"end members" between which the true mineralogical compositions of the rocks are situated. The biotite contents of all the cordierite variants are slightly too low whilst the standard norms are incorrect as well since considerable amounts of cordierite are present in the rocks. Some of the corundum used in the abovementioned reaction certainly represents aluminium which substitutes for silicon or ferric iron. However, for some of the rocks the cordierite variants are quite near to the mode. As an illustration it may be mentioned that the quartz content of a Darling granite is 34,5 weight percent as determined by quantitative X-ray diffractometry which correlates well with the value of 33,91 weight percent Q in the cordierite mesonorm. (The corresponding standard mesonorms has Q = 37,02%). Correlation of the abovementioned mesonorms with modes can never be absolute because the pinitisation of cordierite and saussuritisation of plagioclase have not been taken into account. Accordingly the muscovite-zoisite variants were also calculated for the hybrid granodiorite, according to the relationship:

$$20\ An + 5\ Or = 7\ Ms + 16\ Zo + 2\ Q$$
$$\underline{33\ Cord + 40\ Or = 42\ Ms + 16\ Bi + 15\ Q}$$
$$20\ An + 33\ Cord + 45\ Or = 49\ Ms + 16\ Zo + 16\ Bi + 17\ Q$$

The results (table 11) correlate well with the mode for average hybrid granodiorite reported in chapter IV, except that biotite is a little too low. The biotite values for all the norms can be raised between 0,2 and 0,8 % by using the reaction relationship:

$$9\ Mt + 5\ Or = 6\ Hm + 8\ Bi$$

which is permissible since most of the ore specks are in fact associated with the biotite. Primary hematite is not present in most of the rocks but the ferric iron can enter various silicate structures by ionic substitution.

Enough has now been said to demonstrate that the mesonorms can supply a satisfactory basis for discussion of the quantitative

mineralogy/

mineralogy. An alternative approach to the direct determination of modes of coarsely porphyritic granites by point counting would be to utilise the representative powders painstakingly prepared for chemical analysis, and to measure the X-ray modes. This method requires the preparation of standards and the elimination of preferred orientation of flaky minerals; it was not attempted owing to lack of time.

The mesonorms were used to calculate the Q - Or - Ab - An proportions (table 12). The compositions of the various granites are shown in fig. 36 which illustrates the Q - Or - Ab - An - (H_2O) tetrahedron projected on the Q - Or - Ab surface (after von Platen, 1965). The values derived from the standard mesonorms are shown as solid triangles and the data for the cordierite variants as open triangles. The true position of each granite would be somewhere between these extremes. It is remarkable that DAR and CB both plot on or near their relative cotectic surfaces which form the boundaries between the silica and plagioclase phase volumes. A similar coincidence with the potash feldspar - silica equilibrium surface appears to apply in the case of CCG. The plots for HPG and VG seem to lie within the plagioclase phase volume. Only VG is situated far from the relevant cotectic surface but would coincide with it if 10 equivalent percent of phenocrysts are removed (6m in fig. 36). (The phenocrysts were subtracted in the ratio K - feldspar : plagioclase = 2 : 1 and it was assumed that the potash feldspar holds 25 % Ab and the plagioclase 30 % An). This could mean that the phenocrystal cores are in disequilibrium with the matrix, as also indicated by zonal structures, but in any event the abnormal nature of VG with respect to the other granites is once again demonstrated. Of all the granites, only the finer-grained young granite CB is close to the relevant "minimum melt" composition.

Magmas are suspensions consisting of crystals and liquids and consequently a fair percentage of phenocryst cores must have formed under different P - T conditions than the matrix.

In/

TABLE 12

Q-Or-Ab Values (weight percentage)

		Q	Or	Ab	Ab/An
HPG	S	43,13	29,03	27,84	3,36
	C	38,48	33,09	28,43	
	H	38,67	32,76	28,57	
DAR	S	49,19	25,73	25,08	2,61
	C	45,73	28,78	25,49	
	H	45,79	28,70	25,52	
CPG	S	36,42	32,46	31,12	2,97
	C	34,42	34,20	31,38	
	H	34,50	34,04	31,46	
OG	S	41,67	29,16	29,17	3,75
	C	37,68	32,61	29,70	
	H	37,79	32,41	29,79	
VG	S	41,42	25,25	33,34	2,62
	C	40,94	25,65	33,41	
	H	41,09	25,39	33,53	
CB1	S	41,72	32,05	26,23	5,58
	C	37,29	35,95	26,76	
	H	37,35	38,85	26,80	
CB2	S	42,71	30,70	26,59	4,58
	C	38,41	34,47	27,11	
	H	38,48	34,36	27,16	
CCG	S	34,47	33,74	31,79	10,44
	H	37,52	27,88	34,61	
80:20	S	57,72	17,77	24,51	24,82
	C	41,45	32,08	26,47	
	H	42,15	30,92	26,92	
HbGn1	S	59,52	12,28	28,20	4,00
	C	41,84	22,85	29,92	
	H	47,57	22,30	30,13	
	M	60,07	6,71	33,22	∞
	HM	60,54	5,98	33,48	
HbGn2	S	53,00	11,60	34,40	4,59
	C	41,84	20,87	37,30	
	H	42,16	20,26	37,58	
	M	55,28	2,90	41,82	∞
	HM	55,76	2,06	42,18	
HbGn2C	S	53,67	11,54	34,79	4,66
	C	42,32	20,98	36,70	
	H	42,65	20,37	36,98	
	M	55,35	3,66	40,99	∞
	HM	55,82	2,83	41,35	

S = Standard mesonorm
C = Cordierite variant
H = Hematite-cordierite variant
M = Muscovite (illite)-cordierite variant
HM = Hematite-muscovite-cordierite variant

MESONORMATIVE VALUES PLOTTED IN THE SYSTEM
Q - Or - Ab - An - (H_2O)

▲ : Standard mesonorm △: Cordierite variants e: Eutectic

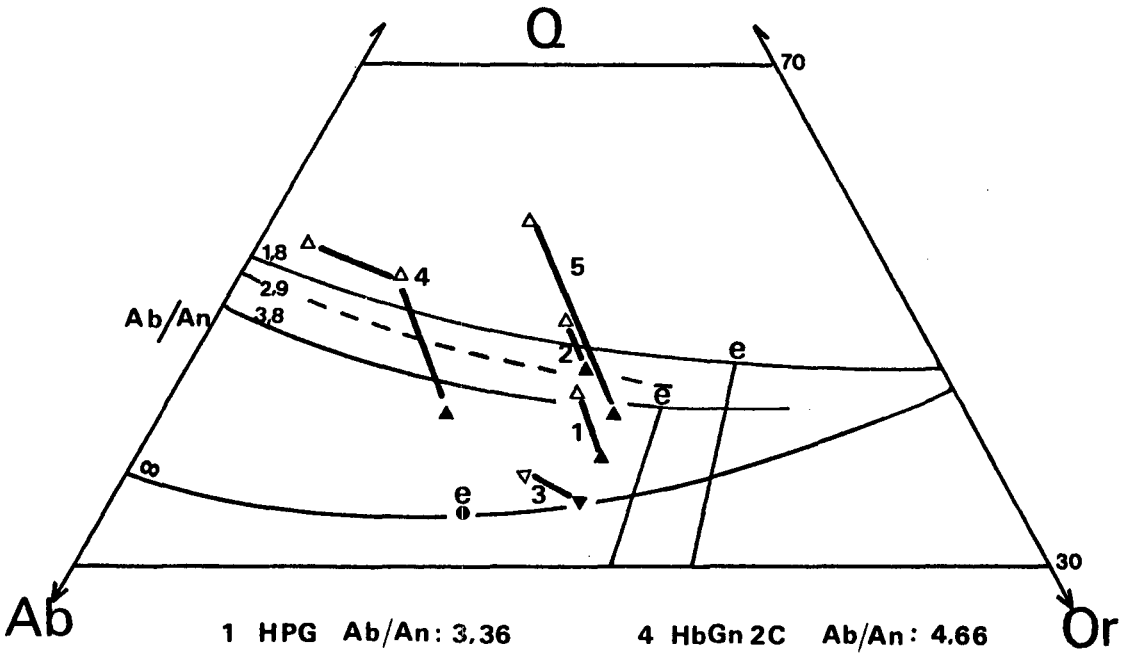

1 HPG Ab/An: 3,36
2 DAR Ab/An: 2,61
3 CCG Ab/An: 10,44
4 HbGn 2C Ab/An: 4,66
5 80 : 20 Ab/An: 24,82

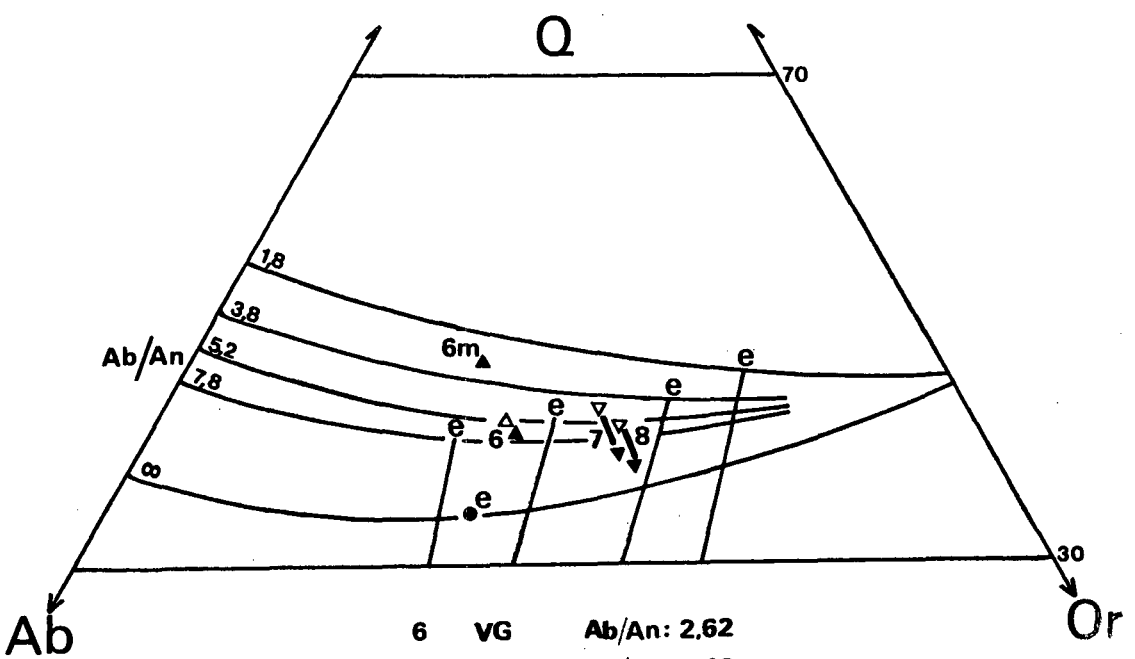

6 VG Ab/An: 2,62
6m VG matrix Ab/An: 2,49
7 CB2 Ab/An: 4,58
8 CB1 Ab/An: 5,58

Fig. 36

In special cases they may even represent xenocrysts from the deep crustal source material where the magma was generated by anatexis or palingenesis. What is remarkable about the data presented above is therefore not the lack of correspondence, as possibly for VG, but that there is a correlation at all. It should be realised that von Platen's diagrams are based on a pressure of 2 000 b in the presence of excess water. That this was in fact the case for all the intrusions discussed is unlikely. Convincing arguments were also recently forwarded that granite magmas may not be water-saturated at all, since they may not have been generated on minimum melting curves but at slightly higher temperatures controlled by the intersection of the stability curves of hydrous minerals in the source rocks with the prevailing geothermal gradients (Burnham, 1967; Brown and Fyfe, 1970). Much more evidence will have to be gathered for the rocks under consideration before truly quantitative answers can be given. One step in this direction would be melting experiments on representative samples of Cape granite.

2. Melting experiments : a pilot study

Since the bulk composition of one of the younger granites, CB, seems to approach "minimum melt" proportions, whilst the older granites approximate divariant compositions, it was decided to test this possibility by direct measurement. Representative material was available in the form of powdered granite prepared with great care for chemical analysis. The powders are exceedingly fine-grained, making microscopic study of the experimental products impractical though presenting a distinct advantage from the viewpoint of attainment of equilibrium. Nevertheless, phenomena such as rounding of grains and appearance of globules of siliceous glass could be observed. Since funds for platinum tubes were not available at this stage, the runs had perforce to be made in silica glass tubes which were closed under vacuum with an oxygen-hydrogen flame. The

expected/

expected reaction with the container proved to be surprisingly slight but increased somewhat in the higher temperature runs. It is emphasized that this work represents a feasibility study designed to compare two samples treated under identical conditions and that it will be followed by more accurate work in platinum with oxygen fugacity control. The runs were of long duration and exceeded the 30 days recommended by Whitney and Luth (1970) by far.

It was decided to apply the quantitative X-ray diffraction technique of Otálora and Hess (1969) and Bristol (1968) for the determination of the modes of fine-grained rocks such as mylonites and volcanites to the experimental products. During gradual melting the major minerals in a granite can be expected to melt together until relatively high temperatures are reached so that the percentage of any one of them in the products of a run will be roughly proportional to the amount of melting. Quartz was selected as indicator mineral as it is easy to determine quantitatively if care is taken with grain size of the powder, and because no other polymorphs of silica were detected by high resolution X-ray diffraction in any of the experimental products. This seems surprising, but there was no sign of high, intermediate or low tridymite, high cristobalite, keatite, or even high quartz in the X-ray diffraction spectra. Low cristobalite is difficult to recognise since the two solitary very intense peaks are obscured by the base of a prominent low quartz and feldspar peak respectively, but if present, it was higher in the original samples than in the products. High quartz must have formed in most of the runs but evidently reverted to low quartz during quenching; this transition is known to be exceedingly rapid. Tridymite would apparently not have formed during the experimental conditions considered here although the conversion temperature for the pure silica system at 1 bar is 870°C. The silica glass tubes used can easily withstand pressures of up to 5 bars, and the pressure during the high temperature runs would certainly have

exceeded/

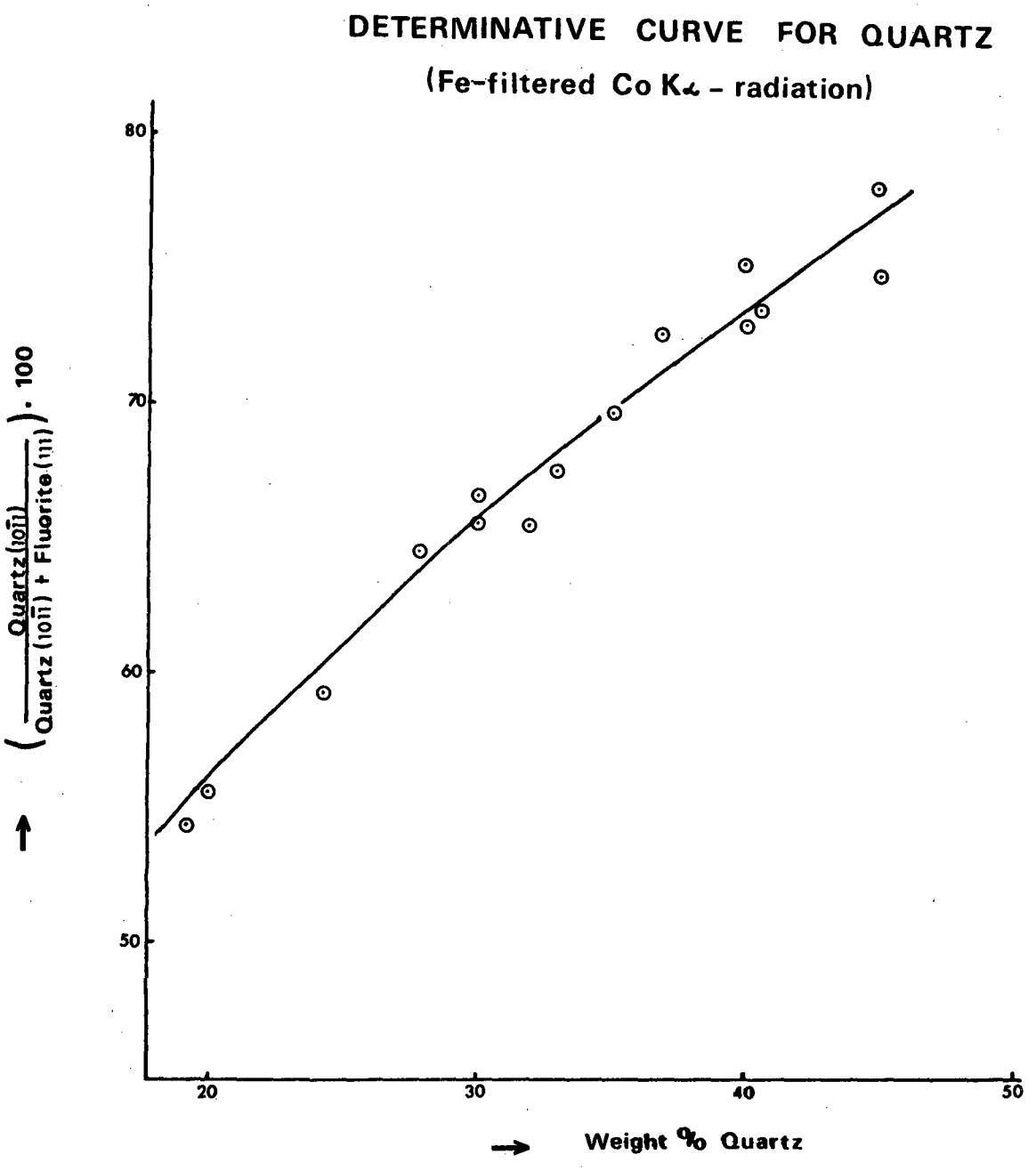

% Quartz	Ratio	Std. error of mean
19,200	54,20	1 ,33
24,610	59,23	0 ,85
30,010	66,54	0 ,78
30,013	65,74	1 ,22
32,980	67,59	0 ,81
36,997	72,80	0 ,84
40,400	74 ,77	0 ,62
39,990	75 ,30	0 ,90
40,004	73 ,04	0 ,98
44,99	74 ,88	0 ,82

Fig. 37

exceeded 1bar owing to internal addition of water during the breakup of biotite and amphibole.

As internal standard 20 weight percent fluorite was added and preferred orientation was minimised by utilisation of a side-packing procedure. Samples were packed several times and no result was accepted before the value for the standard error of the mean ($\sigma/\sqrt{n}$) was satisfactory. Counts were taken by scanning at maximum resolution over the quartz ($10\bar{1}1$) and fluorite (111) peaks which are respectively situated at $2\theta = 31{,}1°$ and $2\theta = 33{,}0°$ respectively for CoKα radiation. Standards were made up by adding pure quartz to a synthetic granite base consisting of pure maximum microcline, plagioclase (An_{60}) and biotite (chlorite-free) mixed in a ratio of 11 : 4 : 1 by weight. The standards held 20, 25, 30, 33, 37, 40 and 45 weight percent quartz and the resulting determinative curve is shown in fig.37. Before utilising the curve for the experimental products it was tested on chemically analysed powdered granites. The value for a sample of Cape Columbine granite, prepared for analysis and taken by J.R. McIver at a point 6,1 m from the Slippers Bay contact, yielded a value of 34,80 $\pm$ 1,50 weight per cent quartz, which is 1,89 percent less than the weight mode equivalent of the published value obtained by conventional point counting (McIver, 1957, p. 552, C). The X-ray modal values for quartz in the Darling area samples submitted for analysis in 1971 are listed in table 13.

The furnaces employed have excellent thermal characteristics with thyristors as switching devices and chromel-alumel thermocouples for both control and measuring. The results of the preliminary experiments are tabled below:

Sample/

Sample	°C	Modal quartz, weight %	Quartz loss, weight %	Time span of run (days)
DAR (1)	-	35,1 ± 1,0	-	-
	670,5 ± 1,0	33,7 ± 1,5	3,99	87
	700 ± 1,0	33,6 ± 1,0	4,27	105
	806 ± 2,6	27,0 ± 3,0	23,08	88
	900 ± 3,1	16,0 ± 2,9	54,42	72
CB (7)	-	34,1 ± 0,7	-	-
	700 ± 1,0	35,8 ± 1,2	0	105
	806 ± 2,6	34,3 ± 2,1	0	88
	845 ± 1,0	30,2 ± 2,8	11,70	87
	900 ± 3,1	18,9 ± 3,2	44,60	72

The slope of the relevant P - T curve is much steeper for the older, coarsely porphyritic Darling granite than for the younger Contreberg granite (fig. 38), since the figures for the weight per cent quartz loss are 0,2/°C and 0,5/°C respectively. The younger granite is therefore nearer to a minimum melt composition than the older granite as expected, although it starts to melt at a higher temperature, which remains unexplained. The water released by the breakdown of biotite plays an important rôle in the melting process (Brown and Fyfe, 1970), but both granites have approximately the same biotite content. In any event, the percentage of melting deduced here would represent maximum values because of addition of a small amount of silica from the container.

TABLE 13

X-ray Modal Values for Quartz
(New Analyses, Table 3)

		Weight % Quartz (± 1,5)	Weight Mode
1	Darling granite	35,1	
2	Darling granite	33,9	
3	Mylonite	22,7	
4	Mylonite	35,9	
5	Biotite granite	34,5	
6	Contreberg granite	31,0	
7	Contreberg granite	34,1	
8	Dassen Island granite	35,7	
9	Dassen Island granite	36,9	
10	Hybrid granodiorite	38,9	28-36
11	Hybrid granodiorite	34,1	
12	Hybrid granodiorite	32,7	
13	Xenolith	41,1	
	Mylonite (A.E. Schoch, 1962, table 4 no.1)	38,7	
	Cape Columbine granite (McIver, 1957, table IIa no. 6; table I, C)	34,8	36,69

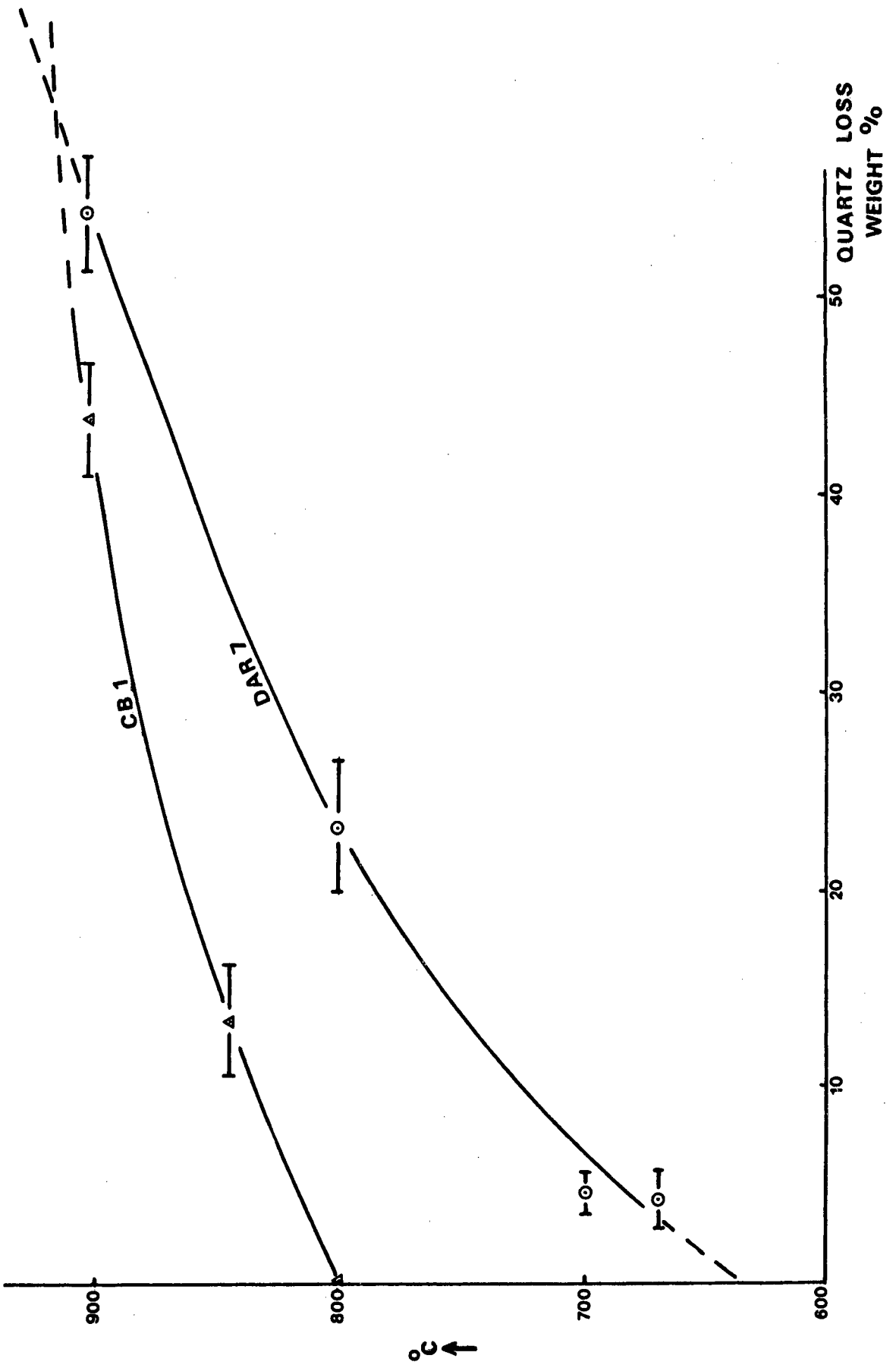

Fig. 38

VIII THERMODYNAMICAL CONSIDERATIONS

The reconstruction of the thermodynamical intensive variants responsible for the phenomena observed at Darling can only be attempted when much more evidence of a detailed nature is available, but certain qualitative deductions are possible. Comparison with a Schreinemakers diagram for granitic rocks developed by Korzhinskii (1959), may be instructive. This synthesis was based on a study of the Archaean complex of Pribaikalie, and seven major phases were considered, namely quartz, orthoclase, plagioclase, biotite, hornblende, pyroxene and hypersthene. Since H_2O may be regarded as completely mobile, the number of minerals equals the number of components, which means that the total paragenesis is invariant at constant temperature and pressure in terms of the phase rule, and that the minerals must have fixed compositions. The plagioclase was taken as An_{33} and the FeO:(FeO + MgO) ratio of the dark minerals as 45,40,20 and 25 for biotite, hornblende, pyroxene and hypersthene respectively. Complete isomorphism between FeO and MgO was assumed.

The constant intensive variants of the system are therefore pressure, temperature, and μH_2O. The construction of the Schreinemakers plot is easily achieved by means of the bundle matrix defined by the assumed compositions of the major phases, provided that K_2O and Na_2O are regarded as mobile components. In the author's opinion this popular assumption is controversial when applied without discrimination, and especially when used to explain phenomena of regional extent, as is indicated by modern studies on K^+ diffusion rates (e.g. Sippel, 1963), although the institution of equilibria based on vapour phase transport of alkalis can be locally important (Orville, 1963). However, when used with caution such chemical potential diagrams can provide much useful information. In the case considered here it is in fact a thermodynamically more precise presentation than plots based on K_2O:Na_2O weight percentages ratios (chapter VI). The inert components in Korzhinskii's synthesis are SiO_2, Al_2O_3,

CaO/

SCHREINEMAKERS DIAGRAM FOR GRANITE UTILISING CHEMICAL POTENTIALS OF K_2O AND Na_2O (After D.S. Korzhinskii)

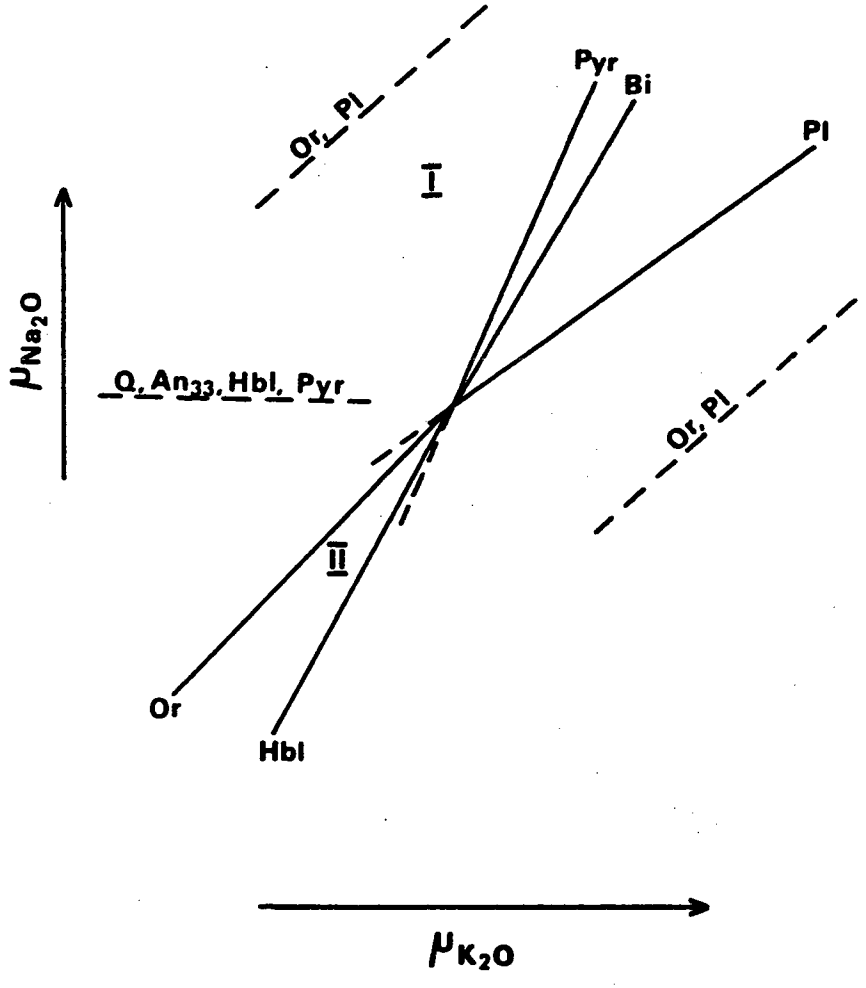

Stable parageneses in fields I and II

I
- Q + Or + Pl + Bi
- Q + Pl + Bi + Hbl
- Q + Pl + Hbl + Pyr

II
- Q + Or + Pl + Bi
- Q + Pl + Bi + Pyr
- Q + Bi + Hbl + Pyr
- Pl + Bi + Hbl + Pyr

[The Q monovariant curve is not shown since only silica-saturated rocks are taken into account]

Fig. 39

CaO, and (MgO + FeO). Amongst the accessory minerals not taken into consideration, magnetite is the most important, and present in all parageneses. The Schreinemakers plot is shown in fig.39.

For purposes of comparison it would be interesting to correlate the theoretical plots with the actual K_2O-Na_2O values for selected Darling-Saldanha granites. The relationship between chemical potential (μ), and concentration of components is given by $\mu_i = \mu^\circ_i + RT \ln N_i f_i$, where $N_i f_i$ is the activity of component i, f the activity coefficient, and $N_i = n_i/(n_1 + n_2 + \ldots\ldots + n_c) = n_i/\sum_i n_i$ if n is given in moles. Since the basic relationship is linear, a plot of $N_i f_i$ values for the alkalis of the granites under consideration would supply the necessary information, but even a graph of N_i data alone would have qualitative value.

The values used for the samples plotted in fig. 25 (chapter VI, the Harpum diagram), were recalculated as naperian logarithms of weight percentages (fig. 40). The same information is displayed as naperian logarithms of molecular percentages in figure 41. On basis of the arguments advanced above , figure 41 can therefore be qualitatively compared with the Schreinemakers diagram which employs a plot of the $\mu_{Na_2O} : \mu_{K_2O}$ ratio (fig. 39).

The majority of the Darling-Saldanha granites considered, have major mineral parageneses of quartz - orthoclase - plagioclase - biotite (Q - Or - Pl - Bi). Most of the plotted points in figure 41 will therefore probably lie to the left of the invariant point in figure 39, that is, in fields I and/or II, which are the fields of the normal granitoids. A different paragenesis has to be considered for the Vredenburg granite (VG), which holds minor amounts of hornblende (Hbl) in addition to the phases mentioned above. . There is a possibility that this granite actually exhibits more than one divariant paragenesis, for instance (Q + Or + Pl + Bi) plus (Q + Pl + Bi + Hbl) or a monovariant paragenesis (Q + Or + Pl + Bi + Hbl), represented by the

Pyr/

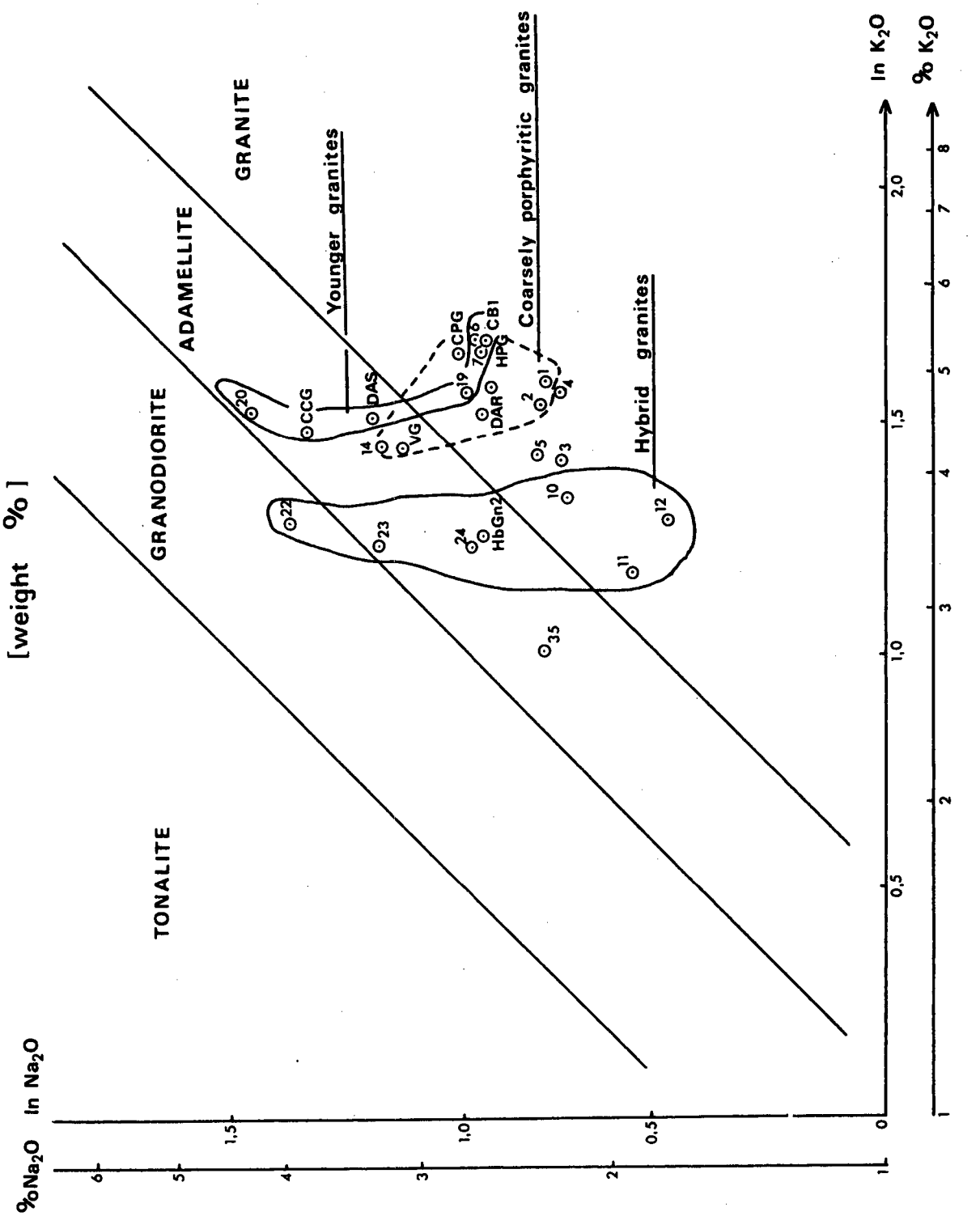

Fig. 40

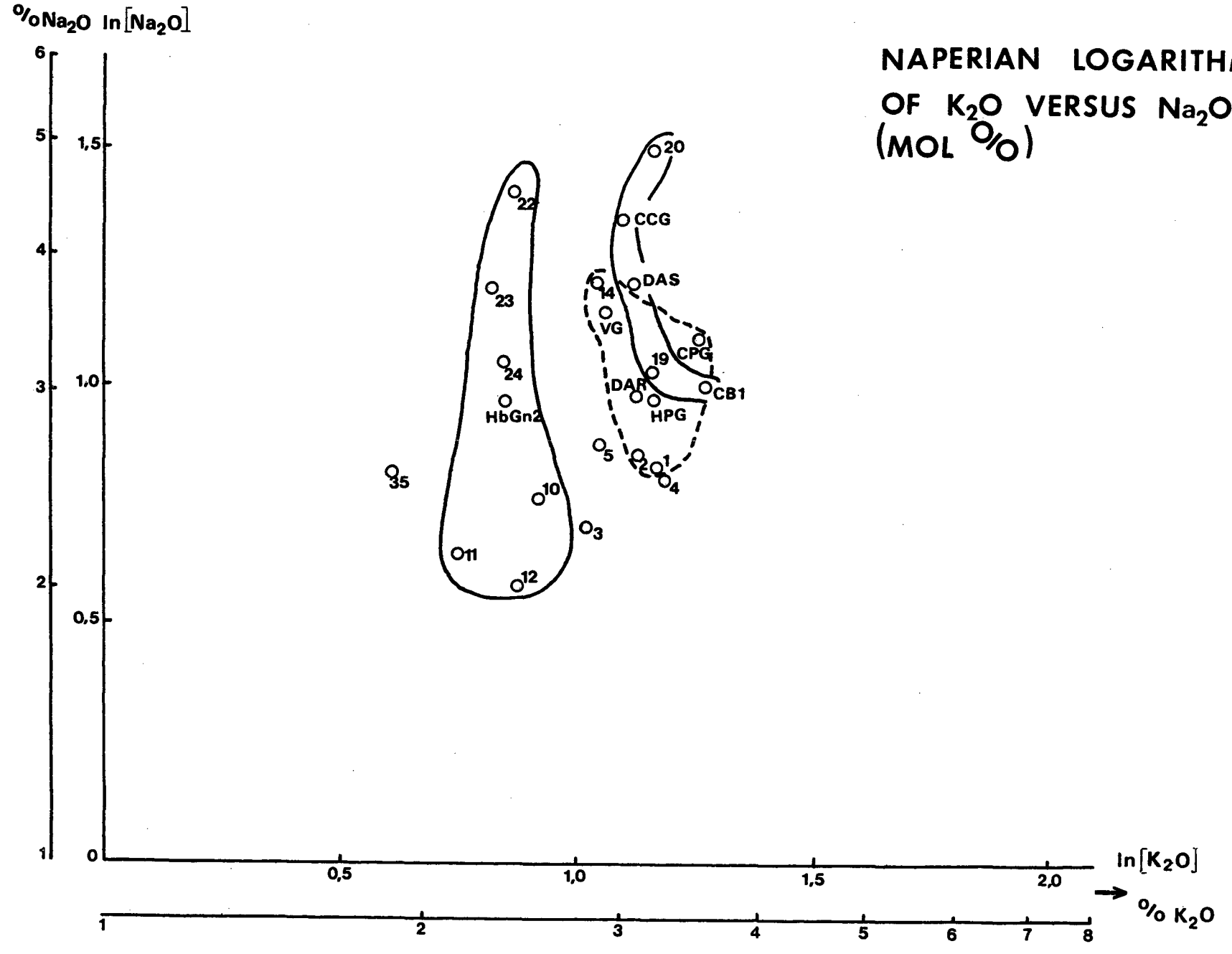

Fig. 41

Pyr curve in figure 39. However, the chemical and mineralogical data available for this granite are still too scant for any firm conclusion to be drawn.

Strictly speaking the hybrid granites should not be taken into account when comparing figures 41 and 39, since cordierite enters as a major phase and was not considered during construction of the Schreinemakers diagram; its presence would affect the slopes of all the curves.

The diagrams deal with constant temperature, pressure and H_2O conditions, which would not have been the same for the older and younger granites. Consequently the positions of these two groups of intrusives on the plots will have to be shifted with respect to each other on a truly quantitative representation, since the invariant point must be at different positions for the two sets of data.

Any curve representing (Or + Pl) has a slope of 45°, because $nCaAl_2Si_2O_8 \cdot mNaAlSi_3O_8 + (\frac{1}{2}K_2O) = nCaAl_2Si_2O_8 \cdot (m-1)NaAlSi_3O_8 + KAlSi_3O_8 + (\frac{1}{2}Na_2O)$ and $d\mu_{Na_2O} : d\mu_{K_2O} = 0$ at constant T and P, $d\mu_{Na_2O} : d\mu_{K_2O} = 1$ (Korzhinskii, 1959). The paragenesis (Q + Pl + Hbl + Pyr) is represented by a horizontal line, since no K_2O is required. In figure 39 plagioclase of An_{33} was assumed, consequently the lines representing (Or + An_{33}) and (Q + An_{33} + Hbl + Pyr) must pass through the centre of the bundle, and those for associations with more basic plagioclase will lie to the right and below the invariant point. A similar argument holds for the equilibrium lines (Q + Pl + Hbl + Bi) and (Q + Pl + Pyr + Bi), which are nearly horizontal.

The average plagioclase of the hybrid products is more basic than for the granites (chapter IV), but the plotted positions in figure 41 are in agreement with the above arguments only if it is assumed that the newer analyses (10, 11, 12) are correct and the older ones (22,23) incorrect. It is also clear that the dark minerals have a greater influence on plagioclase composition than does K-feldspar. More cannot be deduced at the moment

since/

since too little is known of the P-T conditions, the constancy of which could have been violated during the establishment of the zonal feldspars and this would have had an opposite effect to the one suggested.

In the case of the younger granites, it is evident that the clearly displayed trend of Na_2O-enrichment from CB1 to sample 20, crosses a relatively small number of the possible lines of 45° slope. A significant trend in the average anorthite content of plagioclase can therefore not be expected. The observed trend must be ascribed mainly to a change in the orthoclase-plagioclase ratio. The initially gradual slope from CB1 to sample 19 can be explained by a decrease in biotite content.

The artificial nature of a nomenclature of granites based on K_2O-Na_2O ratios only, as in Harpum-diagrams (figs. 25,40), is exposed by the above considerations. Classification of fairly complex systems on such a restricted basis as a few parameters would be of value for petrogenetic purposes only when firmly rooted in thermodynamical theory, according to which the assumptions (constant factors) are always clearly stated. From this viewpoint the μ - μ diagrams have considerable merit. The author doubts, however, whether K_2O and Na_2O can be regarded as mobile components over batholithic dimensions. Trends constructed for multiple batholiths, based on changes in the alkali ratio with time, and which are so popular in current literature (cf, "Granite 71", Symposium, Salisbury, September 1971, to be published), may perhaps be a reflection merely of different levels of temperature and partial melting in the source areas. The breakdown of the potassium mineral biotite, as well as the progressive melting of more anorthite-rich plagioclase, must have played a dominant rôle in these processes. The important influence of anorthite content has been adequately demonstrated by von Platen (1965) in his study of experimental anatexis, and HCl was shown by him to be worthy of consideration as well, but the author is convinced that a similar position will still be given to biotite in future studies on granite genesis. It is

therefore/

therefore necessary to take many more than two components into consideration and the development of a six component experimental granitic system (Or-Ab-An-Q-Bi-H_2O) is an exciting possibility for future work.

The extensive hybridisation features at Darling transpose the problem of petrogenetic reconstruction by observation of "end products" to a complex level, straddling the area between igneous equilibria and metamorphic processes. Much work remains to be done. The first advances will have to come from quantitative reconstruction of ancient intensive variants. Amongst the most important of these are silica activity, total pressure and H_2O fugacity.

Considering the isobaric 1 bar curves of <u>silica activity</u> against temperature reported by Carmichael et al. (1970) and Nicholls et al. (1971), and assuming from the experimental evidence that the granitic liquids of Darling and Saldanha had a temperature of 700 - 900°C, it can be inferred from the presence of zircon rather than baddeleyite that ($-\log a_{SiO_2}$) must have been in excess of 0,4 - 0,6. For a temperature of 1 000°C the corresponding value would be greater than 0,30. Nicholls et al. (1971), have shown how <u>total pressure</u> can be estimated by thermodynamical calculation from mineralogical data. Their isothermal reconstruction (1 000°C) takes into account, amongst others, the mineral pairs sphene-perovskite, orthoclase-leucite, albite-nepheline, and zircon-baddeleyite. Since sphene, orthoclase (microcline), albite (plagioclase), and zircon are present in the Darling granites conclusions may soon be possible on the basis of detailed mineralogical study. The reaction

$$\underset{\text{(annite)}}{KFe_3AlSi_3O_{10}(OH)_2} + \underset{\text{(gas)}}{\tfrac{1}{2}O_2} = \underset{\text{(sanidine)}}{KAlSi_3O_8} + \underset{\text{(magnetite)}}{Fe_3O_4} + \underset{\text{(steam)}}{H_2O}$$

shows promise for the determination of <u>fugacity of H_2O</u> in lavas (Wones and Eugster, 1965) and was used with success by Ewart et al. (1971) for this purpose. Its applicability to more deepseated rocks (such as the Darling-Saldanha granites) is obvious, since

the/

the paragenesis biotite-microcline-magnetite is present.

The reconnaissance nature of the present study makes it impractical to calculate thermodynamical parameters at present, but the author has already started on a study of accessory minerals, with quantitative estimates of such factors as f_{O_2}, f_{H_2O}, total pressure, and temperature in view.

IX THE DARLING BATHOLITH IN REGIONAL PERSPECTIVE

Since the Darling batholith represents only one of a number of Cape granite plutons, it is necessary to consider possible regional correlations. For this purpose geochemical, geochronological and even textural data may be used in addition to geological age relationships.

The closest neighbour of the Darling batholith is the Saldanha batholith which likewise consists of several intrusions eg. the Hoedjies Point granite, Saldanha quartz porphyry, Vredenburg granite and Cape Columbine granite. As pointed out already the coarsely porphyritic Darling granite and the coarsely porphyritic Hoedjies Point granite of the Saldanha batholith are probably interconnected below superficial cover; this correlation is corroborated by the geochemical similarities presented in chapter VI. The regional granites of other plutons in the Southwestern Cape, such as the Cape Peninsula granite, are texturally and mineralogically similar to the abovementioned Saldanha-Darling intrusives. Since critical contacts are not exposed, the Darling granite was originally correlated with the Vredenburg granite of Saldanha but this was corrected after the chemical data became available and just in time for the final editing of Geological Survey Sheet 3318A, -3218C (in print). A synthesis of the regional geochemical variations in geochemical parameters would at present be premature. The excellent paper by P. Kolbe (1966) was a step in this direction, but unfortunately the samples were collected with too little discrimination.

In 1968 Prof. S. Maske arranged with Dr. A. Burger of the Geochronology division, National Physical Research Laboratory, C.S.I.R., for three zircon datings to be done on selected Cape granites. The purpose of this project was to determine whether geochronologically significant differences exist between the various intrusions belonging to the Saldanha batholith, since the author suggested that there are at least four regional ages

of/

of igneous rocks and not three as previously reported. Five samples were collected in collaboration with Prof. D.L. Scholtz and three were eventually selected for zircon-dating, viz. Hoedjies Point granite, Cape Columbine granite and Saldanha quartz porphyry. Additional samples were subsequently supplied at the request of Dr. Burger but the project is still in progress and several anomalies remain to be explained. The following preliminary results are available:

Cape Peninsula granite = 610 m.y.
Darling granite = 560 m.y.
Hoedjies Point granite = 628 m.y.

Previous determinations by other laboratories took only the Cape Peninsula granite into account, and selected values may be tabulated as follows:

Whole rock Rb/Sr : 550 m.y. Biotite K/A : 496 m.y.	}	Allsop and Kolbe, 1965
Biotite Rb/Sr : 630 m.y.		Holmes and Cahen, 1957
Whole rock Pb/Pb : 550 ± 50 m.y.		Aldrich et alia, 1955.

The inter-pluton correlations suggested above on grounds of similarity in chemistry, xenolith content, mineralogy and structure, are therefore corroborated by the available geochronological data.

The Vredenburg granite was first recognised as a separate entity only recently and was provisionally named the Northwest Bay granite (Schoch, 1966). It was renamed by Dr. H.N. Visser on evidence accumulated during the regional mapping of Geological Survey Sheet 3318A - 3218C. Although this granite is coarsely porphyritic like the Hoedjies Point granite, it has geochemical and mineralogical characteristics which are different from the suite discussed above. An approximate age of 800 m.y. is indicated by preliminary determinations on zircon (Dr. A. Burger, personal communication). At first the author was perplexed by these results, and still prefers to reserve judgment until K/A and/or Rb/Sr values are available in addition to more zircon dates, but soon realised that such an ancient genesis cannot be

ruled/

ruled out. The fact is that no exposed contact with the Hoedjies Point granite is known. The Vredenburg granite holds numerous Malmesbury Formation xenoliths, as does the Hoedjies Point granite, so that a date of 800 m.y. would make the Malmesbury considerably older than is generally accepted at present.

It is also interesting to note that the large Colenso fault may extend through the Saldanha batholith into Northwest Bay. This cannot be proved by direct observation due to superficial cover but it seems unlikely that such a major fault would terminate within a few km from its last observed surface expression. Deformation is particularly severe in the granite near the postulated extension of the fault, the most impressive example being the northwesterly trending mylonites of Trekoskraal, just south of a few km of beach in Northwest Bay (Schoch, 1962). If this is true, the portion of the Saldanha batholith to the southwest of the postulated fault consists of the Hoedjies Point granite, intruded by a large pluton of Saldanha quartz porphyry, while the ground to the north-east is occupied by the recently recognised Vredenburg granite, intruded in turn by small northwesterly trending bodies of Cape Columbine granite (cf. table 1). A large age discrepancy between the Hoedjies Point and Vredenburg granites would not be unusual for such a situation.

Unpublished data concerning the structure of the Malmesbury Formation to the south-east of the Darling batholith indicate that the sand-covered southwestern contact may be a regional fault as well. The only granite-hornfels contact known at present, (on Klawervlei), is too small to supply unambiguous evidence but exhibits unmistakable shearing effects. Since the Colenso fault forms the northeastern boundary of the pluton, the Darling batholith may therefore be part of a huge fault block. This interpretation is reinforced when it is realised that the Klipheuwel beds (sensu stricto) show characteristic features of rapid deposition and are situated in the same structure farther to the south-east (Visser, 1967). The postulated fault block may consequently be regarded as a graben. The highly developed

hybridisation/

hybridisation zone with northwesterly trend in the central part of the batholith is considered to be a remnant of the ancient roof zone, which was not preserved in other Cape Granite plutons owing to a less favourable structural situation. This interpretation implies that the southern portion of the Saldanha batholith forms part of the same graben.

Although the extent of the hybridisation phenomena at Darling has no counterpart in other plutons of Cape Granite, similar manifestations are known in the Saldanha batholith. These occurrences exhibit the same level of hybridisation in many cases, but are of course very much smaller. It is interesting to note that spectacular swarms of xenoliths occur in the Hoedjies Point granite at Hoedjies Point and that the largest single exposure of hybrid granite in Saldanha occurs in the same granite east of Langebaan, where the Saldanha batholith is nearest to the Darling pluton. These facts are in agreement with the structural model discussed before. Numerous small hybrid granite occurrences are also present in the Vredenburg granite. The most important localities were described by Scholtz (1946), for instance the hybrid phenomena at Klein Paternoster, Groot Paternoster (Duikereiland), and the Slippers Bay hills. Recent mapping by Dr. H.N. Visser indicated that the lastmentioned occurrence is situated in an isolated body of Cape Columbine granite (Sheet 3318A - 3218C). This was long suspected by the author and was also suggested after a brief investigation by Mr. D.F.F.Garisch in 1959. The miniature contact at Slippers Bay described by McIver (1957), is therefore a junction between Cape Columbine granite and Malmesbury Formation hornfels.

The mylonitisation phenomena occurring mainly as northwesterly orientated bands in the Darling and Saldanha granites, originated from stress pulses which acted from the south-south-west. (Schoch, 1962). The main band on the Northwest Bay coast at Trekoskraal, is covered by recent limestone and dunes toward the south-east and is then obliterated by the quartz porphyry. In 1958 the author observed that the northwesterly trending band of

severe/

severe mylonitisation at Darling reported by Scholtz (1946), is situated approximately in line with the Trekoskraal band, and of equal crushing intensity and development (Schoch, 1962, p. 740). As a result of the research reported in this thesis, it can now be added that the Darling mylonite continues along strike towards Saldanha, broad mylonite zones being present as far to the northwest as Swartberg and Betjieskop. These northwesterly outcrops of the Darling pluton were among the first examined during the field work phase and the author may be excused for recording his delight when he discovered the previously unknown Betjieskop occurrence, nearly halfway between Darling and Trekoskraal, and on the extrapolated strike line! However, the regional synthesis which emerged finally, indicates that we are not dealing with a single band of crushing, but with several sub-parallel ones, and that mylonitisation often grades on strike into gneissic zones of the same orientation.

The final word on the deformation structures peculiar to the Darling-Saldanha granites is yet to be spoken but the main deformation epoch was definitely before the younger intrusives. This is beautifully illustrated by the relationship of the mylonite to the Klipberg granite (map, folder), to the Saldanha quartz porphyry (op.cit., 1962), and to the Cape Columbine granite (Scholtz, 1946; op.cit., 1962). Feebler crushing of later dates left its imprint on all the quoted examples along the same zones as the major deformation, testifying to the gradually waning pulse-like nature of the forces responsible for the mylonitisation. Any geochronological interpretation of these granites will have to take this field evidence into account. Detailed investigations at Trekoskraal have adequately demonstrated that the intrusion and deformational history of the Cape granites are exceedingly complex, and that the outcrops present a deceptive appearance to the casual geological observer not intimately conversant with regional as well as detailed aspects.

The correlation of the younger granites is more problematic

than/

than that of the principal intrusives. These granites are relatively small bodies in the regional setting and local conditions probably played a significant rôle during their genesis. With the exception of the Klipberg granite, the intrusions are always elongated in a northwesterly direction and are possibly of dyke-like habit. Separate ages of granite emplacement should not be postulated unless firm field evidence is available and for this reason the young granites are provisionally regarded as coeval in spite of textural and sometimes mineralogical differences. There are many examples in literature of time-equivalent igneous rocks which were summarily attributed to different ages on the ground of textural data, as in the case of chill phases.

The Klipberg and Contreberg granites may perhaps be correlated with a number of separate bodies of Cape Columbine granite in the Saldanha batholith. The Dassen Island granite is probably a marginal phase of a regional granite and is similar to other nodular tourmaline Cape granites of local occurrence, as in the Bottelary hills near Stellenbosch. The quartz porphyry dykes of Cape St. Martin (Otto, 1957) and Shell Bay, may be younger than the Saldanha quartz porphyry, and this interpretation is corroborated by preliminary geochronological results, but the evidence is too meagre at present for any firm conclusions to be drawn. It can be mentioned that a tentative figure of 670 m.y. was determined for Contreberg granite, but this is probably not reliable because the sample unfortunately yielded very little zircon (Dr. A. Burger, personal communication). This date is older than expected and further work is in progress.

X/

X CONCLUSION

From the evidence presented in the previous chapters, it is now apparent that the Darling Batholith is highly complex. It is multiple in nature - relatively small bodies of younger granite having intruded into the regional Darling granite and its correlates, including the hybrid granites. The young Contreberg granite differs from the Klipberg granite for which very little chemical data are available at present, primarily because it is difficult to obtain unweathered material apart from aplites in the granite. Chill phases are not important in the Darling batholith, except for apophyses of Klipberg granite observed on Wolwefontein. It would seem that conditions of emplacement differed considerably between the older and younger intrusives.

The hybridisation phenomena which developed so markedly at Darling, reflect reaction between the older granite and Malmesbury metamorphites and must have originated under essentially the same physico-chemical conditions as this granite. The position and irregularities of the hybrid granodiorites reflect a remnant roof zone, possibly representing a synform in the eroded overlying rocks. This interpretation is supported by the quantitative distribution of xenoliths and their nature.

Assuming that the relative distribution of rock types on surface is near the actual apportionment in three dimensions, the following planimetrically determined figures can be regarded as volume percentages:

Darling granite (DAR)	50,3	72,8
Porphyritic biotite granite	22,5	33,3
Hybrid granodiorite (HbGn)	10,8	
Klipberg granite (KB)	1,8	3,9
Contreberg granite (CB)	2,1	4,4
Small occurrences of young granite	0,5	
Dassenberg granite	1,3	
Non-porphyritic biotite granite	10,6	
	99,9	

It/

It is clear that the young granites, which occur in different parts of the batholith (fig. 3), are of roughly the same size and that the problematic Dassenberg granite may well be a hybrid variety of one of these. With respect to the batholith as a whole they are relatively insignificant, particularly since much of the non-porphyritic biotite granite probably represents hybrid older granite. The ratio of young granites to hybrid and biotite-rich older granite is of the order of 1 : 6 to 1 : 10. It is therefore likely that the young intrusives represent anatectic products from a nearby subjacent source, a conclusion with which the preliminary experimental results reported in chapter VII are in agreement. The proximity of most younger granites to hybrid granites in both the Darling and Saldanha batholiths may consequently be of petrogenetic significance.

ACKNOWLEDGEMENTS

The author is deeply indebted to Prof. D.L. Scholtz who suggested this project, for his unfailing interest and helpful suggestions. Heartfelt thanks are also due to Prof. W.J. Verwoerd for his stimulating discussions and critical evaluation of the manuscript. The author wishes to thank the C.S.I.R. for a bursary during the first part of the research, which made the completion of most of the field work possible.

The writer expresses his gratitude to his wife, Mrs. M. Schoch, for drawing the lion's share of the text figures under trying circumstances. The continuous and enthusiastic support of his parents, Mr. and Mrs. E.L. Schoch of George, was invaluble to the author. Thanks are also due to Mrs. A.E.R. Verwoerd for the typing of the manuscript.

REFERENCES

ALDRICH L.T., WETHERILL G.W., DAVIS G.L. and TILTON G.R.: Radioactive ages of micas from granitic rocks by Rb-Sr and K-Ar methods.
TRANS. AM. GEOPHYS. UNION, 39, pp. 1124 - 1134, 1958.

ALLSOP H.L. and KOLBE P.: Isotopic age determinations on the Cape Granite and intruded Malmesbury sediments, Cape Peninsula, South Africa.
GEOCHIM. COSMOCHIM. ACTA, 29, pp. 1115 - 1130, 1965.

A.S.T.M., JOINT COMMITTEE ON POWDER DIFFRACTION STANDARDS: Powder Diffraction File, 1970.

AZÁROFF V.L.: Elements of X-ray Crystallography.
McGRAW HILL, 1968.

AZÁROFF V.L. and BUERGER M.J.: The powder method in X-ray crystallography,
McGRAW HILL, 1958.

BAILEY S.W. and BROWN B.E.: See BROWN and BAILEY.

BARTH T.F.W.: Oxygen in rocks: a basis for petrographic calculations.
J. GEOL., 56, pp. 50 - 60, 1948.

BARTH T.F.W.: Principles of classification and norm calculations of metamorphic rocks.
J. GEOL., 67, pp. 135 - 152, 1959.

BATEMAN P.C., CLARK L.D., HUBER N.K., MOORE J.G. and RINEHART C.D.: The Sierra Nevada batholith: A synthesis of recent work across the central part.
GEOL. SOC. AM. PROFESSIONAL PAPER, 414-D, 1963.

BOOCOCK C.: The structural features and inclusions of the Cape Peninsula granite.
TRANS. ROY. SOC. S.AFRICA, 33, pp. 243 - 277, 1951-52.

BRISTOL C.C.: The quantitative determination of minerals in metamorphosed volcanic rocks by X-ray powder diffraction.
CAN. J. EARTH SCI., 5, pp. 235 - 242, 1968.

BROWN B.E. and BAILEY S.W.: Chlorite polytypism: I Regular and semirandom one-layer structures.
AM. MINERALOGIST, 47, pp. 819 - 850, 1962.

BROWN G.C. and FYFE W.S.: The production of granitic melts during ultrametamorphism.
CONTR. MINER. PETR., 28, pp. 310 - 318, 1970.

BURNHAM C.W.: Hydrothermal fluids at the magmatic stage (in BARNES H.L. ed.: Geochemistry of hydrothermal ore deposits).
HOLT, RINEHART and WINSTON, 1967.

BURRI C.: Petrochemische Berechnungsmethoden auf Äquivalenter Grundlage.
BIRKHAUSER VERLAG, 1959.

CARMICHAEL D.M.: On the mechanism of prograde metamorphic reactions in quartz-bearing pelitic rocks.
CONTRIB. MINER. PETR., 20, pp. 244 - 267, 1969.

CARMICHAEL I.S.E., NICHOLLS J., SMITH A.L.: Silica activity in igneous rocks.
AM. MINERALOGIST, 55, pp. 246 - 263, 1970.

CHALMERS B.: Principles of solidification.
JOHN WILEY, 1964.

CHAYES F. and McKENZIE W.S.: Experimental error in determining certain peak locations and distances between peaks in X-ray (powder) diffractometer patterns.
AM. MINERALOGIST, 42, pp. 534 - 547, 1957.

CHAYES F. and MÉTAIS D.: On the relation between suites of CIPW and Barth-Niggli norms.
CARNEGIE INST. WASH. YEARBOOK, pp. 193 - 195, 1964.

CLOOS H.: Einführung in die Geologie.
GEBRüDER BORNTRAEGER, 1936.

CORSTORPHINE G.S.: Geologists' report for 1897.
ANNUAL REP. GEOL. COMM. CAPE OF GOOD HOPE,
pp. 3 - 43, 1897.

DANCHIN R.V.: Aspects of the geochemistry of some selected South African fine-grained sediments, 2 vols.
UNPUBL. Ph.D. THESIS, UNIVERSITY OF CAPE TOWN, 1970.

DARWIN C.: Geological observations on the volcanic islands.
pp. 148 - 150, 1844.

DEER W.A., HOWIE R.A. and ZUSSMAN J.: Rock-forming minerals, 5 vols. LONGMANS, 1962, 1963.

DE VILLIERS J.: The geology of the Baviaans Kloof.
TRANS. GEOL. SOC. S. AFRICA, 44, p. 153,
map, 1941.

DE VILLIERS J.: A review of the Cape Orogeny.
ANN. UNIV. STELLENBOSCH, 22, SECT. A, Nos. 1-14,
p. 186, 1944.

DE VILLIERS J. and BURGER A.J.: Note on the minimum age of certain granites from the Richtersveld area.
GEOL. SURV. S. AFRICA ANN., 6,
pp. 83 - 84, 1967.

DE VILLIERS J., JANSEN H. and MULDER M.P.: Die geologie van die gebied tussen Worcester en Hermanus: Toeligting van Gebiede 3319 (Worcester) en 3419A (Caledon) en dele van Gebiede 3318D(Stellenbosch) en 3418B (Somerset-Wes).
GEOL. SURV. S. AFRICA, 1964.

DUNHAM A.C. and THOMPSON R.N.: The origin of granitic magmas: Skye and Rhum.
J. GEOL. SOC. AUSTRALIA, 14, pp. 339-343, 1967.

ENGEL A.E.J. and ENGEL C.G.: Progressive metamorphism and granitization of the major paragneiss, Northwest Adirondack Mountains, New York.
BULL. GEOL. SOC. AM., 71, pp. 1 - 58, 1960.

ERNST W.G.: Amphiboles.
SPRINGER VERLAG, 1968.

EUGSTER H.P. and WONES D.R.: Stability relations of the ferruginous biotite, annite.
J. PETROL., 3, pp. 82 - 125, 1962.

EWART A., GREEN D.C., CARMICHAEL I.S.E. and BROWN F.H.: Voluminous low temperature rhyolitic magmas in New Zealand.
CONTRIB. MINER. PETR., 33, pp. 128 - 144, 1971.

FRONDEL C.: Danas' The System of Mineralogy, 7th ed., Vol. III: The silica minerals.
JOHN WILEY, 1962.

GEOLOGICAL COMMISSION OF THE CAPE OF GOOD HOPE: Geological map of the Colony of the Cape of Good Hope, Sheet IV.
(Mapped by ROGERS A.W., SCHWARZ E.H.L. and DU TOIT A.L.), 1906.

GEOLOGICAL SURVEY OF THE REPUBLIC OF SOUTH AFRICA, DEPT. OF MINES: Sheet 3318A - 3218C, Saldanha.
(Mapped by VISSER H.N. and SCHOCH A.E.).
In press.

GEOLOGICAL SURVEY OF THE UNION OF SOUTH AFRICA, DEPT. OF MINES: Sheet 247, Cape Town.
(Mapped by HAUGHTON S.H.), 1933.

GOLDSMITH J.R. and LAVES F.: The microcline-sanidine stability relations.
GEOCHIM. COSMOCHIM. ACTA., 5, pp. 1 - 19, 1954.

GOWER J.A.: X-ray measurement of the iron-magnesium ratio in biotites.
AM. J. SCI., 255, pp. 142 - 156, 1957.

"GRANITE 71": Symposium, Salisbury, Rhodesia, 1971, (To be published, GEOL. SOC. S. AFRICA SPEC. PUB.)

GRIGORIEV D.P.: Ontogeny of minerals.
ISRAEL PROGR. SCI. TRANSLATIONS, 1965 (1961).

HALL B. - See PLAYFAIR.

HARPUM J.R.: Petrographic classification of granitic rocks in Tanganyika by partial chemical analysis.
RECORDS GEOL. SURV. TANGANYIKA, 10, pp. 80 - 88, 1963.

HARTNADY C.J.H.: Structural analysis of some pre-Cape formations in the Western Province.
UNIV. CAPE TOWN, PRECAMBRIAN RESEARCH UNIT BULL., 6, pp. 59 - 60, 1969.

HALL A.L.: Analyses of rocks, minerals, ores, coal, soils and waters from Southern Africa.
GEOL. SURV. S. AFRICA, MEM. 32, p. 129, 1938

HAUGHTON S.H.: The geology of Cape Town and adjoining country.
GEOL. SURV. S. AFRICA EXPL. SHEET 247, pp. 32-37, 1933.

HOLMES A. and CAHEN L.: Géochronologie africaine 1956.
ACAD. ROYALE DES SCIENCES COLONIALES, V 1, pp. 33 - 35, 1957.

IIYAMA T.: Optical properties and unit cell dimensions of cordierite and indialite.
MINERALOGICAL J., 1, 372 - 394, 1956.

JAHNS R.H. and BURNHAM C.W.: Experimental studies of pegmatite genesis. I A model for the derivation and crystallisation of granitic pegmatite.
ECON. GEOL., 64, pp. 843 - 864, 1969.

JAMES R. and HAMILTON D.L.: Phase relations in the system $NaAlSi_3O_8$ - $KAlSi_3O_8$ - $CaAl_2Si_2O_8$ - SiO_2 at 1 Kb water vapour pressure.
CONTRIB. MINER. PETR., 20, pp. 111 - 141, 1969.

KLEEMAN A.W.: The origin of granitic rocks: Skye and Rhum. A reply.
J. GEOL. SOC. AUSTRALIA, 14, pp. 345 - 347, 1967.

KOLBE P.: Geochemical investigation of the Cape Granite, South-western Cape Province, South Africa.
TRANS. GEOL. SOC. S. AFRICA, 69, pp. 161 - 199, 1966.

KORZHINSKII D.S.: Physico-chemical basis of the analysis of the paragenesis of minerals.
CONSULTANTS BUREAU, translated 1959. (1957).

KRAUSKOPF K.B.: Introduction to Geochemistry.
McGRAW HILL, 1967.

LOWE K.E.: A graphic solution for certain problems of linear structure.
AM. MINERALOGIST, 31, pp. 425 - 434, 1946.

LUTH W.C., JAHNS R.H. and TUTTLE O.F.: The granite system at pressures of 4 to 10 kilobars.
J. GEOPHYS. RES., 69, pp. 759 - 773, 1964.

McIVER J.R.: On the granite-hornstone contact at Slippers Bay.
ANN. UNIV. STELLENBOSCH, 33, SECT. A, Nos. 1 - 11, pp. 541 575, 1957.

McLACHLAN G.R.: The geology of Dassen Island.
TRANS. GEOL. SOC. S. AFRICA, 52, pp. 377 - 384, 1949.

MASKE S.: The diorites of Yzerfontein, Darling, Cape Province.
ANN. UNIV. STELLENBOSCH, 33, SECT. A, Nos. 1 - 11, pp. 23 - 70, 1957.

MEHNERT K.R.: Migmatites and the origin of granitic rocks.
ELSEVIER, 1968.

MIDDLEMOST E.: Petrology of the Bremen Granite-Syenite Complex, South West Africa.
TRANS. GEOL. SOC. S. AFRICA, 70, pp. 117 - 134, 1967.

MIYASHIRO A.: Cordierite - Indialite relations.
AM. J. SCI., 255, pp. 43 - 62, 1957.

NELL G. and BRINK W.C.: The petrology of the Western Province dolerites.
ANN. UNIV. STELLENBOSCH, 22, SECT.A, Nos. 1 - 14, pp. 27 - 62, 1944.

NICHOLLS J., CARMICHAEL I.S.E. and STORMER J.C.: Silica activity and P total in igneous rocks.
CONTRIB. MINER. PETR., 33, pp. 1 - 20, 1971.

NIGRINI A.: Diffusion in rock alteration systems: I Prediction of limiting equivalent ionic conductances at elevated temperatures.
AM. J. SCI., 269, pp. 65 - 91, 1970.

NUFFIELD E.W.: X-ray diffraction methods.
JOHN WILEY, 1966.

ORVILLE P.M.: Alkali ion exchange between vapor and feldspar phases.
AM. J. SCI., 261, pp. 201 - 237, 1963.

OTÁLORA G. and HESS H.H.: Modal analysis of igneous rocks by X-ray diffraction methods with examples from St. Paul's Rock and an olivine nodule.
AM. J. SCI., 267, pp. 822 - 840, 1969.

OTTO J.D.T.: The dyke rocks of Cape St. Martin.
ANN. UNIV. STELLENBOSCH, 33, SECT. A, Nos. 1 - 11, pp. 387 - 443, 1957.

PEIKERT E.W.: Model for three-dimensional mineralogical variation in granitic plutons based on the Glen Alpine stock, Sierra Nevada, California.
BULL. GEOL. SOC. AM., 76, pp. 331-348, 1965.

PLAYFAIR J. and HALL B.: Account of the structure of Table Mountain and other parts of the peninsula of the Cape, drawn up by Prof. Playfair from observations made by Capt. Basil Hall.
TRANS. ROY. SOC., 7, pp. 269 - 278, 1815.

POLDERVAART A.: Chemistry of the Earth's crust. (In "Crust of the Earth", POLDERVAART A., ed.).
GEOL. SOC. AM. SPEC. PAP. 62, pp. 119 - 144, 1955.

POTGIETER C.T.: The South African pyrophyllite deposits.
ANN. UNIVERSITY OF STELLENBOSCH, SECT. A., Nos. 3- 11, pp. 224 - 265, 1950.

READ H.H.: The granite controversy.
T. MURBY, 1957.

REITAN P.H.: Frictional heat during metamorphism. 2. Quantitative evaluation of concentration of heat generation in space.
LITHOS, 1, pp. 268 - 274, 1968.

ROGERS A.W.: Summary of work done in the Southwestern districts.
FIRST ANNUAL REP. GEOL. COMM. CAPE OF GOOD HOPE, p. 13, 1896.

ROGERS A.W.: Survey of the Stellenbosch district.
ANNUAL REP. GEOL. COMM. CAPE OF GOOD HOPE, pp. 47 - 49, 1897.

ROGERS A.W. and DU TOIT A.L.: An introduction to the geology of the Cape Colony, pp. 22 - 29, p.35.
LONGMANS, GREEN, 1909.

ROOKE J.M.: Geochemical variation in African granitic rocks, and their structural interpretation. (In CLIFFORD T.N. and GASS I.G., editors: African magmatism and tectonics).
OLIVER and BOYD, pp. 255 - 417, 1970.

ROSS M., TAKEDA H. and WONES D.R.: Mica polytypes: systematic description and identification.
SCIENCE, 151, pp. 191 - 193, 1966.

SCHOCH A.E.: The cataclasites of Northwest Bay. ANN. UNIV. STELLENBOSCH, 37, SER.A, Nos. 2-10, pp. 659-808, 1962.

SCHOCH A.E.: Discussion on paper by P. Kolbe.
TRANS. GEOL. SOC. S. AFRICA, 69, p. 257, 1966.

SCHOCH A.E.: The Cape Granites in 1971. (Delivered at symposium "Granite 71" in Salisbury, Rhodesia). To be published. (GEOL. SOC. S. AFRICA SPEC. PAP.)

SCHOLTZ D.L.: On the younger Precambrian granite plutons of the Cape Province. (Anniversary address by the president).
PROC. GEOL. SOC. S. AFRICA, 49, pp. xxxv - lxxxii, 1946.

SCHREINER G.D.L., BASSON H.H. and VERBEEK A.A.: Potassium-Argon dating of the Cape Granite and a granitized xenolith at Sea Point.
TALANTA, 15, pp. 1125 - 1133, 1968.

SCHREYER W. and SCHAIRER J.F.: Compositions and structural states of anhydrous Mg-cordierites: A reinvestigation of the central part of the system $MgO-Al_2O_3-SiO_2$.
J. PETROL., 2, pp. 324 - 406, 1961.

SHAND S.J.: Discussion in "Origin of Granite". (GILLULY J., chairman).
GEOL. SOC. AM. MEM., 28, pp. 137 - 139, 1948.

SHAND S.J.: History of a feldspar crystal.
BULL. GEOL. SOC. AM., 60, pp. 1213 - 1214, 1949.

SIPPEL R.F.: Sodium selfdiffusion in natural minerals.
GEOCHIM. COSMOCHIM. ACTA., 27, pp. 107 - 120, 1963.

SMITH J.V. and YODER H.S.: Experimental and theoretical studies of the mica polymorphs.
MINER. MAG, 31, pp. 209 - 235, 1956.

SÖHNGE P.G. and DE VILLIERS J.: The Kuboos pluton and its associated line of intrusions.
TRANS. GEOL. SOC. S. AFRICA, 51, pp. 1 - 36, 1948.

STRUNZ H., TENNYSON Ch. and UEBEL P.-J.: Cordierite - morphology, physical properties, structure, inclusions, and orientated intergrowth.
MINERALS SCI. ENG., 3, pp. 3 - 18, 1971.

SZÁDECZKY-KARDOSS E.: A genetical system of igneous rocks.
21 INTERNAT. GEOL. CONGR., NORDEN, PART 13, pp. 260 - 274, 1960.

SZÁDECZKY-KARDOSS E., PANTÓ G. and SZÉKY-FUX V.: A preliminary proposition for developing a uniform nomenclature of igneous rocks.
21 INTERNAT. GEOL. CONGR., NORDEN, PART13, pp. 287 - 292, 1960.

TAKEDA H.: Distribution of mica polytypes among space groups.
AM. MINERALOGIST, 56, pp. 1042 - 1056, 1971.

TURNER F.J. and WEISS L.E.: Structural analysis of metamorphic tectonites.
McGRAW HILL, 1963.

TURI B. and TAYLOR H.P.: An oxygen and hydrogen isotope study of a granodiorite pluton from the Southern California batholith.
GEOCHIM. COSMOCHIM. ACTA, 35, pp. 383 - 406, 1971.

TURI B. and TAYLOR H.P.: O^{18}/O^{16} ratios of the Johnny Lyon Granodiorite and Texas Canyon Quartz Monzonite plutons, Arizona, and their contact aureoles.
CONTRIB. MINER. PETR., 32, pp. 138 - 146, 1971.

TUTTLE O.F. and BOWEN N.L.: Origin of granite in the light of experimental studies in the system $NaAlSi_3O_8$ - $KAlSi_3O_8$ - SiO_2 - H_2O.
GEOL. SOC. AM. MEM., 74, 1958.

VAN BILJON S.: The Kuboos batholith in Namaqualand, South Africa.
TRANS. GEOL. SOC. S. AFRICA, 42, pp. 123 - 219, 1939.

VAN ZYL P.J.: The complex dioritic stocks west of the Malmesbury-Paardeberg granite pluton.
ANN. UNIVERSITY OF STELLENBOSCH, VOL. 26, SECT. A, Nos. 3 - 11, pp. 481 - 507, 1950.

VISSER H.N.: Verspreiding en korrelasie van die Formasie Klipheuwel in die Swartland en die Sandveld.
ANN. GEOL. OPNAME S. AFRIKA, 6, pp. 31 - 38, 1967.

VISSER H.N. and SCHOCH A.E.: Geology and mineral deposits of the Saldanha Bay area, Sheet 3318A - 3218C.
GEOL. SURV. S. AFRICA, MEM. (In press).

VON PLATEN H.: Kristallisation granitischer Schmelzen.
BEITR. MINERAL. PETROG., 11, pp. 334 - 381, 1965.

WALKER F. and MATHIAS M.: The petrology of two granite-slate contacts at Cape Town, South Africa.
QUART. J. GEOL. LONDON, 102, pp. 499 - 518, 1946.

WASSERSTEIN B.: South African granites and their boron content.
GEOCHIM. COSMOCHIM. ACTA, 1, pp. 329 - 338, 1951.

WEDEPOHL K.H. (ed.): Handbook of Geochemistry, Vol. II/1.
SPRINGER VERLAG, p. 1-A-5, 1969.

WHITNEY J.A. and LUTH W.C.: Water undersaturated melting of natural granites at 2Kb.
TRANS. AM. GEOPHYS. UNION, 51, abstr. V30, p. 438,1970.

WHITTEN E.H.T.: Process-response models in geology.
BULL. GEOL. SOC. AM., 75, pp. 455 - 464, 1964.

WHITTEN E.H.T.: Quantitative areal modal analysis of granitic complexes.
BULL. GEOL. SOC. AM., 72, pp. 1331 - 1360, 1961.

WONES D.R. and EUGSTER H.P.: Stability of biotite: experiment, theory and application.
AM. MINERALOGIST, 50, pp. 1228 - 1272, 1965.

WYBERGH W. and DU TOIT A.L.: The limestone resources of the Union.
GEOL. SURV. S. AFRICA, MEM. 11, 1918.

WYLLIE P.J. and TUTTLE O.F.: Effect of carbon dioxide on the melting of granite and feldspars.
AM. J. SCI., 257, pp. 648 - 655, 1959.

YODER H. S. and EUGSTER H.P.: Phlogopite synthesis and stability range.
GEOCHIM. COSMOCHIM. ACTA, 6, pp. 157 - 184, 1954.

YODER H.S. and SMITH J.V.: - See SMITH and YODER.

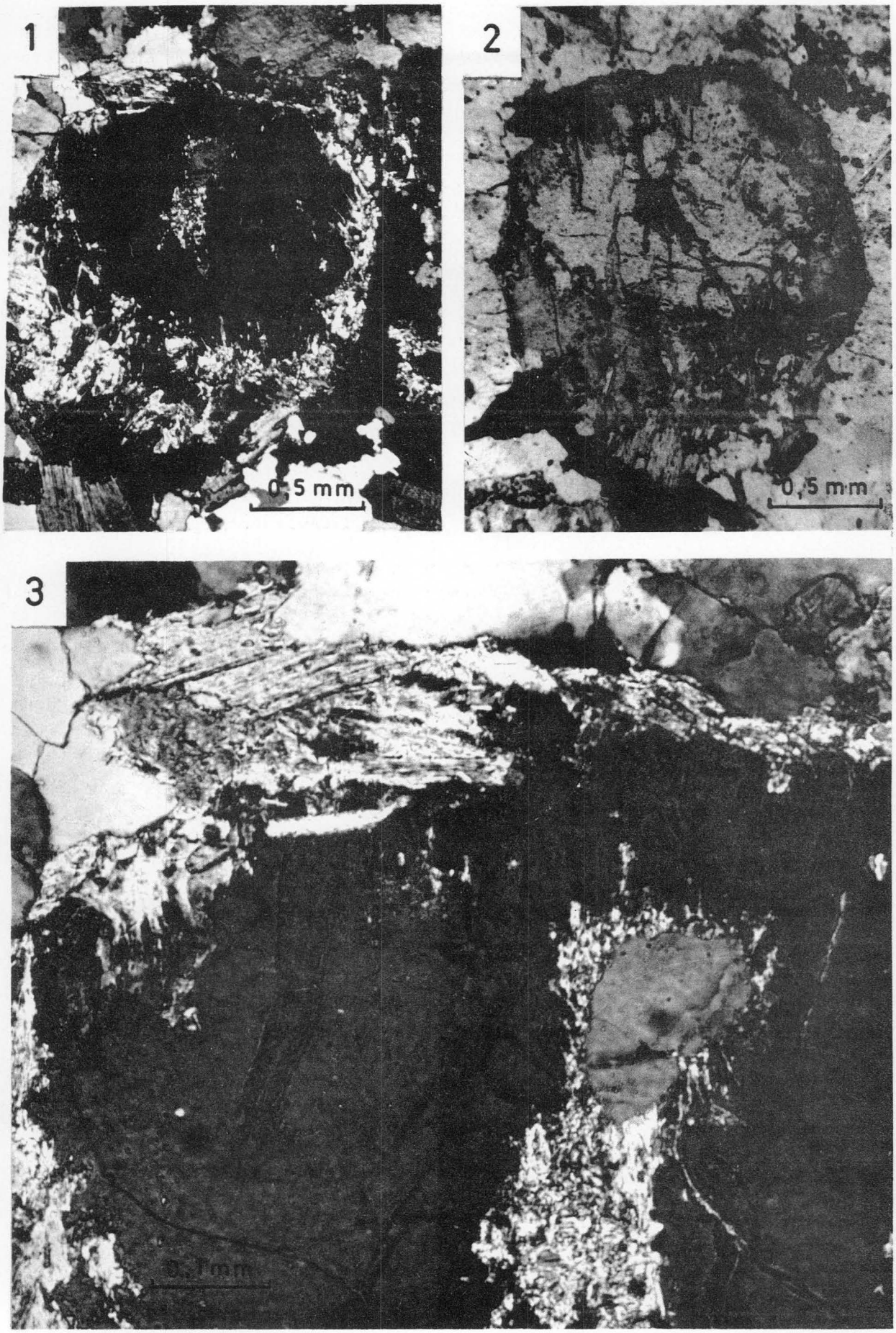

Plate I Marginally pinitised cordierite grain in hybrid granodiorite, Rheboksfontein. 1,3 - Crossed polarisors. 2 - Ordinary polarised light.

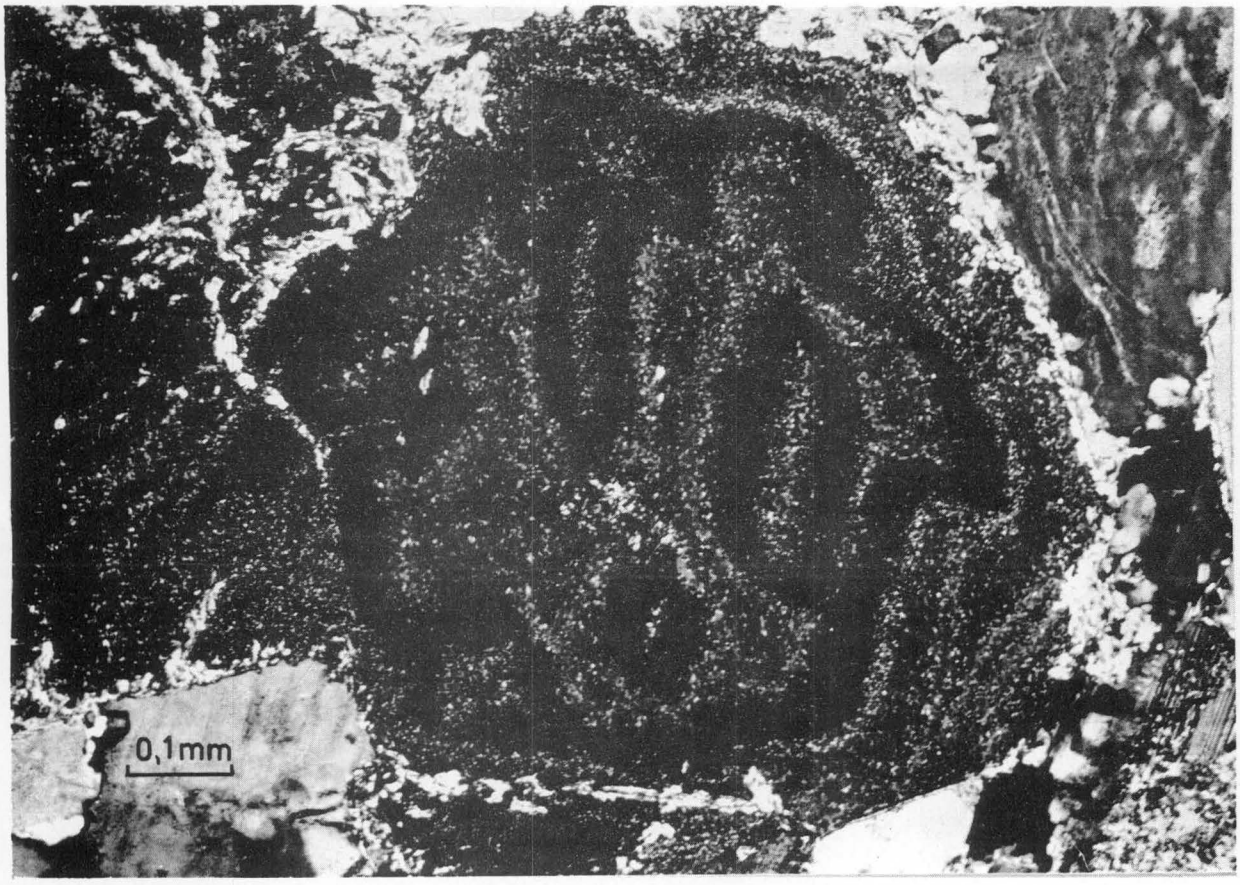

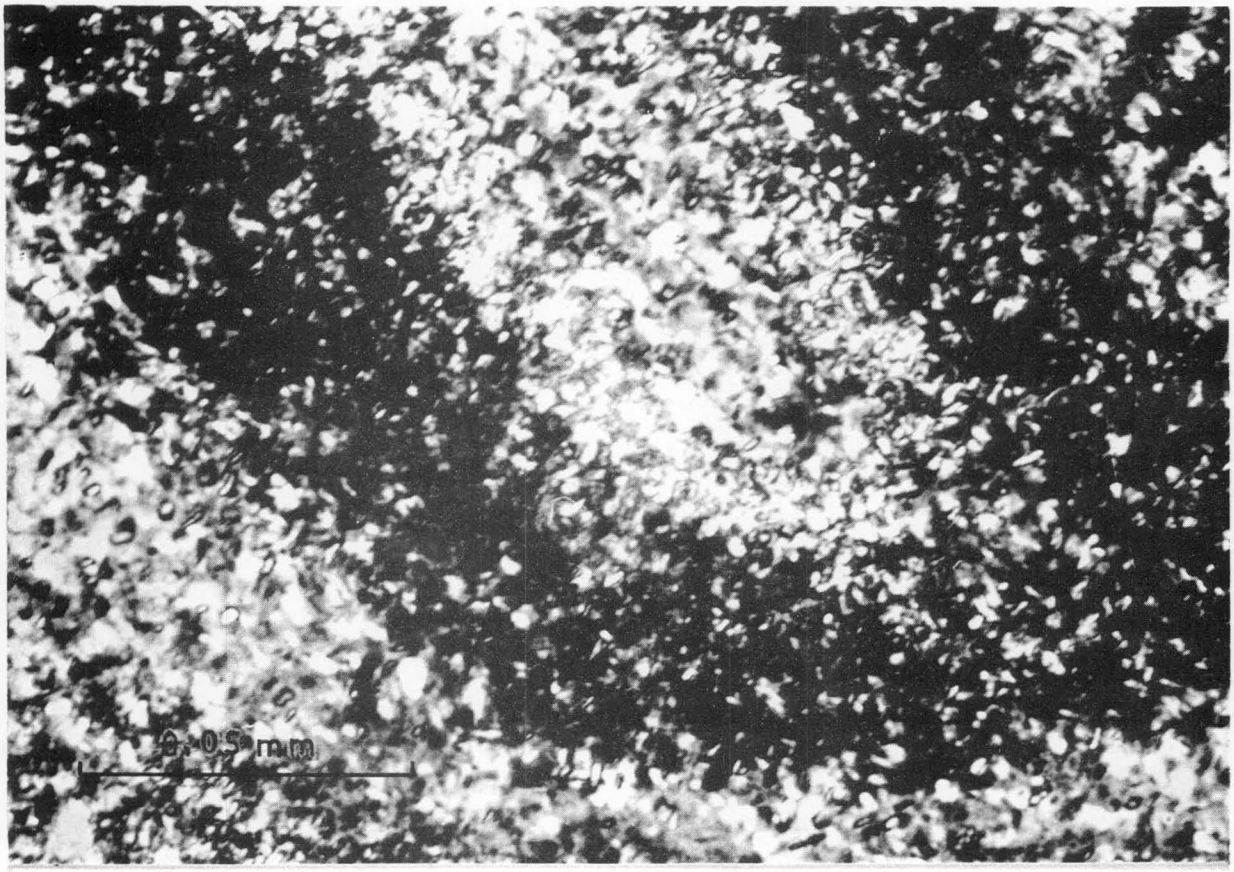

Plate II Wavy structures in the alteration products of completely pinitised cordierite, coarsely porphyritic granite, Klipfontein. Crossed polarisors. Lower photomicrograph illustrates a small portion of upper one.

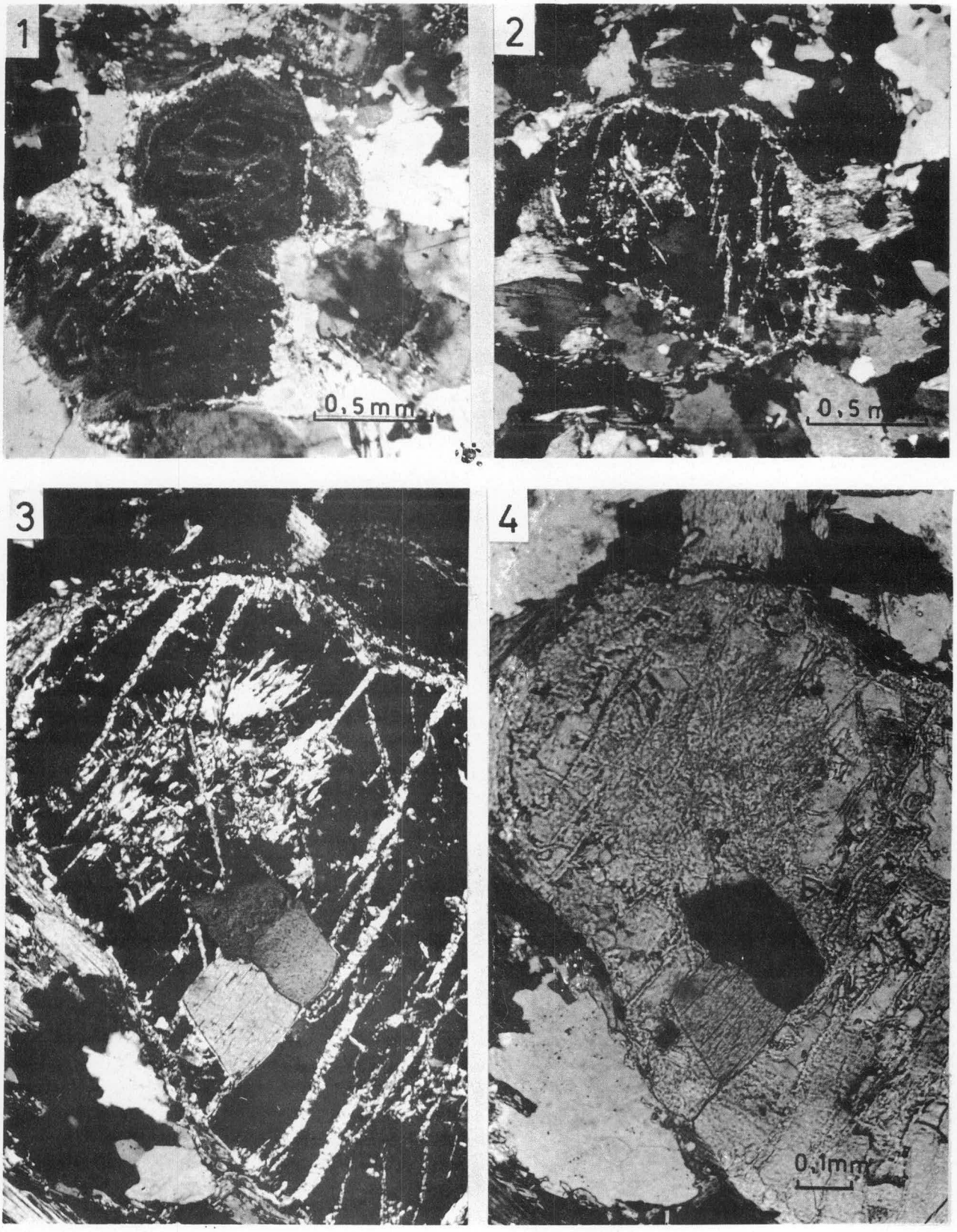

Plate III 1. Completely pinitised cordierite grain, illustrated at higher magnification in plate II. 2,3,4. Marginally pinitised cordierite grain in hybrid granodiorite, Grootberge. 2,3 - crossed polarisors. 4 - ordinary polarised light.

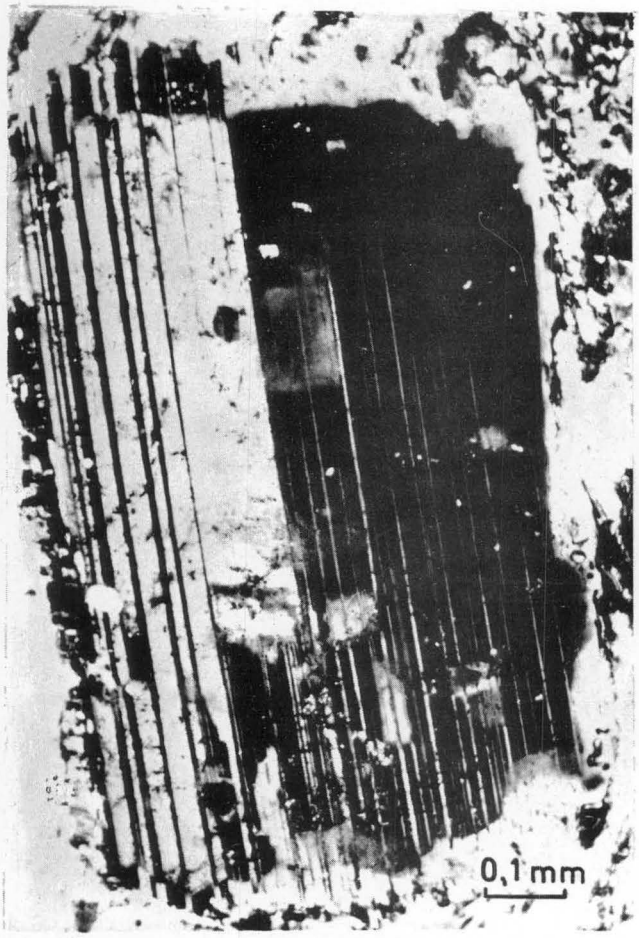

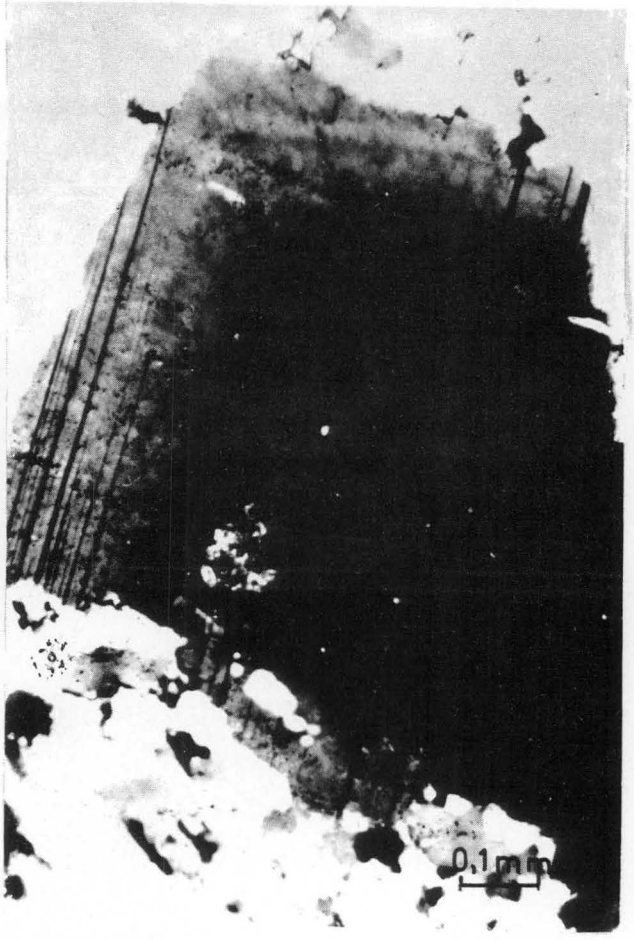

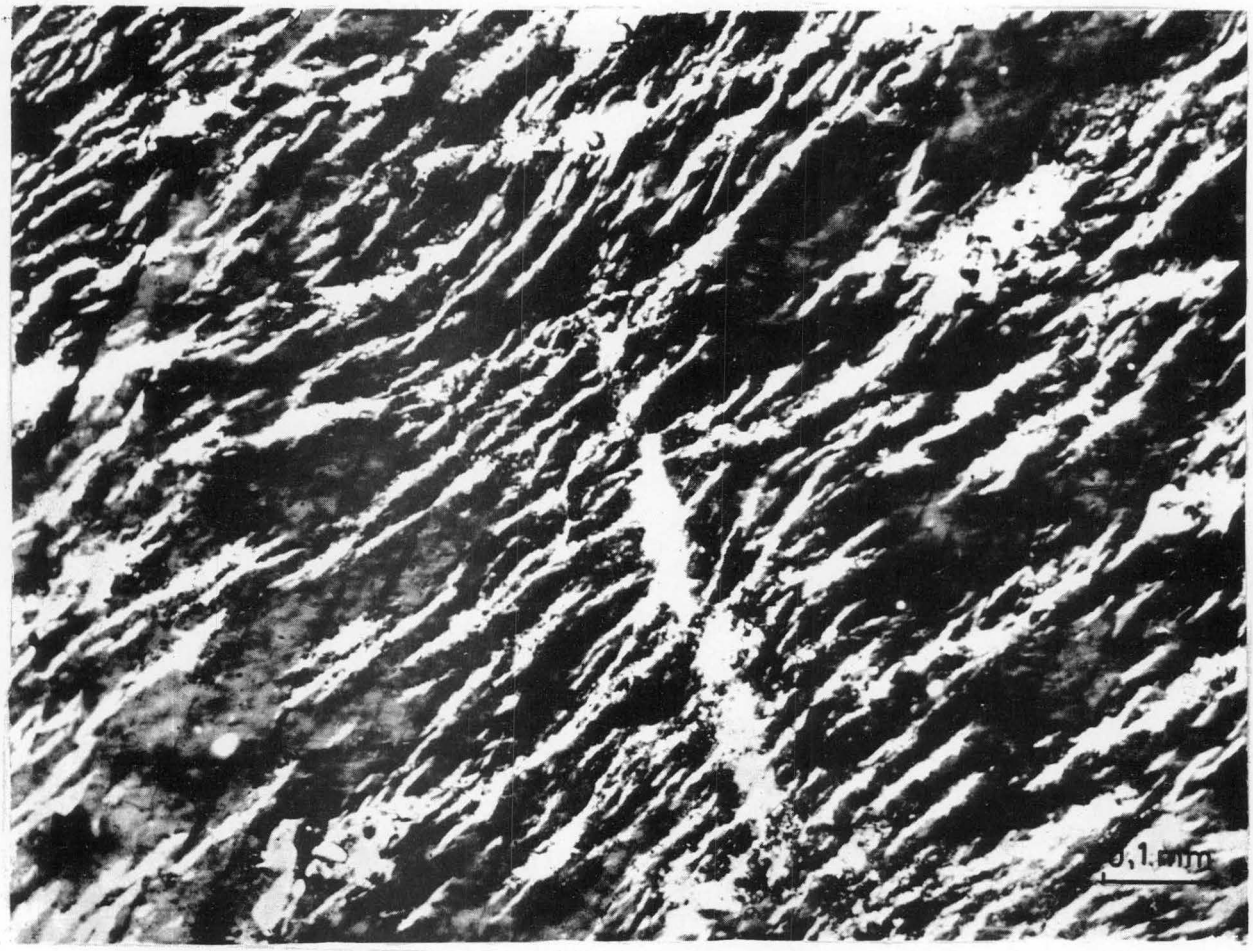

Plate IV Typical feldspars in Darling granite. 1,2. Zonal plagioclase, Swartwater. Crossed polarisors. 3. Microcline perthite, Bonteberg. Crossed polarisors.

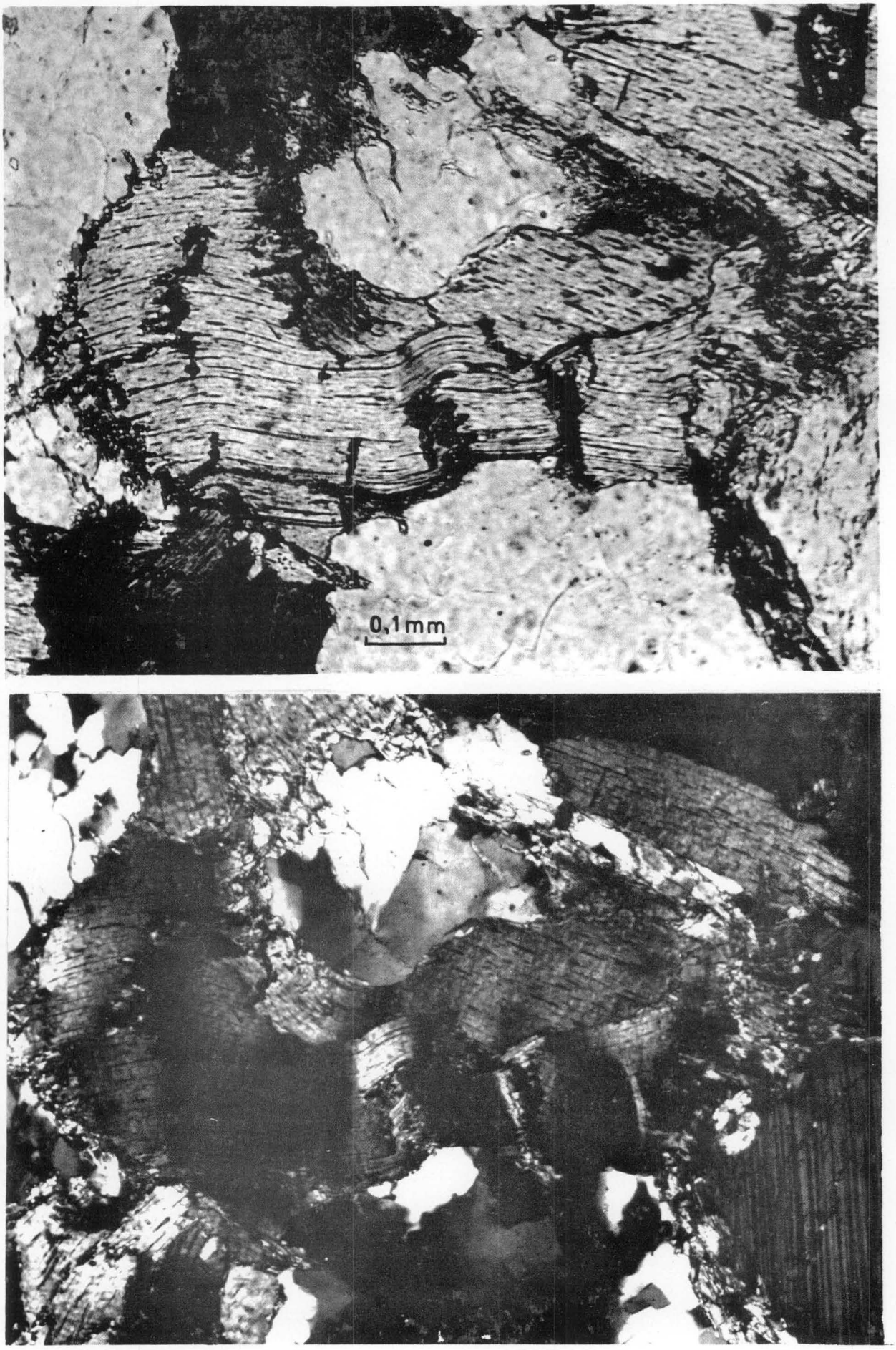

Plate V Deformed biotite in non-porphyritic biotite granite, Nuwepos. Upper and lower photomicrographs respectively with ordinary polarised light and crossed polarisors. Grain in upper right hand corner is zircon.

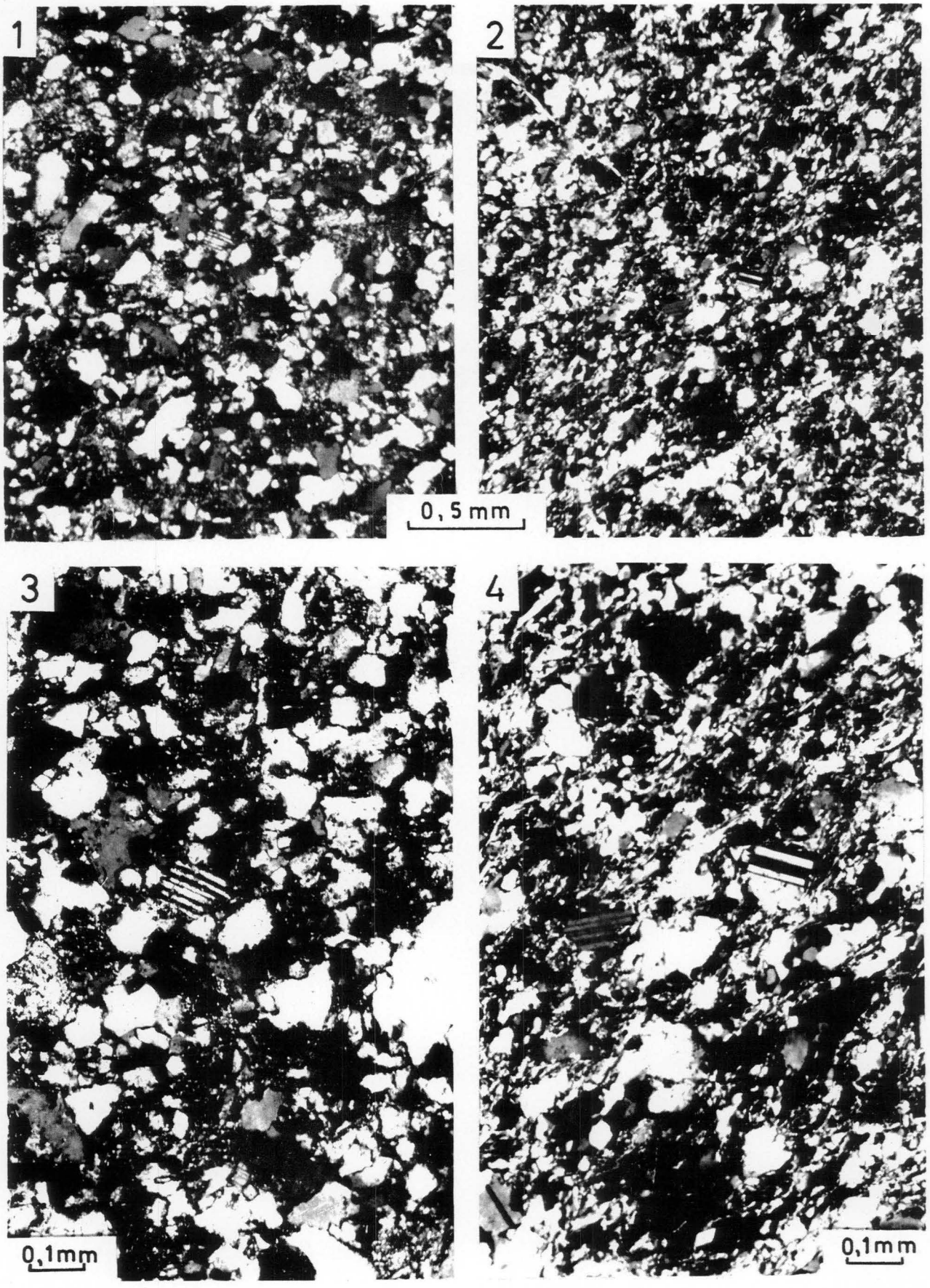

Plate VI Comparison of textures of Malmesbury hornfels and hornfelsic xenoliths in granite. 1,3. Malmesbury hornfels (quartzitic greywacke) from old quarry, De La Rey. 2,4. Xenolith in Darling granite, Grootberge.

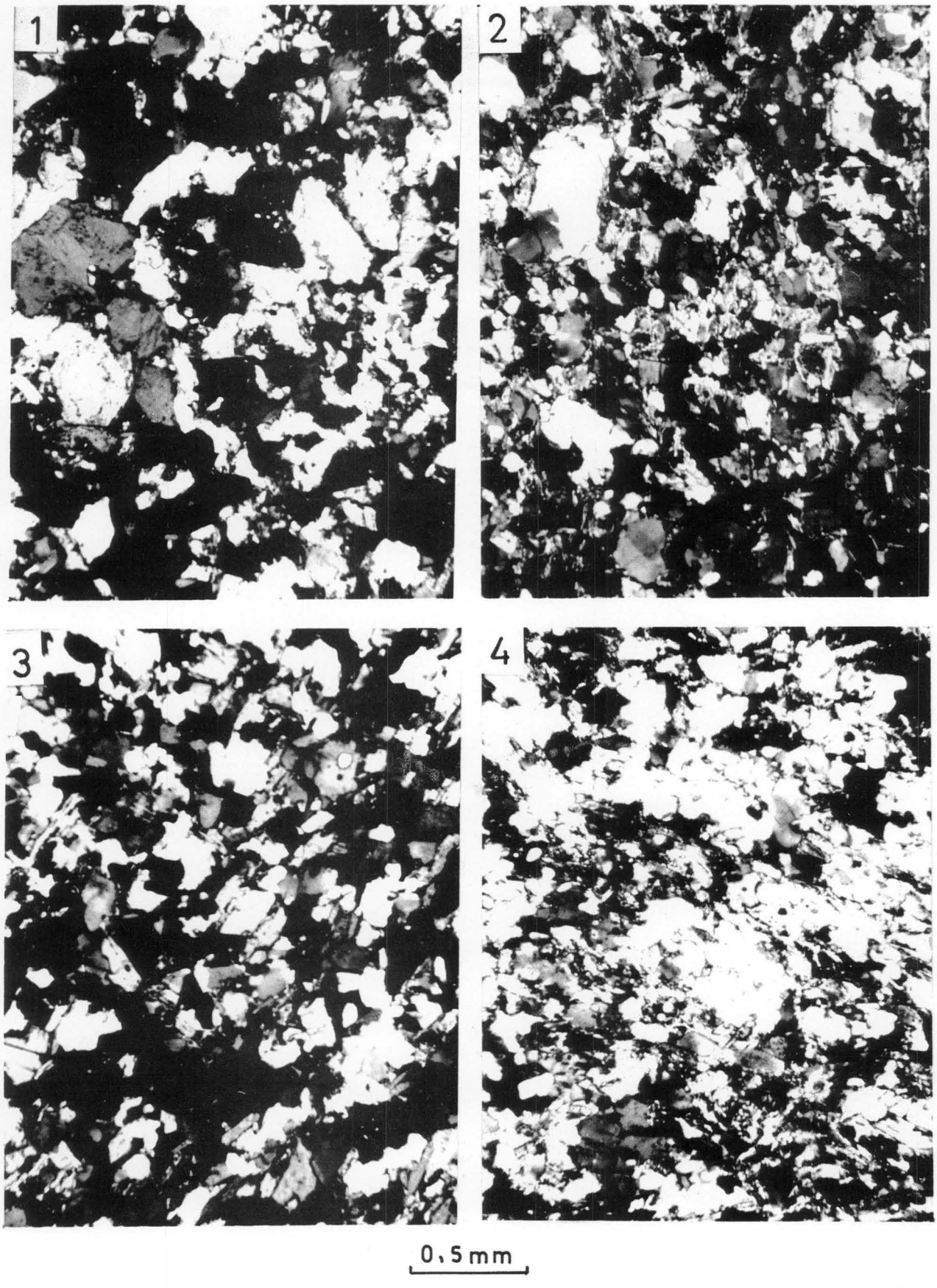

Plate VII Comparison of textures. 1. Quartz fault breccia on Colenso fault, Brakrivier. 2. Pelitic Malmesbury metamorphite, Mamre. 3. Xenolith in coarsely porphyritic biotite granite, Ontongskloof. 4. Xenolith in Darling granite, Grootwater.

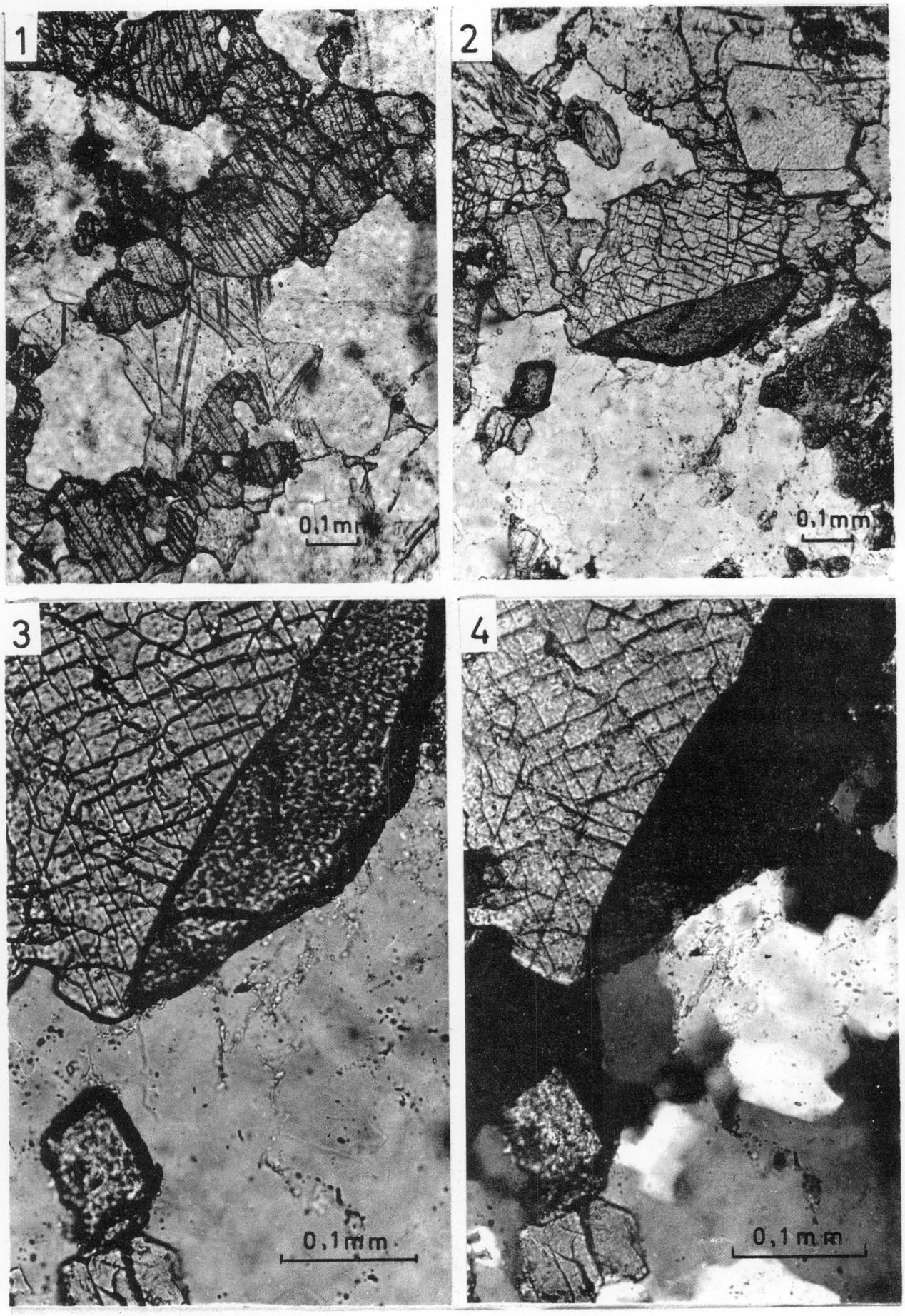

Plate VIII Calcareous xenolith in hybrid granodiorite, Waterkloof. 1. Diopside, calcite, quartz. Ordinary polarised light. 2,3,4. Diopside, sphene, quartz. 2,3 - ordinary polarised light. 3 - crossed polarisors. Photomicrographs 3,4 illustrate a small portion of No.2.

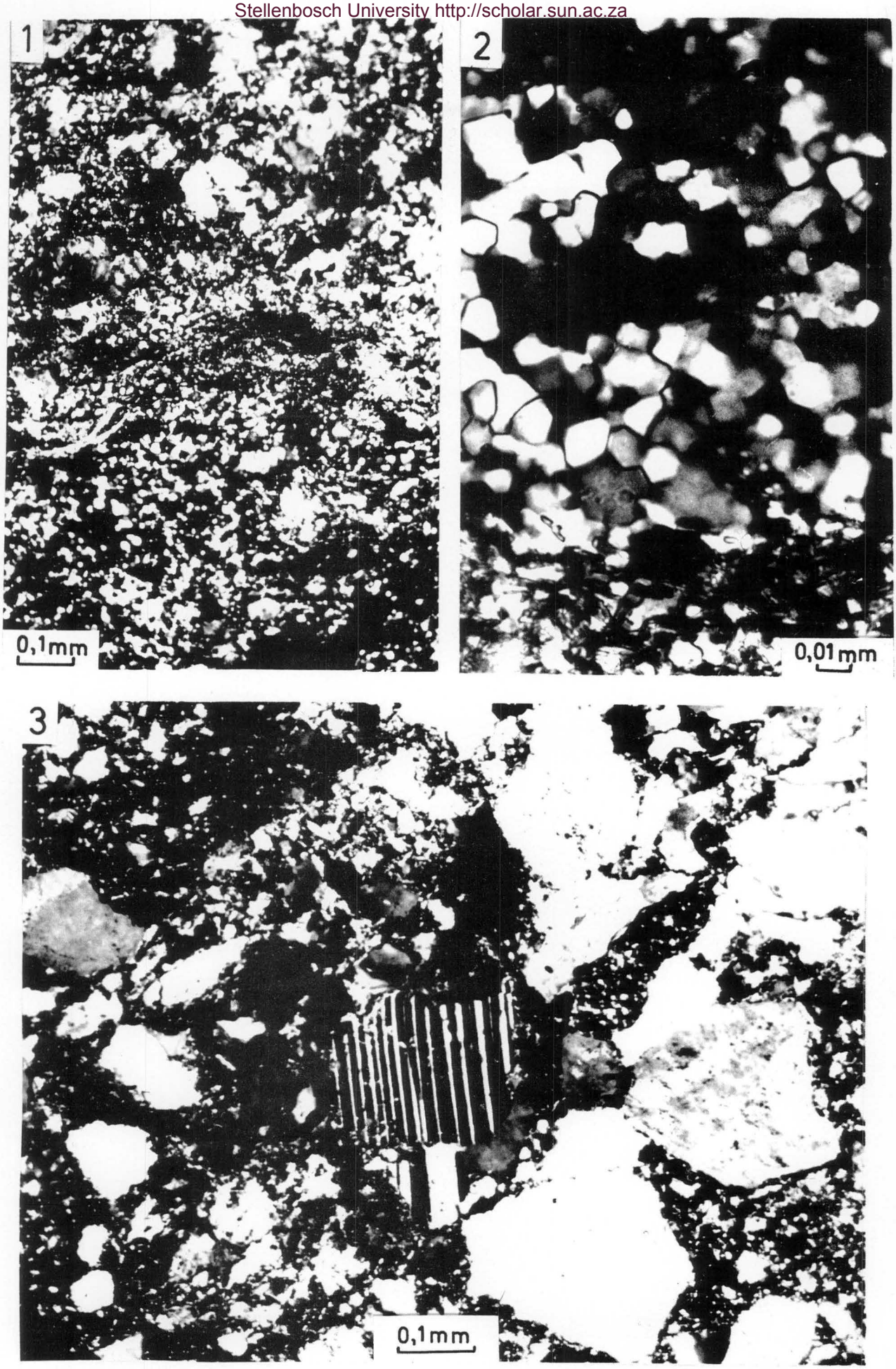

Plate IX Mylonites. 1,2. Mylonite from Klipvlei near Colenso fault. Photomicrograph 2 illustrates a small portion of No.1, and shows details of the microfragmental recrystallised quartz. 3. Mylonite on Colenso fault, Hartbeesvlei.

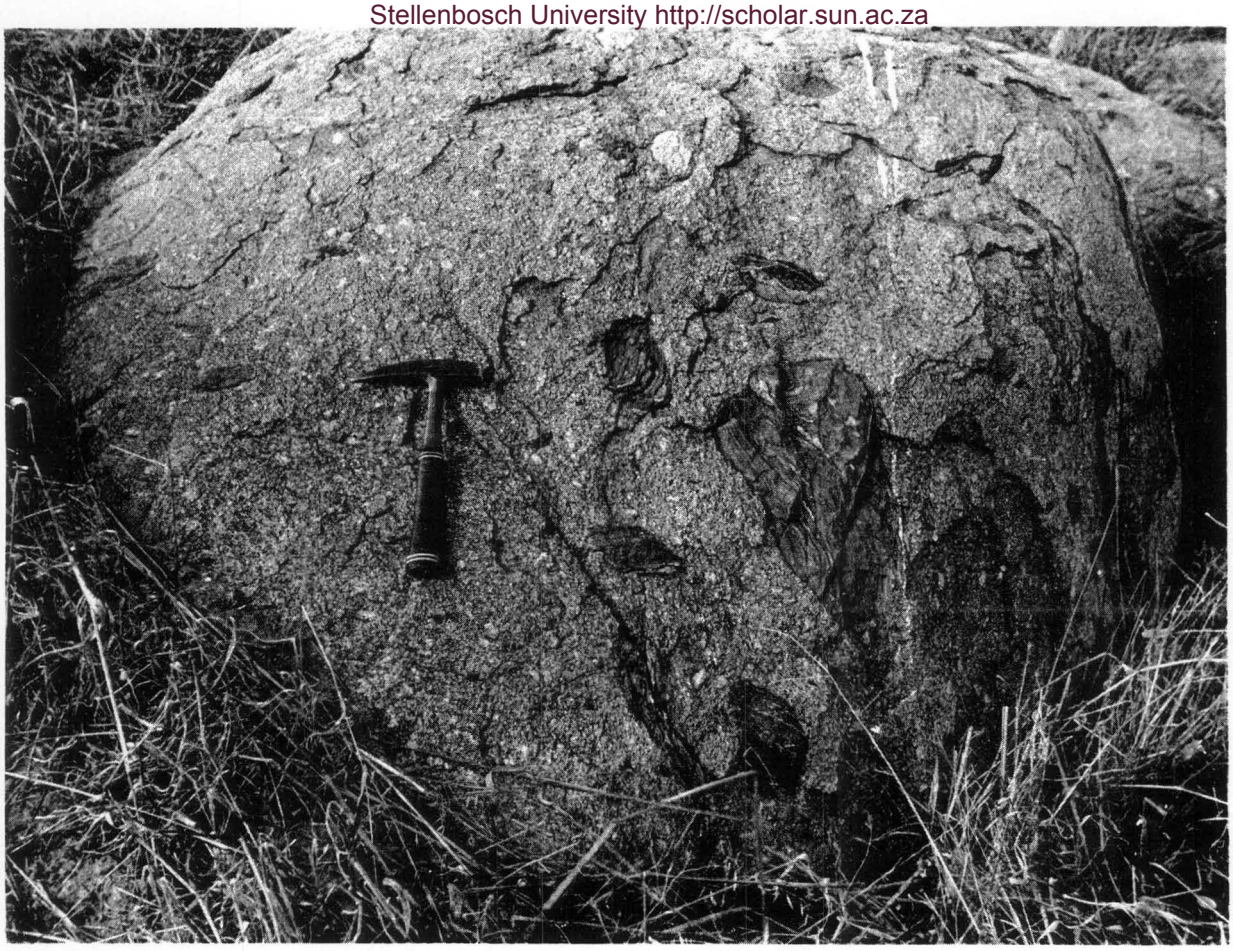

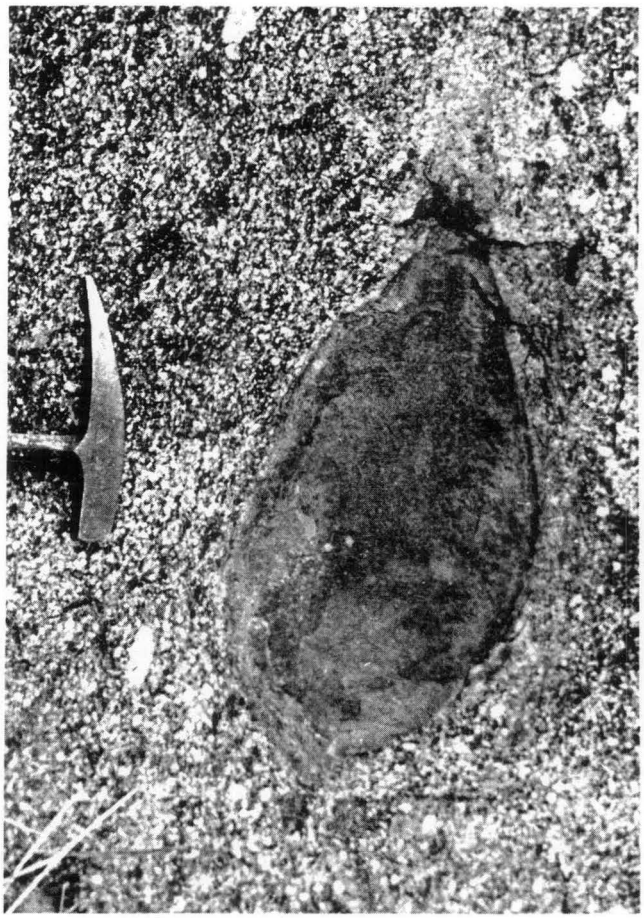

Plate X Xenoliths in hybrid granodiorite.
Above and below, left - Xenolith cluster, Bonteberg. Note various orientations.
Below, right - Typical ellipse-shaped cross-section of metamorphosed quartzitic graywacke, Oranjefontein.

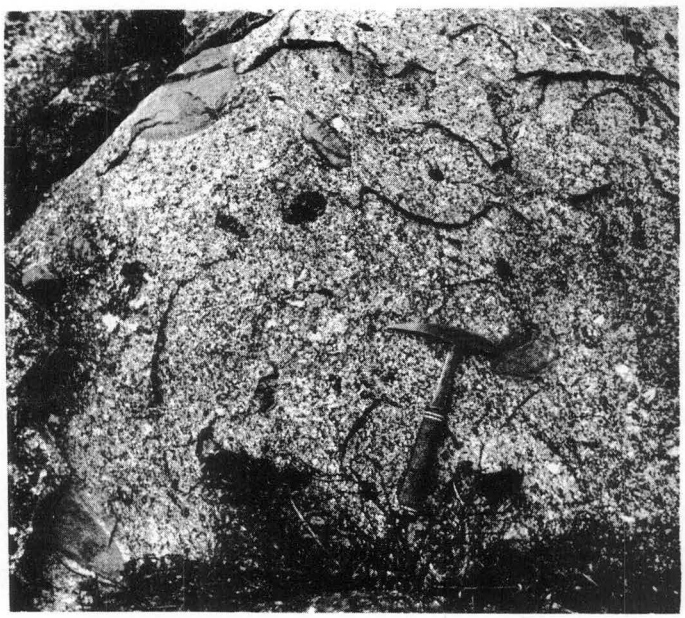

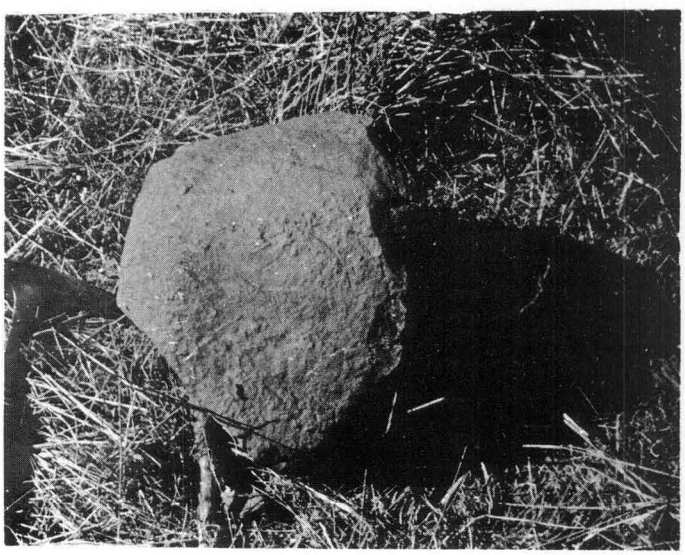

Plate XI Shapes of the xenoliths

Right, below - Central segment of unweathered ellipsoid-shaped xenolith bounded by joint planes (straight edges), and liberated from hybrid granodiorite matrix by weathering, Slangkop. Shadow indicates ellipse-shaped cross-section in the other dimension.
Other photographs - Xenolith clusters in non-porphyritic biotite granite and hybrid granodiorite (middle), looking to the southeast. Left - Vrededal; right, above - Waterkloof; right, middle - Towers.

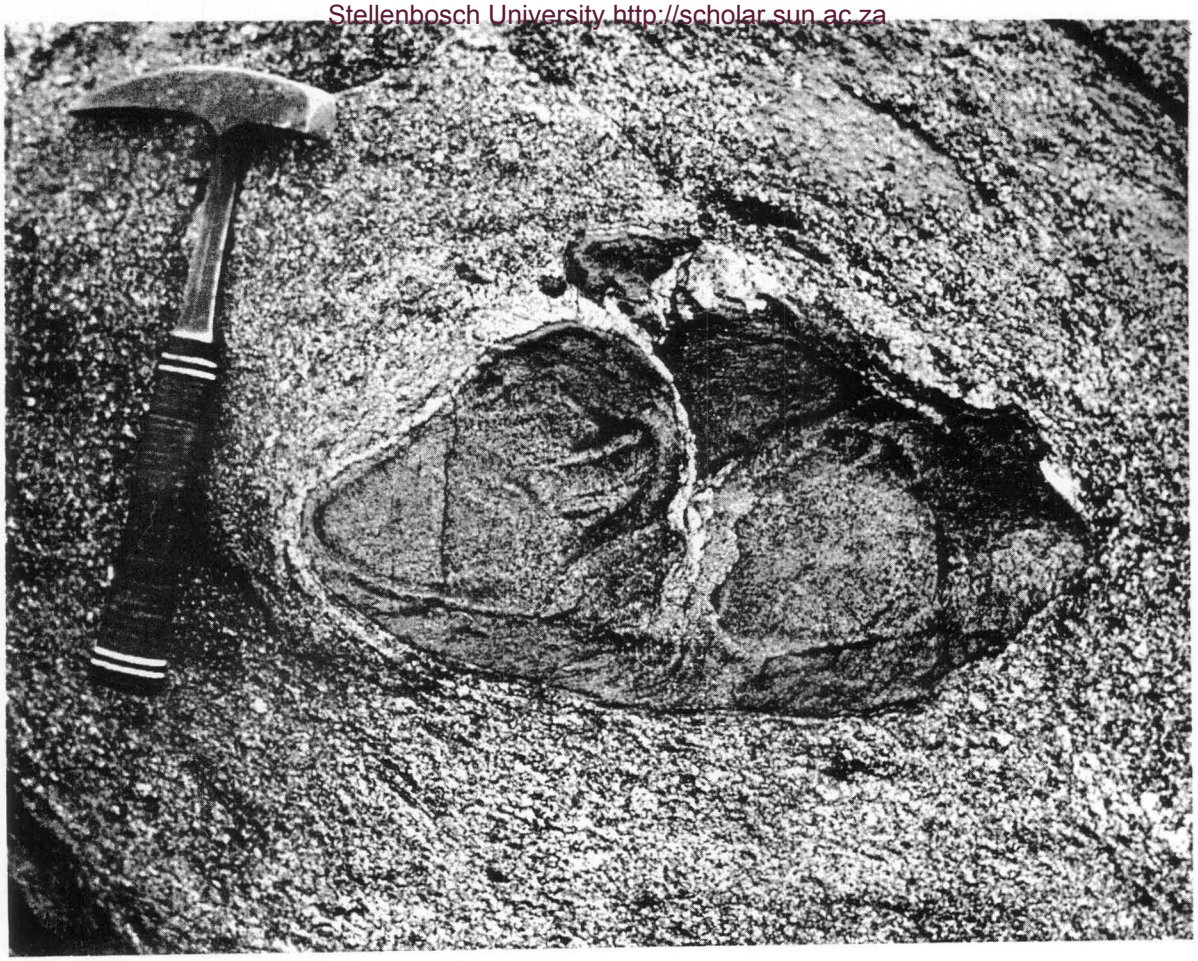

Plate XII Reaction between xenoliths and enveloping hybrid granodiorite. Xenoliths showing both clearcut borders and visible reaction relationship with surrounding medium, Ontongskloof.

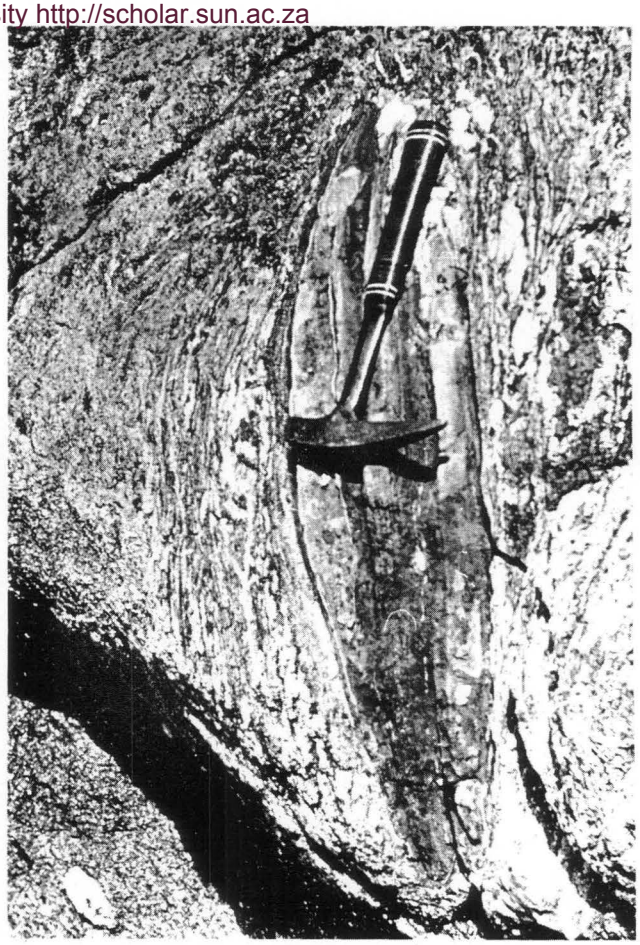

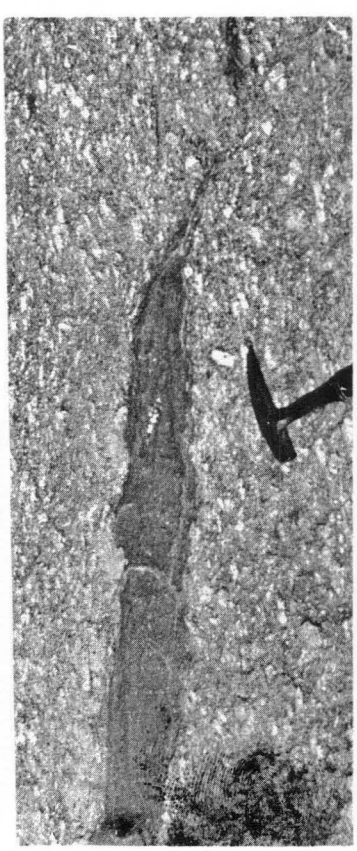

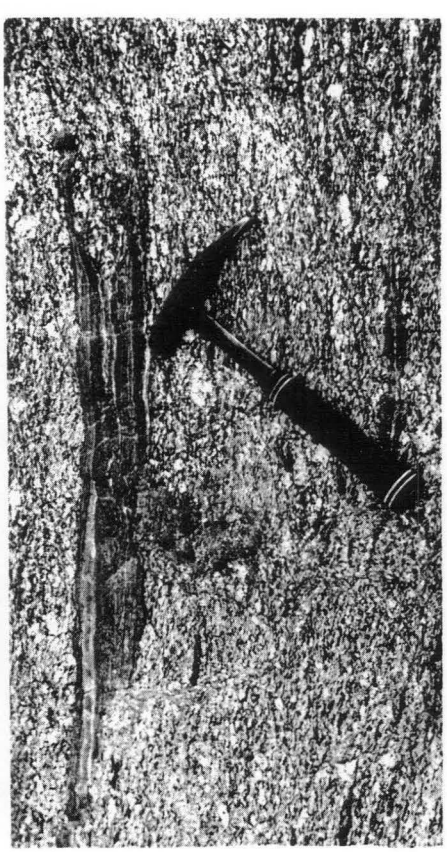

Plate XIII Elongated xenoliths, and autoliths.
Above - Xenoliths in hybrid granodiorite at Wolwefontein (left) and Ontongskloof (right).
Below, left - Possible autolith of finegrained granite in Darling granite, Pampoenvlei. Shaft of hammer orientated east-west.
Below, middle and right - Drawn-out northwesterly orientated xenoliths in coarsely porphyritic biotite granite, respectively at Rheboksfontein and Burgerspost.

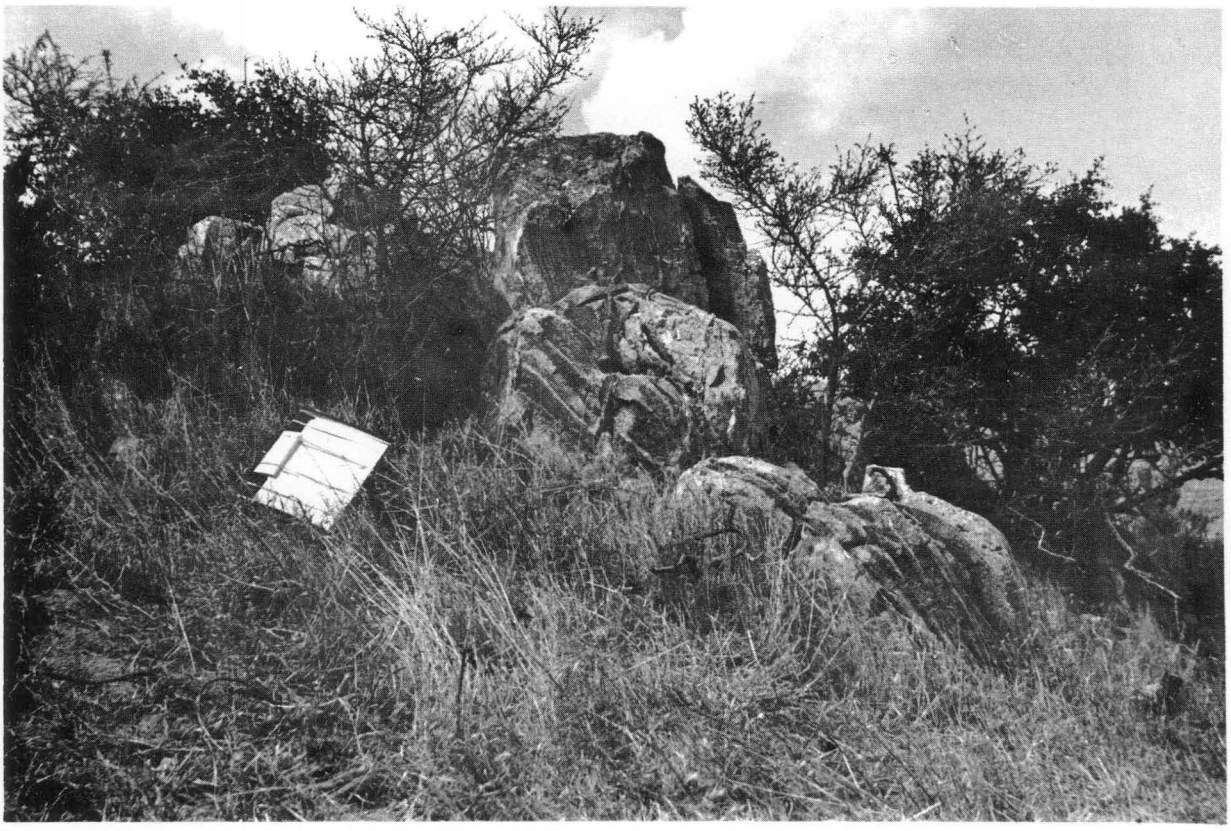

Plate XIV Lime-rich xenoliths.
Large xenolith in hybrid granodiorite (not visible), Oranjefontein. Looking to the southwest.

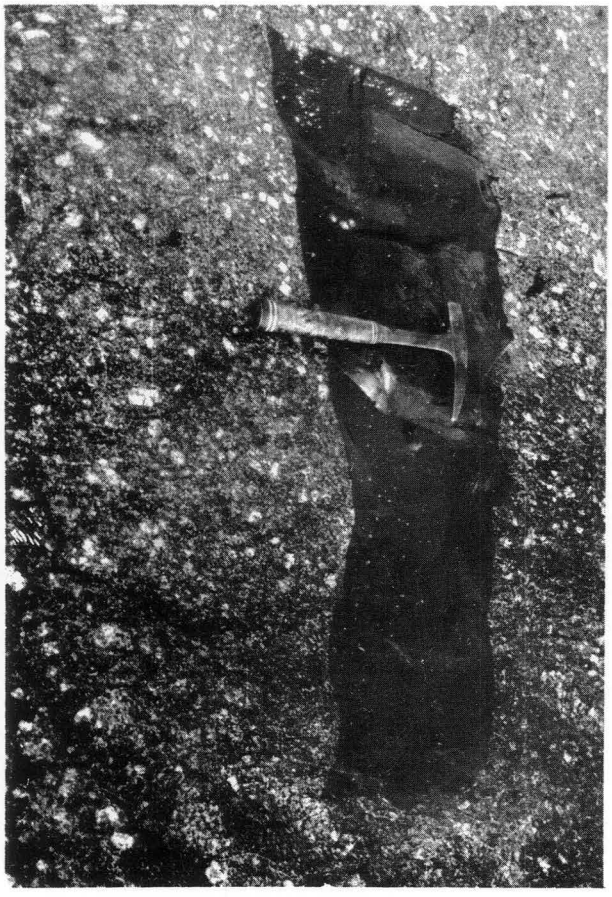

Plate XV Dassen Island - xenoliths

Above and below, left - Hornfelsic xenoliths in coarsely porphyritic granite, and apparently bounded by joint planes, northwestern peninsula.

Below, right - Small ghost inclusion in coarsely porphyritic granite, east coast.

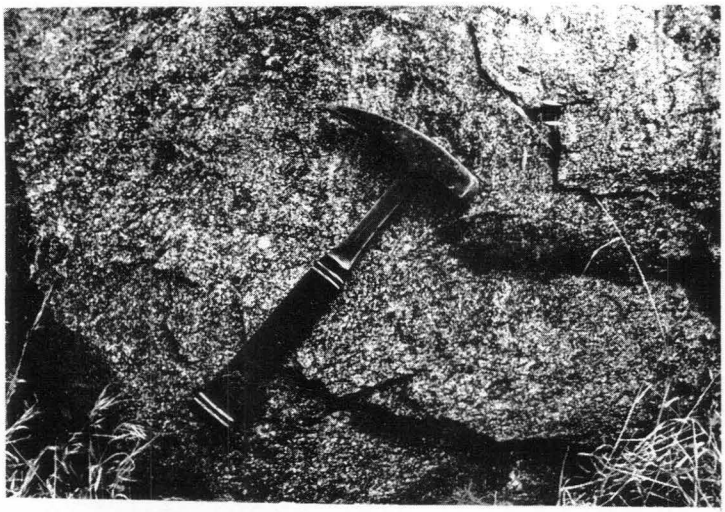

Plate XVI Textures of granites.

Above, left - Weathered surface of biotite rich Darling granite (coarsely porphyritic biotite granite), Rheboksfontein. Note thin oblique shear streak above handle of hammer.

Above, right - Hybrid dioritic rock, on farm Dassenberg.

Middle, right - Typical hybrid granodiorite, Ontongskloof. At this locality the rock holds an average of 4 large xenoliths per m^2 and 2 quartz segregations per m^2.

Below - Left, boulder of Klipberg granite, Wolwefontein. Right, Contreberg granite, on farm Contreberg.

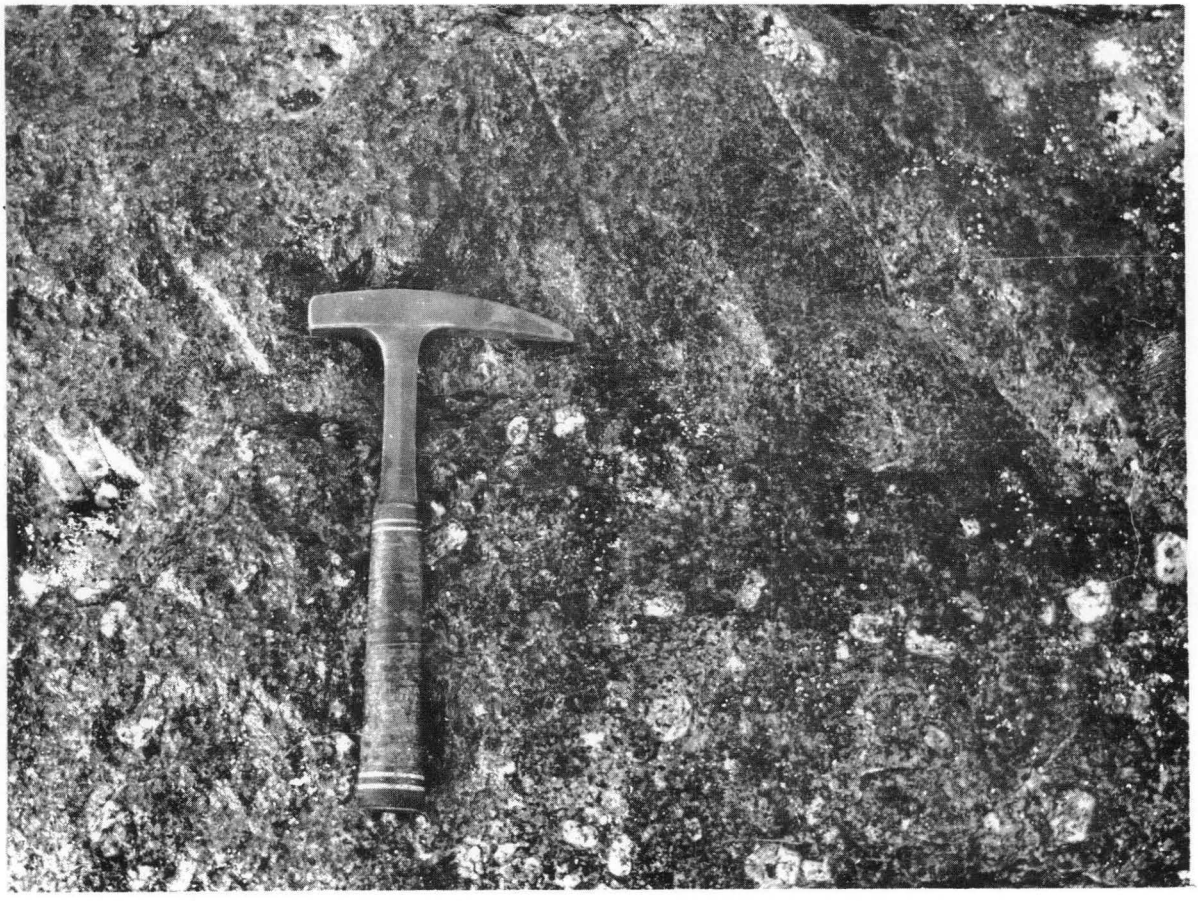

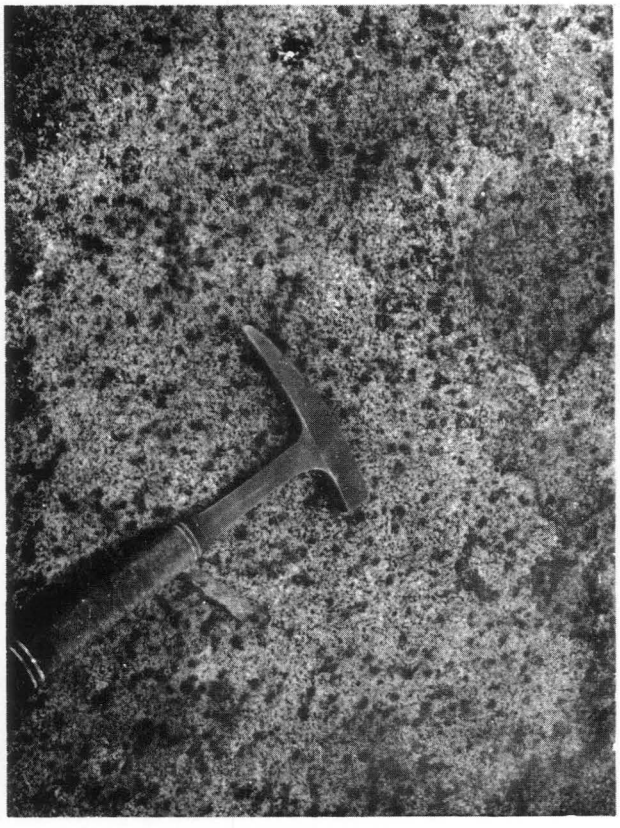

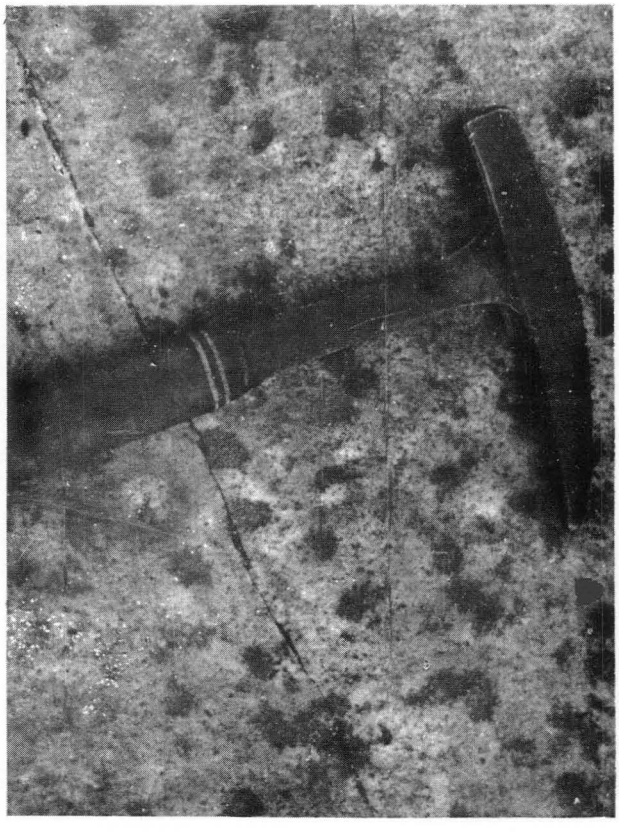

Plate XVII Dassen Island - nodular tourmaline granite.
Above - Contact between coarsely porphyritic granite and finegrained nodular tourmaline granite, north-western peninsula. Note tourmaline nodules with leucocratic borders in upper part of photograph.
Below - Finegrained tourmaline granite with the predominant type of uncollared nodules. Left, small nodules, House Bay. Right, large nodules, east coast.

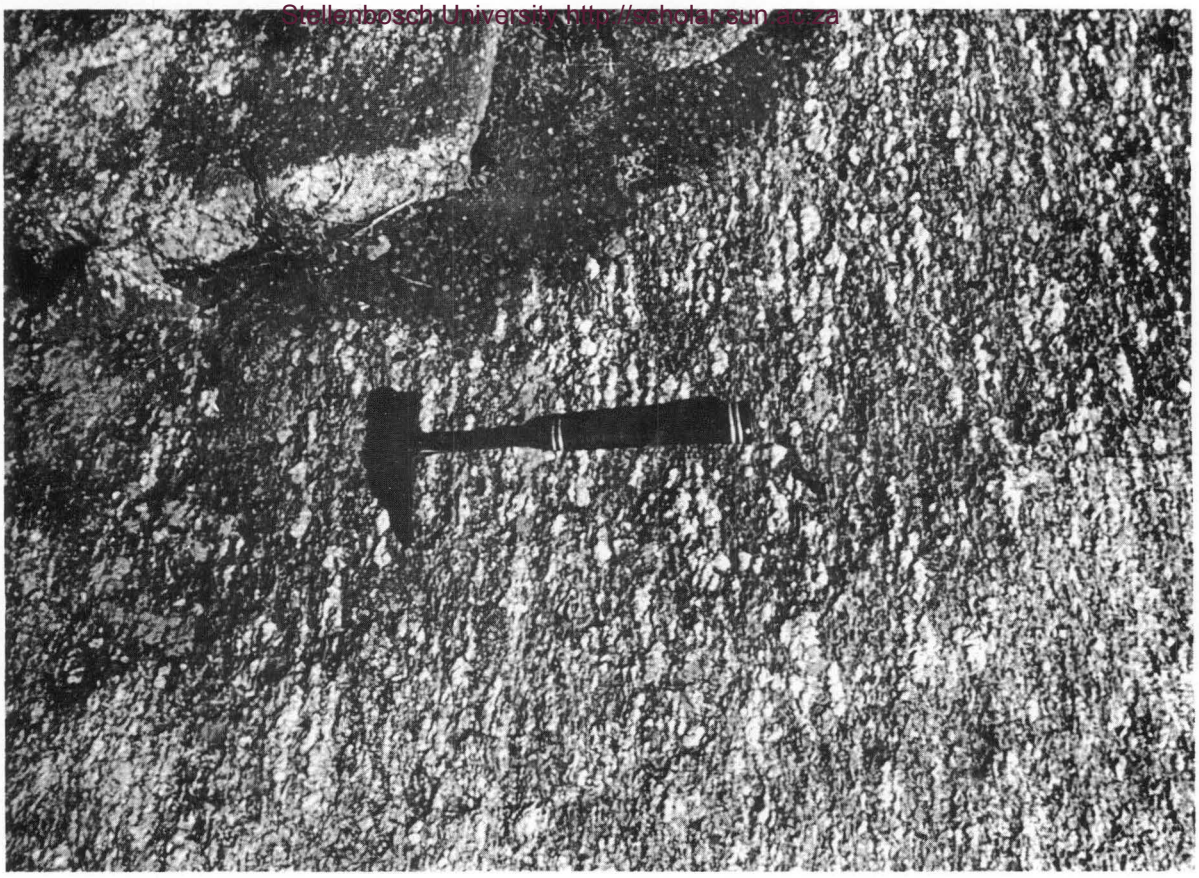

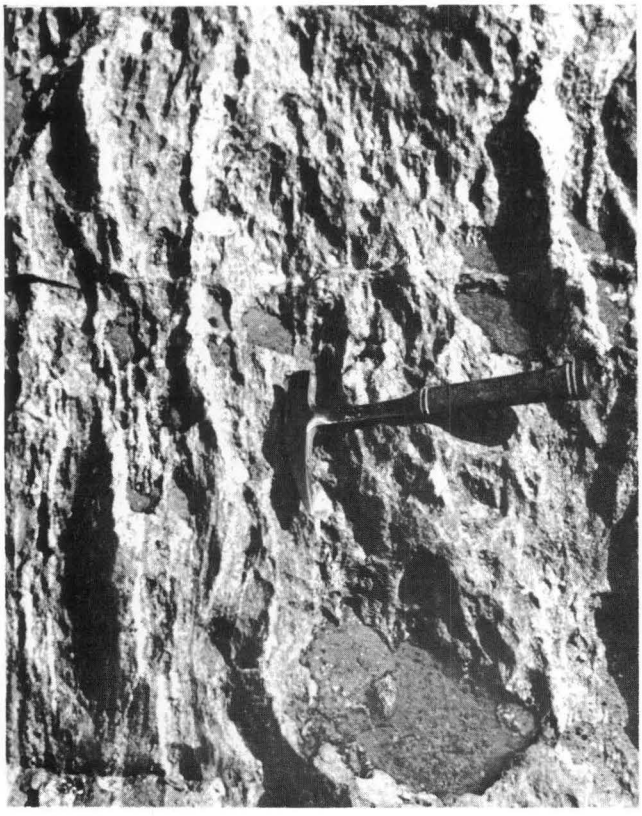

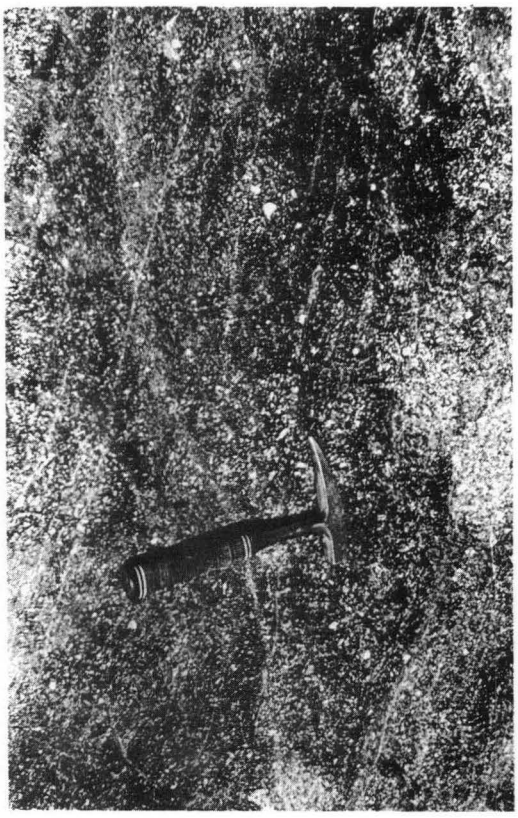

Plate XVIII Directed structures.

Above - Gneissic biotite rich Darling granite with northwesterly orientation, Burgerspost. Situated on strike of a zone of mylonitisation.

Below, left - Schlieric structure, probably due to cataclasis, in area where stringers of Contreberg granite are interdigitated with non-porphyritic biotite granite, Vrededal.

Below, right - Cataclastically deformed hybrid granodiorite, Alexanderfontein East.

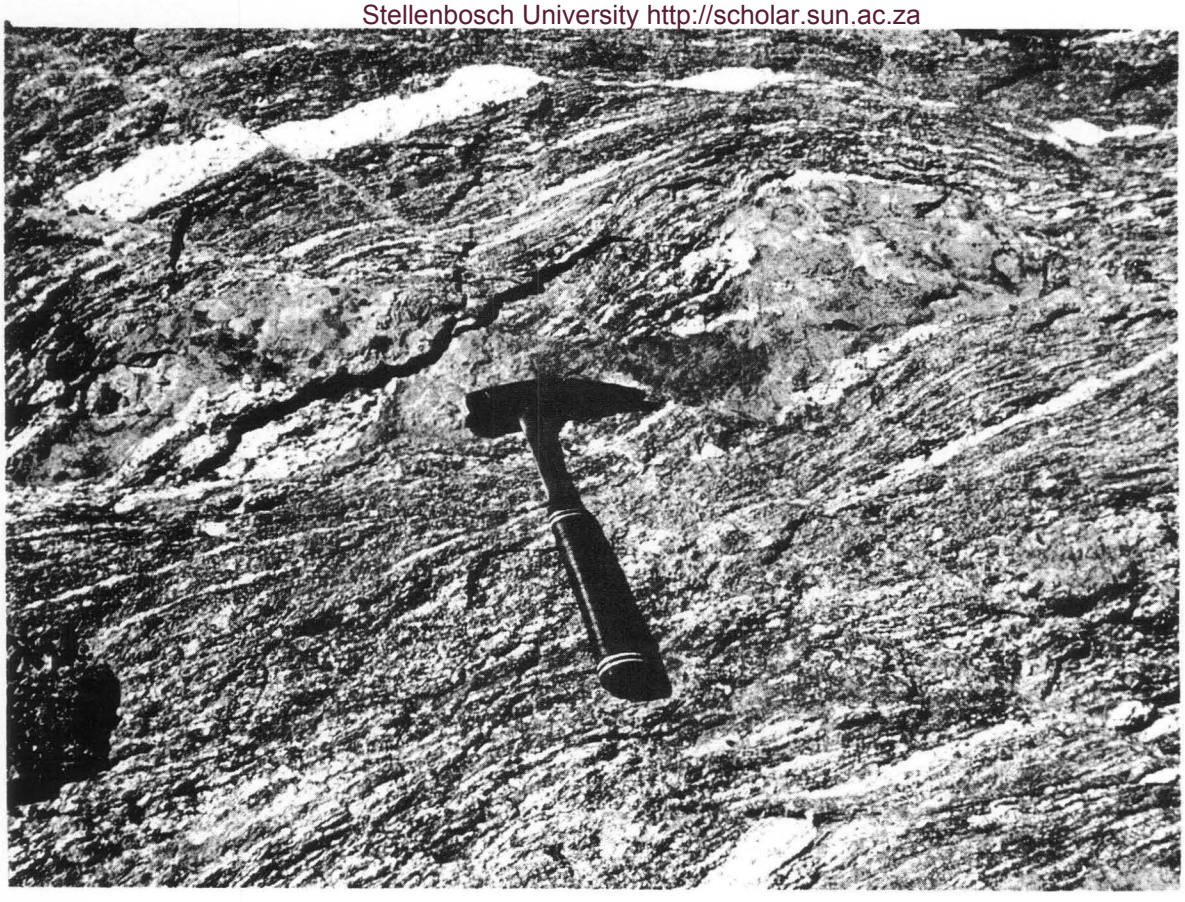

Plate XIX Schlieric structures.

Above and below, left - Northwesterly trending mylonitic zone with aplogranitic stringers traversing hybrid granodiorite, Hill side.

Below, right - Schlieric granite, Oranjefontein. Possibly representing a lit-par-lit relation between Contreberg granite and hybrid granodiorite.

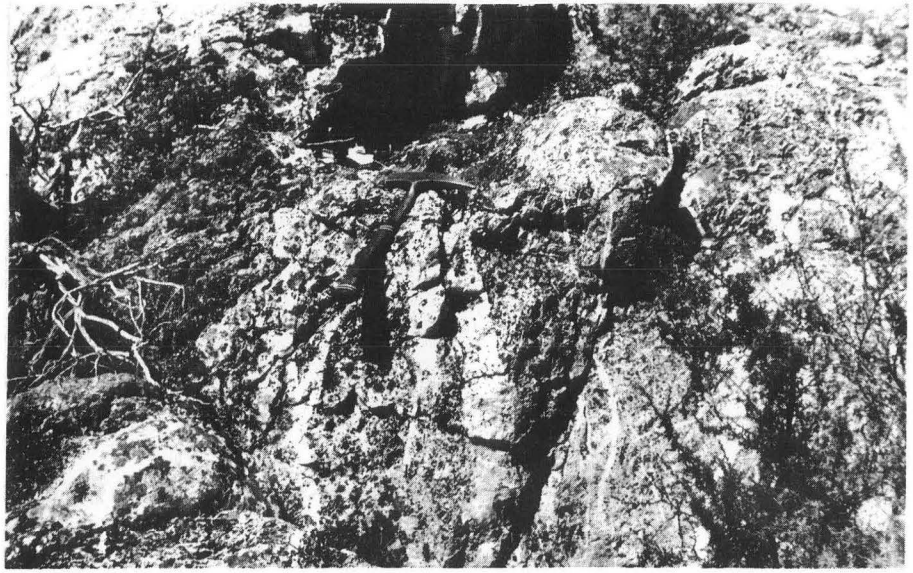

Plate XX. The Colenso fault, outcrops of chalcedonic fault breccia.
In the areas shown the fault breccia forms the only outcrops in flat and featureless terrain. Above, left - Local swing in fault which follows strip of outcrops in foreground but which eventually connects up with outcrops shown on horizon at left. Môrelig, looking to the northwest. Above, right - Intermittent breccia outcrops indicates position of fault. Stipples on right edge of photograph, in background, are the same. Kraalbosdam, looking to the south south-east. Below, left - The fault breccia. At corner between The Granary, Môrelig and Nuwerus. Below, right - Same locality as below, left, showing development of fault breccia. This is the topographic feature referred to as occurring on the horizon, above, left. Looking northwest.

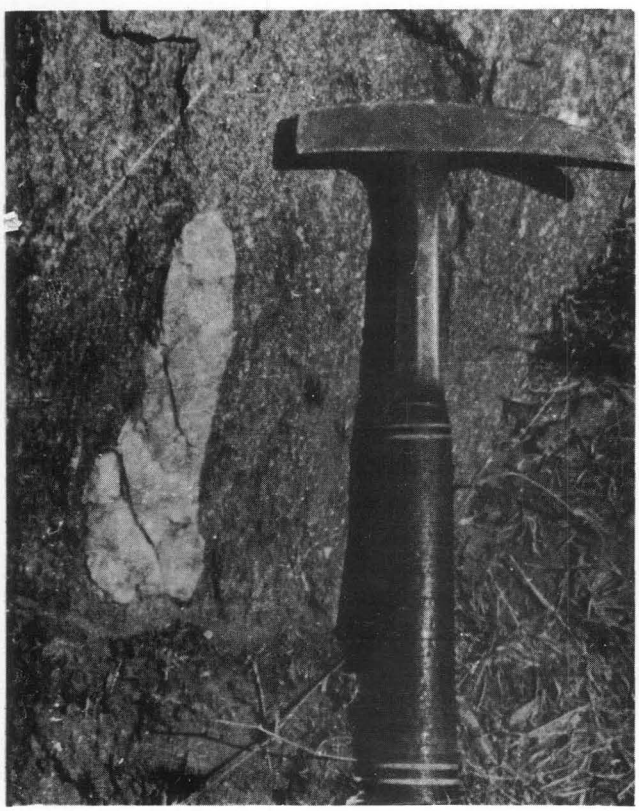

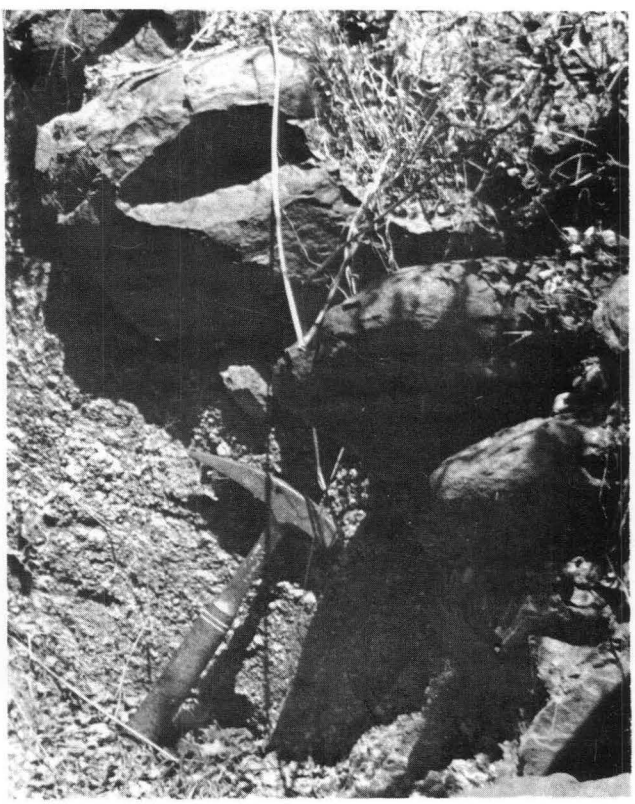

Plate XXI Structure of the Malmesbury formation, and dolerite.
Above, left - Northerly orientated "oscillation ripple marks" in Malmesbury hornfels, Ganzekraal. Note striped cherty marker bed on lower horizon. Above, right - High tide inundating depression marking less resistant beds in the nose of a typical boat-shaped synclinal fold, approximately 250 m from foreground of photograph. Ganzekraal, looking to the north.
Below, left - Typical quartz segregation in hybrid granodiorite, Slangkop. Below, right - Contact between dolerite dyke and weathered hybrid granodiorite, dipping 39° to the south. Exposed in bottom of a donga, Oranjefontein.

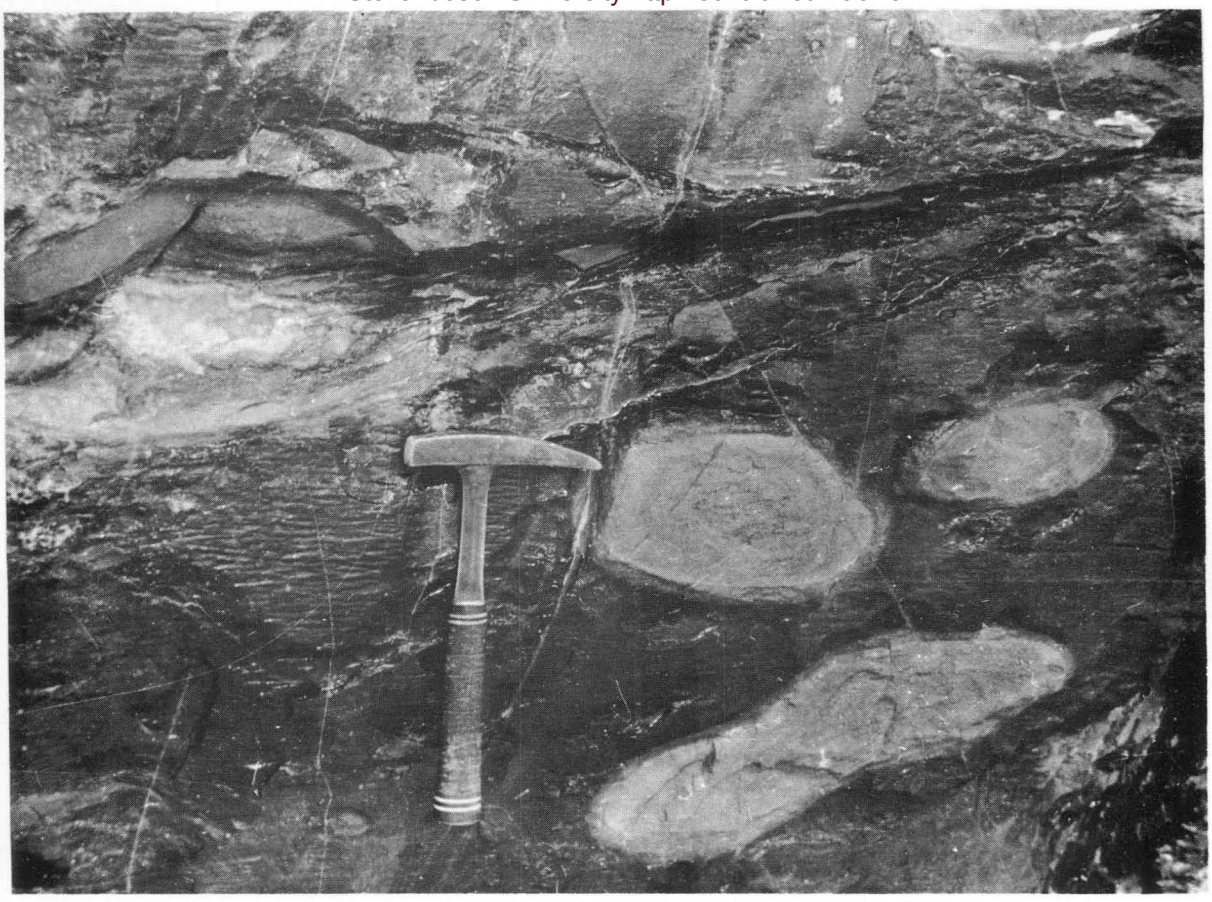

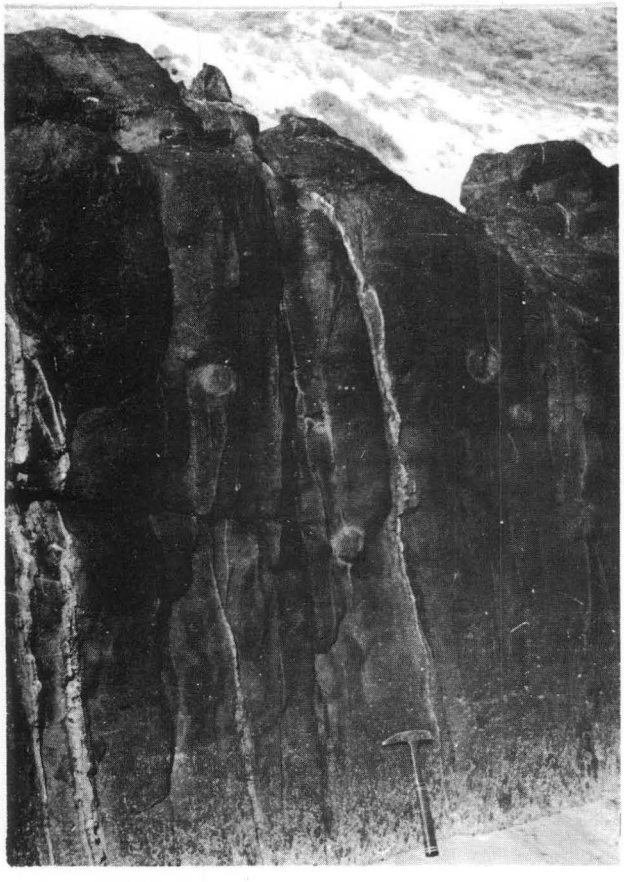

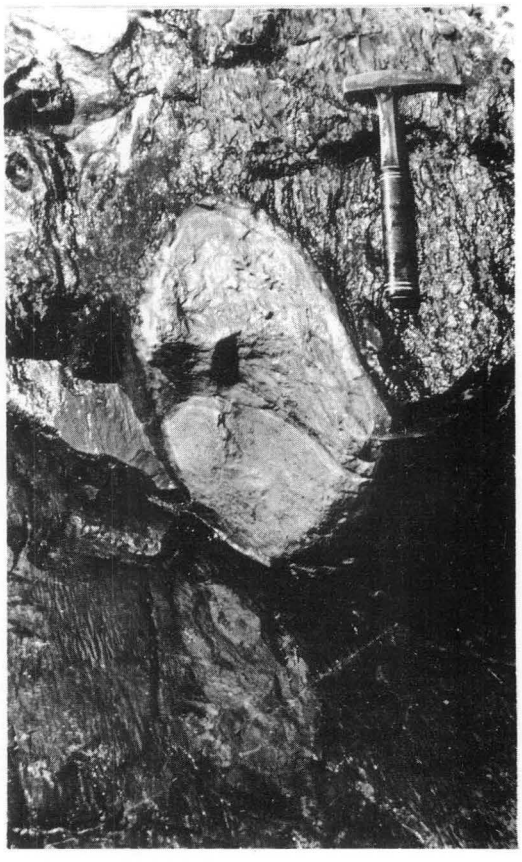

Plate XXII Concretions in Malmesbury formation hornfels.
Above - Concretions showing concentric structure, Mud river. Head of hammer orientated north-south.
Below, right - Showing shape of concretion, same locality.
Below, left - Concretions visible on an axial cleavage plane, and in spotted shale, Ganzekraal. Note quartz veins in cross joints. Sea and surf visible in background, wet sand in foreground.

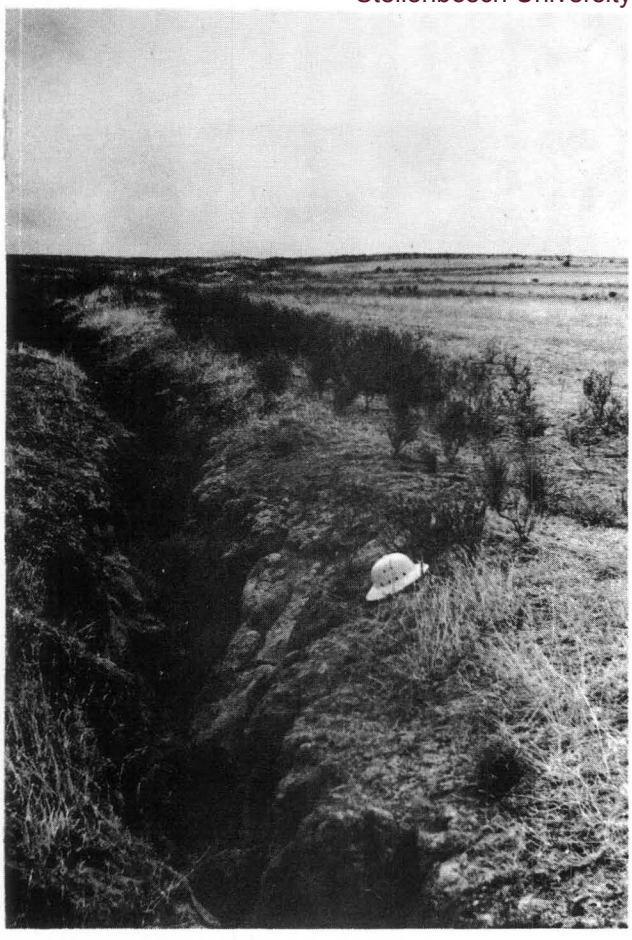

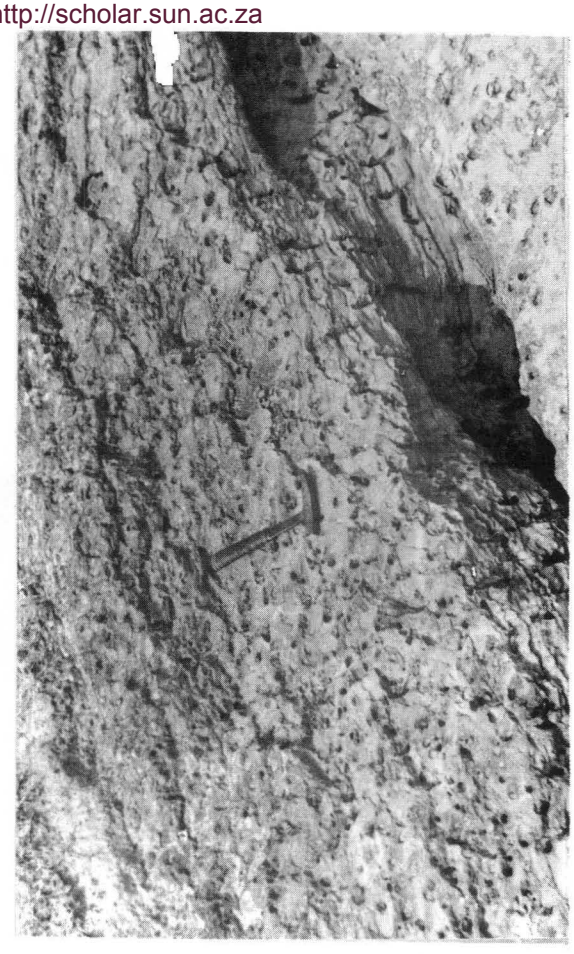

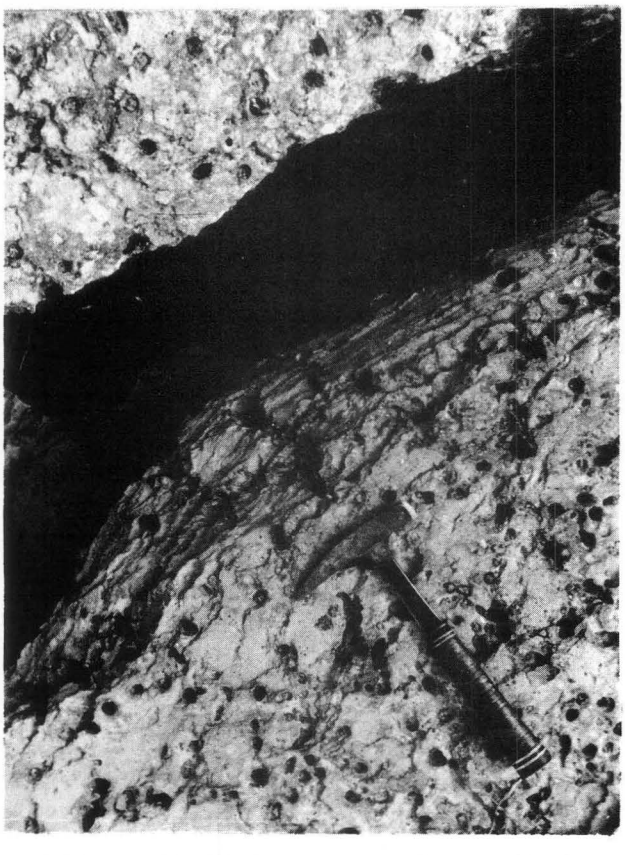

Plate XXIII Formation of ferricrete, Wildschutsvlei.

Above, left - Small donga excavated in weathered hybrid granite, and exposing the beginnings of a laterite layer below the soil cover.

Above, right and below - Numerous pipe-like channels are present in the weathered material, and are either filled with, or rimmed by iron oxides.

(The pipe-like type of laterite illustrated above grades elsewhere into a kind with a boxwork of pipes, and eventually into the familiar nodular ferricrete).

APPENDIX

Data used in figures (chapter VI).

Tables a to i.

Data for K_2O-Na_2O diagram (fig. 25)

		Na_2O	K_2O
HPG		2,56	4,81
DAR		2,60	4,57
CPG		2,92	5,17
VG		3,08	4,19
CCG		3,81	4,36
CB		2,62	5,28
DAS		3,31	4,50
HbGn2		3,50 ±0,01	2,62 ±0,36
	1	2,25	4,84
DAR	2	2,28	4,63
	14	3,26	4,24
	3	2,21	4,09
	4	2,22	4,81
	10	2,14	3,79
	11	1,89	3,21
HbGn	12	1,76	3,63
	22	3,99	3,60
	23	3,30	3,42
	24	2,70	3,42
	5	2,34	4,16
	6	2,63	5,34
CB	7	2,61	5,22
	19	2,68	4,73
	20	4,30	4,53
	35	2,30	2,80
	13	0,34	0,39

Data for Fe_2O_3-FeO diagram (fig. 26)

			Fe_2O_3	FeO
	HbGn2		0,84 ±0,15	5,57 ±0,30
	DAR		0,17 ±0,03	3,59 ±0,33
OG	HPG		0,66	2,92
	CPG		0,33	2,68
	VG		0,42	2,88
	CB 1		0,24	2,01
	DAS		0,44	0,78
	CCG		0,59	0,79
		1	0,19	3,19
	DAR	2	0,11	3,32
		14	0,21	4,25
	MYLONITE	3	0,38	4,17
		10	0,26	4,50
		11	0,85	6,11
	HbGn2	12	1,03	5,39
		22	0,99	6,17
		23	1,09	5,69
		5	0,55	4,61
		19	0,21	1,86
	CB 1	6	0,37	1,94
		7	0,12	2,08
	MALM.	35	2,18	5,34

Data for Fe^{+++}-Fe^{++} diagram (fig. 27)

	Fe^{++}	Fe^{+++}	Fe^{+++}/Fe^{++}
DAR	2,66	0,11	0,041
HPG	2,11	0,08	0,038
VG	2,11	0,06	0,028
32	2,10	0,10	0,048
33	1,47	0,08	0,054
CB 1	1,46	0,11	0,075
34	1,15	0,04	0,035
CCG	0,57	0,08	0,014
HbGn2	4,11 $\pm$0,21	0,53 $\pm$0,11	0,129
35	3,90	1,48	

Data for variation diagrams (figs. 28, 29 and 30)

No.	Si^{++++}	Al^{+++}	$Fe^{+++}+Fe^{++}+Mn^{++}+Mg^{++}$ "fm"	Ca^{++}	$Na^{+}+K^{+}$ "alk"	CATIONS	OH^{-}
10	60,00	15,07	6,52	1,48	7,80	91,54	7,80
11	56,54	16,08	9,58	1,54	6,92	91,72	11,50
12	57,54	16,53	9,13	1,99	7,08	93,18	6,54
22	55,86	16,80	9,43	1,56	11,10	95,39	9,70
23	56,38	17,23	8,83	1,77	9,54	94,27	8,98
14	60,43	14,63	5,24	2,78	10,46	94,12	5,34
32	60,59	15,04	4,36	2,63	9,58	92,77	5,04
33	61,35	14,89	3,49	2,62	9,76	92,52	5,02
34	62,27	15,54	2,34	2,35	9,80	92,53	3,66
22+23	56,12	17,01	9,13	1,66	10,32	94,82	9,34
80:20	55,73	16,47	9,04	1,04	7,66	90,90	14,27
DAR	61,51	14,55	4,63	1,97	9,66	92,52	6,26
HbGn2C	57,77	16,32	8,42	1,71	8,42	93,38	8,92

Curves for the Darling hybrid rocks shown in bold, compared with regional hybridisation curves based on data from D.L. Scholtz (1946) shown by dashed lines. The data for the 80:20 Malmesbury mixture, DAR and HbGn2C have been added for comparison, but were not used during construction of the curves.

Data for "granite differentiation index" diagram (fig.31)

	$\log(FeO+Fe_2O_3+MgO+TiO_2)$	$Na_2O+K_2O+SiO_2$	$\frac{FeO+Fe_2O_3+MgO+TiO_2}{Na_2O+K_2O+SiO_2} \cdot 100$
CCG	0,2672	84,30	2,195
CSM			2,369
CB1	0,5289	79,68	4,242
VG	0,6493	78,64	5,671
HPG	0,7135	76,87	6,726
DAR	0,7497	76,66	7,396

Data for "granite differentiation index" diagram (fig. 32)

	$FeO + Fe_2O_3 + MgO + TiO_2$	$Na_2O + K_2O + SiO_2$
20	0,39	84,78
CCG	1,85	84,30
DAS	1,48	81,92
CB1	3,38	79,68
VG	4,46	78,64
CPG	4,46	77,57
HPG	5,17	76,87
DAR	5,62	76,66
HbGn2	9,98	70,74
19	3,00	79,95
7	3,31	79,69
1	5,43	76,67
14	6,53	75,46
10	7,67	74,31
11	11,38	68,87
12	10,71	69,80
22	10,95	69,85
23	10,08	70,05
24	7,88	73,25
3	7,87	72,03
35	11,05	66,36
13	7,54	68,05

Data for Az° - Si° diagram (fig. 33)

	Az°	Si°
20	0,831	1,744
DAS	0,827	1,864
CCG	0,823	1,802
CB	0,792	1,699
VG	0,778	1,654
HPG	0,770	1,622
CPG	0,771	1,542
DAR	0,766	1,619
10	0,756	1,719
24	0,737	1,557
5	0,739	1,539
HbGn2	0,719	1,462
12	0,715	1,551
11	0,715	1,562
23	0,701	1,311
22	0,690	1,179
35	1,700	1,445

Data for 6alk - 2(al-alk) - (100-2al) diagram (fig.34)

No.	6alk	2(al - alk)	(100 - 2al)
10	67,07	20,84	12,09
11	56,46	25,59	17,95
12	57,32	25,47	17,21
22	70,72	11,84	17,44
23	66,29	17,86	15,85
24	66,85	20,39	12,26
HbGn	64,40	20,11	15,49
DAR	75,95	13,14	10,91
HPG	77,31	14,29	8,40
CPG	81,49	12,25	6,26
VG	79,27	10,85	9,87
CB	83,10	12,78	4,12
CCG	92,05	3,69	4,26

Data for variation diagram (fig. 35)

	Si	al	alk	c	fm
20*	491,83	52,5	45,5	0,4	1,6
DAS	478,83	54,4	39,2	1,9	4,5
CCG	466,54	44,5	39,7	7,0	8,8
19	384	45,1	29,8	10,8	14,3
CB	380,84	45,4	31,0	7,3	16,2
VG	370,74	39,5	28,0	13,3	19,2
CPG	337,61	43,1	29,7	8,2	18,9
HPG	334,68	41,3	26,6	10,1	22,0
DAR	328,05	38,9	25,6	10,8	24,6
5	282,65	36,5	20,9	9,7	32,9
10	309,5	39,1	20,2	7,6	33,4
24	280,9	38,9	20,1	9,3	31,7
HbGn2	256,2	26,4	18,8	7,6	37,1
11	250,5	35,6	15,3	6,8	42,2
12	251,6	36,1	15,5	8,7	39,7
23	224,0	33,7	22,2	6,3	37,8
22	235,3	35,9	19,9	7,3	36,8

* The analysis of P. Kolbe (1966, table 6, no. 151) is obviously of a sample of aplite in Klipberg granite.

Colenso Fault

Colenso Fault

Pelgrimsrus Fault

DARLING

MAMRE

PELLA

YSTERFONTEIN

ATLANTIC OCEAN

DASSEN ISLAND

Burgerspan
Skilpadfontein
Swartberg
Swartbergsvlei
Smutskraal
Driefontein
Ratelberg
Swartwater
Wildschutsvlei
Slangkop
Windhoek
Grootwater
De la Rey
Koffiefontein
Rondeberg
Brakrivier
Kraalbosdam
Jan Swartsvlei
Klipberg
Plattekop
Alexanderfontein
Langfontein
Bosteebeen
The Towers
Rheboksfontein
Döringfontein
Smalpad
Oude Post
Woodlands
Waylands
Oranjefontein
Glen Frank
Groote Post
Ontongskloot
Pompoenvlei
Klowervlei
Mud River
Midlands
Ganzekraal
Colenso
Hebrewsvlei
Morelig
Longa
Kalkop
Pelgrimsrus
Gemsbokkuil
Klipfontein
Mamre Rd
Evening Star
The Granary
Morning Star
Januariekraal
Viededal
Papkuilsfontein
Contreberg
Watterkloof
Commercial Dale
Gabbejaenberg
Nuwepos
Hill Side
Burgerspost
Dassenberg
Katzenberg
Groenfontein
Klein Dassenberg
Green River

LEGEND

- Ferricrete, Silcrete
- Recent limestone
- Chalcedonic fault breccia
- Faults
- Dolerite
- Diorite
- Young granites (Contreberg granite, Klipberg granite)
- Dassenberg granite
- Biotite granite
- Hybrid granodiorite and hybrid adamellite
- Mylonite
- Coarsely porphyritic biotite granite
- Coarsely porphyritic granite (DARLING GRANITE)
- Malmesbury formation metamorphites

- Very large xenolith
- Lime-rich xenolith
- Pegmatoid
- Aplogranite
- Garnet abundant
- Gneissic granite

Kilometres
1 0 1 2 3 4 5